Functional analysis of catalase mutants and their application to the analysis of NADPH-linked pathways in oxidative signaling in Arabidopsis thaliana

Zheng Yang

UNIVERSITÉ PARIS SUD
Comprendre le monde, construire l'avenir

Functional analysis of catalase mutants and their application to the analysis of NADPH-linked pathways in oxidative signaling in *Arabidopsis thaliana*

Thèse de doctorat de l'Université Paris-Saclay
préparée à l'Université Paris-Sud
au sein de l'Institut des Plantes des Sciences de Paris-Saclay, IPS2

École doctorale n°567 :
Sciences du végétal : du gène à l'écosystème, SDV

Spécialité de doctorat : Biologie

Thèse présentée et soutenue à Gif-sur-Yvette, le 15.11.2018, par

Zheng Yang

Composition du Jury :

Dr. Marianne Delarue Professeur, Univ. Paris-Sud, Orsay	Présidente
Dr. Yves Jolivet Professeur, Univ. Lorraine, Nancy	Rapporteur
Dr. Arnould Savouré Professeur, Sorbonne Université, Paris	Rapporteur
Dr. Graham Noctor Professeur, Univ. Paris-Sud, Orsay	Directeur de Thèse

ACKNOWLEDGMENTS

I would like to express my gratitude to everyone who helped me throughout the process of thesis writing. It would not have been so smoothly to finish the work without their support.

My deepest gratitude goes first to Professor Graham Noctor, my supervisor, for his patient guidance, detailed advice and continuous encouragement during my PhD study. It is my great pleasure to have a supervisor with immense knowledge and rigorous attitude to scientific work. His instruction and words helped me a lot in my research and the writing of thesis, and for sure, will influence me more in the future.

I am thankful to the jury members of my defence, Prof. Yves Jolivet (Université de Lorraine, FR), Prof. Arnould Savouré (Sorbonne Université) and Prof. Marianne Delarue (Université Paris Sud, FR) for having accepted to evaluate my PhD work and spending their valuable time to read my thesis.

I would like to thank the former and the current colleagues in our group. Amna Mhamdi, my first officemate, helped me a lot in learning different techniques and in being familiar with the working environment. The scientific discussion with her has benefited me a lot. Her enthusiasm, responsibility and preciseness has set a food example to me in my routine work. I am very grateful to Gilles Chatel-Innocenti and Hélène Vanacker for the opportunity to work on the mutants they had obtained, and for their help and discussions, enabling me to produce the results presented in Chapter 4 of this thesis. I am also thankful to Marie-Sylviane Rahantaniaina for the help in my work and life. Our communication about the culture, food and everything else is so nice and unforgettable. To Caroline Lelarge for salicylic acid analysis. To Emmanuelle Issakidis-Bourguet and Daoxiu Zhou for the valuable scientific discussion and help in life. To Yuan Shen and Xiaoyun Cui for much help in work and friendship in life.

During the PhD career, I obtained much help and support from colleagues in IPS2. It is really lucky to meet these nice people in the institute. Their passionate smile and kindly words have warmed me so much. I would like to express my gratitude to these members, Raynaud Cécile, Linda De Bont, Jingfang Hao, Shengbin Liu, Marie Dufresne, Sophie Massot, Sophie Blanchet, Severine Domenichini, Holger Ornstrup, Jean-paul Bares….

This thesis would not have been possible without the financial support of China Scholarship Council and French Agence Nationale de la Recherche grants ANR12BSV60011 (Cynthiol).

Finally, I would like to take the opportunity to thank my parents and brother for your understanding and support. It is the love of the family that provided continuous power throughout my PhD career.

在这段异国他乡的难忘的博士生涯中，来自家人的爱是支持我在科研道路上不断前进的动力和源泉。所有的经历都因为你们而有意义。亲爱的爸爸，妈妈和哥哥，感谢你们的理解和鼓励，我爱你们！

Abbreviations

2-OG	2-Oxoglutarate
3-AT	3-Aminotriazole
^{3}Chl	Triplet state of chlorophyll
$^3O_2$	Triplet oxygen
5-OPase	5-Oxoprolinase
6PGDH	6-Phosphogluconate dehydrogenase
ABA	Abscisic acid
AO	Ascorbate oxidase
APX	Ascorbate peroxidase
ASC	Reduced ascorbate
C	Cytosine
CAT	Catalase
Chl	Chlorophyll
CPR5	CONSTITUTIVE EXPRESSION OF PR GENES5
cICDH	Cytosolic ICDH
$DCFH_2$-DA	Dichlorodihydrofluorescein-diacetate
DDR	DNA damage response
DHA	Dehydroascorbate
DHAR	Dehydroascorbate reductase
DTNB	5,5'-dithiobis (2-nitro-benzoic acid)
γ-ECS	γ-EC synthetase
EMS	Ethyl methanesulfonate
FNR	Ferredoxin-NADP reductase
G	Guanine
G6PDH	Glucose-6-phosphate dehydrogenase
GA	Gibberellins
Ga3P	Glyceraldehyde-3-phosphate
GGC	γ-Glutamyl cyclotransferase
GGT	γ-Glutamyl transpeptidase
G proteins	GTP-binding proteins
GPX	Glutathione/thioredoxin peroxidase
GR	Glutathione reductase
GRX	Glutaredoxin
GS/GOGAT	Glutamine synthetase/glutamate synthase
GSH	Reduced glutathione
GSH-S	Glutathione synthetase
GSK3	Glycogen synthase kinase 3
GSSG	Glutathione disulfide
GST	Glutathione S-transferase
hCO_2	High CO_2
H_2O_2	Hydrogen peroxide
HPLC	High performance liquid chromatography
HR	Hypersensitive response
ICDH	Isocitrate dehydrogenase
ICS1	Isochorismate synthase1
JA	Jasmonic acid
Ler	*Landsberg erecta*
LD	Long days (16 h photoperiod)
L-Gal	L-Galactose
MAPK	Mitogen-activated protein kinase
MAPKK	MAPK kinase
MAPKKK	MAPK kinase kinase
MDHA	Monodehydroascorbate
MDHAR	Monodehydroascorbate reductase
ME	Malic enzyme
MeJA	Methyl jasmonate

MIPS1	*myo*-Inositol phosphate synthase
NADHK	NADH kinase
NADPH	Reduced nicotinamide adenine dinucleotide phosphate
NADP-ME	NADP-malic enzyme
NO	Nitric oxide
npGAPDH	Nonphosphorylating glyceraldehyde-3-phosphate dehydrogenase
NTR	NADPH-thioredoxin reductase
OPPP	Oxidative pentose phosphate pathway
OXI1	Oxidative signal inducible 1
PCS	Phytochelatin synthase
PEP	Phosphoenolpyruvate
PGA	3-Phosphoglycerate
PR	Pathogenesis-related
PRX	Peroxiredoxin
PS I	Photosystem I
PS II	Photosystem II
PTS1	Peroxisomal Targeting Sequence1
RBOH	Respiratory burst oxidase homolog
RETC	Respiratory electron transport chain
ROS	Reactive oxygen species
RT-PCR	Reverse transcription-Polymerase chain reaction
RuBP	Ribulose 1,5-*bis*phosphate
SA	Salicylic acid
SAR	Systemic acquired resistance
SD	Short days (8 h photoperiod)
SOD	Superoxide dismutase
Sugar-P	Sugar phosphate
T	Thymine
TILLING	Targeting Induced Local Lesions in Genomes
TNT	2,4,6-Trinitrotoluene
TRX	Thioredoxin
TRXox/TRXred	Oxidized/reduced thioredoxin
VPD	2-Vinylpyridine
χ^2	Chi-square

TABLE OF CONTENTS

CHAPTER 1

GENERAL INTRODUCTION

General overview of energy conversion in plants

Plants are sessile organisms and so cannot move away from adverse conditions. Because they are constantly challenged by environmental changes such as pathogen infection, fluctuations in temperature and light intensity, water availability and chemical pollution, plants have developed extensive physiological systems to cope with a range of stimuli and to maintain normal growth and development. Photosynthesis and respiration are two fundamental physiological processes in plants because they play a critical role in balancing carbon fixation and efflux, as well as energy transfer and production. Photosynthesis captures light energy to fix CO_2 into carbohydrates such as sugars. This is driven by reduced nicotinamide adenine dinucleotide phosphate (NADPH) and ATP, which are produced by the activities of photosystem II (PSII), the cytochrome b_6/f complex, photosystem I (PSI) and the ATP synthase. Because photosynthesis takes place in an oxygen-rich environment and involves highly energetic reactions, it is accompanied by generation of reactive oxygen species (ROS) such as singlet oxygen in PSII and superoxide in PSI (Foyer et al., 2012). Photorespiration, which occurs alongside CO_2 fixation, is initiated by the oxygenation of ribulose 1,5-bisphosphate (RuBP) in the chloroplast. The product, phosphoglycolate, is transferred to the peroxisomes and undergoes a reaction catalyzed by glycolate oxidase, in which hydrogen peroxide (H_2O_2) is produced. Thus, H_2O_2 can be produced at high rates during photosynthesis, either in the peroxisome directly from O_2 or in the chloroplast following dismutation of superoxide. The rate of H_2O_2 production through both of these routes is influenced by environmental conditions such as temperature, water availability, and light intensity.

Mitochondrial respiration is another essential energy-transducing reaction that can also give rise to ROS formation. During this process carbohydrates and O_2 are consumed to produce CO_2, water and energy. Unlike photosynthesis which relies on light, respiration is not directly dependent on light and can produce energy in the dark. Like the photosynthetic electron transport chain, the respiratory electron transport chain (RETC) can also produce H_2O_2 via superoxide. However, respiration probably makes only a relatively minor contribution to overall cellular ROS production, at least in the light. It has been estimated that reactions associated with photosynthesis and photorespiration are the major

sources of ROS within plant cells in the light (Foyer and Noctor, 2003).

Increased ROS production can modify intracellular redox state. Because ROS production is influenced by external conditions, these molecules have become recruited by plants as important signals that provide information on environmental conditions relative to the internal status of plant cells. Under non-stressful physiological conditions, intracellular redox homeostasis is maintained by various systems. When the environment becomes more challenging, ROS accumulation can occur, leading to the perturbation of physiological processes that depend on cellular redox state. Depending on its intensity, context and duration, such perturbations can lead to increased resistance in plants through acclimation processes. Alternatively, they may lead to cell death. These responses are well known as outcomes of stress, although it is important to note that even cell death is not necessarily deleterious to plant function and can be used, for instance, as a strategy to resist pathogen invasion.

There is keen interest in understanding plant responses to stress, as they can often determine agricultural yields. The central role of ROS in stress responses explains the explosion of research interest in these molecules over recent decades. While earlier concepts saw ROS as toxic byproducts, they are now considered to be key signaling molecules involved in many physiological processes (Foreman et al., 2003; Wagner et al., 2004; Han et al., 2013a, b; Foyer et al., 2017). It is important to note that, in the natural and field environments, plants are often exposed to more than one type of stress condition simultaneously. For instance, a plant might have to cope with soil pollutants, excessive salt, and pathogen attack at the same time. Although it is accepted that ROS are key regulators of the outcome of such conditions, the network that controls ROS and plant responses to ROS remains to be elucidated. As explained below, one of the key gaps in our knowledge is the specific role of different enzymes that are involved in controlling accumulation of ROS and cell redox state. This is the context within which the work presented in this thesis has been conducted.

1.1 ROS in plants

1.1.1 ROS: definition

The term ROS refers to a group of derivatives of O_2 that are more reactive than O_2 itself. Since 2.7 billion years ago, when significant amounts of O_2 began to accumulate in the earth's atmosphere following the evolution of PSII in O_2-evolving cyanobacteria, plants have had to evolve mechanisms to deal with ROS generation within their cells (Mittler et al., 2004). The production of ROS relies on the distinct molecular characteristics of O_2. As a diatomic radical, O_2 has two unpaired electrons with the same spin quantum number. Because of the spin restriction, O_2 prefers to accept electrons one at a time, which initially produces superoxide. Photodynamic excitation of O_2 can also lead, without reduction, to singlet oxygen (Krieger-Liszkay, 2005). Both of these processes lead to the generation of partially reduced or activated derivatives of O_2 which are, collectively, known as ROS (Halliwell, 2006). As well as the superoxide anion and singlet oxygen, ROS include H_2O_2 and the very reactive hydroxyl radical (Figure 1.1).

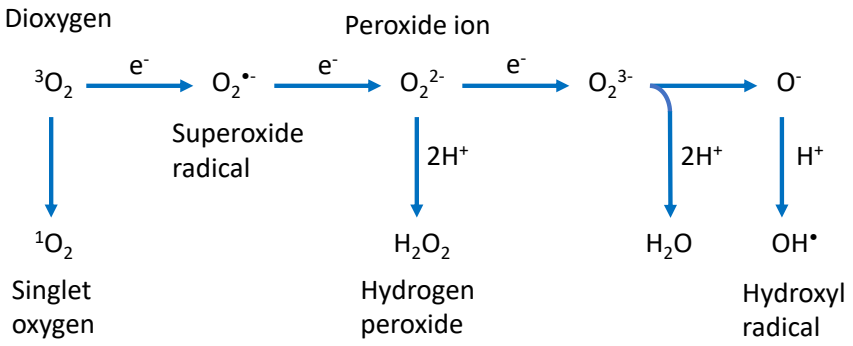

Figure 1.1. Generation of different ROS forms.

Singlet oxygen is a highly reactive form of ROS that is formed in PSII within chloroplasts. It has a short half-time of around 200 ns in cells and can react with various biomolecules such as lipids, proteins and DNA/RNA (Gorman and Rodgers, 1992). Singlet oxygen can be generated during photoinhibition, which is caused by excess photosynthetically active radiation (Hideg et al., 1998;

Krieger-Liszkay, 2005). Photosensitizers like Rose Bengal can also lead to the generation of singlet oxygen (Gutiérrez et al., 2014). Singlet oxygen production and signaling have been well studied in *flu* mutants in which a defect in a chlorophyll (Chl) biosynthesis regulator leads to ROS accumulation (Laloi et al., 2007; Lee et al., 2007).

As noted above, superoxide, a short-lived anion radical, is produced as a byproduct of electron transport chains during photosynthesis and respiration. Plasma membrane NADPH oxidases are another source of superoxide anion in plants. Such enzymes translocate electrons from NADPH in the cell across the membrane to O_2, which is reduced at the cell surface (Foyer and Noctor, 2000; Mittler et al., 2004; Li et al., 2017). Because of its high reactivity and toxic characteristic, superoxide anion is then converted to H_2O_2 and O_2 by chemical transformation or by dismutation catalyzed by superoxide dismutase (SOD).

H_2O_2 has received particular attention as an oxidant and signaling molecule because of its relative stability. As well as being produced secondarily from superoxide (Figure 1.1), H_2O_2 can be generated at high rates by a two-electron reduction of O_2 catalyzed by enzymes such as the photorespiratory glycolate oxidase (Foyer and Noctor, 2003). H_2O_2 is not a free radical, and it has a relatively long lifespan compared with other ROS. This property allows it to traverse cellular membranes and migrate between different compartments to function in physiological processes. H_2O_2, however, is highly oxidizing, with a standard redox potential of +1.32 V at pH 7.0 (Winterbourn, 2013). Despite this potential oxidizing power, it reacts poorly with most biological molecules because of a high activation energy barrier that explains its relative stability. Therefore, the reactions of H_2O_2 are kinetically rather than thermodynamically driven. This means that they are largely dependent on catalysts such as enzymes. Among various types of enzymes that can metabolize H_2O_2, catalase (CAT) has received attention because it is highly abundant and active and because it can catalyze the dismutation of H_2O_2 without the requirement of any reducing co-factor other than H_2O_2 itself.

The hydroxyl radical is the three-electron reduction product of O_2, and can notably be produced by metal-catalyzed reductive cleavage of H_2O_2 (Figure 1.1). As a free radical, it is short-lived, and is

considered the most reactive ROS. It is highly destructive of cellular components, and can attack lipids, proteins, DNA and RNA. Therefore, it is kept at a minimal level compared with the superoxide anion and H_2O_2, although it is thought to be important in the formation of cell wall polymers. The hydroxyl radical can notably be produced via the Fenton reaction involving suitable transition metals (Halliwell and Gutteridge, 2015; Li et al., 2017). Plants lack enzymatic mechanisms to scavenge the hydroxyl radical, but its formation can be prevented by metal chelators and rapid removal of H_2O_2 via a variety of enzyme systems that are discussed below. Together, these mechanisms act to limit Fenton-induced damage through the hydroxyl radical (Genaro-Mattos et al., 2015).

1.1.2 ROS generation

1.1.2.1 ROS generation and compartmentation

Many developmental processes involve signaling through ROS that are probably generated at lower levels than those associated with stress. It has been well established that reactions associated with photosynthesis, photorespiration and respiration are major sources of ROS. As described above, ROS can also be generated at the extracellular surface by NADPH-dependent oxidases, as well as in the apoplast by peroxidases and oxidases (Figure 1.2; Corpas et al., 2001; Foyer and Noctor, 2003; Asada, 2006; Mhamdi et al., 2012; Noctor et al, 2017) .

The chloroplast was one of the very first sources of ROS to be described in plants (Mehler, 1951; Asada et al., 1974). ROS generation occurs during photosynthesis at the sites of both PSI and PSII (Asada et al., 2006; Foyer et al., 2017). Specifically, singlet oxygen is produced by the photosensitizer Chl in the reaction center of PSII. When light absorption exceeds the capacity of photosynthetic electron transport, the lifetime of excited triplet states of Chl (^{3}Chl) increases, favoring transfer of the absorbed light energy to ground-state triplet oxygen ($^3O_2$) to form singlet oxygen (Hideg et al., 1998; Krieger-Liszkay, 2005). In contrast, PSI is considered to be a less important contributor to singlet oxygen generation in photosynthetic organisms. However, it is the major site for the generation of superoxide anion and H_2O_2; that is, reduced forms of O_2 (Mehler, 1951; Asada, 2000; Fryer et al.,

2002).

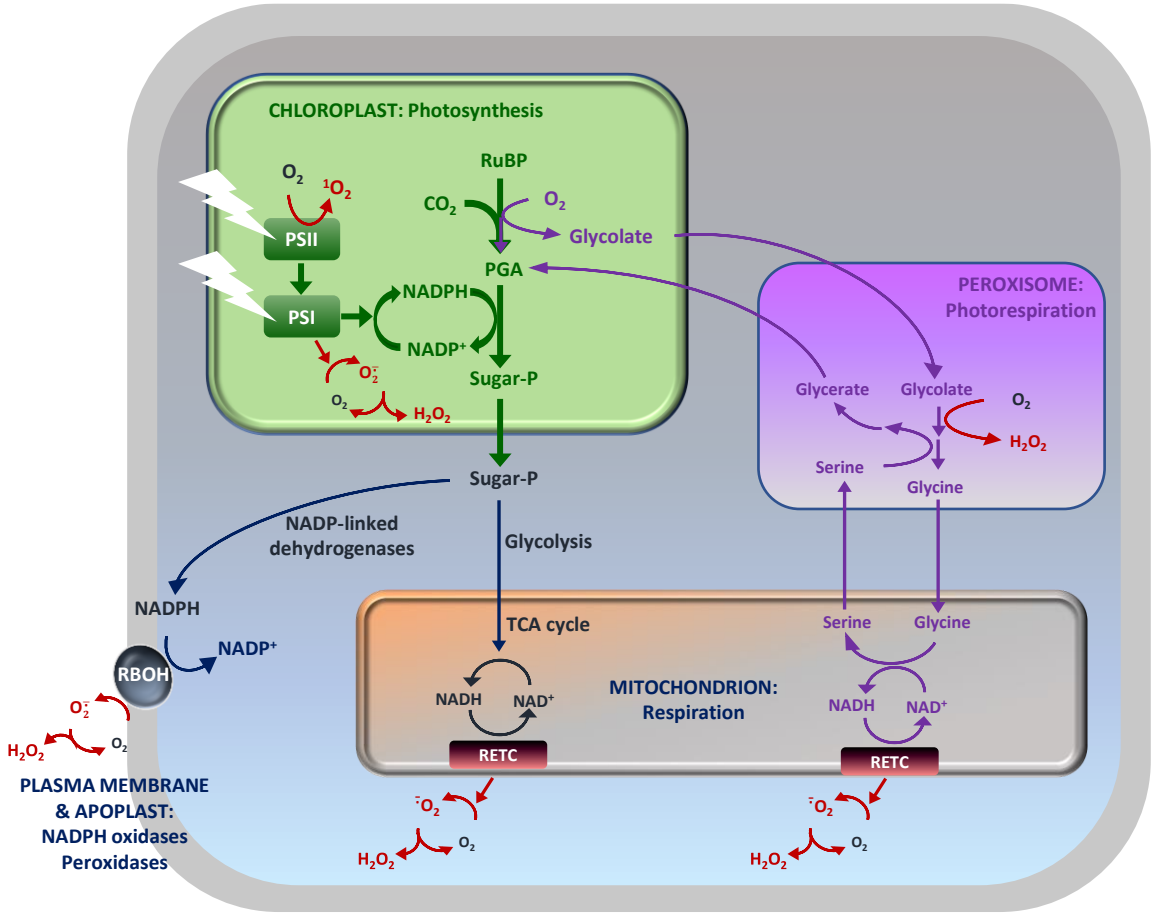

Figure 1.2. The basics of ROS formation in plants. PGA, 3-phosphoglycerate. PSI/II, photosystem I/II. RBOH, respiratory burst oxidase homolog. RETC, respiratory electron transport chain. RuBP, ribulose 1,5-bisphosphate. Sugar-P, sugar phosphate. Figure taken from Noctor et al. (2017).

As well as the chloroplast, the peroxisome is an important site of ROS generation within plant cells, notably through photorespiration-related reactions (Mhamdi et al., 2012). During this pathway, which can be rapid, H_2O_2 is generated by the enzymatic activity of glycolate oxidase which catalyzes the oxidation of glycolate to glyoxylate. In addition, for oilseed plants such as Arabidopsis, fatty acid catabolism is a major source of ROS in peroxisomes during germination. The breakdown of lipid storage by β-oxidation leads to H_2O_2 accumulation as a result of acyl-CoA oxidase activity (Graham and Eastmond, 2002; Nyathi and Baker, 2006). In addition, H_2O_2 can also be formed by other enzyme systems such as xanthine oxidase coupled to SOD (Corpas et al., 2006).

In animals, the mitochondrial electron transport chain is a major site of ROS generation (Liu et al., 2002). Complex I and III are the main sites of ROS production in mitochondria, whereby O_2 is reduced to superoxide anion (Møller, 2001; Jezek and Hlavata, 2005). Subsequently, the superoxide anion is converted to H_2O_2 either by the action of MnSOD or by spontaneous dismutation (Finkel and Holbrook, 2000). Compared to chloroplasts and peroxisomes, the rate of H_2O_2 generation in plant mitochondria is probably lower (Foyer and Noctor, 2003; Halliwell and Gutteridge, 2015). In the light at least, the mitochondria are not regarded as a major source of ROS in leaves, although this obviously does not exclude an important function for these organelles in ROS-related signaling.

The apoplast is a major site of ROS generation. For example, during plant-pathogen interactions, ROS-producing enzymes are thought to be largely responsible for the apoplastic oxidative burst (Qi et al., 2017). This system consists chiefly of NADPH oxidases, cell wall peroxidases and amine oxidases (Petrov and Van Breusegem, 2012; Sierla et al., 2013). NADPH oxidases, also called respiratory burst oxidase homologs (RBOHs), are one of the major ROS-generating enzymes in plants (Umezawa et al., 2010; Mittler et al., 2011). As noted above, they transfer electrons from cytosolic NADPH to apoplastic oxygen, leading to the production of the superoxide anion, which is then converted to H_2O_2 spontaneously or by SOD. Ten NADPH oxidase genes have been identified in Arabidopsis. Among them, AtrbohD and AtrbohF play important roles in the hypersensitive response (HR; Torres et al., 2006; Chaouch et al., 2012; Kadota et al., 2015).

1.1.2.2 Stress and ROS

In optimal physiological conditions, redox homeostasis is maintained and ROS levels are relatively low. However, as sessile organisms, plants often endure environmental challenges that limit growth, reproductive success, yield, quality, or other traits desirable to humans. Collectively, these conditions are defined as stress, and are typically divided into abiotic and biotic stresses. Abiotic stress refers to the negative impact of non-living factors on organisms. Examples are excess salt, heavy metals, heat, chilling, insufficient water or high irradiance. The second is biotic stress that occurs due to damage instigated by other living organisms including bacteria, fungi, viruses, parasites, insects and other

native or cultivated plants. A central theme in many stress responses is the accumulation of ROS and ROS-induced changes in cellular redox state. This condition is commonly known as oxidative stress (Foyer and Noctor, 2000; Dat et al., 2001; Pastori and Foyer, 2002).

Pollution linked to heavy metals that are redox-active may result in superoxide anion formation because of autoxidation, and subsequently lead to H_2O_2 production via Fenton-type reactions (Li and Trush, 1993; Schutzendübel and Polle, 2002). Drought is another abiotic stress condition in which the roles of ROS have received much attention. In drought conditions, stomatal closure is induced, causing a drop in intracellular CO_2 concentrations. This effect tends to favor RuBP oxygenation, thereby increasing glycolate production and accelerating H_2O_2 production in the peroxisomes (Cornic and Briantais, 1991; Noctor et al., 2014). Moreover, drought stress favors electron flux to O_2 and restricts $NADP^+$ regeneration. The rise in NADPH:$NADP^+$ ratio will lead to promotion of the Mehler reaction, and increased photosynthetic control will tend to promote singlet oxygen production. Furthermore, over-reduction of the electron transport chain in chloroplasts and decreased availability of other oxidants for the chain during drought may enhance singlet oxygen, superoxide anion or H_2O_2 production (Asada, 2006; Fischer et al., 2013).

The above paragraph describes examples of how abiotic stress conditions can alter ROS production by their effects on basal metabolism. In addition to such effects, rapid programmed production of ROS, known as “oxidative bursts”, may also occur. Such processes have received particular attention for their importance in responses to biotic stress (Torres et al., 2006). Indeed, the first documented “oxidative burst” in plants was described following infection of potato tubers with the pathogenic oomycete, *Phytophthora infestans* (Doke, 1983). Since then numerous studies have shown that ROS production at the cell wall and apoplast is involved in biotic stress responses. Plasma membrane NADPH oxidases and cell wall peroxidases are thought to be the major sources of ROS production during plant-pathogen interactions, although intracellular redox reactions are also involved. NADPH oxidases, especially RBOHD and RBOHF in Arabidopsis, play a key role in apoplastic ROS generation in immune responses (Torres et al., 2002; Nühse et al., 2007; Zhang et al., 2007). In addition, it has been reported that class III apoplastic peroxidases PRX33 and PRX34 are essential for

ROS production in response to flg22 and elf18 in Arabidopsis (Daudi et al., 2012).

1.1.3 ROS signaling

A long-held view of the biological role of ROS was that they are toxic by-products of plant metabolism through the processes described above (Asada, 1999). According to this view, they would have little or no importance in physiological processes, but rather cause damage to lipids, proteins and DNA in the stressed cells, leading to the notion that resistance to stress could be engineered by enhancing antioxidative capacity or by avoiding the production of ROS (Noctor and Foyer, 1998; Asada, 1999; Maxwell et al., 1999; Mittler, 2002). However, since the beginning of this century, substantial experimental data suggests that ROS are highly controlled signaling molecules. For ROS to be effective as signaling components, living cells have very efficient antioxidant systems to keep them under precise control (Foyer and Noctor, 2005a,b). Secondary messengers activated by ROS can regulate downstream pathways that are physically non-adjacent to the original ROS signaling pathway (Nathan, 2003). All these characteristics render ROS able to set specificity as signaling molecules. ROS function is intimately involved in the activation of gene expression, the induction of specific protein kinases and calcium signatures, the interaction with NADPH oxidases, hormone signal transduction, and the requirement of specific gene modulation for ROS-induced cell death (Figure 1.3; Kovtun et al., 2000; Desikan et al., 2001; Foreman et al., 2003; Kwak et al., 2003; Vandenabeele et al., 2003; Wagner et al., 2004; Vandenbroucke et al., 2008; Sewelam et al., 2016).

1.1.3.1 ROS and photosynthesis

Chloroplasts were one of the very earliest sources of ROS to be described in plants. As described above, ROS production in the thylakoid membrane is notably determined by the balance between light capture and the utilisation of light energy by the photosynthetic electron transport chain, which in turn depends on metabolic consumption of ATP and reductant for its continued operation. Any change or

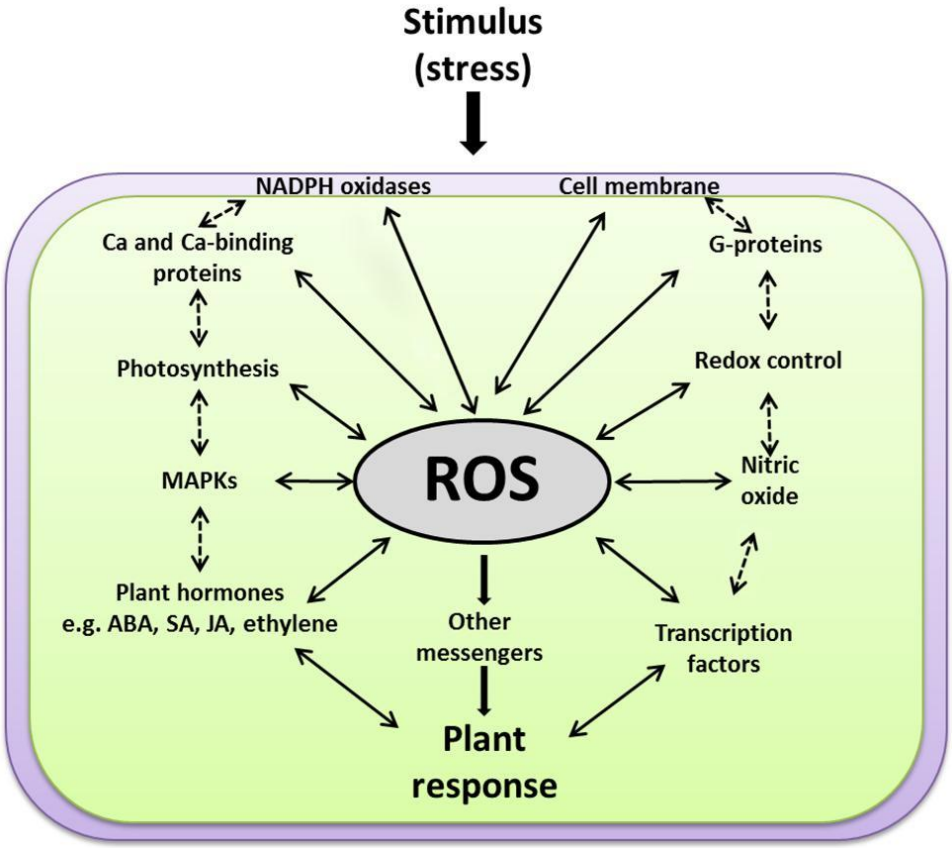

Figure 1.3. A scheme explaining how ROS function at the cross-roads of various key signaling events. ROS work upstream and downstream of the other signaling components, e.g. membranes, NADPH oxidases, G-proteins, calcium, redox homeostasis, photosynthesis, MAPKs, plant hormones [such as salicylic acid (SA), jasmonic acid (JA), abscisic acid (ABA), and ethylene] and transcription factors. Solid arrows for direct ROS interactions with other signaling components, dashed arrows for expected indirect interactions. Figure taken from Sewelam et al. (2016).

imbalance associated with photosynthesis in the chloroplast can affect, directly or indirectly, other functions in plants. It is not surprising that plants have evolved mechanisms to sense photosynthesis-associated ROS accumulation induced by environmental challenges, to enable the ensuing change of redox states in the chloroplast to influence other signaling pathways and lead to appropriate physiological responses (Huner et al., 1996). It has been shown that signal transmission from the chloroplast can change nuclear gene expression, which is proposed to act as a retrograde signaling pathway (Koussevitzky et al., 2007; Pogson et al., 2008; Pfannschmidt et al., 2009; Leister, 2012; Godoy Herz et al., 2014; Sewelam et al., 2016). For example, when pharmacological approaches were used to block carotenoid synthesis and hence increase the ability of ROS production in chloroplasts,

Arabidopsis seedlings suffered severe photo-oxidative damage. Simultaneously, ROS-responsive marker genes were rapidly up-regulated (Kim and Apel, 2013). Another approach used a genetic system of glycolate oxidase overexpression to perturb H_2O_2 levels in chloroplasts. The resulting ROS accumulation induced early signaling responses by regulating gene transcription and secondary signaling messengers, providing further evidence for ROS-dependent retrograde signaling pathways (Sewelam et al., 2014). The redox state of the plastoquinone pool, which plays a key role in electron transport in photosynthesis, was suggested to modulate the expression of cytosolic ascorbate peroxidase (APX) under excess light stress (Karpinski et al., 1997). Other studies also show that ROS signaling from chloroplast is involved in abiotic and biotic stress responses (Fryer et al., 2003; Agrawal et al., 2004; Joo et al., 2005; Belhaj et al., 2009; Zurbriggen et al., 2009; Serrato et al., 2013).

1.1.3.2 ROS and redox homeostasis

Redox regulation is an essential factor to keep energy conversion and consumption in plants under good control. When suffering environmental challenges, ROS perturbation is perceived and transformed into redox signals, followed by responses at various levels of regulation and in different subcellular compartments (Scheibe and Dietz, 2012). The major soluble non-protein redox couples in plants like glutathione, ascorbate, NAD and NADP, are at the hub of the redox network surrounding ROS generation and control. It was reported that photorespiration-derived H_2O_2 led to a photoperiodic effect on redox signaling, in which intracellular glutathione state was perturbed by the accumulation of glutathione disulfide (GSSG; Queval et al., 2007). The changes of intracellular redox state could mediate various signaling events through their interaction with many other secondary messengers such as protein kinase and phosphatases, phytohormones and calcium. Much evidence indicates that ROS-antioxidant interactions act as a metabolic interface between environmental changes and the ensuing signaling responses (Foyer and Noctor, 2005a, 2012), and this is partly accomplished through modifications of redox state (Dietz, 2008). The plant antioxidative systems that promote redox homeostasis in the face of constant ROS production are discussed further in Section 1.2.

1.1.3.3 ROS and Mitogen-activated protein kinase (MAPK)

MAPK signaling pathways have been well accepted as a general signal transduction mechanism in eukaryotes. These pathways consist of three functionally linked protein kinases: MAPK, MAPK kinase (MAPKK) and MAPK kinase kinase (MAPKKK). By protein phosphorylation cascades from MAPKKK to MAPK, this system links different receptors to their cellular and nuclear targets (Tena et al., 2001). MAPK signaling cascades in Arabidopsis are complex, involving multiple isoforms of each MAPK gene and more than 20 pathways (Wrzaczek and Hirt, 2001; Ichimura et al., 2002).

Many environmental constraints were found to stimulate MAPK cascades, like cold, heat, drought, wounding, and pathogens, while these cascades are also involved in phytohormone signaling (Bowler and Fluhr, 2000). In plants and eukaryotes in general, it has been demonstrated that the transmission of oxidative signals is controlled by protein phosphorylation involving MAPKs (Kyriakis and Avruch, 1996; Gustin et al., 1998; Pitzschke and Hirt, 2006; Xing et al., 2008). It was reported that H_2O_2 initiated MAPK signaling by activating ANP1, an isoform of MAPKKK. This effect led to the phosphorylation of MPK3 and MPK6 (Kovtun et al., 2000). Oxidative signal inducible 1 (OXI1), a protein kinase, is also involved in the activation of MPK3 and MPK6. Infection by virulent fungal pathogens caused HR in *oxi1* null mutant, concomitantly the activation of MPK3 and MPK6 by oxidative stress was compromised (Rentel et al., 2004). Protein phosphorylation was also demonstrated to trigger Ca^{2+}-dependent ROS production, which was mediated by NADPH oxidases in Arabidopsis. This study also suggested the existence of a positive feedback regulation of Ca^{2+} and ROS (Kimura et al., 2012).

1.1.3.4 ROS and phytohormones

Plant stress responses are highly integrated with hormone signaling to regulate biological processes. Salicylic acid (SA) signaling is associated with resistance to biotrophic pathogens as well as abiotic stress (Vlot et al., 2009). Intracellular and extracellular ROS accumulation can induce SA production, pathogenesis-related (PR) gene expression, and cell death (Chamnongpol et al., 1998; Torres et al.,

2005; Chaouch et al., 2010). All these effects can be reverted in the *cat2* mutant by blocking SA synthesis, showing that H_2O_2-triggered cell death and related responses are not a direct consequence of damage (Chaouch et al., 2010). Intriguingly, the defence responses triggered by increased peroxisomal availability of H_2O_2 in *cat2* occur in a photoperiod-dependent manner: the PR responses such as lesions and SA accumulation appear when plants are grown in long days (LD) but not short days (SD) (Queval et al., 2007; Chaouch et al., 2010). ROS-induced SA accumulation can have several effects, notably including enhanced resistance to pathogens through the induction of PR proteins and phytoalexins. In addition, it can also promote stomatal closure, which may also contribute to defence against pathogens that enter plants by this route (Khokon et al., 2011). The application of SA can also induce ROS production via a peroxidase-catalyzed reaction, which also favors stomatal closure (Melotto et al., 2006; Miura et al., 2013).

Unlike SA, JA and the related compound methyl jasmonate (MeJA) are involved in the response to necrotrophic pathogens and wounding (Devoto and Turner, 2005). Accumulating evidence reveals a strong relationship between ROS and JA signaling. For instance, ROS derived from NADPH oxidases are critical for JA-induced gene expression regulated by MYC2, a transcription factor involved in JA-mediated response (Maruta et al., 2011). It was revealed that JA signaling in response to intracellular oxidative stress requires an accompanying accumulation of glutathione (Han et al., 2013b). A complex relationship between SA and JA in physiological processes has been elucidated. Many studies show the opposite effect between JA signaling and SA-dependent pathways (Dangl and Jones, 2001; Spoel et al., 2003; Takahashi et al., 2004; Koorneef et al., 2008). However, the two pathways may interact positively and can also be induced together. For example, it was demonstrated that increased H_2O_2 levels in *cat2* induced both SA and JA signaling pathways, and that both pathways are less induced when glutathione accumulation is genetically blocked by the *cad2* mutation (Han et al., 2013b). These observations point to some glutathione-dependent signaling process in the link between H_2O_2 and induction of phytohormone pathways, an issue that will receive attention in Chapters 4 and 5 of this thesis.

As well as SA and JA, other phytohormones are also involved in stress responses. ABA is known to be

induced together with ROS production in different environmental stress responses. It has been reported that ABA-induced stomatal closure during stress is mediated by ROS which is derived from NADPH oxidases (Kwak et al., 2003). Besides, ABA is found to be required for H_2O_2 production in chloroplasts, mitochondria and peroxisomes under water stress (Hu et al., 2006). Moreover, ABA has been considered to play a negative role in biotic stress signaling orchestrated by SA, JA and ethylene (Coego et al., 2005). Ethylene is well documented to be a key player in programmed cell death during senescence, ozone stress or pathogen infection (Orzaez and Granell, 1997; Lund et al., 1998; Overmyer et al., 2000). Gibberellins (GA), a cyclic diterpene compound with multiple functions in the plant life cycle, are linked with ROS through DELLA proteins which modulate transcript levels of antioxidant enzymes (Achard et al., 2008).

1.1.3.5 Other components involved in ROS signaling

In addition to the aspects mentioned above, there are also some other second messengers such as GTP-binding proteins (G proteins) and Ca^{2+} which mediate the ROS signals. The role of G proteins in stress responses, especially in plant-pathogen interactions, has been extensively reported (Assmann, 2005; Trusov et al., 2009; Maruta et al., 2015). It was revealed that under ozone stress, the first biphasic oxidative burst is greatly attenuated or absent in mutants lacking Gα protein or Gβ protein (Joo et al., 2005). AtRbohD and AtRbohF were suggested to receive initial signals from G proteins to mediate ozone responses in guard cells (Suharsono et al., 2002). Calcium signaling is involved in many signal transduction pathways. Elevations in cytosolic Ca^{2+} represent an early response to many different biotic and abiotic stresses (McAinsh and Pittman, 2009; Dodd et al., 2010). ABA and H_2O_2 treatments are among those that can increase cytosolic Ca^{2+} concentrations. Moreover, Ca^{2+} has been reported to work both upstream and downstream of ROS production in signaling pathways (Bowler and Fluhr, 2000; Abuharbeid et al., 2004; Monshausen et al., 2009; Sewelam et al., 2013).

1.2 ROS processing

The above discussion underlines the close integration of ROS-dependent redox signaling in numerous physiological processes, while also revealing that our knowledge of the details of redox signaling remains incomplete. Although many downstream responses to ROS have been described, the key redox events that lie at the heart of ROS-triggered signaling remain to be elucidated. A key player in enabling and regulating ROS signals is the plant antioxidative system. This system is complex and includes efficient enzymatic and non-enzymatic mechanisms that have been developed during evolution. Enzymatic systems consist of CAT, APX, SOD, various types of peroxiredoxins (PRX), glutathione/thioredoxin peroxidases (GPX) and glutathione S-transferases (GST). Non-enzymatic components include glutathione and ascorbate, which can be considered major components of a redox hub, but also tocopherol, carotenoids and phenolic compounds. Through the network of these mechanisms, plants regulate ROS accumulation and maintain redox homeostasis (Figure 1.4； Noctor et al., 2017).

1.2.1 Catalase

CAT was the first discovered antioxidative enzyme. All known CAT forms in eukaryotes are haem-dependent. Among them two main types have been characterized, which are monofunctional CATs (also known as typical CATs) and bifunctional CAT-peroxidases (Zamocky et al., 2008). They can be distinguished by the affinity for H_2O_2 and the sensitivity to the inhibitor 3-amino-1,2,4-triazole (3-AT) (Margoliash and Novogrodsky, 1960; Regelsberger et al., 2002). Unlike monofunctional CATs, which exist in diverse organisms, the CAT-peroxidases are only found in some fungi and prokaryotes (Mutsuda et al., 1996; Regelsberger et al., 2002).

The typical CAT reaction is the dismutation of H_2O_2. The reaction is initiated by splitting the O-O bond of H_2O_2 to produce a molecule of H_2O, as well as an oxy-ferryl enzyme intermediate (compound I) and a porphyrin cation radical. Then a second H_2O_2 is oxidized to O_2. Simultaneously, compound I is reduced back to the initial state by releasing the bound O which is involved in the formation of the second molecule of water (Regelsberger et al., 2001; Alfonso-Prieto et al., 2009). Intriguingly,

monofunctional CATs can also catalyze some H_2O_2-dependent peroxidation of reducing substrates, making the functional division between the two types of CAT indistinct. During this process, the reduction of compound I is performed by the interaction with small compounds like ethanol instead of the second H_2O_2 (Zamocky et al., 2008). CAT-associated peroxidation has been reported in both mammalian and plants (Havir and McHale, 1989; Kirkman and Gaetani, 2007), but its physiological significance remains as yet unclear.

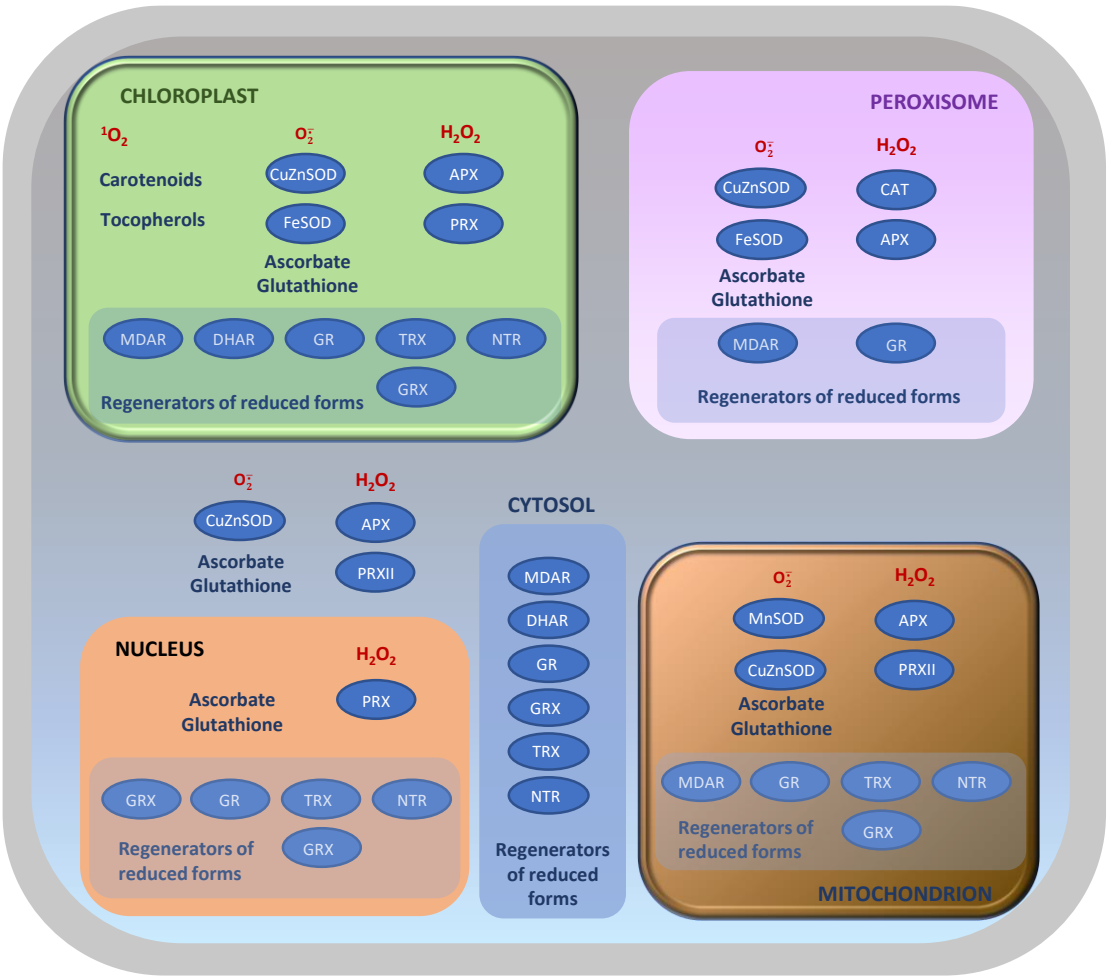

Figure 1.4. Plant antioxidative systems and their localization within the cell. APX, ascorbate peroxidase. CAT, catalase. DHAR, dehydroascorbate reductase. GR, glutathione reductase. GRX, glutaredoxin. MDHAR, monodehydroascorbate reductase. NTR, NADPH-thioredoxin reductase. PRX, peroxiredoxin. SOD, superoxide dismutase. TRX, thioredoxin. Figure taken from Noctor et al. (2017).

CATs are notably distinguished from other H_2O_2-metabolizing enzymes based on two factors. Firstly, when functioning as a dismutase, CAT function does not require reductant other than H_2O_2. Secondly,

CAT has high specificity for H_2O_2. So far three CAT genes have been identified in angiosperm species such as Arabidopsis, rice, tobacco, maize and pumpkin (Willekens et al., 1995; Frugoli et al., 1996; Guan and Scandalios, 1996; Esaka et al., 1997; Iwamoto et al., 2000). In Arabidopsis, *CAT1* and *CAT3* are located contiguously on chromosome 1 while *CAT2* is located on chromosome 4 (Frugoli et al., 1996). According to the classification system based on tobacco genes and first proposed by Willekens et al. (1995), Class I CATs are mainly expressed in photosynthetic tissues, Class II CATs are associated with vascular tissues, while Class III CATs are notably expressed in seeds and reproductive tissues. For Arabidopsis, *CAT1*, *CAT2* and *CAT3* correspond to Class III, Class I and Class II, respectively (Table 1.1). The *CAT1* gene is mainly expressed in pollens and seeds and at very low levels in leaves, *CAT2* is expressed in photosynthetic tissues but also in roots and seeds, while *CAT3* is associated with vascular tissues. It has been reported that compared to *CAT1*, the transcript levels of *CAT2* and *CAT3* are much higher in mature Arabidopsis rosettes (Frugoli et al., 1996; McClung, 1997). In addition, *CAT2* transcripts show a day-night rhythm with a peak expression at the night/day transition, which is opposite to that of *CAT3* (Zhong et al., 1994; Mhamdi et al., 2010a). Studies on subcellular localization showed that CATs exist mainly in peroxisomes in plants. Evidence supporting this conclusion includes the high CAT activity in peroxisomes and the identification of an import mechanism due to a Peroxisomal Targeting Sequence 1 (PTS1) pathway (Mullen et al., 1997).

Table 1.1. Probable classification of the three CATs found in different plant species (taken from Mhamdi et al., 2010a)

	Class I	Class II	Class III
Tobacco	Cat1	Cat2	Cat3
Arabidopsis	CAT2	CAT3	CAT1
Maize	Cat2	Cat3	Cat1
Pumpkin	cat2	cat3	cat1
Rice	CatC	CatA	CatB

Previous studies on gene-specific T-DNA insertion mutants showed that *CAT2* encodes the major leaf CAT isoform and this enzyme makes the major contribution to leaf CAT activity (Queval et al., 2007; Mhamdi et al., 2010a). In *cat2* knock-out mutants, the CAT activity in rosettes is decreased by around

90% compared with that in wild type, and root CAT activity is also attenuated, though less severely (Bueso et al., 2007). In *cat3*, there is around 20% activity lost. In contrast, the effect of the *cat1* mutation on leaf CAT activity is negligible. This is consistent with its relatively low transcript levels in leaves. To date, therefore, it seems that CAT2 and CAT3 may play the major roles in Arabidopsis rosette tissue. However, the relative contribution of these CAT isoforms changes according to the developmental stage of the plants (Zimmermann et al., 2006). For instance, as a senescence-associated gene, *CAT3* transcripts increase with leaf age.

Because of the close association with photorespiration, Arabidopsis *CAT2*-deficient mutants (*cat2*) have been extensively used in various studies of plant development and physiology. Under conditions where photorespiratory H_2O_2 production is highly active, CAT function deficiency leads to increased availability of endogenous H_2O_2, with effects on cell redox state. The intracellular H_2O_2 signal can be modulated by changing photorespiration-related growth conditions, such as CO_2 concentration and irradiance (Queval et al., 2007). When grown in air (400 μL CO_2 L^{-1}) with a moderate irradiance of 200 μmol m^{-2} s^{-1} at the surface of leaves, *cat2* shows a dwarf phenotype accompanied by redox perturbation, evidenced by the decreases in the GSH:GSSG ratio and increases in total glutathione. By contrast, it has a wild-type phenotype when grown in high CO_2 (hCO_2; 3000 μL L^{-1}) or if the irradiance is lower than 50 μmol m^{-2} s^{-1}, both conditions in which photorespiration is rather inactive.

Among the most obvious phenotypes of *cat2* grown in air at moderate light intensity are necrotic lesions. This phenotype is photoperiod-dependent. When grown in a 16 h photoperiod (LD), *cat2* shows spreading necrotic lesions. By contrast, no lesions are observed in plants grown in an 8 h photoperiod (SD), even though the dwarf phenotype and redox perturbation are as marked as in LD (Queval et al., 2007, 2009). The lesion appearance in *cat2* bears a striking resemblance to the HR, and includes SA accumulation, *PR* genes induction (e.g. *PR1* and *PR2*), activation of camalexin and its synthesis pathway, and induced resistance to bacterial challenge. As well as necrotic lesions, all these effects are absent in SD. By the combination of pharmacological and genetic approaches, it is revealed that exogenous SA treatment could induce these responses in SD and revert it in LD when SA synthesis is genetically blocked. All these observations show that SA is involved in the peroxisomal

H_2O_2-triggered HR-like lesion formation in *cat2* grown in LD air condition (Chaouch et al., 2010).

Because of their influence on cell redox state, peroxisomal CATs act as regulators to fine-tune redox signaling, which is also a function of the carbon flux through photorespiration. This makes *cat2* mutants an interesting model system to investigate the possible relationship between photorespiration and other metabolic, transcriptional and physiological processes, especially those possessing a redox component. Reductive pathways for H_2O_2 processing appear to compensate quite rapidly when CAT is deficient. Even though glutathione redox status is perturbed within hours after the onset of photorespiratory H_2O_2 production in *cat2*, little or no change is found in the redox states of glutathione-associated redox compounds, like ascorbate/dehydroascorbate or NADPH/$NADP^+$ (Queval et al., 2007; Mhamdi et al., 2010b,c). Glutathione status appears to play an active part in the H_2O_2-triggered signal transduction provoked by CAT deficiency. For example, the *GR* knockout line *gr1*, which shows qualitatively similar changes in glutathione to those observed in *cat2*, has a wild-type phenotype, but nevertheless shows gene expression patterns that partly recapitulate those observed in *cat2*. Further, when the *gr1* mutation is introduced into the *cat2* background, H_2O_2-associated transcript profiles are significantly affected, suggesting that glutathione plays a role in transmitting H_2O_2-induced signals (Mhamdi et al., 2010b). Further evidence for this conclusion was obtained by analysis of *cat2* lines in which glutathione accumulation was genetically impaired (Han et al., 2013a,b).

Extensive evidence reveals that phytohormones are important in determining *cat2* phenotypes. Transcriptome analysis of *cat2* roots points to the modulation of ethylene and auxin signaling (Bueso et al., 2007). Another study showed that the decreased CAT activity in *cat2* induced effects on ABA signaling (Jannat et al., 2011). Glutathione was shown to be a key player in linking H_2O_2 to SA signaling (Han et al., 2013a). It was also reported that CAT2 participates in SA-mediated repression of auxin accumulation and JA biosynthesis during pathogen infection (Yuan et al., 2017). Another study reported that CAT2 and APX1 work in a coordinated way during the nuclear DNA damage response (DDR). Compared with the *cat2* single mutant, the *apx1 cat2* double mutant is more tolerant to oxidative stress imposed by high light, heat and paraquat application, and genome-wide

transcriptome analysis shows an activation of typical DDR hallmarks (Vanderauwera et al., 2011).

1.2.2 Ascorbate and glutathione in ROS metabolism

Many compounds function as effective antioxidants in cells by regulating ROS accumulation. Among the best studied players are the cellular redox buffers, ascorbate and glutathione. They are well accepted to be key in controlling concentrations of ROS, although both metabolites are involved in multiple physiological processes (Cobbett et al., 1998; Vernoux et al., 2000; Dowdle et al., 2007). Ascorbate and glutathione are distinguished from most other antioxidant small molecules by (1) specific enzyme systems (peroxidases) that couple them to H_2O_2 metabolism; (2) the relative stability of their oxidized forms; (3) recycling of oxidized forms to reduced compounds by high-capacity reductases and associated systems that depend on the key electron carrier, NAD(P)H. Based on these features, ascorbate and glutathione can effectively regulate cellular redox state by repeated redox cycling (Foyer and Noctor, 2011). The pools of these two metabolites are generally highly reduced (over 95%) within the cytosol, chloroplasts and mitochondria, while the oxidized forms accumulate in compartments lacking efficient redox-recycling mechanisms like the vacuole and the apoplast (Schwarzländer et al., 2008; Queval et al., 2011; Noctor et al., 2016).

1.2.2.1 Glutathione in plants

Glutathione (γ-glutamylcysteinylglycine) is the principal low-molecular-weight thiol in most cells. It is an essential metabolite with multiple functions in plant development, biosynthetic pathways, detoxification, antioxidant biochemistry, and redox homeostasis. The fundamental function of glutathione is in thiol-disulfide interactions, in which the interconversion of reduced glutathione (GSH) and GSSG allows an appropriate cell redox state to be achieved. The concentration of cellular glutathione is high, as is its reduction state in the absence of stress. Under optimal physiological conditions the average ratio of GSH:GSSG in tissues such as leaves is at least 20:1 (Mhamdi et al., 2010a; Han et al., 2013a). However, this value may be higher (e.g. cytosol) or lower (e.g. vacuole) in specific subcellular compartments (Meyer et al., 2007; Queval et al., 2011).

In plants glutathione is synthesized by two ATP-dependent steps which rely on the activity of γ-EC synthetase (γ-ECS) and glutathione synthetase (GSH-S) (Rennenberg, 1980; Meister, 1988; Noctor et al., 2002; Mullineaux and Rausch, 2005). Each synthetic enzyme is encoded by a single gene (May and Leaver, 1994; Ullman et al., 1996), and both are indispensable to plant growth and development. Knocking out *GSH1*, the gene encoding γ-ECS, leads to lethality at the embryo stage (Cairns et al., 2006) while knocking out *GSH2*, the gene encoding GSH-S, causes a seedling-lethal phenotype (Pasternak et al., 2008). In Arabidopsis γ-ECS is located in plastids (Wachter et al., 2005), while GSH-S is found in both chloroplasts and cytosol, with the latter compartment considered to contain the major form of GSH-S because of the higher abundance of the corresponding transcript (Wachter et al., 2005). Glutathione synthesis, which responds to factors such as oxidative stress or heavy metals, can be modulated by regulating γ-ECS expression and activity, or by changing cysteine availability (Strohm et al., 1995; Noctor et al., 1998; Creissen et al., 1999; Harms et al., 2000; Noji and Saito, 2002; Wirtz and Hell, 2007). Both *GSH1* and *GSH2* transcripts respond to phytohormone and heavy metals (Xiang and Oliver, 1998; Sung et al., 2009), as well as to light, drought and pathogens.

While glutathione synthesis is stress-responsive, degradation is also important to achieve appropriate levels. In Arabidopsis there are four different types of enzyme which have been implicated in glutathione degradation. These are phytochelatin synthase (PCS), γ-glutamyl transpeptidase (GGT), γ-glutamyl cyclotransferase (GGC), and 5-oxoprolinase (5-OPase). Most attention has thus far focused on GGT, which is considered to degrade mainly GSSG located in the vacuole or the apoplast (Masi et al., 2007; Ferretti et al., 2009; Ohkama-Ohtsu et al., 2011; Su et al., 2011).

1.2.2.2 Ascorbate in plants

Ascorbate, also known as vitamin C, is a highly abundant metabolite and a water-soluble antioxidant in both animals and plants. It occurs in a reduced form (ascorbic acid) and two oxidized forms, which are the immediate product of one-electron oxidation (monodehydroascorbate, or MDHA) and dehydroascorbate (DHA), which has lost two electrons compared to ascorbate and is largely the result of MDHA dismutation. Homeostasis between reduced and oxidized ascorbate is essential for plants to

cope with environmental stress. Ascorbate is found in different subcellular compartments like chloroplasts, mitochondria, peroxisomes, and vacuoles (Jiménez et al., 1997, 1998; Noctor et al., 2002; Takahama, 2004; Zechmann, 2011). It has been well documented that ascorbate can be synthesized through the L-galactose (L-Gal) pathway starting from glucose (Linster and Clarke, 2008; Wheeler et al., 1998, 2015; Bulley and Laing, 2016). It was shown that *vtc1* and *vtc2* mutants, deficient in the enzymes associated with this pathway, contain only 25-30% and 10-20% of wild type ascorbate levels, respectively. Furthermore, the loss of ascorbate biosynthetic capacity in the *vtc2 vtc5* mutant cannot be compensated by other identified ascorbate biosynthetic pathways (Dowdle et al., 2007). Hence, the L-Gal pathway is suggested to be the primary pathway that generates ascorbate in most plant organs. Nevertheless, alternative ascorbate biosynthetic pathways through galacturonate and glucuronate have also been proposed (Li et al., 2010). Ascorbate has been considered of great importance in plants with key functions in growth development, metabolism and stress responses (Noctor and Foyer, 1998; Smirnoff, 2000; Pastori et al., 2003; Anjum et al., 2014). The finding that near-total ascorbate depletion in the *vtc2 vtc5* mutant is associated with seedling lethality (Dowdle et al., 2007) suggests that, like glutathione, ascorbate is an indispensable player during at least some stages of plant development.

1.2.2.3 Ascorbate-glutathione pathway

While ascorbate and glutathione can react chemically with ROS, and also have other functions as enzyme co-factors and in defense, their roles in the ascorbate-glutathione pathway continue to be a major research focus. The pathway is involved in ROS metabolism in plant cells by removal of H_2O_2 (Figure 1.5； Foyer and Noctor, 2009). Like CATs, APX has high specificity for H_2O_2. APX can reduce H_2O_2 to water by consuming two molecules of ascorbate, which leads to the generation of two molecules of MDHA. This primary oxidation product can be converted back to ascorbate by MDHA reductase (MDHAR) in an NAD(P)H-dependent reaction. If not reduced rapidly, MDHA will disproportionate to ascorbate and DHA because of its characteristic as a short-lived radical. GSH can reduce DHA to regenerate ascorbate, a reaction catalyzed by DHA reductases (DHAR), accompanied by the production of GSSG. In addition to MDHAR and DHAR, non-enzymatic routes for ascorbate

regeneration exist, including the reduction of DHA by GSH or of MDHA by chloroplast ferredoxin (Polle, 2001; Smirnoff, 2011; Gest et al., 2013; Johnston et al., 2015; Noctor, 2015). Consumption of GSH in this pathways leads to GSSG, which can be reduced back to GSH by the action of glutathione reductase (GR). This reaction needs electrons provided by NADPH. During this sequence of reactions, ascorbate and glutathione are not consumed: instead they are involved in a cyclic transfer of reducing equivalents by the action of four enzymes, which permits the reduction of H_2O_2 to H_2O using electrons derived from NAD(P)H (Foyer and Halliwell, 1976; Noctor and Foyer, 1998; Foyer and Noctor, 2009).

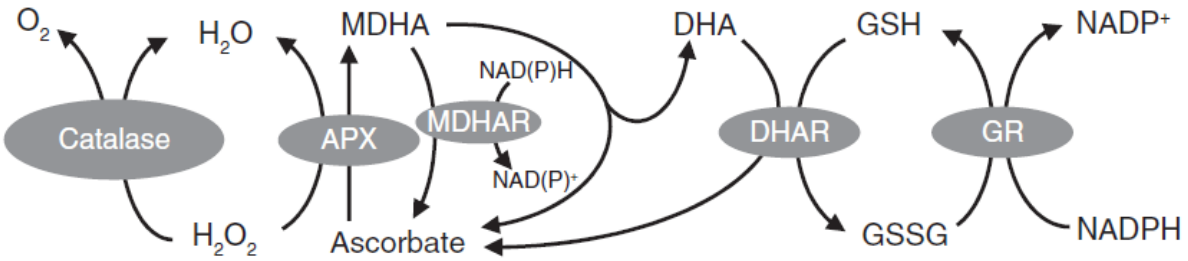

Figure 1.5. Two of the major pathways for H_2O_2 metabolism in plants. APX, ascorbate peroxidase; MDHA, monodehydroascorbate; MDHAR, monodehydroascorbate reductase; DHA, dehydroascorbate; DHAR, dehydroascorbate reductase; GSH, reduced glutathione; GSSG, glutathione disulfide; GR, glutathione reductase. Figure taken from Foyer and Noctor (2009).

Both ascorbate and glutathione are abundant and stable antioxidants which may be maintained at thermodynamic equilibrium with each other under optimal conditions. Within the highly reducing intracellular context, ROS accumulation can lead to the transient or sustained adjustment of this system, and such adjustments can be sensed by signaling pathways, leading to downstream responses. For glutathione, there is a close correlation between its status and the expected intracellular ROS availability. For example, it has been extensively reported that pharmacologically or genetically blocking CAT activities causes glutathione to become both more oxidized and more abundant (Smith et al., 1985; May and Leaver 1993., Willekens et al., 1997; Queval et al., 2009; Mhamdi et al., 2010a). Work going back over two decades has pointed to novel outcomes of modulating parts of the ascorbate-glutathione pathway, suggesting that the pathway does not function simply as an

antioxidative system but may also act in redox signaling. For example, cytosolic DHARs are involved in the regulation of glutathione status triggered when H_2O_2 metabolism shifts from CAT to reductive pathways. Genetically blocking these enzymes weakens, rather than reinforces, cell death and defense responses induced by CAT deficiency (Rahantaniaina et al., 2017). Another report showed that MDHAR can act as a pro-oxidant rather than an antioxidant by conferring sensitivity to soil-borne pollutant 2,4,6-trinitrotoluene (TNT) on Arabidopsis (Johnston et al., 2015; Noctor, 2015).

One current view is that perturbation of the status of the ascorbate-glutathione pathway may be important in signaling, i.e., the pathway has a dual antioxidant-signaling role in which some downstream responses are triggered by increased H_2O_2 metabolism through the pathway, rather or in addition to increased H_2O_2 concentrations (Foyer and Noctor, 2016). In such a scenario, glutathione status seems likely to be an influential player, based on possible interactions with protein thiol-disulfide groups. In contrast to glutathione, the ratio of ascorbate to DHA is less likely to be involved in the transmission of ROS signals. Instead, ascorbate limits the lifetime of ROS signals by scavenging ROS chemically and enzymatically. Ascorbate contents are sensitive to factors such as irradiance (Gatzek et al., 2002; Smirnoff et al., 2011), and this response may be partly related to functions in tocopherol regeneration and xanthophyll cycle.

1.2.2.4 Other pathways of ROS processing

In addition to CATs and the ascorbate-glutathione pathway, plants also contain other antioxidative systems to cope with H_2O_2 accumulation. Among them, PRX has been well documented to function in maintaining appropriate H_2O_2 levels, at least in chloroplasts (Awad et al., 2015). PRX is a thiol-dependent peroxidase existing in almost all organisms. Depending on the isoform, PRX regeneration from the oxidized form to the reduced state can be accomplished by glutaredoxin (GRX), thioredoxin (TRX), NADPH-thioredoxin reductase (NTR), glutathione or ascorbate (Dietz, 2003; Rouhier and Jacquot, 2005; Meyer, 2008; Pérez and Cejudo, 2009; Liebthal et al., 2018). GPX is also able to remove H_2O_2 but these enzymes are likely to function with TRX instead of GSH (Herbette et al., 2002; Iqbal et al., 2006). GST could also play a role as GSH-dependent peroxidases to remove H_2O_2 (Dixon

et al., 2009), although their exact importance in this respect is still not clear.

All the enzymes discussed above are found in the aqueous cell phases. Within the membrane phase, carotenoids and tocopherols are well known as important compounds to control the accumulation of ROS and derived molecules. Carotenoids can act either to avoid ROS production (e.g. by quenching excited Chl states) or react with existing ROS by quenching singlet oxygen (Fischer et al., 2013). Most evidence available so far suggests that the functions of tocopherols (vitamin E) are more essential in seeds than in leaves. Tocopherol-deficient mutants of Arabidopsis show clear effects associated with enhanced lipid peroxidation and the activation of defense pathways during germination (Sattler et al., 2006).

1.2.2.5 NADPH-linked reaction in plants

NADPH is a key redox carrier in the aqueous phase of many cells and plays a crucial role in physiological processes like cell growth, proliferation, detoxification, redox homeostasis and biosynthesis. It is the reductant required for sugar-phosphate production in the photosynthetic Calvin-Benson cycle and is also required for other key anabolic pathways such as lipid and amino acid synthesis. Alongside its roles in biosynthetic pathways, NADPH functions in defence reactions and the regulation of cellular redox status. For example, in the ascorbate-glutathione pathway, NADPH is required for the reactions catalyzed by GR and MDHAR (Figure 1.5; Noctor, 2006) while TRX needs NADPH to protect against oxidative damage (Nordman et al., 2003). The functions of NADPH are not limited to providing electrons for biosynthetic reactions and antioxidative enzymes. Indeed, NADPH may have a pro-oxidant function, for example, in providing reductant for plasma membrane NADPH oxidase that produce suyperoxide and, subsequently, H_2O_2 (Foreman et al., 2003; Torres et al., 2006). NADPH is also a cofactor for the generation of nitric oxide (NO) from arginine, catalyzed by animal-type NO synthases (Corpas et al., 2009), although the existence of such enzymes in plants is controversial.

The regeneration of NADPH in plants is accomplished by several systems. The primary source in the

chloroplast is ferredoxin-NADP reductase (FNR). This enzyme mediates electron transfer from ferredoxin to $NADP^+$ in a light-dependent manner (Arakaki et al., 1997). Another source of NADPH is via glucose-6-phosphate dehydrogenase (G6PDH) and 6-phosphogluconate dehydrogenase (6PGDH), both of which work in the oxidative pentose phosphate pathway (OPPP). Other NADPH-producing dehydrogenases include isocitrate dehydrogenase (ICDH), nonphosphorylating glyceraldehyde-3-phosphate dehydrogenase (npGAPDH) and malic enzyme (ME). Moreover, NADH kinase (NADHK) may also contribute to the production of NADPH (Figure 1.6; Foyer and Noctor, 2009). While the primary function of FNR is considered to be in photosynthesis, the physiological roles of other NADPH-generating enzymes remain unclear. The following sections present a concise overview of some of these NADPH-producing systems in plants.

1.2.2.5.1 Glucose-6-phosphate dehydrogenase

G6PDH is the first and rate-limiting enzyme in the OPPP，which is a source of NADPH in non-photosynthetic tissues as well as in leaves in the dark (Emes and Neuhaus, 1997; Thom et al., 1998). It catalyzes the oxidation of glucose-6-phosphate to 6-phosphogluconolactone accompanied by the conversion of $NADP^+$ to NADPH. The NADPH thus produced can subsequently be used for the various NADPH-requiring reactions discussed above. Many studies have shown that G6PDH is associated with various environmental stress responses. G6PDH activity can be stimulated by exogenous application of H_2O_2 and NaCl, as well as drought and pathogen attack (Wang et al., 2008; Scharte et al., 2009; Li et al., 2011; Dal Santo et al., 2012; Corpas and Barroso, 2014). It has been reported that drought stress activated the expression of G6PDH as well as its activity (Liu et al., 2013), and overexpression of G6PDH-encoding genes could enhance the resistance to drought stress (Scharte et al., 2009). Although many of the studies have been correlative in nature, attention has focused on relationship between G6PDH and the ascorbate-glutathione pathway (Wang et al., 2008).

In plants, 6 *G6PD* genes have been identified. They encode four plastidic isoforms (G6PD1-4) and two cytosolic isoforms (G6PD5 and G6PD6). Moreover, the plastidic isoforms are separated into classes

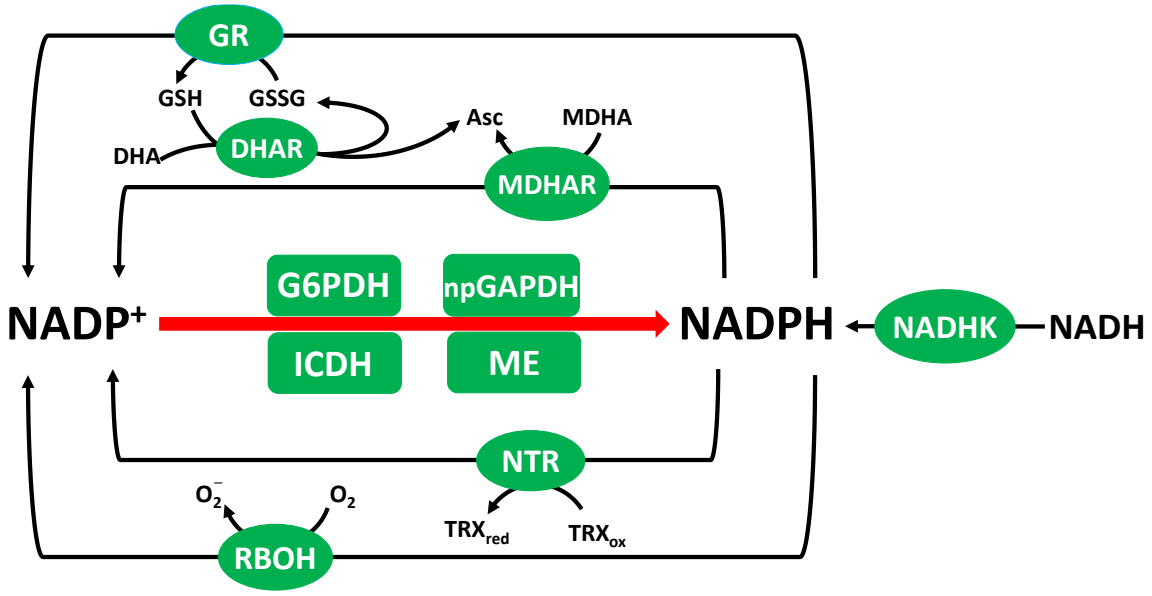

Figure 1.6. Some NADPH-producing and consuming reactions in the cytosol. G6PDH, glucose-6-phosphate dehydrogenase; npGAPDH, nonphosphorylating glyceraldehyde-3-phosphate dehydrogenase; ICDH, isocitrate dehydrogenase; ME, malic enzyme; NADHK, NADH kinase; NTR, NADPH-thioredoxin reductase; RBOH, respiratory burst oxidative homolog; TRXox/TRXred, oxidized/reduced thioredoxin. Figure taken from Foyer and Noctor (2009).

P1 and P2, which can be distinguished by specific antibodies, regulatory mechanisms, and expression patterns (Wendt et al., 1999; Wakao and Benning, 2005). In Arabidopsis G6PD1 and G6PD2 may play the major roles in the plastid because T-DNA insertions in the *G6PD3* gene do not affect the activity in zymograms and G6PD4 activity and mRNA abundance are very low. In terms of cytosolic isoforms, G6PD5 is highly expressed in leaves but at lower levels in other tissues. By contrast, G6PD6 is extensively expressed in all tissues. As well as expression, kinetic characteristics may determine the influence of each isoform. For instance, the K_M $NADP^+$ of G6PD6 is considerably higher than that of G6PD5 (Wakao and Benning, 2005). Seeds of a *g6pd5 g6pd6* double mutant showed higher oil content and weight compared to the wild type, suggesting that deficiency of cytosolic G6PDH may modulate the metabolism of developing seeds (Wakao et al., 2008). Moreover, cytosolic G6PDH-produced NADPH has been described as a factor that influences tobacco responses to pathogen attack, an effect the authors explained in terms of reductant for NADPH oxidases (Scharte et al., 2009). It has also been reported that the activity of G6PDH can be stimulated by glycogen synthase kinase 3 (GSK3) during salt stress, leading to the alteration of redox status and favoring ROS metabolism in stress conditions

(Dal Santo et al., 2012).

1.2.2.5.2 Isocitrate dehydrogenase

ICDHs mediate the oxidative decarboxylation of isocitrate to 2-oxoglutarate (2-OG), accompanied by the production of NADPH and CO_2. As a carbon skeleton, 2-OG is required for ammonia assimilation through the glutamine synthetase/glutamate synthase (GS/GOGAT) pathway (Hodges, 2002). In Arabidopsis there are three genes encoding different ICDH isoforms located in the cytosol, chloroplasts/mitochondria and peroxisomes. Among them cytosolic ICDH (cICDH) is the major isoform in leaves, accounting for more than 90% of the $NADP^+$-dependent activity in leaf extracts (Kruse et al., 1998; Hodges, 2002; Mhamdi et al., 2010c). ICDH has been shown to provide NADPH for the promotion of redox signaling or homeostasis in response to oxidative stress (Møller & Rasmusson 1998; Hodges et al., 2003). Deficiency of cICDH in the *cat2* mutant exacerbates glutathione oxidation and lesion formation, and also enhances *PR* transcripts and bacterial resistance, pointing to some role for cICDH in redox signaling linked to pathogenesis responses (Mhamdi et al., 2010c). Moreover, ICDH activity is found to be stimulated by O_3 treatment in a day length-dependent manner (Dghim et al., 2013).

1.2.2.5.3 Nonphosphorylating glyceraldehyde-3-phosphate dehydrogenase

npGAPDH mediates the irreversible oxidation of glyceraldehyde-3-phosphate (Ga3P) to 3-phosphoglycerate (3-PGA), accompanied by the production of NADPH (Arnon et al., 1954; Iglesias, 1990). This enzyme is a conserved cytosolic protein in higher plants (Arnon et al., 1954; Mateos and Serrano, 1992; Gao and Loescher, 2000), and is encoded by a single gene (Bustos and Iglesias, 2002; Rius et al., 2006). It is also found in green algae and some specialized bacteria (Mateos and Serrano, 1992; Brunner and Hensel, 2001; Iddar et al., 2005). Its function provides an alternative route for Ga3P oxidation in glycolysis, as a bypass to oxidation by NAD-dependent GAPDH and 3-PGA kinase (Iglesias, 1990; Plaxton, 1996).

The function of npGAPDH in plants remains unclear. In photosynthetic cells, it was suggested to be involved in a shuttle system which exports photosynthetic NADPH from the chloroplast to the cytosol (Kelly and Gibbs, 1973). Reduction of sugars to polyols in plants may also require NADPH derived from npGAPDH (Rumpho et al., 1983; Gao and Loescher, 2000). In non-photosynthetic cells, npGAPDH was found to be a target for posttranslational phosphorylation (Bustos and Iglesias, 2002). It can be phosphorylated by the interaction with 14-3-3 proteins in heterotrophic tissues. This leads to a lower activity and enhanced sensitivity to regulation by adenylates and inorganic pyrophosphate (Bustos and Iglesias, 2003). It was also recently reported that npGAPDH influences PR responses triggered by hCO_2 (Mhamdi and Noctor, 2016).

1.2.2.5.4 NADP-malic enzyme

NADP-malic enzyme (NADP-ME) mediates the reversible oxidative decarboxylation of malate to produce pyruvate and CO_2, simultaneously reducing $NADP^+$ to NADPH (Chang and Tong, 2003). Its substrate malate is a crucial tricarboxylic acid cycle intermediate and plays different roles in plant physiological processes, like defense responses, stomatal movement and metabolite signaling (Lee et al., 2008; Parker et al., 2009; Finkemeier et al., 2013). One of the products of the NADP-ME reaction, pyruvate, is involved in multiple pathways. It is notably the final product of glycolysis, where it is produced from phosphoenolpyruvate (PEP) in the cytosol, before being translocated to the mitochondria for metabolism through the TCA cycle. Apart from oxidative decarboxylation, NADP-ME can also catalyze the reductive carboxylation of pyruvate and the decarboxylation of oxaloacetate (Gerrard Wheeler et al., 2008).

NADP-ME is involved in many kinds of biological processes. It not only takes part in the photosynthetic pathway in some C_4 and CAM species, but also functions as a non-photosynthetic isoforms in many plants (Drincovich et al., 2001). To date four NADP-ME genes encoding specific isoforms have been identified in Arabidopsis. Among them NADP-ME 1-3 are localized in the cytosol and NADP-ME 4 is plastidic (Gerrard Wheeler et al., 2005). These isoforms exhibit different kinetic, regulatory and structural properties (Gerrard Wheeler et al., 2005, 2008; Maurino et al., 2009). Genetic

analysis indicates that NADP-ME2 is responsible for most of the activity analyzed in mature plant tissues. Recent studies show that the loss of function of NADP-ME2 alters metabolic profiles (Brown et al., 2010; Voll et al., 2012). This enzyme is activated in response to various environmental challenges (Voll et al., 2012; Li et al., 2013). The overexpression of a cytosolic NADP-ME of rice in Arabidopsis enhances the tolerance to osmotic and salt stress (Cheng and Long, 2007; Liu et al., 2007).

1.3 Lesion-mimic mutants in plants

One outcome of excess ROS availability is induced cell death. Current concepts suggest that ROS-dependent cell death is not just due to cell collapse caused by damage but rather is under genetic control. Indeed, components required for ROS-induced cell death in plants (EXECUTOR proteins) have been identified by genetic studies (Wagner et al., 2004). As described in detail above, the extensive studies of *cat2* reveal that loss of this antioxidative enzyme leads to an HR-like phenotype in which plants present lesions on the leaves linked to SA accumulation. Many other mutations have been described that lead to similar, spontaneous lesion formation. To date, more than 40 lesion-mimic mutants have been identified in Arabidopsis (Bruggeman et al., 2015). The appearance of lesions in lesion-mimic mutants is often accompanied by phenomena associated with pathogen attack, like SA induction, defense marker gene expression, and altered resistance to biotic challenge (Lorrain et al., 2003).

The first lesion-mimic mutant described was *lsd1* (Dietrich et al., 1994). This mutant presents lesions on the leaves in a day length-dependent manner. When plants are grown in LD or transferred from SD to LD, lesions form and gradually spread until consuming the entire leaf. *LSD1* codes for a zinc finger protein which may act as a negative regulator of a pro-death signal. By binding to the transcription factor AtbZIP10, LSD1 stops it from entering the nucleus and thereby suppresses cell death (Dietrich et al., 1997; Kaminaka et al., 2006). A second mutant that shows a similar phenotype is *mips1*, a mutant defective in the synthesis of *myo*-Inositol (Meng et al., 2009). This mutant exhibits spontaneous cell death which is affected by both the amount of light and day length. Studies strongly

suggest that *myo*-Inositol plays important roles in regulating cell death formation and this regulation is closely linked to phytohormones like SA (Meng et al., 2009; Donahue et al., 2010).

1.4 Arabidopsis: a model to aid quick progress in understanding plant function

Arabidopsis has been well accepted as the most important model plant system by the scientific community. It has a relatively small size, as well as a small genome, compared with other plant species. Since the sequencing of its whole genome in 2000, lots of genetic tools have become available. Nowadays both scientific information and biological materials are easily accessible through various databases and biological stock centers, and it is relatively easy to produce genetic resources. Indeed, Arabidopsis is an excellent model for both classical (forward) genetics studies and analyses using reverse genetics. These two approaches can both be powerful and are distinguished as follows. Forward genetics aims to identify the sequence change that underlies a specific mutant phenotype, by which we can find genetic determinants of a specific physiological process or a signaling pathway. A big advantage of forward genetics is that this approach does not depend on prior assumptions. Instead, all the genes are considered, in an unbiased fashion, to find mutations that affect the phenotype of interest. Chemical mutagenesis by agents such as ethyl methanesulfonate (EMS) are most popular in forward genetics, although screens can also be conducted on other collections, such as T-DNA insertion mutants (Page and Grossniklaus, 2002; Peters et al., 2003; Qu and Qin, 2014). Reverse genetics, in contrast to forward genetics, begins with a clearly identified gene of interest. Plants carrying a mutation in this gene are then analyzed to determine if it is associated with any interesting phenotype, with the advantage relative to forward genetics that the phenotypic analysis can be more extensive and conducted at different levels (visible, molecular, biochemical). Key resources for reverse genetics are T-DNA and transposon-tagged mutant collections, in which expression of given genes are modified. More recently, TILLING (Targeting Induced Local Lesions in Genomes) has also become a commonly used reverse genetic strategy, in which random chemical mutagenesis is combined with PCR-based screening to identify point mutations in genes of interest. This technology allows a time

and cost-saving discovery of induced point mutations in a big population of mutagenized individuals (McCallum et al., 2000; Greene et al., 2003)

1.5 Aims of the project

The overall objectives of this thesis were to continue the group's work on enzyme systems involved in metabolizing H_2O_2 in plants, with a particular focus on CATs and enzymes involved in or related to the ascorbate-glutathione pathway. Most available functional analysis of CAT has been focused on CAT2 functions in leaves. As the major leaf isoform, CAT2 accounts for most of the extractable CAT activity and it has been demonstrated to play an important role in oxidative stress signaling. When grown in LD, but not SD, *cat2* shows spreading necrotic lesions, SA accumulation, *PR* gene induction, accumulation of camalexin and its synthesis pathway, and enhanced resistance to bacterial challenge (Chaouch et al., 2010). Although the SA pathway and related genes are only strongly induced in LD, many other genes, including numerous oxidative stress marker genes, are induced more strongly in SD (Queval et al., 2012). Irrespective of the growth day length, all of the stress responses triggered by loss of *CAT2* function can be prevented by growth at hCO_2 or low light (Queval et al., 2007). These characteristics make *cat2* a useful stress mimic tool to investigate the importance of components involved in oxidative signaling. One issue is whether the influence of day length on oxidative signaling is related to differences in stress intensity or not. A second issue bears on the specific functions of *CAT1* or *CAT3*, for which there is as yet little information. To explore these questions, single and double CAT mutants were investigated and the results obtained are presented in Chapter 2.

As described above, NADPH is a crucial component in cell redox homeostasis. The production of NADPH relies on several different enzymes. G6PDH is one of the major NADPH-producing enzymes that could play important roles in oxidative stress conditions, when the enzyme would traditionally be considered likely to play an antioxidative role. However, according to unpublished work in our group, a knockout for a specific isoform (*G6PD5*) was found to abolish, rather than exacerbate, the *cat2* lesion phenotype. Moreover, the abolition of *cat2*-induced lesions by *G6PD5* deficiency appears to be linked to inhibition of *cat2*-triggered activation of the SA pathway. To investigate the processes that

might be involved, we carried out a forward genetic screen on *cat2 g6pd5*, based on identifying mutants that allow lesions to be observed in this genetic background. This work is described in Chapter 3.

One of the pathways for which NADPH is required is the ascorbate-glutathione pathway, which becomes particularly important in stress conditions. In total, four enzymes are involved in the ascorbate-glutathione pathway. Unlike the other three (APX, DHAR, GR), little genetically based information is available on the role of specific MDHAR isoforms. As discussed above, ascorbate can be regenerated from MDHA or DHA by enzymatic and non-enzymatic processes, some of which require GSH and/or NADPH. Recent work in our group showed that the loss of all three DHAR functions does not affect leaf ascorbate pools in either optimal growth conditions or oxidative stress (Rahantaniaina et al., 2017). The ability to maintain a largely reduced leaf ascorbate pool when DHAR activity is negligible may be explained by other routes, such as MDHAR. To explore the roles of specific isoforms of MDHAR in the ascorbate-glutathione pathway, mutants for three MDHAR-encoding genes were obtained and analyzed in both Col-0 and *cat2* oxidative stress backgrounds. The functional analysis of these lines is presented in Chapter 4.

CHAPTER 2

The function of specific catalases in plants

A modified version of this chapter has been submitted for publication by the following authors:

Yang Z, Mhamdi A and Noctor G. Analysis of single and double catalase mutants in Arabidopsis underscores the essential role of CATALASE2 for plant growth and day length-dependent oxidative signalling in leaves.

Summary

Three genes encode CAT in Arabidopsis. While the role of *CAT2* in photorespiration is well established, the importance of the different CATs in other processes is less clear. In this work, we examined CAT functions by using T-DNA mutants for *cat1*, *cat2*, *cat3*, as well as *cat1 cat2* and *cat2 cat3* double mutants. In roots and in leaves, the *cat2* mutants showed the largest effect on activity. Like rosette growth, root growth was inhibited in all *cat2*-containing lines. Root growth inhibition was prevented by growth at hCO_2, suggesting that it is an indirect effect of oxidative stress in the leaves. Marked phenotypes were not identified in single *cat1* or *cat3* mutants, but analysis of double mutants suggested some overlap between *CAT2* and *CAT3* in leaves and *CAT1* and *CAT2* in seeds. The response of H_2O_2 marker genes to equal-time exposure of *cat2* to oxidative stress was highly influenced by growth day length context. Similar responses in *cat2* and *cat2 cat3* suggest that this is not related to day length effects on *CAT3* expression. The non-specific CAT inhibitor, 3-aminotriazole (3-AT), produced qualitatively similar day length-dependent effects to those observed in *cat2*. Together, our data (1) underline the importance of CAT2 in Arabidopsis; (2) suggest that CAT1 and CAT3 are mainly “back-up” enzymes; and (3) establish that day length-dependent responses to CAT deficiency are independent of the duration of oxidative stress.

2.1 Introduction

Among the many enzymes that plants may use to remove H_2O_2, CAT is the most rapid and is strongly expressed (Tuzet et al., 2018). Accordingly, under standard assay conditions, CAT shows a very high extractable activity (Noctor et al., 2016). Enzyme capacity is particularly high in photosynthetic tissues but activities are also considerable in other plant parts (Mhamdi et al., 2012). Most plants so far examined contain three genes encoding CAT (Frugoli et al., 1996; Dat et al., 2001; Mhamdi et al., 2010a). One of these (*CAT2* in Arabidopsis) is essential for optimal plant growth in C_3 plants growing in air, but the roles of the other two (*CAT1* and *CAT3* in Arabidopsis) remain much less clear.

The expression patterns of the Arabidopsis CATs suggested that *CAT2* encodes the photorespiratory CAT (Frugoli et al., 1996) that genetic studies in barley and tobacco showed to be important in leaves (Kendall et al., 1983; Willekens et al 1997). An RNAi construct based on the *CAT2* sequence produced Arabidopsis plants that were smaller, more sensitive to high light, and that showed induction of oxidative stress-responsive genes (Vandenabeele et al., 2004; Vanderauwera et al., 2005). Analysis of gene-specific T-DNA knockouts confirmed that *CAT2* is responsible for a large part of the leaf activity in Arabidopsis and identified the encoded enzyme as an important player in photorespiration (Queval et al., 2007).

While the importance of *CAT2* in photorespiration is clear, less is known about other possible functions of this gene. In addition to loss of most of the leaf CAT activity, the *cat2* mutant was previously reported to produce a 50% decrease in root activity (Bueso et al., 2007). The mutant also shows decreased post-germinative growth that, like phenotypes observed in mature leaves, was linked to auxin signaling (Gao et al., 2014; Liu et al., 2017). Auxin is one of a number of phytohormones whose contents or signaling pathways are modified by the oxidative stress caused by loss of *CAT2* function (Chaouch et al., 2010; Mhamdi et al., 2010b; Tognetti et al., 2010; Han et al., 2013a, b).

Interestingly, the effect of *cat2*-induced oxidative stress in leaves has been linked to day length. Loss of *CAT2* function causes lesions when plants are grown in LD but not in SD, and this effect seems to

be under genetic control (Queval et al., 2007; Chaouch et al., 2010; Li et al., 2014). Transcriptomes elicited by the *cat2* mutation are also different in LD compared to SD (Queval et al., 2007, 2012), but the significance of this observation with respect to photoperiod-dependent signaling is potentially obscured by the differences in the duration of exposure to photorespiration (and, therefore, oxidative stress).

Available evidence does not suggest that there is a great difference in the biochemical properties between the three CATs. Gene sequences have high similarity and promoter-swap studies revealed that *CAT3* under the control of the *CAT2* promoter, but not *CAT2* under the control of the *CAT1* or *CAT3* promoter, can fully rescue *cat2* phenotypes (Hu et al., 2010). This suggests that any specificity of function may be largely controlled by differences in expression. For example, CAT3 protein increases relative to CAT2 as leaves age (Zimmermann et al., 2006) and *CAT1* expression is closely associated with reproductive tissues (Mhamdi et al., 2010a). However, the roles of *CAT1* and *CAT3* remain largely unknown and, while mutants for these genes have been briefly described (Mhamdi et al., 2010a), they have not been the focus of any in-depth study.

Since the *CAT2* gene is located on a different chromosome from the *CAT1* and *CAT3* genes, double mutants for *cat1 cat2* and *cat2 cat3* are relatively straightforward to obtain. In contrast, it is difficult to obtain the *cat1 cat3* combination by simple crossing because the two genes are located adjacently on chromosome 1. A very recent study using CRISPR technology reported a triple loss-of-function line but the plants were not analyzed in depth (Su et al., 2018). In the present study, we used gene-specific mutants to analyze the roles of the three CAT genes in Arabidopsis. Our aims were (1) to examine potential roles for *CAT1* and *CAT3* in plant growth and development; (2) to assess the importance of *CAT2* in organs other than leaves; (3) to establish whether day length-dependent oxidative signaling in *cat2* leaves is independent of stress duration and whether it is influenced by *CAT3*.

2.2 Material and methods

2.2.1 Plant material

The T-DNA CAT mutants were obtained from Nottingham Arabidopsis Stock Centre (NASC), Nottingham University, UK. While *cat2* and *cat3* are from the SALK collection and are in the Col-0 background, *cat1* is in the Col-3 background. The polymorphisms were SAIL_311_d07 for *cat1*, SALK_076998 for *cat2* (*cat2-1*, Queval et al., 2009), and SALK_092911 for *cat3*. Genotyping was performed by PCR using the primers listed in Supporting Information Table S1. Double mutants were generated by crossing *cat2* with *cat1* or *cat3*. After verification that mutations were heterozygous in F1 generation by PCR, double homozygotes were identified in F2 by the same way. F3 seeds were used for experiments.

2.2.2 Growth conditions and sampling

For all experiments, plants were grown at a temperature of 20°C (day)/18°C (night) at an irradiance of 200 $\mu mol.m^{-2}s^{-1}$ at the leaf surface (16h light: 8h dark). For analysis of effects on roots, plants were grown on 0.5 Murashige-Skoog medium for up to two weeks in the presence or absence of added sucrose (1%), either in air (400 $\mu L.L^{-1}$) or 3000 $\mu L.L^{-1}$ CO_2 (hCO_2), which was used to decrease photorespiration to very low levels.

For experiments investigating processes in leaves or rosettes, plants were grown in soil in a controlled environment growth chamber and given nutrient solution twice a week, as in Queval et al. (2007). In these conditions, the day length was either 8h (SD) or 16h (LD) and the CO_2 concentration either air or hCO_2. Unless otherwise stated, plants were grown to the age of 19-21d (LD) or 26-28d (SD), at which point samples were taken. In experiments to analyze the effect of day length on oxidative stress marker gene expression, plants were grown at hCO_2 in either short or LD and then transferred to air for 8h, and samples were taken before and after the transfer. All samples were rapidly frozen in liquid nitrogen and stored at -80°C.

2.2.3 Enzyme activities

Enzyme assays were performed as described in detail in Noctor et al. (2016). About 100 mg root or shoot tissue was ground in liquid nitrogen then extracted into phosphate buffer (pH 7.5), 1 mM EDTA. Centrifuged extracts were desalted on a NAP-5 column, and immediately used for spectrophotometric assay. CAT was measured as the disappearance of H_2O_2 at 240 nm, APX as the H_2O_2-dependent disappearance of ascorbate at 290 nm, DHAR as the GSH- and extract-dependent formation of ascorbate at 265 nm, and GR as the GSSG-dependent oxidation of NADPH at 340 nm.

2.2.4 Measurements of transcript abundance

Total RNA was extracted with Trizol following the manufacturer's protocols, and qPCR procedures were performed as in Queval et al. (2007), except that transcripts were normalized to two independent constitutive genes, which were *ACTIN2* and *RCE1*. Gene-specific primer sequences used in this study are listed in Supporting Information Table S1.

2.2.5 Ascorbate, glutathione and ROS assays

Ascorbate and glutathione were measured by plate-reader spectrophotometry following the procedures described by Queval and Noctor (2007). ROS visualization was performed by dichlorodihydrofluorescein-diacetate ($DCFH_2$-DA) staining of the primary roots of ten individual plants of each genotype in each condition, using a method adapted from Mhamdi et al. (2010b). 10 day-old seedlings were incubated in 50 µM staining solution at room temperature for 20 min in dark. Then seedlings were washed three times with phosphate buffer for 5 min in dark. Fluorescence was observed with a Zeiss Axio Imager 2 fluorescence microscope.

2.3 Results

2.3.1 *CAT* expression and activity in roots

We first analyzed transcript levels of all three CATs in the roots of seedlings grown in the presence or absence of added sucrose (Figure 2.1A). The *cat1*, *cat2* and *cat3* mutations decreased respective transcripts to low levels, although low transcript signals and variability in roots meant the differences were not always significant relative to the wild-type. Both *CAT2* and *CAT3* tended to be higher in plants grown on sucrose, with a significant increase in *CAT2* in *cat3* and in *CAT3* in *cat2* ($P < 0.05$). Compensatory changes in the expression of other CATs were also observed for some of the mutants in both growth conditions (Figure 2.1A). *CAT1* transcripts were increased in the two *cat3* backgrounds while *CAT3* transcripts were higher in *cat2* backgrounds other than *cat2 cat3*, although the increase in *CAT3* was not significant in *cat1 cat2* grown with added sucrose.

Consistent with previous reports for activities measured in leaves (Mhamdi et al., 2010a), the *cat1* mutant showed wild-type levels of CAT activity (Figure 2.1 B). This was observed when *cat1* was compared to either Col-0 or Col-3, which showed very similar root CAT activities (Supporting Information Figure. S1). As in leaves (Queval et al., 2007), loss of *CAT2* function caused a substantial decrease in root activity (Figure 2.1B). Like *cat1*, the *cat3* mutation alone had no significant effect on activity. However, in *cat2 cat3* grown without added sucrose, the activity was decreased compared to *cat2*, although this effect was not apparent when plants were grown on sucrose (Figure 2.1B).

2.3.2 Root and seed phenotypes in *CAT* mutants

Growth analysis revealed that *cat2* had a substantial impact on root length in plants grown without sucrose in air (Figure 2.2A, left). A slight effect of *cat3* was observed in the *cat2 cat3* double mutant. The *cat1* mutant showed no decrease in root length (Figure 2.2A, left). The effects on growth were broadly correlated with ROS signals estimated using $DCFH_2$-DA (Figure 2.2B and Supporting Information Figure. S2), with the strongest ROS signals observed in *cat2* genotypes, although some

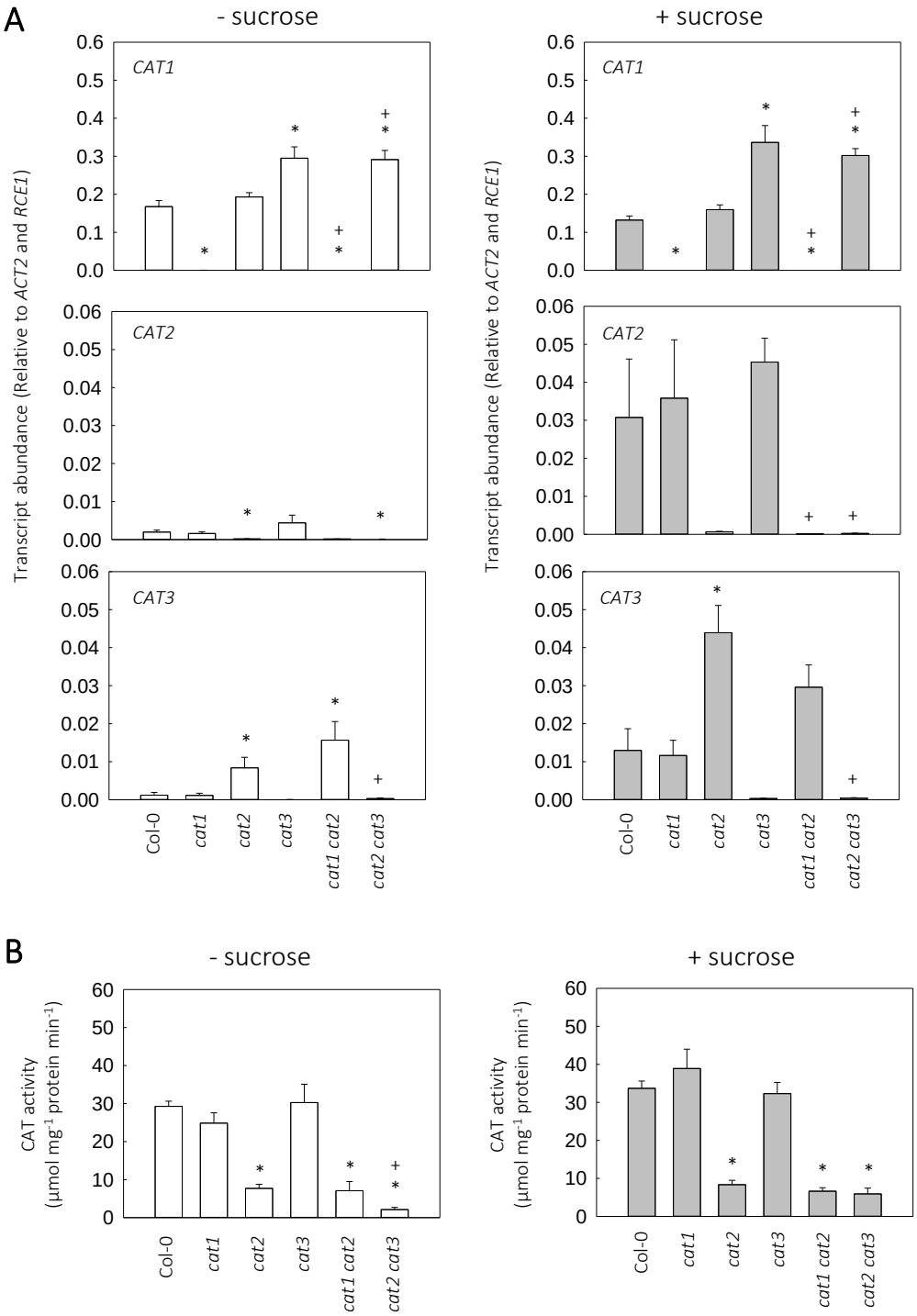

Figure 2.1. Catalase transcript levels (A) and extractable catalase activities (B) in the roots of single and double catalase-deficient mutants. Plants were grown on 1/2MS ± sucrose for 14 d in LD air. Then approximately 100 mg root samples were collected for analysis. Left, no sucrose. Right, 1% sucrose. For transcript analysis, data are means ± SE of three (*cat1, cat1 cat2*) or six (other genotypes) biological replicates. For activities, all data are means ± SE of three biological replicates. * indicates significant difference from wild type at $P < 0.05$; $^{+}$ indicates significant difference between double mutants and *cat2* at $P < 0.05$.

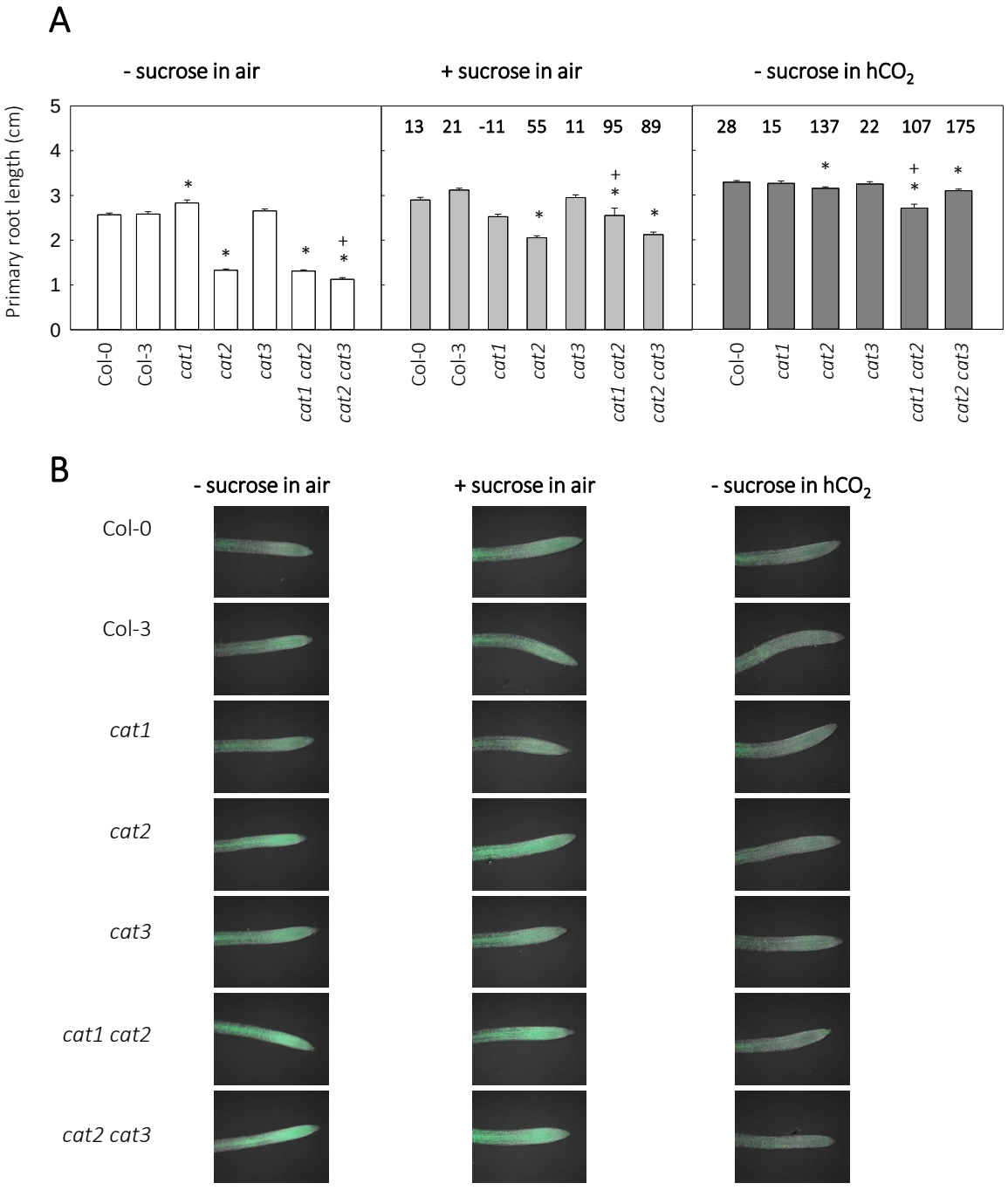

Figure 2.2. Effects of added sugar and CO_2 regime on primary root length (A) and ROS signal intensity (B) in catalase mutants ten days after germination. Left, no sucrose, air. Center, +1% sucrose, air. Right, no sucrose, hCO_2. Data shown in A are means ± SE of at least 18 plants and up to more than 150 plants grown in 9 different experiments. * indicates significant difference from wild-type at $P < 0.05$. $^+$ indicates significant difference between double mutants and *cat2* at $P<0.05$. In the center and on the right, the numbers above the bars indicate percent stimulation of root length by sucrose (center) or by hCO_2 (right) relative to no sucrose, air (left). ROS signals in B were detected using $DCFH_2$-DA. For each condition/genotype, one representative photograph was selected from the ten images shown in Supporting Information Figure S4.

increased staining was also apparent in *cat3* (Figure 2.2B). The impact of *cat2* on growth was substantially alleviated by added sucrose, with all three *cat2* genotypes showing a substantial stimulation (55-95%) of root length compared to the condition without sucrose (Figure 2.2A, middle). This effect was not correlated with changes in ROS signals, which were similar in *cat2* genotypes grown in the presence or absence of sucrose (Figure 2.2B, middle). When plants were grown at hCO_2 (without added sucrose), the effect of *cat2* on growth was almost completely annulled (Figure 2.2A, right). This effect was accompanied by a decrease in ROS signals in these genotypes (Figure 2.2B, right).

To explore root responses to increased ROS signals in the mutants, we analyzed APX activity and APX1 transcripts, as well as two markers for oxidative stress. All these factors have been well documented to be strongly induced in *cat2* leaves (Queval et al., 2007; Mhamdi et al., 2010a,b; Noctor et al., 2016). Despite the increased ROS signals in the roots of *cat2* genotypes (Figure 2.2B), no substantial increase in root APX activity was observed (Figure 2.3A). *APX1* transcripts increased somewhat in *cat2* and *cat1 cat2* in plants grown without added sucrose, but this effect was not apparent in plants grown with sucrose. No increase in either *GSTU24* or *UGT73b3*, two markers for oxidative stress responses, was observed (Figure 2.3B). We also measured ascorbate and glutathione, as well as GR activity, in the mutants. No difference in GR activity was observed (Supporting Information Figure. S3) and ascorbate and glutathione remained at wild-type levels in *cat2* (data not shown).

To investigate the functional impact of the three CATs in reproductive tissues, seed number and seed formation were analyzed in the different genotypes. A slight but significant decrease in the number of seeds per silique was observed in *cat1* and *cat3*, and this was slightly stronger when these mutations were combined with *cat2* (Supporting Information Figure. S4, top). The *CAT* mutations also had some impact on the number of aborted seeds per silique: averaged over at least 100 siliques, the % aborted seeds rose from below 1% in the wild-type to over 4% in *cat1 cat2*, with slight but significant increases also observed in *cat2* and *cat3* (Supporting Information Figure. S4, bottom).

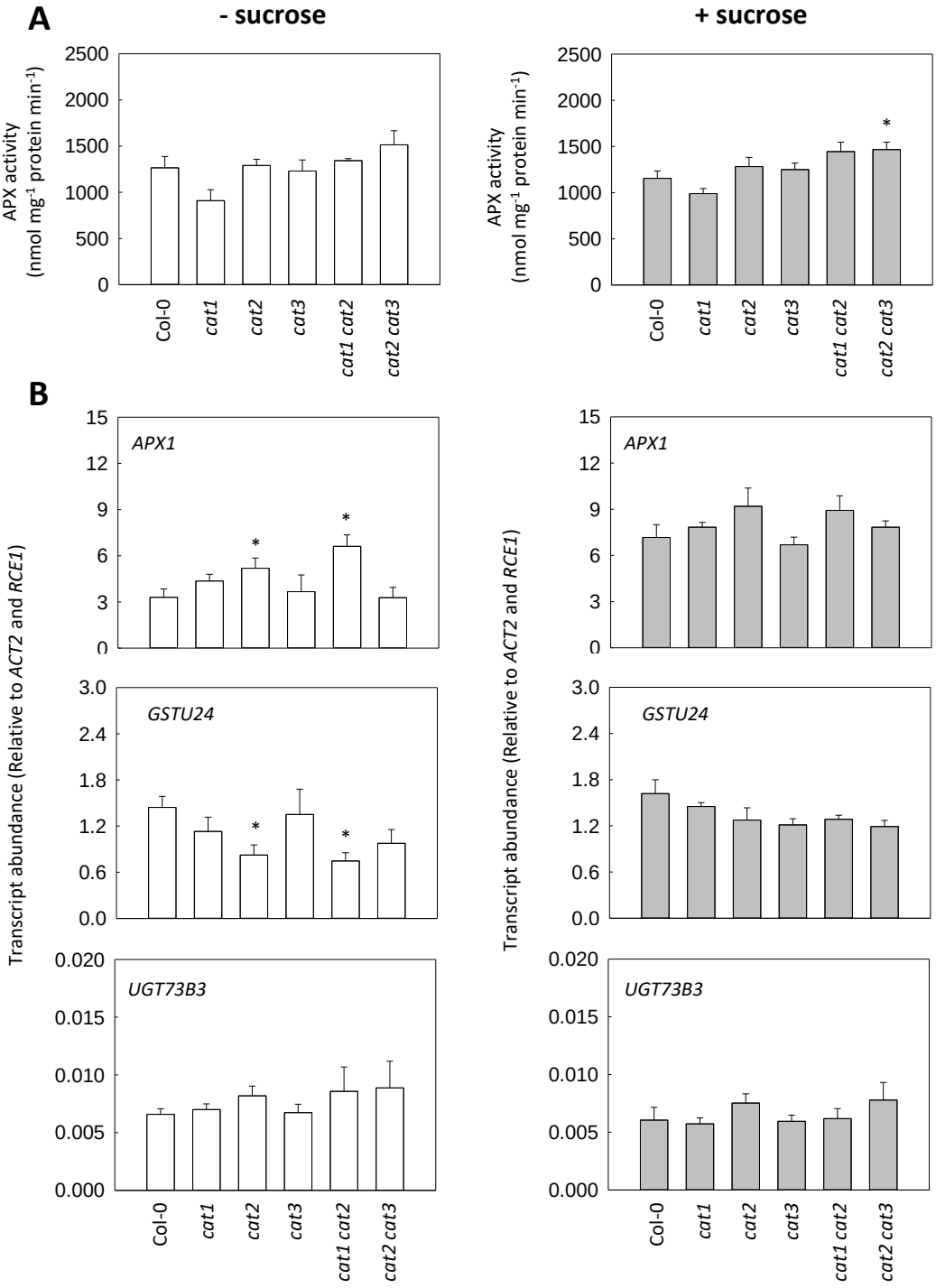

Figure 2.3. Oxidative stress markers in the roots of single and double catalase-deficient mutants. Plants were grown in the presence and absence of sucrose. Left, no sucrose. Right, 1% sucrose. A, extractable ascorbate peroxidase activity. B, three oxidative stress marker transcripts (*APX1*, *GSTU24*, *UGT73b3*). Data are means ± SE of three biological replicates. * indicates significant difference from wild type at $P < 0.05$; $^{+}$ indicates significant difference between double mutants and *cat2* at $P < 0.05$.

2.3.3 CAT2 and CAT3 function in leaves

As shown above, *CAT2* is essential for optimal root growth, adding to observations that expression of this gene is required for rosette development (Queval et al., 2007; Gao et al., 2014; Mhamdi et al., 2010a). *CAT1* does not seem to make a significant contribution to leaf CAT activity, with *CAT3* responsible for most of the CAT2-independent activity (Mhamdi et al., 2010a). We therefore focused on the respective roles of *CAT2* and *CAT3* in ensuring optimal rosette growth. When plants were grown in air, where photorespiration is relatively rapid, *cat3* rosettes were similar to the wild-type, in contrast to *cat2*, in which the rosette was much smaller (Figure 2.4, right). The additional presence of the *cat3* mutation in *cat2 cat3* did not exacerbate the effect of *cat2*. At hCO_2, both *cat2* and *cat3* showed wild-type rosette characteristics, but a significant decrease in rosette size and mass was observed in *cat2 cat3* (Figure 2.4, left). Further, the *cat2 cat3* mutation increased time to flowering significantly compared to both Col-0 and *cat2* in LD (Supporting Information Figure. S5).

The effects on rosette size were specific to growth in hCO_2 in LD: all three mutant lines showed wild-type rosette size when grown at hCO_2 in SD (Supporting Information Figure. S6). The day length-dependent effect was not obviously correlated to differences in CAT activity, which was affected similarly by mutations in both growth conditions. Leaf activity was decreased by about 75% in *cat2*, 15-25% in *cat3* and about 90% in *cat2 cat3* (Figure 2.5). When measured in plants growing at hCO_2, other antioxidative enzymes showed either no effect of the *CAT* mutations or day length (GR, DHAR) or slight increases linked to the *cat2* mutation (APX1), although this was only statistically significant in *cat2 cat3* (Supporting Information Figure. S7).

The above observations in plants grown at hCO_2 point to some photorespiration-independent function of *CAT3* that becomes apparent when *CAT2* function is lost. Moreover, it suggests that such an effect may be conditional on growth day length. We have previously described an interaction between oxidative signaling in *cat2* and growth day length, in that both *cat2* phenotypes and transcriptomes are markedly different in LD and SD (Queval et al., 2007, 2012; Chaouch et al., 2010; Mhamdi et al.,

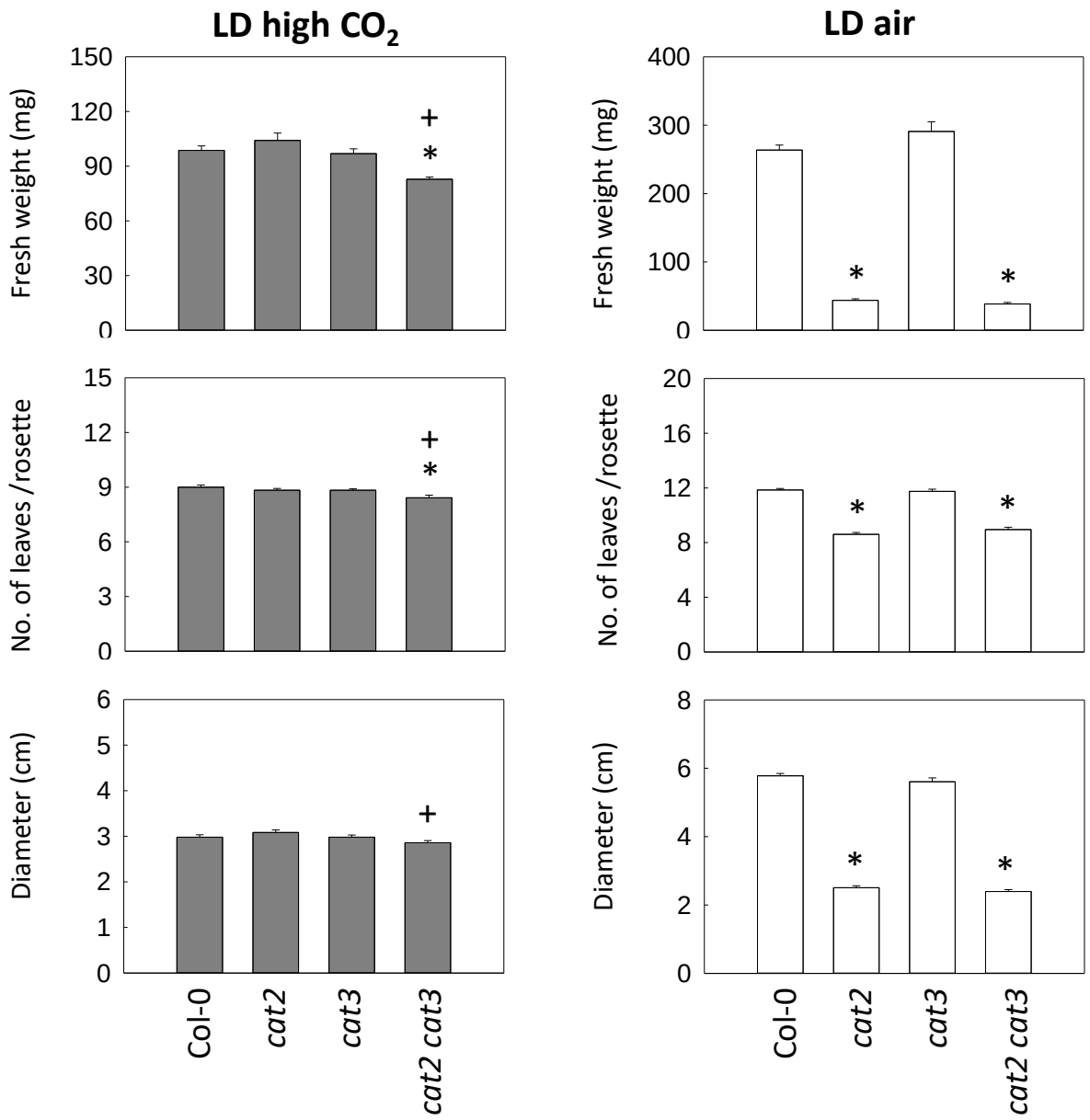

Figure 2.4. Comparison of rosette phenotype in Col-0, *cat2*, *cat3* and *cat2 cat3*. Plants were grown in LD hCO_2 or LD air for 20 d. Data are means ± SE of 24 plants. Significant differences to Col-0 at $P<0.05$ are indicated by *. $^{+}$ indicates significant difference between *cat2 cat3* and *cat2* at $P < 0.05$.

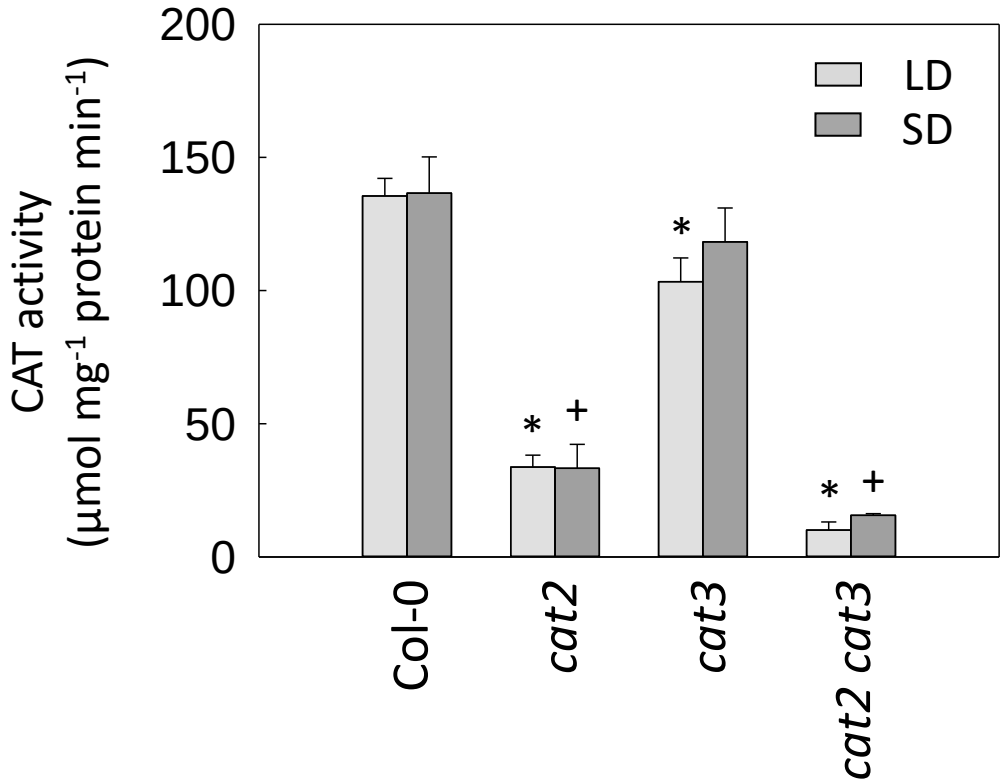

Figure 2.5. Comparison of catalase activity in leaves of catalase mutants grown in LD and SD at hCO_2. Plants were grown in LD hCO_2 for 20 d or SD hCO_2 for 26 d. Leaf samples were taken from different plants. Data are means ± SE of 3 biological replicates. * indicates significant difference between mutants and Col-0 in LD at $P < 0.05$; $^+$ indicates significant difference between mutants and Col-0 in SD at $P < 0.05$.

2010b; Li et al., 2014). However, interpretation of this effect is complicated by the simultaneous variation in the duration of photorespiratory H_2O_2 production. Here, we devised a new experimental protocol to circumvent this problem (Figure 2.6A). With the dual aims of (1) separating the influence of day length from duration of oxidative stress and (2) analyzing the possible roles of CAT3 in influencing day length-dependent oxidative signaling, plants were grown to similar developmental stages in either SD or LD at hCO_2 to prevent photorespiration and the associated oxidative stress in *cat2* genotypes. They were then transferred to air at the beginning of the photoperiod for an equal time exposure to photorespiration (Figure 2.6A). In addition to the *cat2*, *cat3*, and *cat2 cat3* lines, we included a treatment of the wild-type with the CAT inhibitor 3-AT. As Figure 2.6A shows, the phenotypes and size of the plants were quite comparable in the two day-length regimes. As shown in

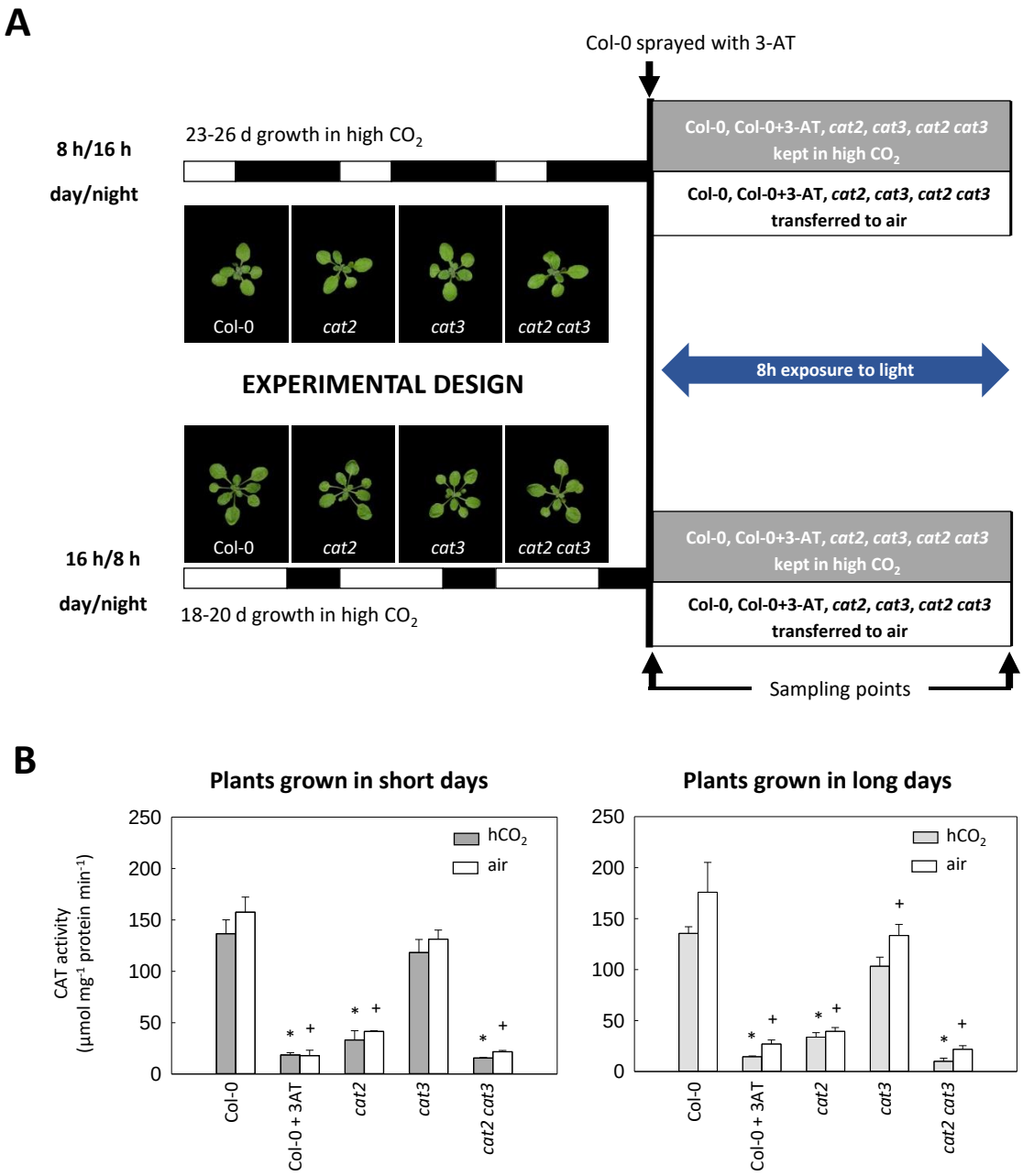

Figure 2.6. Experimental design (A) and catalase activities (B) in different lines and wild-type treated with the catalase inhibitor, 3-AT. The different genotypes were grown in LD hCO_2 or SD hCO_2 to a similar developmental stage. At the beginning of the light period, a group of Col-0 plants were sprayed with the catalase inhibitor 3-AT. All five types of plant (Col-0, Col-0+3-AT, and the three catalase mutant lines) were either kept at hCO_2 to maintain the inhibition of photorespiration or transferred to air to allow photorespiration to occur. After 8h in the light, rosette samples were taken and used for analysis of catalase activity (B), or to obtain the results described in Figures 2.7 and 2.8 and Supporting Information data. For catalase activity, data are means ± SE of 3 biological replicates. Significant differences to Col-0 in hCO_2 at $P < 0.05$ are indicated by *; significant differences to Col-0 in air at $P < 0.05$ are indicated by $^{+}$.

Figure 2.6B, treating the wild-type with 3-AT decreased CAT activities to those observed in *cat2 cat3*. In all cases, CAT activities at the end of the experiment were similar in the two day length conditions (Figure 2.6B). Exposure to air for several days after growth at hCO_2 increases CAT2-dependent CAT activity (Queval et al., 2007), but such effects were minor in the shorter-term (8h) exposure used here (Figure 2.6B). Accordingly, *CAT2* and *CAT3* transcripts were not markedly different between plants kept at hCO_2 or transferred to air for 8h (Supporting Information Figure. S8). As reported for roots (Figure 2.1), the *cat3* mutation was associated with some induction of *CAT1* transcripts, although this was independent of the CO_2 regime (Supporting Information Figure. S8). Similarly, little evidence of marked up-regulation of other antioxidative enzymes was apparent within the short exposure to air (Supporting Information Figure. S9). It is also noteworthy that 3-AT did not affect the activity of these enzymes (Supporting Information Figure. S9).

Despite this stability of key members of core antioxidative systems over the course of the experiment, 8h exposure of *cat2* to air was sufficient to strongly induce two oxidative stress marker genes (Figure 2.7A, middle panels). Strikingly, however, induction of both genes was strongly dependent on the day length in which the plants had been growing prior to transfer to air. Induction of *GSTU24* in LD plants was modest while *UGT73b3* was not induced in *cat2* (Figure 2.7A). By contrast, in SD plants, *GSTU24* and *UGT73b3* were induced about 100-fold and 10-fold respectively (Figure 2.7B, note the log scale). Equally strikingly, the influence of day length was also apparent for 3-AT treatment, with both genes being much more strongly induced after treatment of SD-grown plants than LD-grown plants. It is also noteworthy that 3-AT treatment of the wild-type produced an effect that was about 10 times stronger than the *cat2* mutation for both genes (Figure 2.7).

In a second experiment, we included *cat3* and *cat2 cat3* genotypes. Similar effects of growth day length were apparent for *cat2* and the 3-AT treatment, although this time 3-AT induced the marker genes only about 2-3 times more strongly than *cat2* in SD (Figure 2.8). The single *cat3* mutation did not cause a significant induction, while induction in *cat2 cat3* showed a similar pattern to that observed in *cat2* (Figure 2.8).

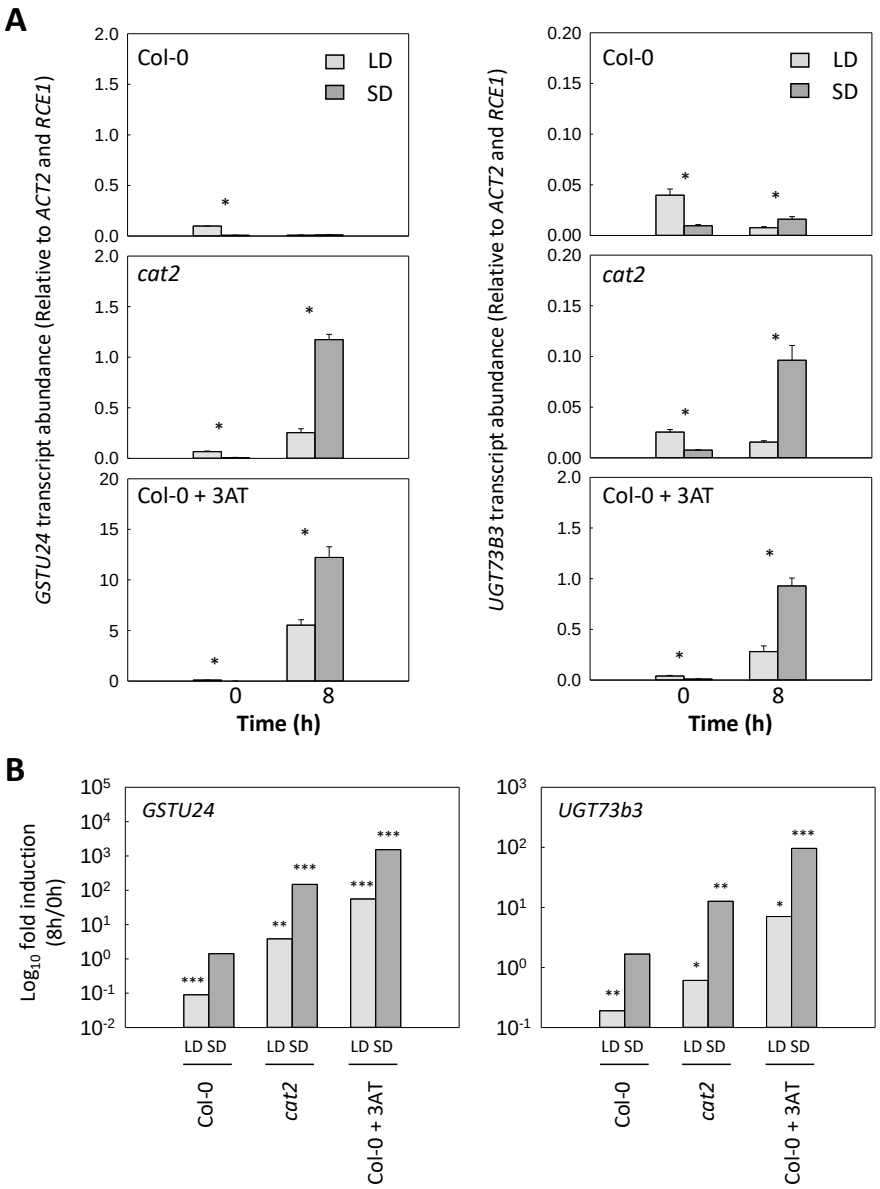

Figure 2.7. Analysis of light-dependent induction of oxidative marker gene transcripts in Col-0 and *cat2* after growth at different photoperiod regimes. Left, *GSTU24*. Right, *UGT73b3*. Plants were grown as described in Figure 2.6A in LD hCO_2 (light grey column) or SD hCO_2 (dark grey column). A set of Col-0 plants were sprayed with 3-AT and untreated and treated Col-0 plants were transferred to air alongside a group of *cat2* plants. Samples were taken either immediately before (0h) or after the treatment/transfer (8h). A, Transcript abundance relative to constitutive genes. Top, Col-0. Middle, *cat2*. Bottom, Col-0+3-AT. Note the different y-axis scale for the bottom two graphs. Data are means ± SE of 3 biological replicates. *Indicates significant difference between LD and SD at $P < 0.05$. B, Logarithmic plots of transcript induction by transfer to air following growth at hCO_2 in LD or SD. Data are means ± SE of 3 biological replicates. Mean values at 8h were divided by mean values at 0h. Significant difference for the three biological replicates at 0h and 8h is indicated at *$P < 0.05$, **$P < 0.01$ and ***$P < 0.001$.

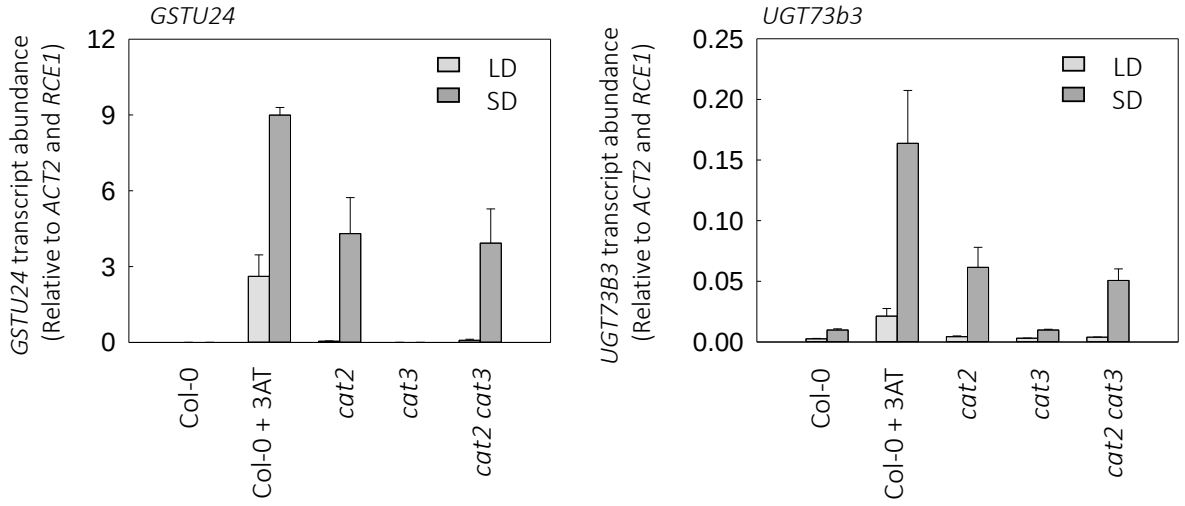

Figure 2.8. Effect of the *cat3* mutation on the modulation of oxidative stress responses by growth day length. Plants were grown in LD hCO_2 or SD hCO_2, then treated as described in Figures 2.6 and 2.7. After 8h in air, samples were taken for RNA extraction and analysis of oxidative stress marker transcripts. Data are means ± SE of 3 biological replicates. No significant difference (P<0.05) was observed for either marker transcript between *cat2* and *cat2 cat3* in either condition.

Finally, we examined whether the stronger gene induction in SD plants was linked to photorespiration by analyzing effects in plants kept at hCO_2 for the 8h test period. Under these conditions, none of the mutant lines showed a marked induction of the two genes (Figure 2.9). Both genes showed some induction by 3-AT treatment, although less than in plants exposed to air (cf. Figures 2.7 and 2.8). In contrast with the effects of the *cat2* mutation and 3-AT treatment when plants were exposed to air, there was no evidence that 3-AT treatment in hCO_2 induced the two genes more strongly in plants grown in SD.

2.4 Discussion

Our aim in this study was to conduct an in-depth comparative analysis of the roles of the three CATs in growth and development of Arabidopsis. To this end, we exploited a *cat2* mutant line that has been well-studied at the leaf level (Queval et al., 2007) and *cat1* and *cat3* mutants that have been previously reported but which have not been investigated in detail (Mhamdi et al., 2010a). Below, we discuss the major issues coming out of this work.

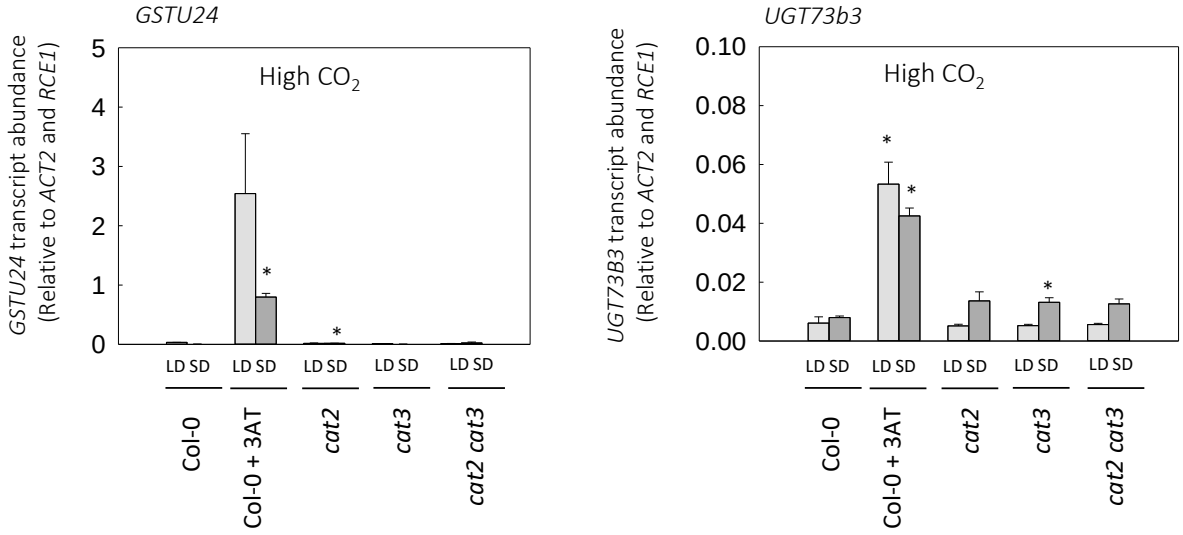

Figure 2.9. Analysis of effect of growth day length on oxidative marker gene transcripts in plants kept at hCO_2. Plants were grown in LD hCO_2 or SD hCO_2 as for Figure 2.8 except that plants were kept at hCO_2 instead of being transferred to air. Samples were taken for RNA extraction and analysis of oxidative stress marker transcripts. Data are means ± SE of 3 biological replicates. *Indicates significant increase at $P < 0.05$ compared to Col-0 in the same condition.

2.4.1 Decreased root growth is specific to *cat2* and is a secondary effect

It was reported previously that the *cat2* mutation causes a decrease of about 80% in extractable leaf CAT activity in leaves and about 50% in roots (Bueso et al., 2007; Queval et al., 2007). Our present data are largely consistent with these earlier reports, although we found a greater decrease in roots than did Bueso et al. (2007). This is possibly due to differences in root age (three weeks in the earlier study compared to two weeks here). The remaining root activity when *CAT2* function is lost appears to be attributable to *CAT3*, since when plants were grown without sucrose, the *cat2 cat3* double mutant had very low activity whereas *cat1 cat2* had similar activity to *cat2* (Figure 2.1). Interestingly, when sucrose was included in the medium, *cat2 cat3* and *cat2* activities were similar. This suggests possible induction of *CAT1* by sucrose, although we note that *CAT1* transcripts were similar in plants grown in the presence and absence of sucrose.

Analysis of leaf responses in *cat2* has established that this mutation causes alterations in leaf redox state, reconfiguration of transcriptomes, and induction of enzymes of the ascorbate-glutathione

pathway (Queval et al., 2007, 2009; Mhamdi et al., 2010b; Vanderauwera et al., 2005). By contrast, increased ROS signals are not so easy to detect (Mhamdi et al., 2010b, Chaouch et al., 2012), possibly due to technical difficulties or due to rapid removal of H_2O_2 by alternative enzymes (Noctor et al., 2016; Tuzet et al., 2018). ROS analysis with the $DCFH_2$-DA stain, which is not easy to use in leaves, revealed a clear increase in root signals in *cat2* genotypes and, to a lesser extent, in *cat3*. More intense ROS signals were accompanied by decreased root growth in all *cat2* genotypes grown in the absence of sugar (Figure 2.2).

A recent analysis of 5-day old seedlings also described decreased root growth in *cat2*, an effect that was completely annulled by growth on sucrose (Liu et al., 2017). While we also found that the *cat2*-dependent inhibition was sensitive to sucrose, this effect was only partial (Figure 2.2). Moreover, Liu et al. (2017) reported that sucrose decreased DAB staining in cotyledons, but we found little evidence that root ROS signals were decreased when root growth was favored. This is in line with a changing perception of ROS. Long considered to be potentially damaging molecules, their positive role in plant growth is now being increasingly recognized (Foyer & Noctor, 2005; Dietz et al., 2016; Foyer et al., 2017; Mittler, 2017). Liu et al. (2017) reported that CAT activity was decreased by growing wild-type seedlings on sucrose, perhaps due to a less developed capacity for photosynthesis (and, hence, photorespiration). Our root-specific analyses found no evidence that sucrose decreased the CAT activity in genotypes other than *cat2 cat3*, in which the activity was stimulated by added sugar. Further, *CAT2* transcripts were more abundant in the roots of plants grown with sugar (Figure 2.1).

The lack of a simple correlation between root growth, root CAT activity and root ROS signals perhaps suggests that any effect of the *cat2* mutation on root development is an indirect consequence of effects in the shoot. Direct evidence that this is the case comes from the almost complete reversion of the *cat2* root phenotype by growing the plants at hCO_2 (Figure 2.2). While we cannot exclude an effect of hCO_2 on biochemical pathways in the root, this observation probably reflects the inhibition of photorespiration, which poses a stress on *cat2* leaves and leads to an indirect effect on root growth.
Further evidence in support of this conclusion comes from an analysis of antioxidative enzymes and H_2O_2 marker transcripts in roots. Both of these factors respond strongly to stress in *cat2* leaves but we

found little evidence of a concerted oxidative stress response in *cat2* roots (Figure 2.3). Interestingly, however, the increase in root ROS signals in *cat2* was accompanied by a slight induction of *APX1*. Since root ROS signals were decreased to wild-type levels in all *CAT* mutants grown at hCO_2 (Figure 2.2), this raises the intriguing possibility that ROS may be produced in the roots as a secondary response to oxidative stress in *cat2* shoots. While we cannot discount direct translocation of ROS, a more likely explanation is activation of cell-to-cell propagation of ROS production through components such as NADPH oxidases (Mittler et al., 2011) which have been implicated in systemic signaling in *cat2* leaves (Chaouch et al., 2012).

2.4.2 The enigmatic roles of non-photorespiratory CATs in Arabidopsis

While our data add to previous studies that attest to the essential function of *CAT2* in Arabidopsis, they do not provide substantial evidence for important biological roles for *CAT1* and *CAT3*. Although *CAT3* appears to encode most of the *CAT2*-independent CAT activity in leaves and roots (Figures 2.1 and 2.5), the *cat3* mutation did not produce a significant effect on growth, despite some evidence of increased ROS signals (Figure 2.2). In the double *cat2 cat3* mutant grown in air, loss of *CAT3* function did not reinforce the *cat2*-dependent effect on growth. However, the *cat2* mutation in itself is sufficient to produce a marked dwarf phenotype. To circumvent this effect, and to analyze possible roles of CAT3 in metabolizing H_2O_2 produced through processes other than photorespiration, we examined effects of *cat3* in plants grown at hCO_2, where *CAT2* is not required for optimal growth. In this condition, rosette size in *cat2 cat3* was slightly but significantly decreased compared to Col-0, *cat2*, and *cat3* (Figure 2.4). This suggests that when *CAT2* is absent, *CAT3* plays some role in the processing of either residual photorespiratory H_2O_2 or photorespiration-independent H_2O_2 in leaves. Interestingly, this effect was not observed in *cat2 cat3* grown in SD at hCO_2, pointing to a day length-dependent role for *CAT3*. *CAT3* expression increases in the older leaves of Arabidopsis grown in LD (Zimmermann et al., 2006). Indeed, *CAT3* is annotated as a senescence-associated gene. Perhaps as an indication of this role, we found that *cat2 cat3* was significantly slower to produce a flowering stem compared to Col-0 and *cat2*, although the *cat3* single mutation had no effect (Supporting Information Figure. S5).

Our data suggests that when other CATs are functional, CAT1 makes at most a minor contribution to overall activity in roots and leaves (Figure 2.1; Mhamdi et al., 2010a). *CAT1* expression is strongest in reproductive tissues, including stamens, pollen and seeds (Mhamdi et al., 2010a). It is interesting that the *cat1* mutation did produce some effect on silique viability when introduced into the *cat2* background (Supporting Information Figure. S4). Nevertheless, this effect points to overlapping roles of *CAT1* and *CAT2* these organs, since the *cat1* mutation alone had no significant effect, and the effect of *cat2* alone was minor and similar to that *cat3*. Despite the apparently low *CAT1*-linked activity, evidence for functional overlap with *CAT2* in roots perhaps comes from the experiments in which plants were grown at hCO_2, where growth in the *cat1 cat2* double mutant showed the biggest difference from wild-type (Figure 2.2).

As well as their expression patterns in different organs, the different CATs show cell- and tissue-specificity within organs (Zimmermann et al., 2006). Despite such specificity, our data identify a number of compensatory responses in specific *CAT* transcripts in response to loss of other CAT functions. This is most obvious for *CAT3* transcripts in the *cat2* background and *CAT1* transcripts in *cat3* and *cat2 cat3* lines (Figure 2.1; Supporting Information Figure. S8). Taken together, our data perhaps suggest that CAT1 and CAT3 may be mainly back-up players to CAT3 and CAT2, respectively. Triple *CAT* mutants that have very recently been reported (Su et al., 2018) may enable a functional analysis of overlap between *CAT1* and *CAT3* functions.

2.4.3 Growth day length affects oxidative signaling independent of oxidative stress duration

While previous reports have documented day length-specific outcomes of the *cat2* mutations at the level of phenotypes and gene expression, they have not established that this effect is independent of stress intensity. The transcripts of many oxidative stress-sensitive genes accumulate more strongly in *cat2* grown in SD than in LD (Queval et al., 2007, 2012), but it is not clear whether this simply reflects attenuation of the response after a certain duration of oxidative stress. Here, we sought to establish, first, whether or not this is the case and, second, whether day length-dependent effects on oxidative

stress transcriptomes can be explained by differences in *cat2*-independent CAT activity in LD compared to SD.

Data shown in Figures 2.7 and 2.8 suggest that the impact of day length on *cat2*-triggered gene expression is not the result of differences in the duration of oxidative stress. When the responses of two H_2O_2 marker transcripts to equal-time exposure to oxidative stress were examined, plants grown in SD clearly showed much stronger induction in response to CAT deficiency than those grown in LD. Interestingly, this was the case whether CAT deficiency was provoked by the *cat2* mutation or by treatment with 3-AT, a general inhibitor of CAT activity. Moreover, 3-AT produced a stronger effect on gene expression than did the *cat2* mutation. The similarity between gene induction in *cat2* and *cat2 cat3* suggest that this was not due to additional inhibition of *CAT3*, even though extractable CAT activity after 3-AT treatment was very similar to that in the double mutant (Figure 2.6). While 3-AT is an inhibitor of histidine biosynthesis, it has been commonly used as an inhibitor of CAT (Ferguson & Dunning, 1986; May & Leaver, 1993). It is effective in knocking down CAT activities within hours after spraying (Figure 2.6) without affecting the extractable activities of several other enzymes involved in the ascorbate-glutathione pathway (Supporting Information Figures S7 and S9).

It is interesting that when 3-AT treatment was performed at hCO_2, the two marker genes were not more strongly induced in SD than in LD. This perhaps suggests that the interaction between day length and oxidative signaling is linked somehow to photorespiration, a process that is tightly embedded into photosynthetic and respiratory metabolism in C3 plants (Foyer et al., 2009). Our observations add to the growing awareness of the impact of nutritional and environmental conditions on defence signalling (Kangasjärvi et al., 2012). They are consistent with previous studies showing that responses of plants to ozone exposure are influenced by the day length context (Vollsnes et al., 2009; Dghim et al., 2013). For instance, ozone-triggered lesions in Arabidopsis are more easily induced by equal-time exposure in LD compared to SD (Dghim et al., 2013), similar to LD-dependent lesion formation in *cat2* (Chaouch et al., 2010). Such effects may be related to circadian clock rhythms, which have been reported to interact with oxidative stress and related phytohormone signaling (Nitschke et al., 2016). Here, by using a short-term exposure to oxidative stress of intracellular origin, we have shown that

gene expression responses in leaves are strongly dependent on the history of the plant, and that this cannot be explained by day length-dependent differences in *CAT3* expression. Although we cannot exclude a stressful effect of 3-AT that is additional to CAT inhibition, it is possible that the stronger effect of 3-AT compared to *cat2* and *cat2 cat3* may be another reflection of the redundancy between the three enzymes.

ACKNOWLEDGMENTS

Z.Y. thanks the China Scholarship Council for the award of a PhD grant. This work received financial support from the French Agence Nationale de la Recherche grants ANR12BSV60011 (Cynthiol) to G.N.

CHAPTER 2: Supporting Information

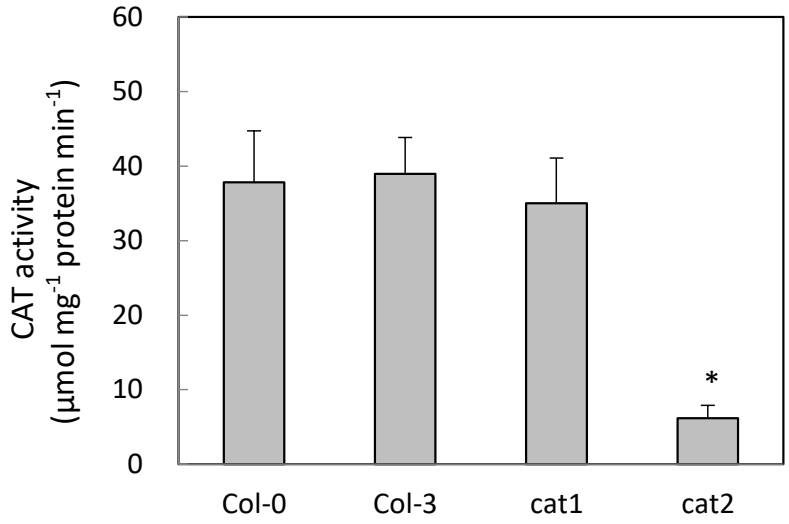

Supporting Information Figure S1. Catalase activities in the roots of Col-0, Col-3, *cat1* and *cat2* backgrounds. Plants were grown for 14d in 0.5 MS in the absence of added sucrose. Data are means ± SE of three biological replicates. * indicates significant difference to Col-0 at $P < 0.05$.

A. Plants grown in air in the absence of sucrose

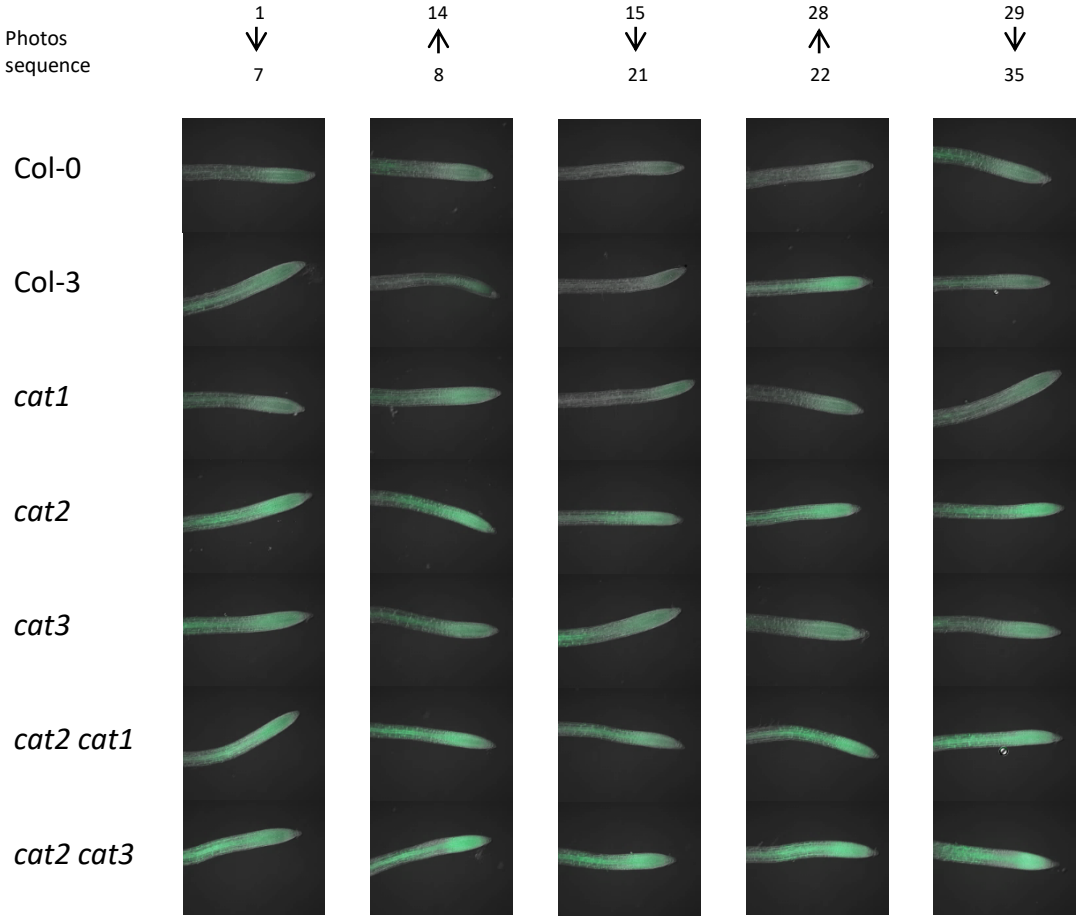

Supporting Information Figure S2. Comparison of ROS signals in root tips using $DCFH_2$-DA in lines grown in different conditions. The images of 10 biological replicates were obtained from plants 10 d after germination. The numbering and arrows indicate the order of image acquisition. designed to minimize time-dependent effects on signal intensity.

A. Plants were grown in air in the absence of added sucrose.

B. Plants were grown in air in the presence or 1% added sucrose.

C. Plants were grown at hCO_2 in the absence of added sucrose.

A. Plants grown in air in the absence of sucrose (continued)

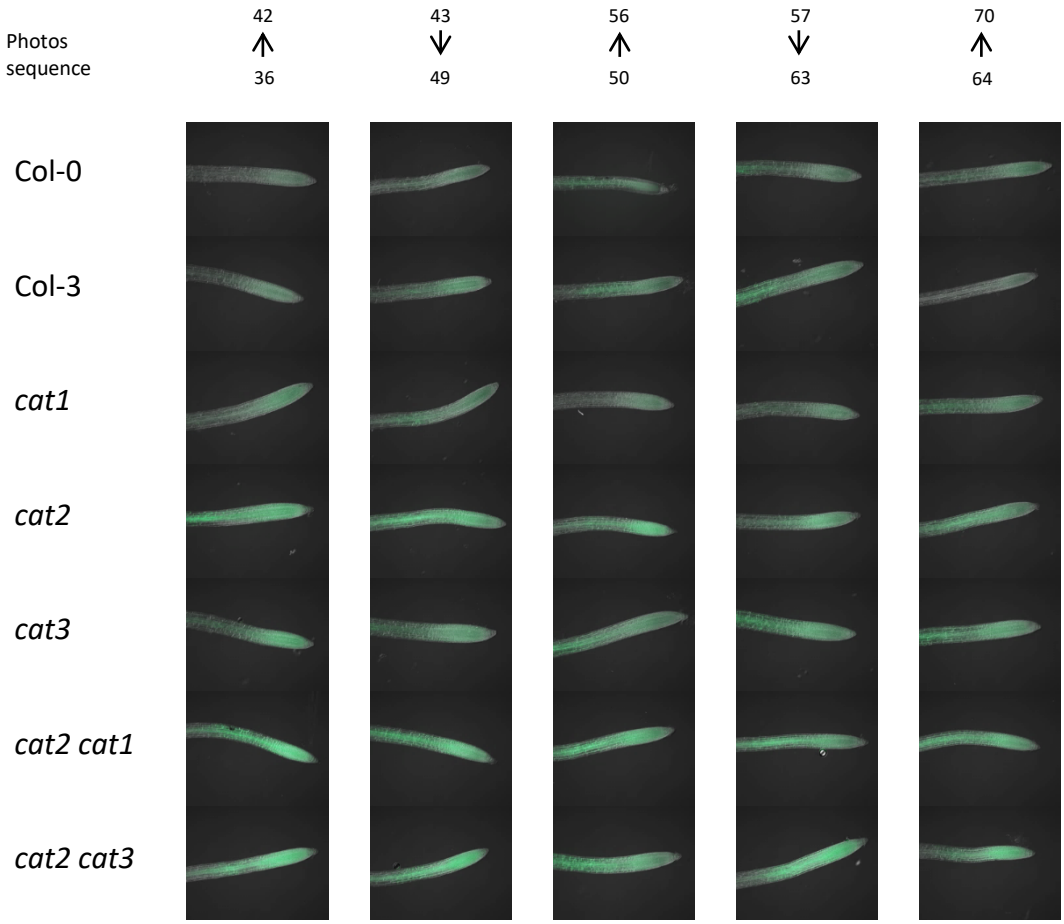

Supporting Information Figure S2. Continued

B. Plants grown in air in the presence of 1% sucrose

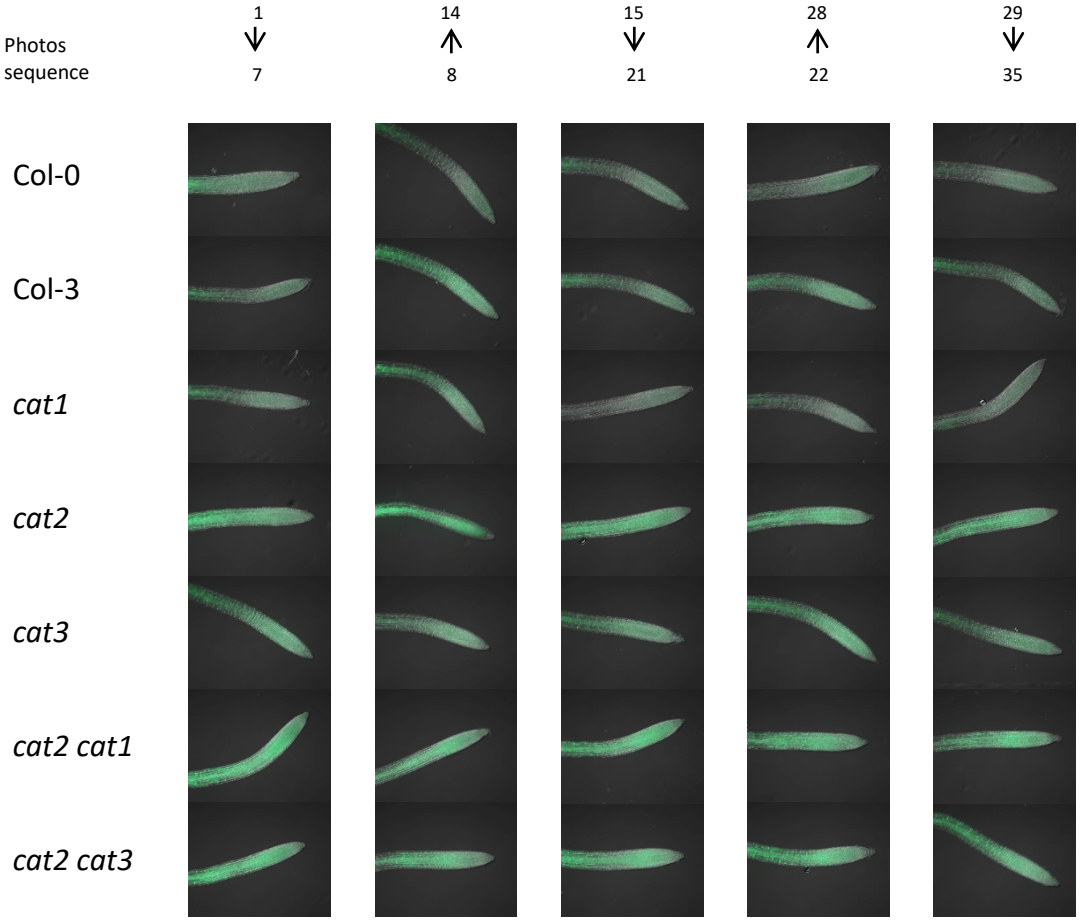

Supporting Information Figure S2. Continued

B. Plants grown in air in the presence of 1% sucrose (continued)

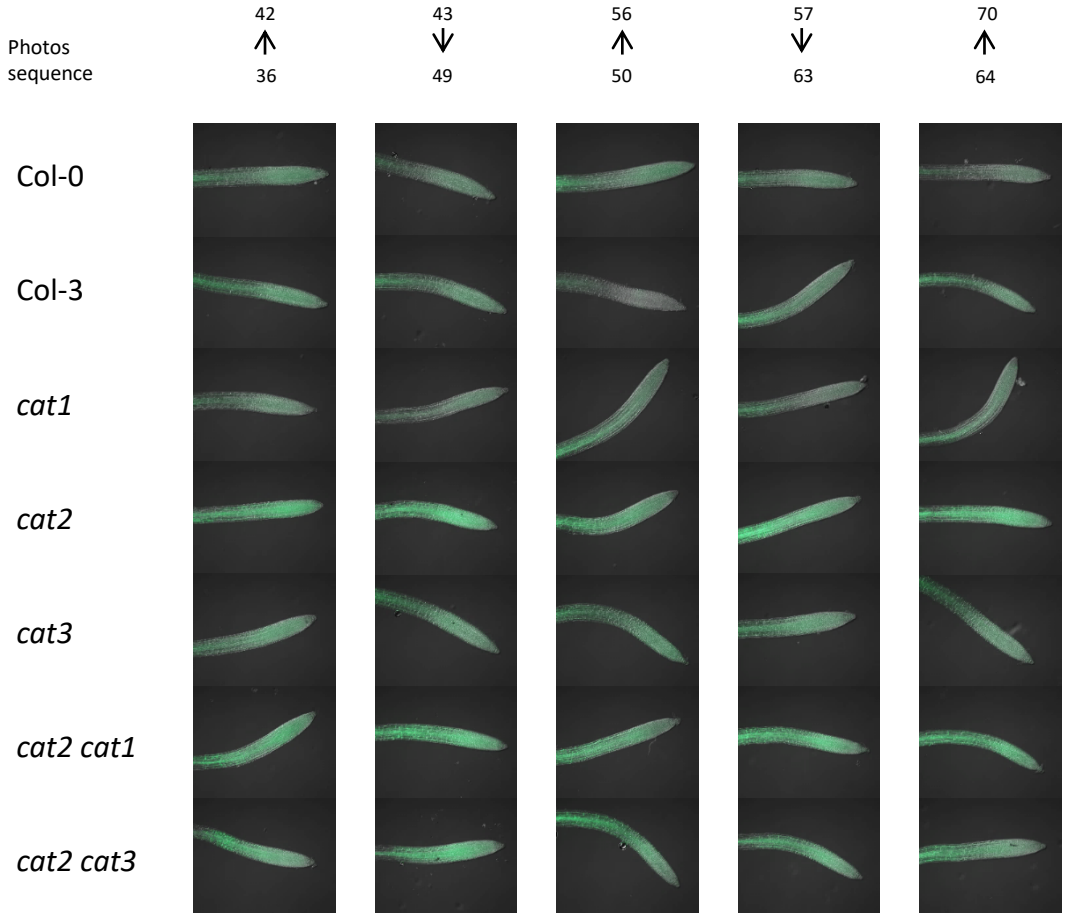

Supporting Information Figure S2. Continued

C. Plants grown at hCO_2 in the absence of sucrose

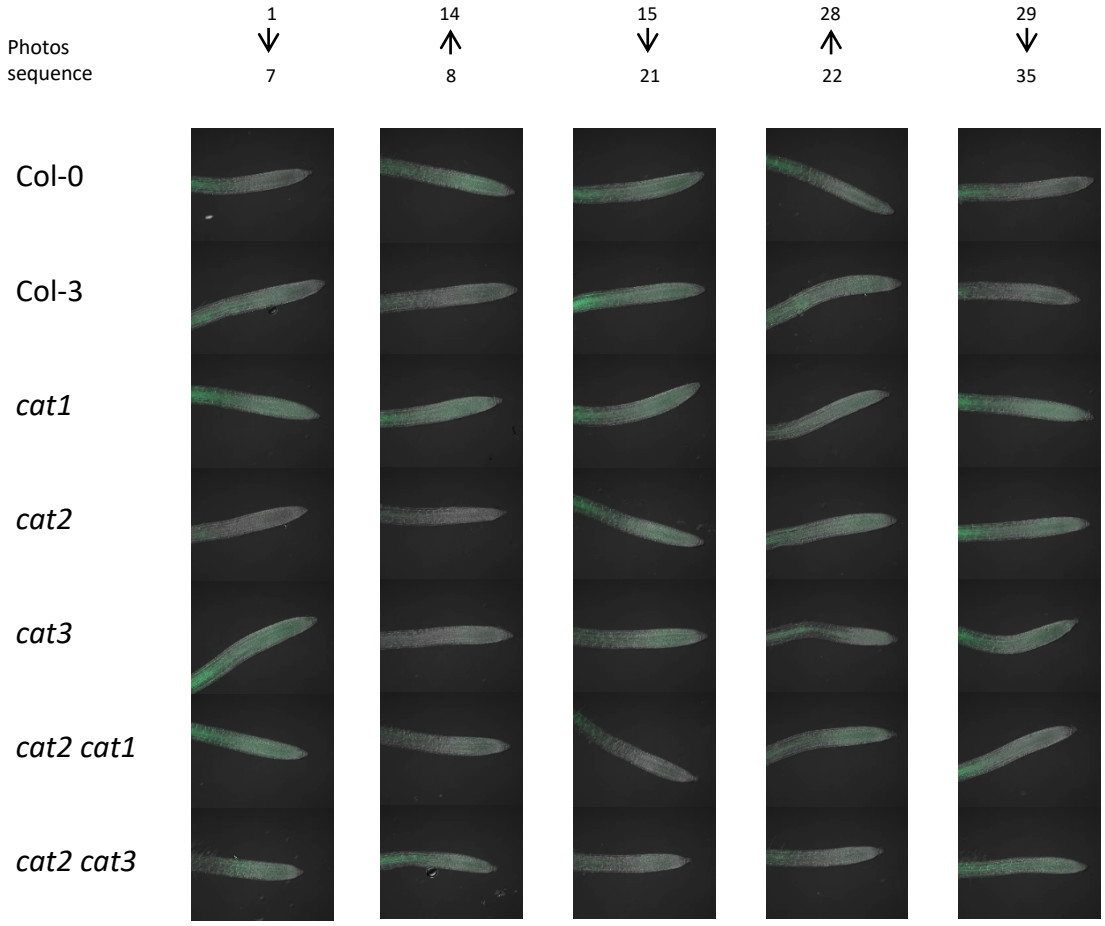

Supporting Information Figure S2. Continued

C. Plants grown at hCO_2 in the absence of sucrose (continued)

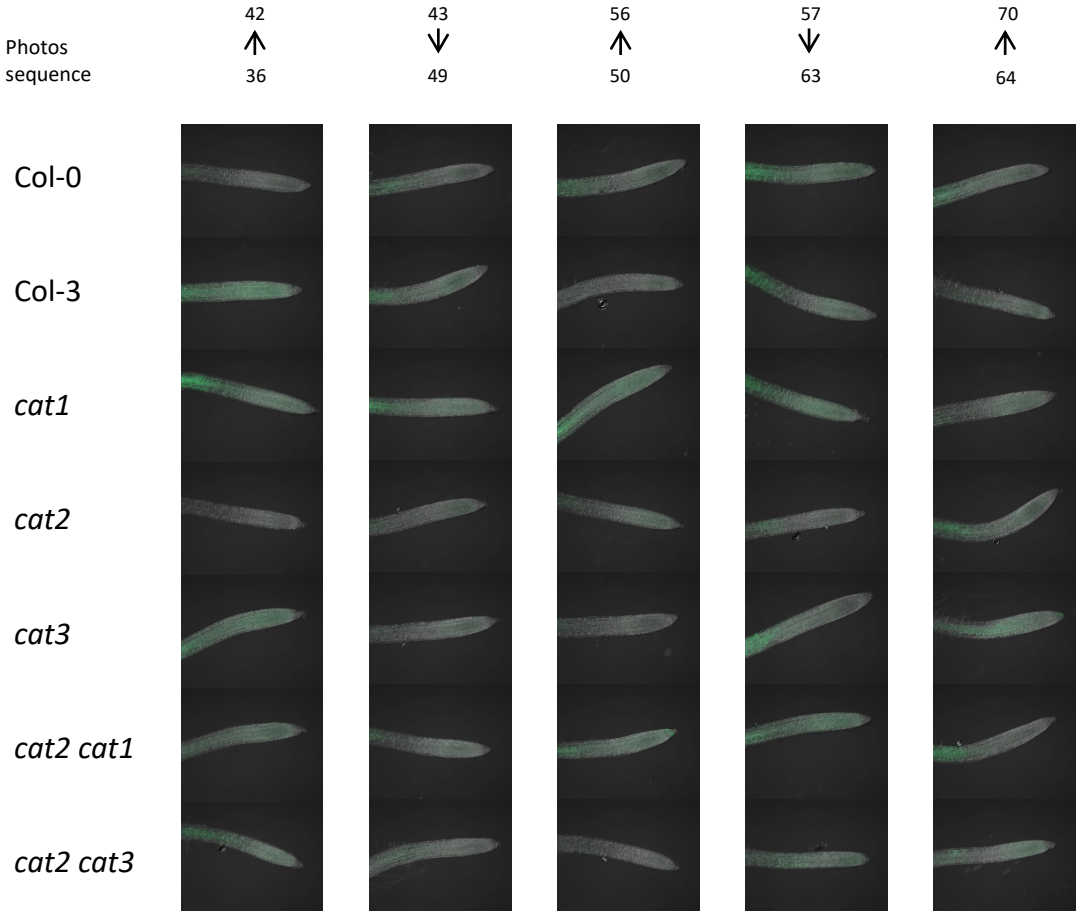

Supporting Information Figure S2. Continued

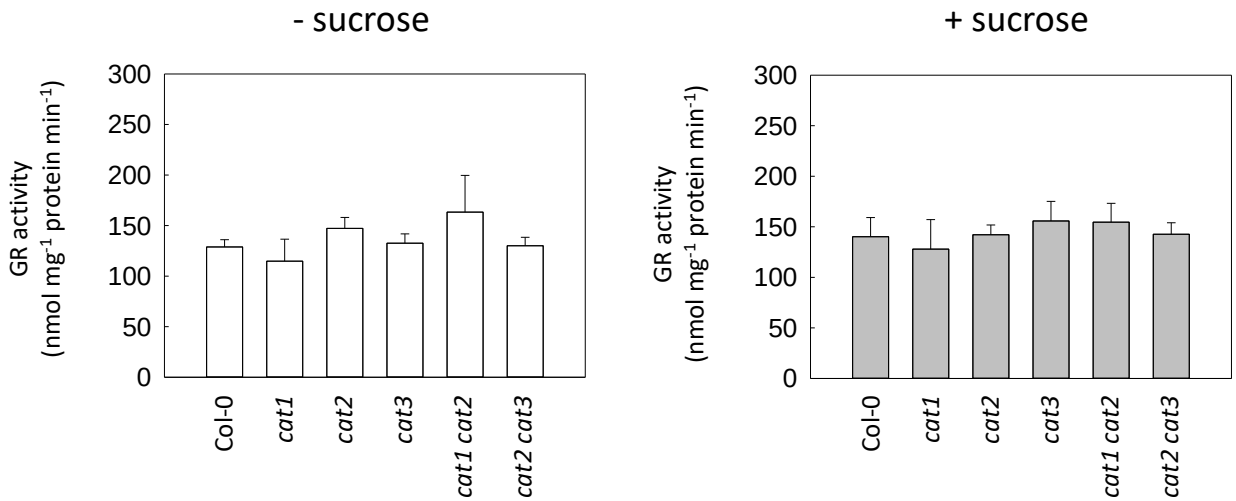

Supporting Information Figure S3. Glutathione reductase activities in roots of single and double catalase-deficient mutants. Plants were grown on 0.5 MS ± sucrose for 14 d in LD air. Then around 100 mg root samples were collected for analysis. Data are means ± SE of three biological replicates. * indicates significant difference from wild type at $P < 0.05$; $^{+}$ indicates significant difference between double mutants and *cat2* at $P < 0.05$.

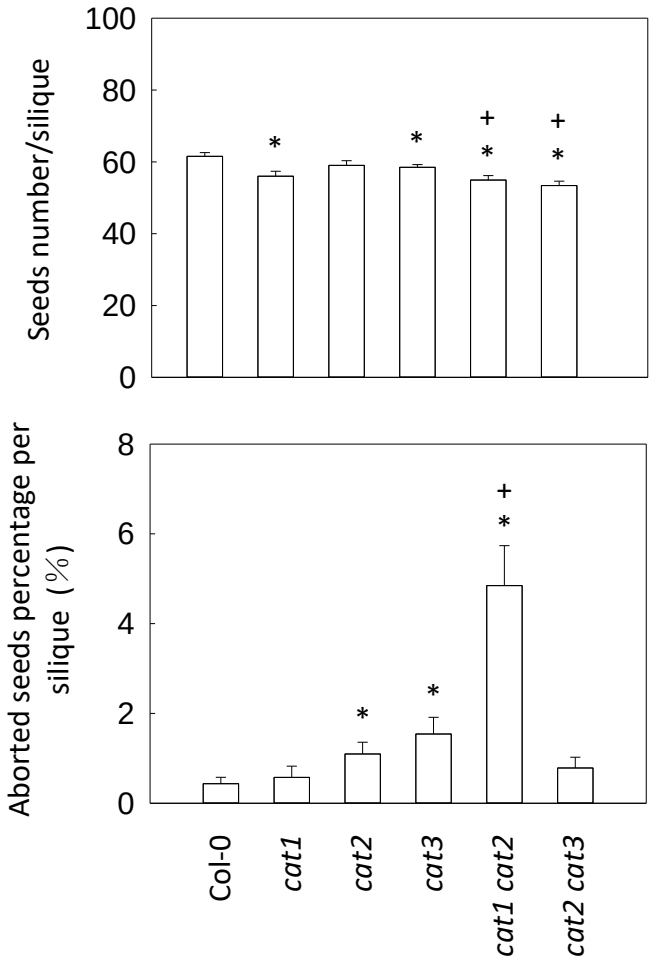

Supporting Information Figure S4. Comparison of siliques in catalase-deficient mutants grown in LD air. Data are means ± SE of at least 20 plants and up to 35 plants (5 siliques per plant) grown in 2 different experiments. * indicates significant difference from wild-type at P<0.05. $^{+}$ indicates significant difference between double mutants and *cat2* at P<0.05.

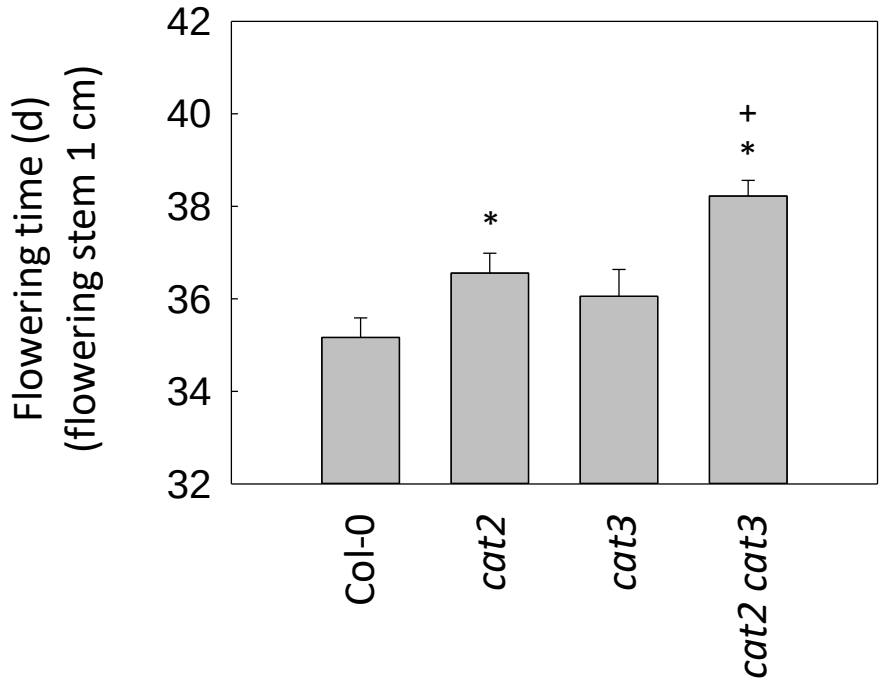

Supporting Information Figure S5. Comparison of flowering time in Col-0, *cat2*, *cat3* and *cat2 cat3* grown in LD hCO_2. The time each plant took to develop a 1 cm flowering stem was recorded. Data are means ± SE of 18 plants. Significant differences to Col-0 at $P < 0.05$ are indicated by *. Significant differences between double mutant and *cat2* at $P < 0.05$ are indicated by +.

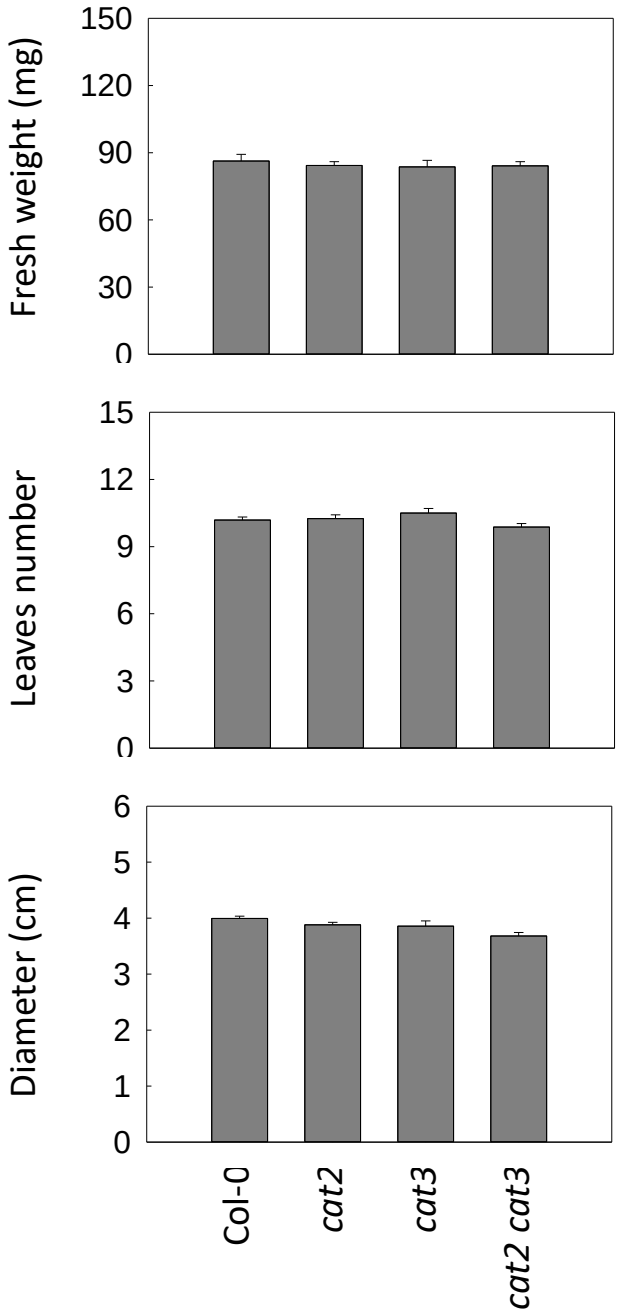

Supporting Information Figure S6. Comparison of rosette phenotype in Col-0, *cat2*, *cat3* and *cat2 cat3* grown in SD hCO_2 for 26 d. Data are means ± SE of 24 plants. Significant differences to Col-0 at $P<0.05$ are indicated by *.

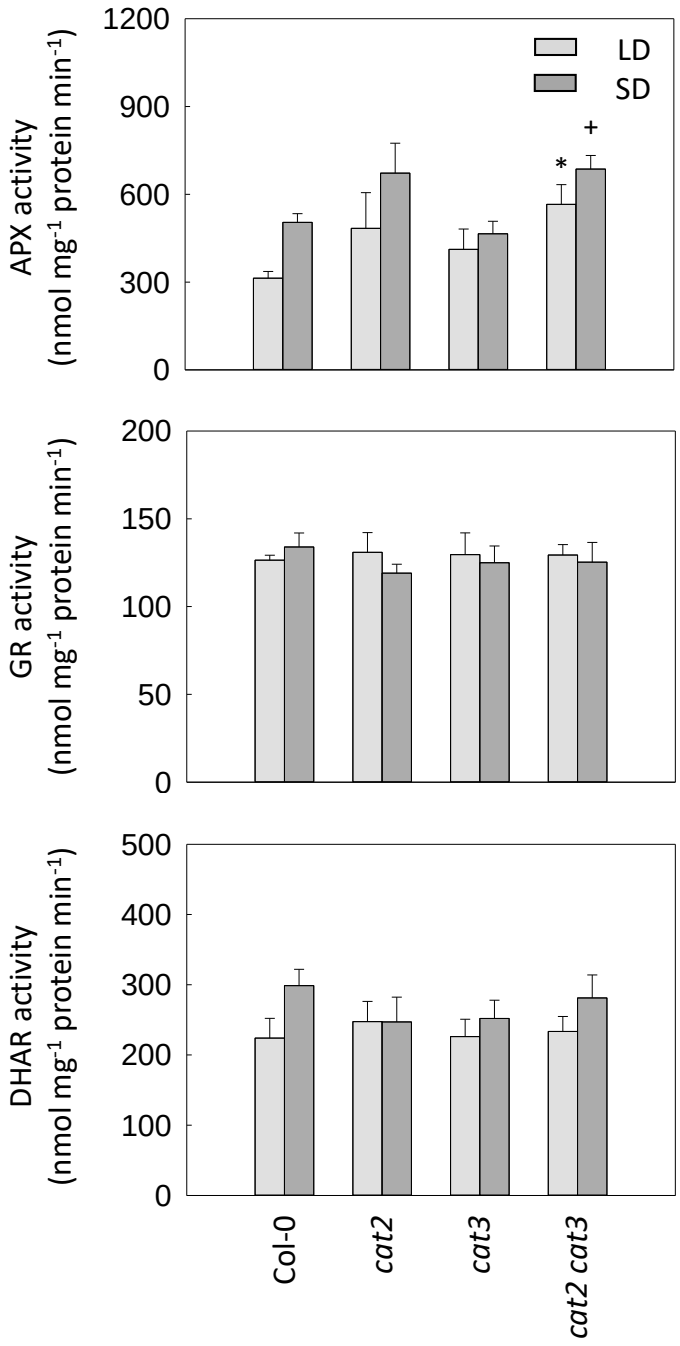

Supporting Information Figure S7. Comparison of antioxidative enzyme activities in leaves of different catalase-deficient mutants. Plants were grown in LD hCO_2 for 20 d or SD hCO_2 for 26 d. Leaf samples were then collected from different plants. Data are means ± SE of 3 biological replicates. * indicates significant difference between mutants and Col-0 in LD at $P<0.05$; $^{+}$ indicates significant difference between mutants and Col-0 in SD at $P<0.05$.

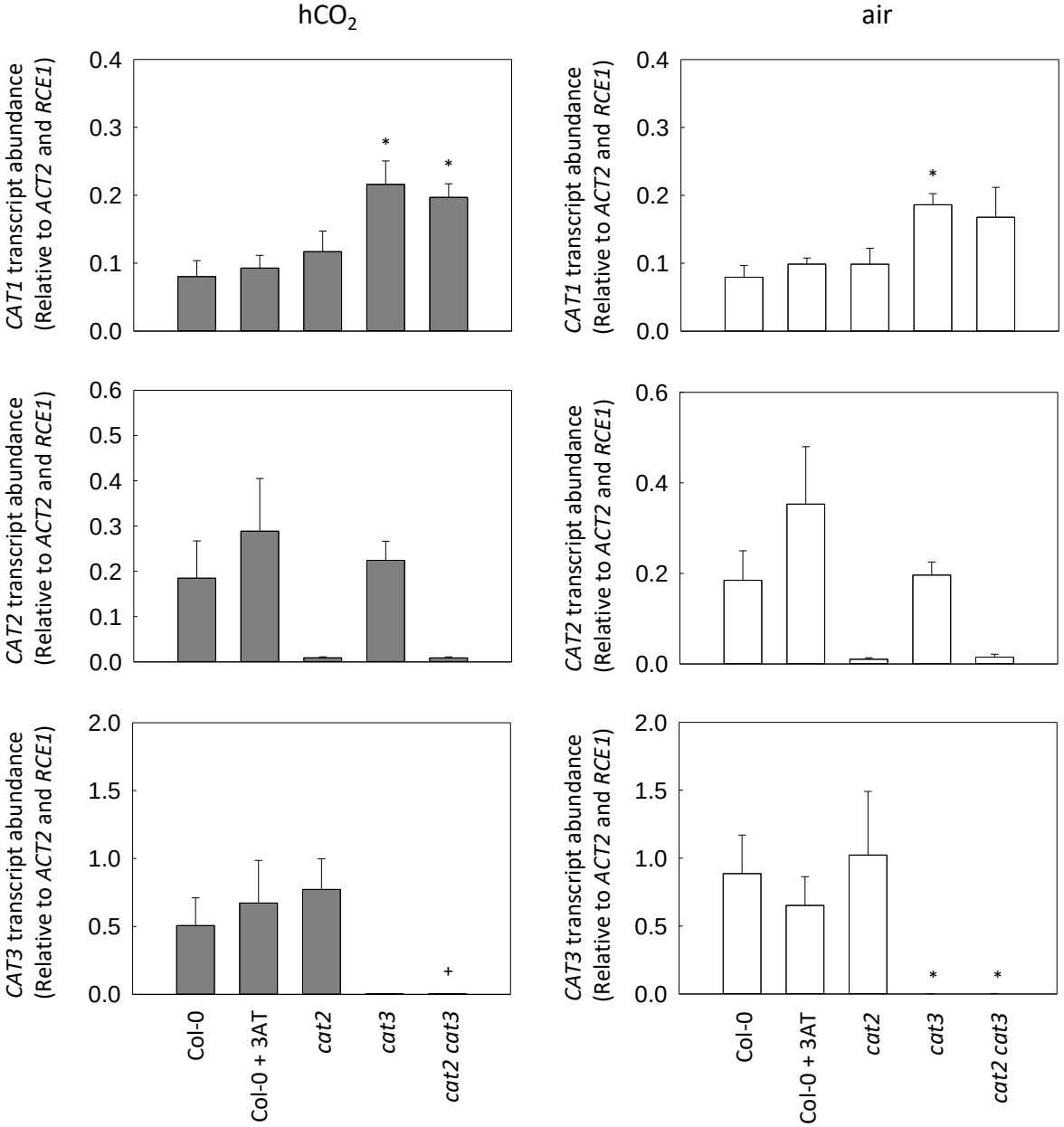

Supporting Information Figure S8. Analysis of catalase transcripts in catalase-deficient mutants in LD hCO_2 or after transfer to air, following the experimental design shown in Figure 2.6. Data are means ± SE of 3 biological replicates. * indicates significant difference from Col-0 at $P<0.05$; $^{+}$ indicates significant difference between double mutant and *cat2* at $P<0.05$.

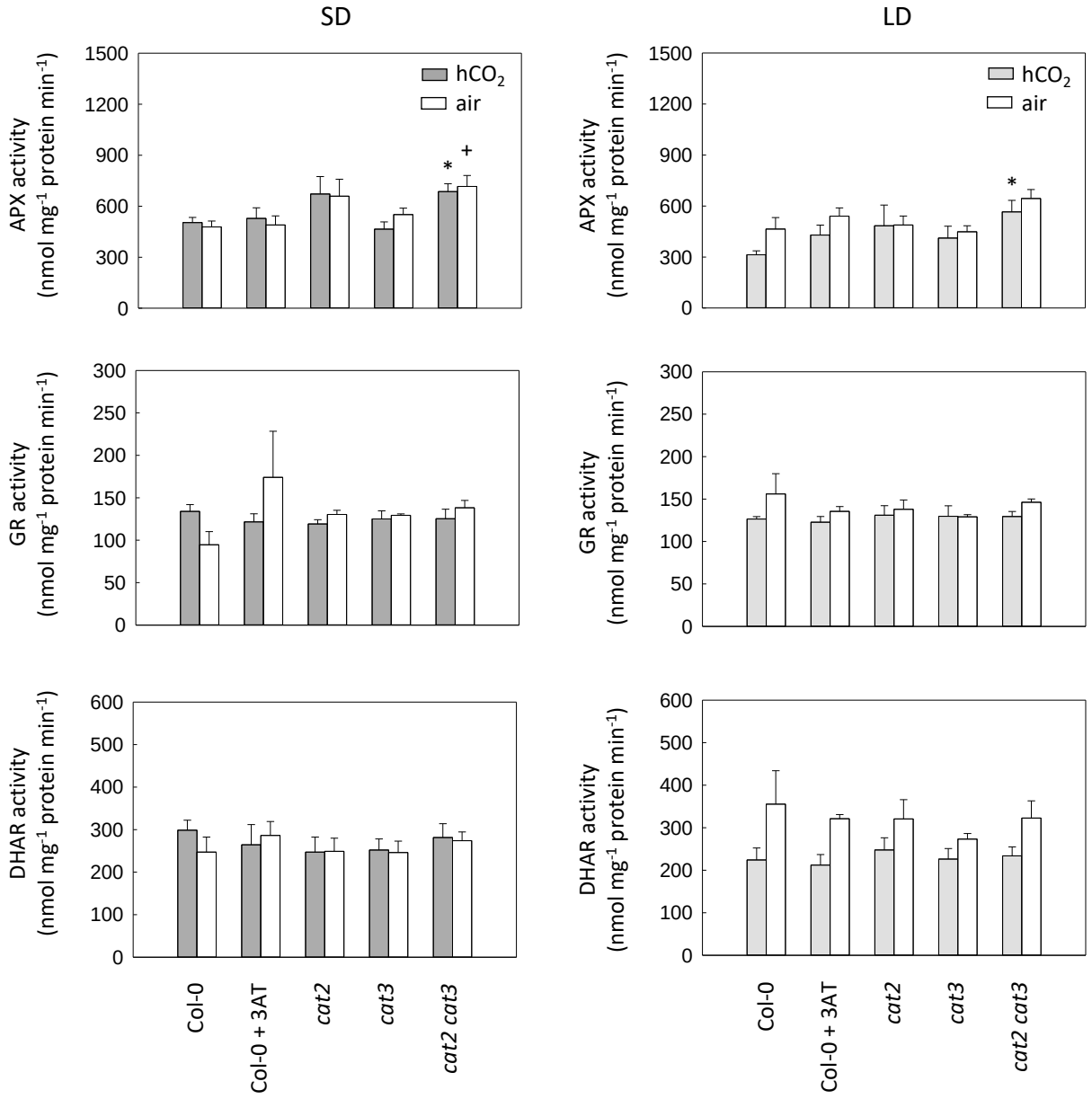

Supporting Information Figure S9. Analysis of antioxidative enzymes activity in catalase-deficient mutants in hCO_2 or after transfer to air, following the experimental design shown in Figure 2.6. Data are means ± SE of 3 biological replicates. * indicates significant difference between mutants and Col-0 in hCO_2 at $P<0.05$; $^{+}$ indicates significant difference between mutants and Col-0 in air at $P<0.05$.

Supporting Information Table S1. Oligonucleotide sequences used in this study

N°	Oligonucleotide	Sequence	Technique
1	ForCAT1	TCCAGGTCAATTACTTCCCTTCA	Genotyping
2	RevCAT1	AGGCTCCGAAAGCGCTTCAA	Genotyping
3	ForCAT2	CCCAGAGGTACCTCTTCTTCTCCCATG	Genotyping
4	RevCAT2	TCAGGGAACTTCATCCCATCGC	Genotyping
5	ForCAT3	TCGATTGTTTAGACGTCCGAC	Genotyping
6	RevCAT3	AGGTTTGAAATGTCATGGGTG	Genotyping
7	Lb1	TGGACCGCTTGCTGCAACTCT	Genotyping
8	LBSail	GAAATGGATAAATAGCCTTGCTTCC	Genotyping
9	ForACTIN2	CTGTACGGTAACATTGTGCTCAG	qRT-PCR
10	RevACTIN2	CCGATCCAGACACTGTACTTCC	qRT-PCR
11	ForRCE1	CTGTTCACGGAACCCAATTC	qRT-PCR
12	RevRCE1	GGAAAAAGGTCTGACCGACA	qRT-PCR
13	ForCAT1	AAGTGCTTCATCGGGAAGG	qRT-PCR
14	RevCAT1	CTCCGAAAGCGCTTCAAC	qRT-PCR
15	ForCAT2	TGCTGGAAACTACCCTGAATGG	qRT-PCR
16	RevCAT2	TCAACACCATACGTCCAACAGG	qRT-PCR
17	ForCAT3	CCACTTGATGTGACCAAGATCTG	qRT-PCR
18	RevCAT3	GTAGATTCCAGGAACCACAAGACC	qRT-PCR
19	ForGSTU24	TCCATAGCTGGTTTGCAGTG	qRT-PCR
20	RevGSTU24	TAGCGACGCTCTCTCTCTCC	qRT-PCR
21	ForUGT73B3	CCTCACCACACCTCTCAACTC	qRT-PCR
22	RevUGT73B3	TCTGGTAACCCGAGATCCAC	qRT-PCR
23	ForAPX1	GCACTATTGGACGACCCTGT	qRT-PCR
24	RevAPX1	GCAAACCCAAGCTCAGAAAG	qRT-PCR

CHAPTER 3

Effect of a specific isoform of glucose-6-phosphate dehydrogenase on H_2O_2-induced SA signaling: a genetic screen for revertant lines

Summary

Lesion formation and associated salicylic acid (SA) signaling triggered by the *cat2* mutation can be abolished by inactivating the SA synthesis pathway through the *sid2* mutation. Interestingly, knocking out a specific isoform of glucose-6-phosphate dehydrogenase (G6PD5) in the *cat2* background produces a very similar effect, but the reasons remain to be elucidated. To identify genes involved in linking intracellular H_2O_2 and G6PD5 in SA signaling, a classical (forward) genetics screen was employed. Seeds of *cat2 g6pd5* were mutagenized with ethyl methanesulfonate and the M2 population was visually screened for individuals that show a similar phenotype to *cat2* (lesions on the leaves). Six candidate revertants with this phenotype were obtained. Following at least one backcross to *cat2 g6pd5*, DNA was isolated from pooled F2 individuals that showed lesions and candidate genes were identified by genome sequencing. The data show that four of these six lines are mutated in genes known to be involved in cell death regulation linked to the SA pathway. Of these four, three carry mutations in the gene encoding *myo*-INOSITOL PHOSPHATE SYNTHASE 1 (MIPS1) while one is mutated in *CONSTITUTIVE EXPRESSOR OF PR GENES 5* (CPR5). In the other two lines, the identified mutations were not in recognized players involved in lesion formation, providing interesting perspectives for further work to characterize the roles of the genes involved.

3.1 Introduction

Pathogen attack is one of the common constraints during plant growth and development. The perception of an invading pathogen commonly stimulates an oxidative burst in infected tissues, with accumulation of H_2O_2. Although there are several sources of pathogen-induced H_2O_2 accumulation, NADPH oxidases have received particular attention (Torres and Dangl, 2005). The high level of H_2O_2 triggers rapid death of plant cells directly in contact with or close to the pathogen. This effect is termed the hypersensitive response (HR; Mur et al., 2008). HR is a widespread phenomenon which contributes to the activation and establishment of plant immunity to disease. As one of the most efficient and immediate resistance reactions, it plays a crucial role in preventing the infection from spreading by sacrificing both infected and adjacent cells. It can also lead to systemic acquired resistance (SAR), a mechanism with enhanced resistance against a wide range of pathogens following an earlier localized attack by a pathogen (Dietrich et al., 1994; Torres et al., 2006; Van Breusegem and Dat, 2006). Accompanied by lesion formation and SAR, the interaction of plants and pathogen also cause *PR* genes induction and SA accumulation (Takahashi et al., 1997; Chamnongpol et al., 1998; Mittler et al., 1999).

The *cat2* mutant has been well described as a lesion-mimic mutant because it shows spontaneous localized lesions similar to those observed in response to bacterial pathogens. As mentioned in the last chapter, oxidative stress responses in *cat2* leaves, including lesion formation, are day length-dependent. Previous work in our group revealed that *cat2* plants grown in LD, but not SD, show obvious lesions (Queval et al., 2007). The lesion phenotype in *cat2* is associated with accumulation of SA and activation of pathogenesis response pathways. The *sid2* mutant is defective in ISOCHORISMATE SYNTHASE1 (ICS1), an enzyme associated with SA synthesis in Arabidopsis challenged with pathogens. When the *sid2* mutation was introduced into the *cat2* background, the lesion phenotype observed in LD condition was reverted, and this effect was accompanied by inhibition of oxidative stress-induced SA accumulation and induction of *PR* genes (Figure 3.1). Furthermore, treatment of rosette leaves with SA restored the lesion phenotype in *cat2 sid2* in LD and also triggered lesion formation in *cat2* in SD. These results demonstrate that H_2O_2-induced lesion and

pathogenesis associated response are dependent on SA through the isochorismate pathway (Chaouch et al., 2010).

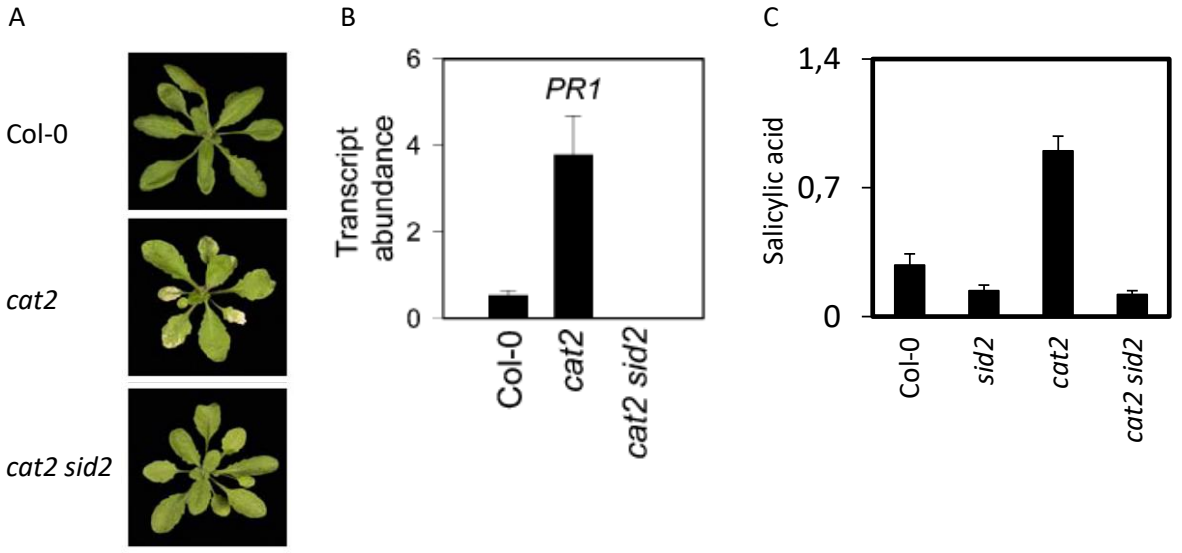

Figure 3.1. Effects of *sid2* mutation on *cat2*-induced lesion and SA signaling. Figures taken from Chaouch et al. (2010)
A. Phenotype of rosette of plants grown in LD air for 25 d.
B. *PR1* transcript relative to *ACTIN2* transcripts.
C. SA accumulation in different genotypes. Results derived from metabolite profiling by GC-MS analysis.

NADPH is a crucial component required for ROS metabolism by the ascorbate/glutathione pathway and TRX pathway, as well as ROS production by NADPH oxidases. The production of NADPH relies on several different enzymes (Foyer and Noctor, 2009). As noted in Chapter 1, G6PDH is a potentially important source of intracellular NADPH and may be involved in various environmental stress responses. In Arabidopsis, the different isoforms are distinguished by their separate localization and function. When I arrived in the laboratory, it was known from the unpublished work of Amna Mhamdi that knocking out a specific cytosolic isoform of G6PDH (*G6PD5*) abolished the *cat2* lesion phenotype (Figure 3.2A). Further, transcriptome analysis showed that most of the genes induced in *cat2* were much less induced when *G6PD5* function is lost (Figure 3.2B). Strikingly, the abolition of *cat2*-induced lesions by *G6PD5* deficiency is very similar to that caused by the *ICS1* mutation. Microarray analyses revealed a significant overlap between the *cat2 g6pd5* and *cat2 sid2* transcriptomes. For instance, for the top 50 genes that are highly induced in *cat2* (relative to Col-0),

the *g6pd5* and *sid2* secondary mutations produced a very similar effect and repressed many of these transcripts to the Col-0 level (Figure 3.2C). These results demonstrate that *g6pd5* mutation mimics the *sid2* mutation in abolishing transcriptome responses triggered by intracellular H_2O_2. In order to get mechanistic insights on the function of G6PD5 in transducing H_2O_2 signals, a first strategy that the group took before the start of my PhD, was to analyze links between the production of NADPH by G6PDH and the function of NADPH-dependent RBOHs. These and other approaches are ongoing. In this chapter, I describe work that introduced a forward genetics approach to elucidate the role of G6PD5 in H_2O_2-triggered lesion formation.

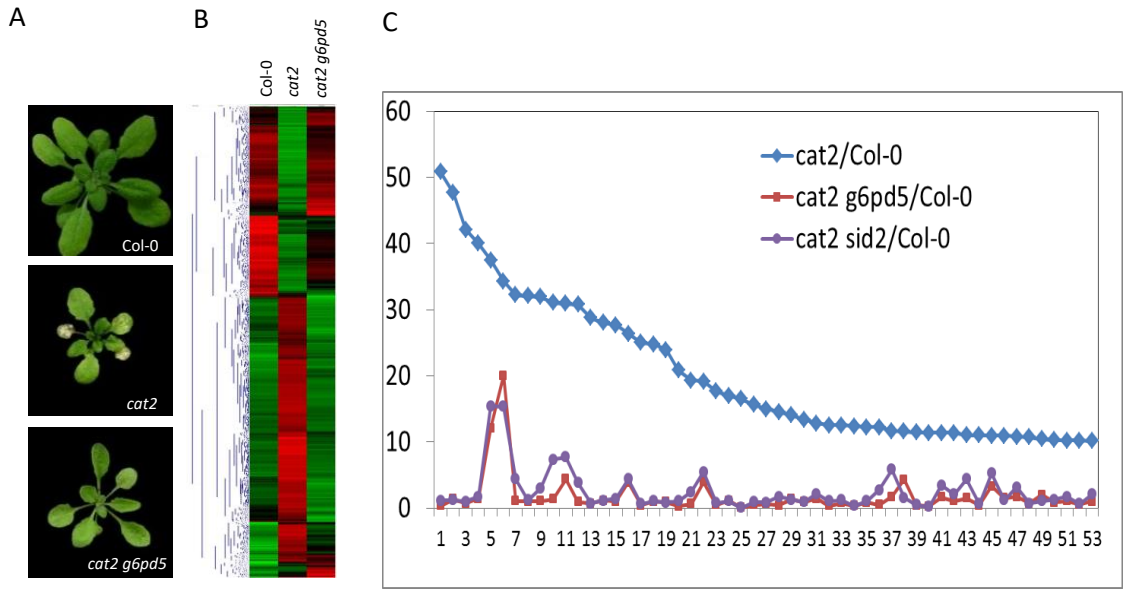

Figure 3.2. Effects of the secondary *g6pd5* mutation on *cat2* phenotype and genes expression. Figures taken from Mhamdi et al. (unpublished)

A. Phenotypes of plants grown in LD air for 3 weeks from seeds.

B. Transcriptome comparison among Col-0, *cat2* and *cat2 g6pd5*.

C. *cat2 g6pd5* transcriptome overlap with *cat2 sid2*. The figure includes the top 50 transcripts highly induced in *cat2* relative to Col-0.

With the completion of genome sequencing programmes, emphasis in genomics has shifted from sequence analysis to gene function investigation. For example, with a sequenced reference genome from the Columbia (Col-0) accession (The Arabidopsis Genome Initiative, 2000), Arabidopsis has been used extensively as a model organism to understand plant development, physiology, and

metabolism. Over the past few decades, many techniques of forward and reverse genetics have been developed to identify causative mutations in *Arabidopsis thaliana*, like chemical, irradiation and insertional mutagenesis (Page and Grossniklaus, 2002; Peters et al., 2003; Henikoff and Comai, 2003). Forward genetics has been proven to be a powerful tool for identifying the components involved in a specific biological process or a signaling pathway. In comparison to reverse genetics approaches such as that described in Chapter 2, this strategy is much less reliant on prior knowledge, and can therefore uncover novel functions for genes through an unbiased approach.

Among all methods in forward genetics, T-DNA insertion and chemical mutagenesis such as EMS are the most widely used. The insertional mutations tend to result in complete knockouts of the gene, making it difficult to link a phenotype other than death with essential genes. Therefore the mutational spectrum with effects on gene function can be limited. In addition, plants mutagenized with T-DNA typically have only one to three insertions per line. So the size of a "saturated population", ie, one in which at least one insertion mutation is randomly generated for most genes, is typically extremely high. Screening so many plants can be prohibitive if the mutant screen being performed is laborious or slow. As a complementary approach, chemically induced mutants have been shown to provide an efficient alternative. Firstly, chemical mutagenesis may produce promoter or missense mutations in the coding region, resulting in a non-lethal knock-down rather than a potentially lethal knockout of a protein function. Consequently, it is easier to understand the functions of essential genes by generating weak non-lethal alleles. Because each individual line can bear single point missense and nonsense substitutions in hundreds of genes, an allelic series of induced mutations with different effects on a given gene's function can be isolated by screening a few thousand mutagenized plants. An additional potential advantage of chemical mutagenesis is that it can be used not only to identify the function of a given gene but also to understand the role of specific amino acids in protein function, thanks to the production of short deletions or point mutations.

As a chemical mutagen, EMS may preferentially induce alkylation of guanine (G), forming O6-ethylguanine which pairs with thymine (T) instead of cytosine (C). Thereafter the single-base change leads to the conversion of C/G pairs to T/A during the subsequent DNA repair. This substitution occurs

at a high frequency during the mutagenesis, even though EMS also generates G/C to C/G or G/C to T/A transversions by 7-ethylguanine hydrolysis or A/T to G/C transition by 3-ethyladenine pairing errors. The efficiency of this mutation effect may be dose-dependent. In general, the higher the EMS concentration used to treat seeds, the larger the number of mutations induced in each individual (Martín et al., 2009). In addition, some genotypes may be more susceptible to EMS treatment than others. Other factors that affect mutation frequency are the gene's position in the genome and the treatment condition during mutagenesis. For example, effects such as embryo-lethality and mutations that cause decreases in Chl are directly related to the length of exposure to a fixed concentration of EMS (Koornneef et al., 1982).

Identification of the genetic basis of a mutant phenotype has become much easier and faster within the past few years. Until recently, map-based cloning or positional cloning was still required, which are relatively lengthy and onerous (Arondel et al., 1992; Meyer et al., 1994). This strategy is usually based on outcrossing the mutant plant to a divergent Arabidopsis accession, often involving crosses between Col-0 and *Landsberg erecta* (Ler). In the F2 generation, the mutant phenotype is scored and molecular markers are then used to provide an approximate location of the mutated gene's physical position. Finally, plants with intra-chromosomal recombination events are used to narrow down the genetic interval. The recombination frequency has been shown to vary across the genome with low recombination frequencies hindering fine mapping (Lynn et al., 2002; Drouaud et al., 2006). Further, the whole mapping processes can be difficult if the mutant phenotype is subtle and if assaying the phenotype is labor-intensive. To avoid this time-consuming effect, traditional map-based cloning has progressively been replaced by direct identification through sequencing. Initially, a pool of DNA isolated from bulked segregants was sequenced and used for simultaneous mapping and mutant identification (Schneeberger et al., 2009; Cuperus et al., 2010; Austin et al., 2011). Although these approaches are fast and straightforward, the considerable phenotypic variation in F2 populations from crosses between different accessions impairs the recognition of mutants with subtle phenotypic alterations. In addition, if genetic screens involve modifiers of a preexisting mutant, the mapping depends on the availability of the primary mutant in another suitable accession, the introgression of the mutation in such a background, or the laborious additional genotyping for the presence of the first-site

mutation. However, these limitations have largely disappeared with the advent of very rapid genome sequencing technology. This allows direct identification of mutations, meaning that mapping is no longer necessary. Currently, a simpler approach of backcrossing mutants to their non-mutagenized progenitor can be used (Abe et al., 2012; Hartwig et al., 2012; Thole and Strader, 2015). Combined with bulk segregation analysis and comparative whole genome sequencing, the number of causal candidates identified in the genome of the mutated plant can be reduced to an acceptable level.

In this part of the work, an EMS mutagenesis of *cat2 g6pd5* was performed and a genetic screen for revertants that present lesions was conducted. Our aim was to further investigate the underlying mechanisms by which G6PD5 is required for lesion formation and, thereby, to define novel components that might link G6PD5 to the activation of SA-associated pathways.

3.2 Results

3.2.1 The evaluation of mutagenesis efficiency

To produce a population of chemically induced mutant lines for the forward genetics study, we treated around 2000 seeds of *cat2 g6pd5* homozygotes (M0) with 0.3% EMS (Qu and Qin, 2014) for 15 h with gentle rotation. Subsequently, these mutagenized seeds (M1) were sown in square pots (nine seeds per pot). Plants were self-pollinated and seeds of the first generation (M2) were harvested in pools. To estimate the efficiency of the mutagenesis, we quantified embryo lethality in siliques of M1 plants as an indicator (Till et al., 2003; Martín et al., 2009). This is performed by estimating the proportion of fully or nearly fully sterile fruits (class A) and the proportion of semi sterile or normal fertile fruits (class B and C). We dissected ten siliques from each of five individual plants selected randomly. As is shown in Table 3.1, among all fifty siliques dissected, only one class B and one class C fruit were observed. Therefore the frequency of class (B+C) is 4%, which is in accordance with the expected range between 2% and 35% (Martín et al., 2009). The efficiency of the EMS mutagenesis was towards the high end of this range, but was considered adequate to continue the genetic screen.

Table 3.1. Embryo lethality degree in the siliques of M1 plants. Ten siliques from each of five M1 Plants (50 in total) were examined for aborted seeds. Siliques were categorized into three classes based on the visual determination of normal and aborted seeds number. Class A: aborted seeds > 20 %; class B: 20 % ≥ aborted seeds ≥ 6.7 %; class C: aborted seeds < 6.7%.

Class category	Number of siliques
A (aborted > 20 %)	48
B (20 % ≥ aborted 6.7 %)	1
C (aborted < 6.7%)	1
(B+C)%	4

3.2.2 The revertant screen

All M2 seeds were pooled together and used for the screen. As is shown in Figure 3.3A, the strategy was based on a screen for lesion phenotypes. Any plants that showed lesions were analyzed by PCR at the *CAT2* and *G6PD5* loci to confirm their homozygosity for the T-DNA insertions, and confirmed *cat2 g6pd5* homozygotes were self-fertilized and individually harvested. After further confirmation of the phenotype and genotype in the next generation, they were backcrossed with *cat2 g6pd5*. Subsequently, segregants showing cell death were pooled for sequencing to find the candidates for the causal mutation.

Specifically, the screen was carried out with plants sown and grown in soil. Nine seeds were sown in each square pot and more than 1600 seeds were planted in total for each batch of screened individuals. As negative and positive controls for phenotyping and genotyping, Col-0, *cat2* and *cat2 g6pd5* were always grown simultaneously alongside mutated plants. After two days in a cold room at 4 °C in dark, plants were transferred to a controlled-environment growth chamber room in LD (16 h light/8 h dark). In *cat2*, lesions initially develop after about two weeks growth and then spread clearly on the rosette area within the following week. Hence, the lesion phenotype screen was performed on plants at 21-25 d of age to make sure that any revertants to the *cat2* phenotype would be visible. Plants showing clear cell death were screened and first genotyped by PCR to check that they were *cat2 g6pd5* homozygotes. To date, six M2 plants that show a *cat2*-like lesion phenotype have been identified using this strategy (Figure 3.3B). It should be noted that while these plants are all *cat2 g6pd5* genotypes that

show *cat2*-like lesions, they do present some differences in leaf shape and rosette size. In some lines, the rosettes have a similar size to *cat2* while others are much smaller. These screened plants were conserved and seeds of M3 were harvested for confirmation of the lesion phenotype and *cat2 g6pd5* homozygous genotype in M3 plants.

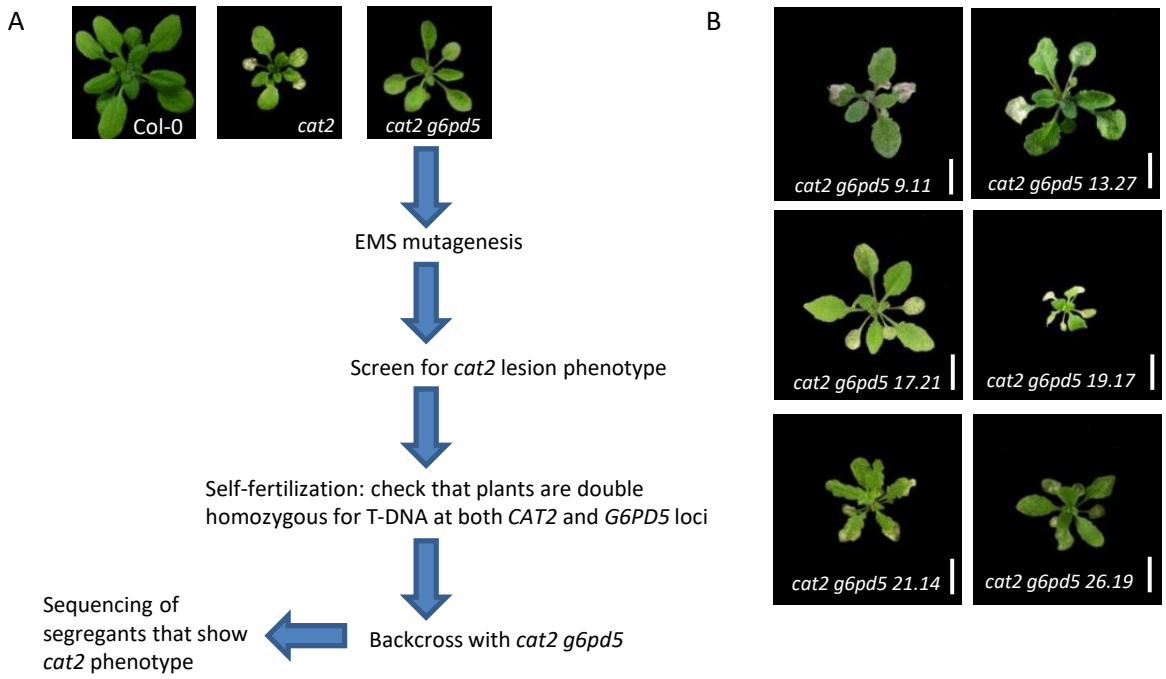

Figure 3.3. Screening strategy (A) and photographs of revertant plants (B). Photographs were taken after grown in LD air for three weeks.

3.2.3 Backcross to *cat2 g6pd5* and segregation analysis

Because EMS mutagenesis induces multiple point mutations in each plant, the high rate of mutagenesis makes it possible that relatively few plants in the screen will be enough to find those with the phenotype of interest. On the other hand, a high mutation density implies that undesired background mutations in selected mutant lines need to be cleaned up to identify the causal mutation. This is partly accomplished by backcrossing the newly identified plants with their parental lines (Weigel and Glazebrook, 2002). An example is shown in Figure 3.4 for the first identified line, 9.11.

The M3 plants of line 9.11, all of which showed clear lesions, were first backcrossed with their

parental line *cat2 g6pd5*. The principle behind this approach is that the causal mutation of line 9.11 introduced by EMS mutagenesis is homozygous in M3. In contrast, other introduced mutations unlinked to the lesion phenotype are likely to be random in zygosity. Backcross with *cat2 g6pd5* does not change the homozygous genotype at the *CAT2* and *G6PD5* loci but the causal mutation should be heterozygous in the F1 backcross. Therefore, the phenotype of F1 plants provides a first indicator to distinguish if the causal mutation is dominant or recessive. Specifically, if F1 plants do not show lesions, the mutation should be recessive; otherwise it is likely to be dominant. This information is also an important reference for the following phenotype segregation. By now the six lines we have obtained are all recessive mutations according to the phenotype of the F1 after backcross (Table 3.2).

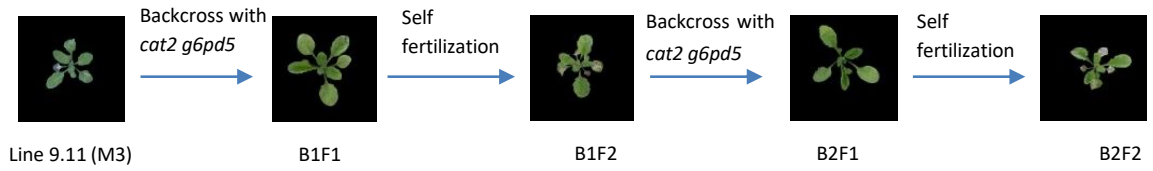

Figure 3.4. Example of backcross for line 9.11. This plant was found to show cell death during the original screen. After the phenotype and the *cat2 g6pd5* homozygous genotype were confirmed in the next generation (M3), it was backcrossed to *cat2 g6pd5*. The *cat2 g6pd5* genotype was confirmed for all the following generations. F1 plants did not show lesions (B1F1). Segregants showing lesions in the next generation (B1F2) were backcrossed to *cat2 g6pd5* again. Then F2 plants with lesions (B2F2) were pooled for sequencing.

From the self-fertilized F1 plants, F2 seeds were harvested from several individual plants and the phenotype segregation was checked for each plant. According to the number of plants showing lesions or not in F2, we can obtain the phenotype segregation ratio for each F1 plant. These data provide an indicator to infer the likely number of causal mutations involved in the phenotype effect and to confirm whether causal mutations are dominant or recessive. For instance, if one quarter of the plants shows lesions, the simplest explanation would be a single causal mutation that is recessive. If three quarters show lesions, this would be consistent with the causal mutation being single and dominant. For more complicated cases, e.g. if two unlinked recessive mutations are involved, the segregation ratio should be 1/16. After re-confirming the *cat2 g6pd5* homozygote genotype, plants with lesions were used for the second backcross and segregation was checked once again. Details of the backcross and segregation in F2 generation were shown in Tables 3.2 and 3.3 respectively. To evaluate how well

Table 3.2. Phenotype segregation for identified revertants after backcross to *cat2 g6pd5*. Three lines have been backcrossed with *cat2 g6pd5* twice. For the other three, the first backcross has just been completed. The phenotypes of each generation during backcross were recorded after growth in LD air for three weeks.

line	phenotype	1st backcross		2nd backcross	
		F1	F2	F1	F2
9.11	Obvious lesions Rosette size smaller than *cat2*	No lesions	27/193 plants with lesions	No lesions	27/230 plants with lesions
13.27	Obvious lesions Rosette size similar to *cat2*	No lesions	21/320 plants with lesions	No lesions	42/367 plants with lesions
17.21	Obvious lesions Rosette size smaller than *cat2*	No lesions	32/255 plants with lesions	No lesions	57/493 plants with lesions
19.17	Obvious lesions Rosette size very small	No lesions	72/377 plants with lesions	No lesions	--
21.14	Obvious lesions Rosette size very small	No lesions	22/326 plants with lesions	No lesions	--
26.19	Obvious lesions Rosette size very small	No lesions	24/119 plants with lesions	--	--

the segregation data fit the predicted segregation ratio of 3:1, we performed Chi-square (χ^2) statistical test (Table 3.3). In this study we only focused on lesion phenotype, so two classes are involved: lesions and no-lesions. Therefore, the degree of freedom (*df*) is 1. For each segregation result, the calculated values of χ^2 were compared with $\chi^2_{0.999}$ which is 10.827 (Weigel and Glazebrook, 2002). Those ratios lower than 10.827 were considered acceptable for 3:1 segregation, which is consistent with the phenotype being caused by a single recessive mutation. As shown in Table 3.3, the majority of the segregation ratios are lower than 1/4 and higher than 1/16. The skewed ratios may be an effect of several factors, such as the segregation of multiple unrelated mutations in a mutagenized background, partial lethality in the male or female gametes, or growth conditions (Weigel and Glazebrook, 2002). We also cannot exclude a partly lethal effect of the causal mutation during embryonic and post-embryonic growth, which would be a simple explanation of lesion phenotype ratios below 1/4.

Table 3.3. Phenotype segregation ratios for individual plants. For each line, segregation ratios were determined in an F2 population for at least two to five F1 plants. Ratios of plants showing lesions to the total number of viable plants are presented. * Indicates classes with segregation data fitting the hypothesis of 3:1 ratio according to Chi-square test. *df* = 1, $\chi^2_{0.999} = 10.827$ ($P < 0.001$).

line	1st backcross (plants with lesions/total plants)					2nd backcross (plants with lesions/total plants)			
	F1 plant1	F1 plant2	F1 plant3	F1 plant4	F1 plant5	F1 plant1	F1 plant2	F1 plant3	F1 plant4
9.11	8/44*	7/49*	6/52*	6/48*	--	12/58*	3/59	7/60*	5/53*
13.27	4/64	0/64	5/64*	4/64	8/64*	9/95	15/96*	12/89*	6/87
17.21	7/69*	2/58	16/77*	7/51*	--	20/137*	22/128*	0/119	15/109*
19.17	33/204*	39/173*	--	--	--	--	--	--	--
21.14	11/68*	13/85*	22/84*	8/96	--	--	--	--	--
26.19	10/43*	14/76*	--	--	--	--	--	--	--

After at least one backcross event, multiple leaf samples of F2 plants displaying a lesion phenotype were pooled together and the bulked DNA was subjected to whole-genome sequencing along with non-mutated parental *cat2 g6pd5* DNA as the reference. For each line we collected the sample from at least 50 plants that presented lesions. This is because, during the backcross, the phenotype should segregate with the causal mutation, while non-causal mutations should be distributed more evenly in F2 (unless they are closely linked genetically to the causal mutation). As shown schematically in Figure 3.5, after self-fertilization, line 9.11 showed phenotype segregation in F2. Plants showing lesions are homozygotes for the causal mutation, but those that are wild-type or heterozygous at the affected locus do not have a lesion phenotype. The more plants included in the pooled sample for DNA extraction, the higher the frequency of the causal mutation should be relative to non-causal mutations. Following the recommendations of our collaborators in Ghent, we used 50 lesion-bearing plants to obtain the pooled DNA (Figure 3.5).

3.2.4 Identification of causal mutations

During whole-genome sequencing of both novel mutants and the parental line *cat2 g6pd5*,

SHOREmap was used to identify the causal mutations. The causal mutation should show the highest frequency among all EMS-induced changes (Ossows*ki* et al., 2008; Schneeberger et al., *2*009;

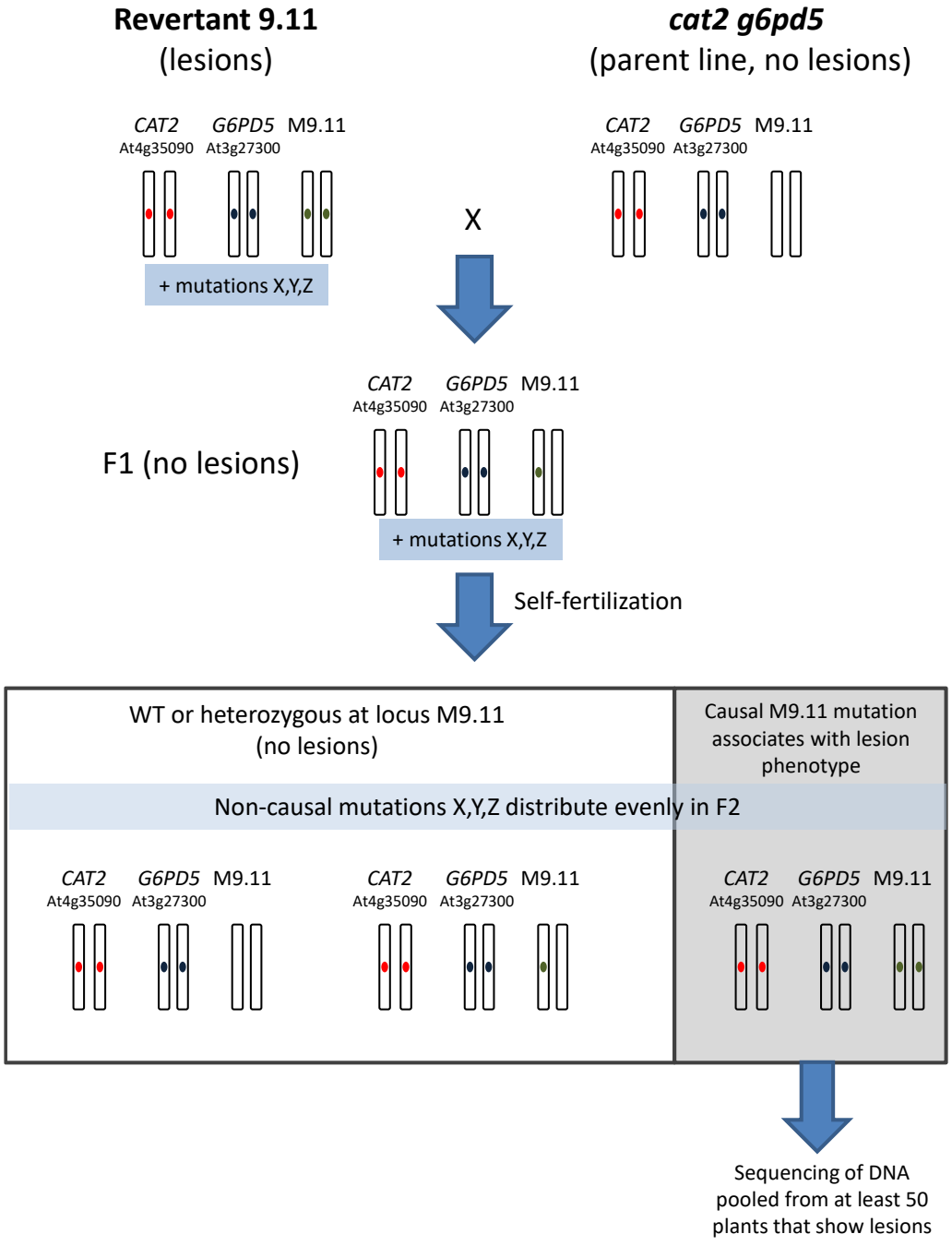

Figure 3.5. Principle of pooled F2 plants for DNA sequencing. After a cross between the revertant M9.11 and the parental line, F1 plants are heterozygous for the causal mutation and show no lesions. In F2, plants that show lesions should be homozygous for the causal mutation. Non-causal mutations present in the original revertant, defined as mutations that do not promote lesion formation, should distribute evenly and be less well represented in the sequencing data.

Hartwig et al., 2012). To date, the putative causal mutations in four of the six lines have been tentatively identified by sequencing. In three lines, the top candidate is *MIPS1*, a gene encoding *myo*-Inositol phosphate synthase, while *CPR5,* encoding CONSTITUTIVE EXPRESSION OF PR GENES5 is the most probable candidate in another line (Table 3.4). As discussed below, mutations in both of these genes have previously been reported to be involved in lesion formation. In the other two lines, several novel candidates for the causal mutation were identified (Table 3.4), but further work is required to establish which of them is responsible for lesion formation in the *cat2 g6pd5* background.

Table 3.4. Identification of mutations. For each line, at least 50 plants of the segregants showing lesions were pooled for DNA extraction and whole-genome sequencing. In parallel, their parental line *cat2 g6pd5* was also sequenced to distinguish between the novel mutations and the genetic background. At the end, all EMS-induced mutations were selected for SHOREmap to identify the causative changes with the highest frequency.

Line	Candidate gene
9.11	MIPS1
13.27	MIPS1
17.21	Several novel candidates
19.17	CPR5
21.14	MIPS1
26.19	Several novel candidates

3.3 Discussion

NADPH is an essential component required in plant metabolism and cellular redox homeostasis (Noctor, 2006; Foyer and Noctor, 2009). Within the context of biotic stress and SA-related signaling, potentially important functions are providing reductant for NADPH oxidases, but also reduction of ascorbate, glutathione, and cytosolic TRXs, all of which have been implicated in PR signaling (Pastori et al., 2003; Torres et al., 2006; Parisy et al., 2006; Tada et al., 2008). It has been well established that NADPH can be generated by several enzymatic approaches. One of the major pathways in the chloroplast is the FNR that provides NADPH for CO_2 assimilation and related reactions (Arakaki et al., 1997). In the cytosol, where many signaling processes occur, NADPH is generated by at least four major NADP-dependent dehydrogenases (Emes and Neuhaus, 1997; Thom et al., 1998; Kruse et al., 1998; Hodges et al, 2003; Arnon et al., 1954; Iglesias, 1990; Chang and Tong, 2003). Even though

some conclusions have been drawn based on pharmacological and genetic studies (Valderrama et al., 2006; Dizengremel et al., 2009; Mhamdi et al., 2010c; Piattoni et al., 2011; Dghim et al., 2013; Li et al., 2013; Wang et al., 2008), the relative importance of different NADPH-generating enzymes remains unclear. Unpublished work in our group over the last several years has revealed that the loss of function of *G6PD5*, encoding a specific isoform of G6PDH, abolishes the *cat2* lesion phenotype, as well as *cat2*-induced transcriptomes (Figure 3.2). Because these effects on *cat2* are quite similar to those caused by the *sid2* mutation (Figure 3.1), this suggests some role for *G6PD5* in regulating SA signaling and lesion formation in *cat2*. The present study aimed to explore components that might be involved in this process by genetically screening revertants of the *cat2 g6pd5* phenotype.

The first revertant line we identified carries a mutation in *MIPS1*. MIPS catalyzes the conversion of glucose-6-phospate to *myo*-inositol phosphate, which is the rate limiting step for *myo*-inositol biosynthesis (Loewus and Loewus, 1983; Loewus and Murthy, 2000). *myo*-Inositol is a ubiquitous compound with diverse biological functions in plants, such as a possible precursor for ascorbate synthesis, and roles in signal transduction and stress tolerance (Loewus and Murthy, 2000). *mips1*, a mutant defective in MIPS, has previously been identified as a lesion-mimic mutant (Meng et al., 2009; Donahue et al., 2010). Interestingly, like lesions in *cat2*, the lesion phenotype in *mips1* was initially linked with day length. When grown in SD it is indistinguishable from the wild type in rosette phenotype, but transferring plants from SD to LD leads to spontaneous cell death formation within several days. However, this phenomenon is more closely linked with the higher quantity of light received in LD (Meng et al., 2009). As in *cat2* and several other lesion mimic mutants, the lesion formation in *mips1* is regulated by SA. Previous work in our laboratory showed that the isochorismate pathway of SA synthesis is involved in the lesion formation and associated defense responses in *cat2* (Chaouch et al., 2010).

Although the *cat2*-induced lesions are light- and day length-dependent, the characteristics seem to somewhat different from those of *mips1*. Cell death in *cat2* was only observed in LD, but not SD, even if higher irradiance is used in SD (Queval et al., 2007). Nevertheless, it is worth mentioning that the functions of both MIPS1 and G6PD5 require glucose-6-phospate as the substrate, and both are located

in the cytosol. These similarities suggest it is worthwhile investigating the relationships between these two enzymes, even though G6PD5 participates in the catalysis of 6-phosphogluconate synthesis, a biological reaction different from that catalyzed by MIPS1.

The second gene we identified by sequencing revertant lines was *CPR5*. Like *mips1*, the *cpr5* mutant has previously been reported to be a member of the lesion-mimic mutant family. Lesion formation in *cpr5* is accompanied by induction of *PR* gene expression, SA accumulation and enhanced resistance to pathogens. Unlike *cat2*, the *cpr5* lesion phenotype is not dependent on environmental conditions such as photoperiod (Bowling et al., 1997). In addition to spontaneous lesion formation, it also exhibits the characteristic of accelerated leaf senescence, indicating that *CPR5* controls multiple physiological processes in Arabidopsis (Jing et al., 2002, 2007, 2008; Yoshida et al., 2002; Trotta et al., 2011).

EMS mutagenesis introduces multiple mutations in the genome. Even if non-causal mutations can be cleaned by backcrossing, it is difficult to remove their influence completely without a series of multiple, time-consuming backcrosses. The principle of identifying the causal mutation is based on its occurring at the highest frequency among all modifications induced by the mutagenesis. To confirm the phenotype effect of these identified genes, one of the approaches will be to obtain T-DNA insertion mutants and to cross them into the *cat2 g6pd5* background. Hence, T-DNA mutants of *mips1* and *cpr5* will be crossed with *cat2 g6pd5* to get triple homozygotes, and the resulting plants will be analyzed to confirm that the candidate genes are indeed responsible for the observed reversion. *PR* gene expression and SA content can be analyzed and compared with *cat2 g6pd5* to establish the pathways underlying the lesion phenotype.

A key remaining question is whether the mutations identified in the revertant screen are dependent on the presence of the *cat2* mutation and, therefore, on oxidative stress induced by intracellular H_2O_2. Our main aim in conducting this screen was to shed light on the mechanisms by which loss of *G6PD5* function modulates the *cat2*-triggered response. To this end, we focused on revertants that show a similar phenotype to that observed in *cat2*. Several other potential revertants were observed that showed symptoms such as yellowing or early senescence but such plants were disregarded because

these phenotypes do not correspond to those observed in the *cat2* single mutant. To date, we cannot judge to what extent the lesion phenotypes linked to the mutations identified in the different revertant lines are dependent on the *cat2* mutation. Indeed, the fact that *mips1* and *cpr5* have already been identified as lesion mimic mutants (i.e., their mutation alone is sufficient to induce lesions) suggests that some of their effects might be independent of the presence of *cat2*. This question could be elucidated by comparing the different genotypes under our growth conditions. For example, a comparison of *mips1*, *cat2 mips1*, *g6pd5 mips1* and *cat2 g6pd5 mips1* could shed some light on this issue. A second approach would be to transform the *cat2 g6pd5* revertant with the wild-type CAT2 sequence. However, as described in the next chapter, the use of a targeted reverse genetics approach to analyze an NADPH-requiring enzyme involved in the ascorbate-glutathione pathway has identified an interesting avenue of inquiry concerning the biochemical mechanisms underlying the effect of the *g6pd5* mutation on responses in *cat2*.

CHAPTER 4

Analysis of the roles of monodehydroascorbate reductases in H_2O_2 metabolism using gene-specific mutants

Summary

Together with catalase, the ascorbate-glutathione pathway is considered to be a key player in metabolizing H_2O_2 produced inside the cell. Literature data suggest that flux through the ascorbate-glutathione pathway is accelerated during stress and in genetic systems that mimic stress, such as the *cat2* mutant. Four different types of enzymes function in the ascorbate-glutathione pathway, and each is encoded by more than one gene. One of these enzymes is NAD(P)H-dependent monodehydroascorbate reductase (MDHAR), for which five genes are annotated in Arabidopsis. To analyze the importance of specific MDHAR isoforms, gene-specific mutants were obtained for one peroxisomal isoform (MDHAR1) and two cytosolic isoforms (MDHAR2, MDHAR3). The consequences of the loss of these MDHAR functions were analyzed in a wild-type and catalase-deficient background. While none of the *mdhar* mutations had a marked effect on growth or rosette phenotype in the wild-type background, *mdhar2* produced several striking effects on *cat2*-triggered changes in redox state and activation of the SA pathway. Compared to *cat2*, a double *cat2 mdhar2* mutant showed much-decreased lesion formation accompanied by weaker activation of the SA pathway. These effects were linked to perturbation of the ascorbate-glutathione pathway, and most notably enhanced oxidation of glutathione compared to *cat2*. Together, the findings suggest that a specific cytosolic MDHAR plays important roles in signaling responses to intracellular H_2O_2.

4.1 Introduction

As noted previously in this thesis, plants are often exposed to various stress conditions in the field. A central theme in most stress responses is the accumulation of ROS, such as H_2O_2, and ROS-induced perturbation on intracellular redox state (Queval et al., 2007). Plants have evolved several enzymatic antioxidative systems to escape from oxidative damage (Mittler et al., 2004). As one of the major enzymes to metabolize ROS, CATs can initiate a dismutation reaction in which H_2O_2 is decomposed into water and O_2. Alongside CAT, the ascorbate-glutathione pathway is also considered to be an essential system to protect plants from oxidative stress by consuming H_2O_2. In this pathway, H_2O_2 can obtain electrons from ascorbate and can thereby be converted to water. This reaction is catalyzed by APX and accompanied by the production of MDHA. As a short-lived radical, MDHA can be recycled immediately to reduced ascorbate (ASC) by MDHAR via electron transfer from NAD(P)H. Alternatively, it disproportionates spontaneously to ascorbate and DHA. DHA can be reduced back to ascorbate, which is catalyzed by glutathione-dependent DHAR (Foyer and Halliwell, 1977; Nakano and Asada, 1981). The product of glutathione oxidation, GSSG, is reduced by GR using NADPH as an electron donor. Among all these enzymes, DHAR and MDHAR may be important for maintaining ascorbate in its reduced state. Interestingly, although the degradation of H_2O_2 in plant peroxisomes is primarily attributed to CATs, the affinity of CAT for H_2O_2 is much lower than that of APX. This leads to the suggestion that APX/MDHAR system might have a much higher efficiency to scavenge H_2O_2 when its concentration is lower (Bunkelmann and Trelease, 1996; Mullen and Trelease, 1996). Nevertheless, modelling analyses suggest that both CAT and APX can function together to maintain H_2O_2 at low levels (of the order of 1 μM: Tuzet et al., 2018).

Although the ascorbate-glutathione pathway is considered to be a key player in metabolizing H_2O_2, the relative importance of specific MDHAR isoforms is not clearly established. Activity of MDHAR has been reported in various plant cell compartments such as chloroplasts (Hossain et al., 1984), the cytosol (Dalton et al., 1993), mitochondria and peroxisomes (Jiménez et al., 1997). Cytosolic MDHAR has been purified from cucumber fruits (Hossain and Asada, 1985), soybean root nodules (Dalton et al., 1992) and potato tubers (Borraccino et al., 1986). A mitochondrial MDHAR has been

purified from potato tubers (De Leonardi S et al., 1995) and a chloroplast MDHAR from spinach leaves (Sano et al., 2005). Analysis of the Arabidopsis genome has revealed that five genes encode *MDHAR* (Table 4.1). The encoded proteins are approximately 50 kDa in mass, and are targeted to various subcellular compartments (Table 4.1). Among them, *MDHAR1* and *MDHAR4* are targeted to the peroxisomal matrix and membrane, respectively. *MDHAR2* and *MDHAR3* are targeted to the cytosol (Lisenbee et al., 2005) while *MDHAR5/6* is targeted to mitochondria or chloroplasts, depending on the different transcription initiation sites (Obara et al., 2002).

Table 4.1. Summary of different *MDHARs* and T-DNA mutants available in the laboratory

List of genes	Localization	Protein molecular mass	T-DNA mutants available
MDHAR1	Peroxisome	50.2 KDa	*mdhar1-1*, *mdhar1-2*
MDHAR2	Cytosol	47.5 KDa	*mdhar2-1*
MDHAR3	Cytosol	48.3 KDa	*mdhar3-1, mdhar3-2, mdhar3-3*
MDHAR4	Peroxisome	53.5 KDa	*mdhar4-1, mdhar4-2*
MDHAR5/6	Chloroplast/Mitochondrion	53.3 KDa	--

As one of the enzymes in the ascorbate-glutathione cycle, MDHAR may play an important role in various physiological processes. Overexpression of *MDHAR* has been reported to enhance tolerance to temperature and methyl viologen in tomato (Li et al., 2010). *MDHAR* genes are involved in the response to abiotic stresses through maintaining redox status in acerola (Eltelib et al., 2011). As well as possible roles in abiotic stresses, *MDHAR* genes were found to play a negative role in pathogen recognition in wheat (Feng et al., 2014a, 2014b; Abou-Attia et al., 2016). In Arabidopsis, *MDHAR1* and *MDHAR4* were proposed to be important for ascorbate recycling in the peroxisomes (Lisenbee et al., 2005). *MDHAR* genes may also be involved in the resistance to ozone, salt and polyethylene glycol (Eltayeb et al., 2007). Fungi such as *Piriformospora indica* can cause accumulation of *MDHAR* transcripts (Vadassery et al., 2009). *MDHAR4* was found to influence seed storage oil hydrolysis and seedling growth (Eastmond, 2007). Recently, evidence was presented for a new pro-oxidant effect of *MDHAR6* in mediating TNT toxicity by promoting reactive oxygen production (Johnston et al., 2015; Noctor, 2015). Further work is required to elucidate the precise roles of the different isoforms.

Very recent work in our group showed that *dhar* mutations did not affect leaf ascorbate pools in optimal and oxidative stress conditions, even though the *cat2*-induced glutathione oxidation and total glutathione accumulation is decreased by multiple *dhar* mutations (Rahantaniaina et al., 2017). The negligible effect of *DHAR* mutation on ascorbate status leads us to investigate the potential importance of other routes reducing DHA or else avoiding its formation by consuming MDHA. Are MDHAR isoforms important in maintaining the ascorbate redox state by catalyzing the reduction of MDHA? To answer this question, we generated loss-of-function mutants for different *MDHAR* genes in Arabidopsis. We also introduced these mutants into a *CAT*-deficient background (*cat2*) to obtain double mutant lines. Because *CAT2* encodes the irreplaceable photorespiratory CAT enzyme, *cat2* itself has been extensively used as a system in which H_2O_2 signals can be switched on and off by transferring plants between photorespiratory and non-photorespiratory conditions (Queval et al., 2007). Decreased CAT activity forces H_2O_2 metabolism through alternative systems that are dependent on cellular reductants, notably the ascorbate-glutathione pathway (see Figure 1.4). For example, it has notably been shown that a specific isoform of GR that is mainly located in the cytosol is essential to allow glutathione regeneration when CAT function is lost (Mhamdi et al., 2010b). Here, we used a similar strategy to analyze the roles of genes encoding MDHAR in Arabidopsis, with a focus on *MDHAR1*, encoding a peroxisomal enzyme, and *MDHAR2* and *MDHAR3*, which encode cytosolic enzymes. For this, a series of *mdhar* and *cat2 mdhar* mutants were analyzed that had been obtained and partially characterized in the laboratory by Gilles Chatel-Innocenti and Hélène Vanacker.

4.2 Results

4.2.1 Identification of *mdhar* single mutants

To analyze the specific roles of different *MDHAR* genes, we obtained at least one line of T-DNA insertion mutants for *MDHAR1*, *MDHAR2*, *MDHAR3* and *MDHAR4* (Table 4.1). In a first analysis, a single line for each gene was chosen for functional analysis. Among them, *mdhar1*, *mdhar2* and *mdhar3* are mutants with T-DNA insertions in the corresponding coding sequence, while for *mdhar4* the T-DNA is located in the promoter (Figure 4.1). All four mutants were identified to be homozygotes

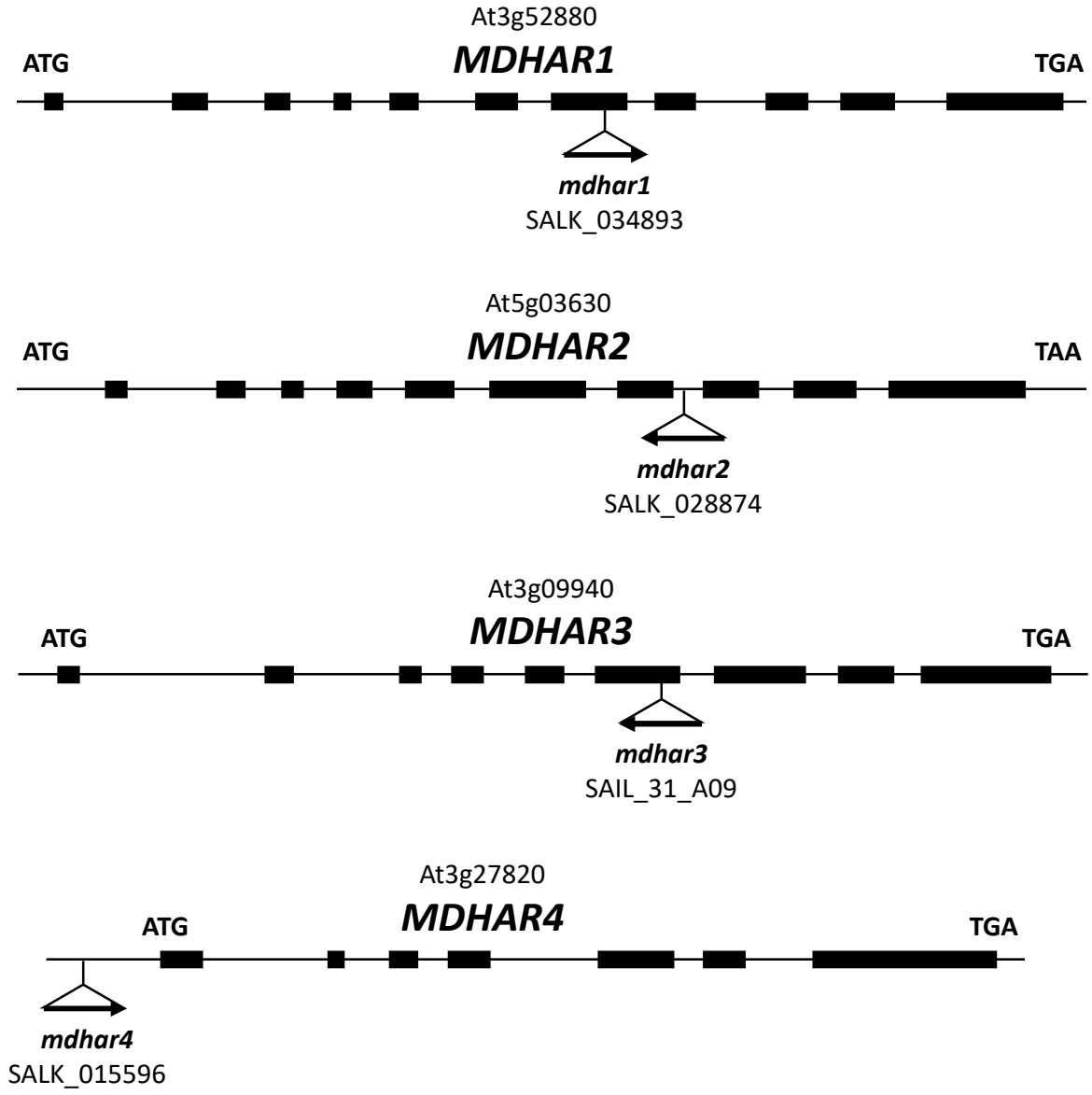

Figure 4.1 Schematic diagram of T-DNA insertion in Arabidopsis *mdhar* mutants. Exons and introns are depicted to scale by boxes and lines, respectively. The coding region of the gene is shown as black boxes. The position of the T-DNA is indicated by the triangle and the arrow indicates the direction of the T-DNA insertion. Seeds of Arabidopsis (*Arabidopsis thaliana*) mutants in the ecotype Columbia (Col-0) background were obtained from the Nottingham Arabidopsis Stock Center (http://nasc.nott.ac.uk).

by PCR genotyping (Figure 4.2A). The results of reverse transcription-polymerase chain reaction (RT-PCR) suggest that *mdhar1*, *mdhar2* and *mdhar3* are true knockouts, which is consistent with the location of insertions in the coding sequences. In contrast, *mdhar4* is not affected by the T-DNA insertion at the level of transcript (Figure 4.2B), suggesting that the insertion in the promoter did not significantly modify expression of the gene. To study the functional impact of single *mdhar* mutations, plants were grown in standard conditions. Little difference in rosette phenotype was found when compared with Col-0 after three weeks' growth in LD, even though the *mdhar4* mutation caused a slight but significant decrease in fresh weight (Figure 4.2C and D). This suggests functional redundancy among MDHAR isoforms or with other systems when plants are grown in non-stressful conditions. Because expression of the corresponding gene did not seem to be altered in *mdhar4*, we focused on the *mdhar1, mdhar2,* and *mdhar3* mutants in the rest of the study described below.

4.2.2 *MDHAR* transcripts in response to intracellular oxidative stress

Based on current concepts of the ascorbate-glutathione pathway as an important player in the plant antioxidative system, we explored the importance of the three *MDHAR* genes in oxidative stress conditions. Because of its enhanced intracellular H_2O_2 availability, *cat2* has been well established as a system to mimic oxidative stress (Queval et al., 2007; Mhamdi et al., 2010bc). Hence, we crossed each *mdhar* mutant into the *cat2* background to produce double mutants. F1 plants were identified as heterozygotes at both the *CAT2* and *MDHAR* loci. Subsequently, homozygotes were identified by PCR genotyping in the F2 generation (Figure 4.3A). RT-PCR confirmed the absence of *CAT2* and *MDHAR* transcripts (Figure 4.3B). F3 seeds were used for functional analysis.

qRT-PCR analysis confirmed that the mutations in *mdhar1* and *mdhar2* decreased the respective transcripts to low levels. The *mdhar3* mutation also decreased the *MDHAR3* transcript to very low levels, although the difference to the wild-type is not statistically significant because of some variability between the Col-0 replicates (Figure 4.4). Interestingly, loss of *CAT2* function induced the expression of *MDHAR2* and *MDHAR3* but not *MDHAR1*. Moreover, the induction of *MDHAR3* was

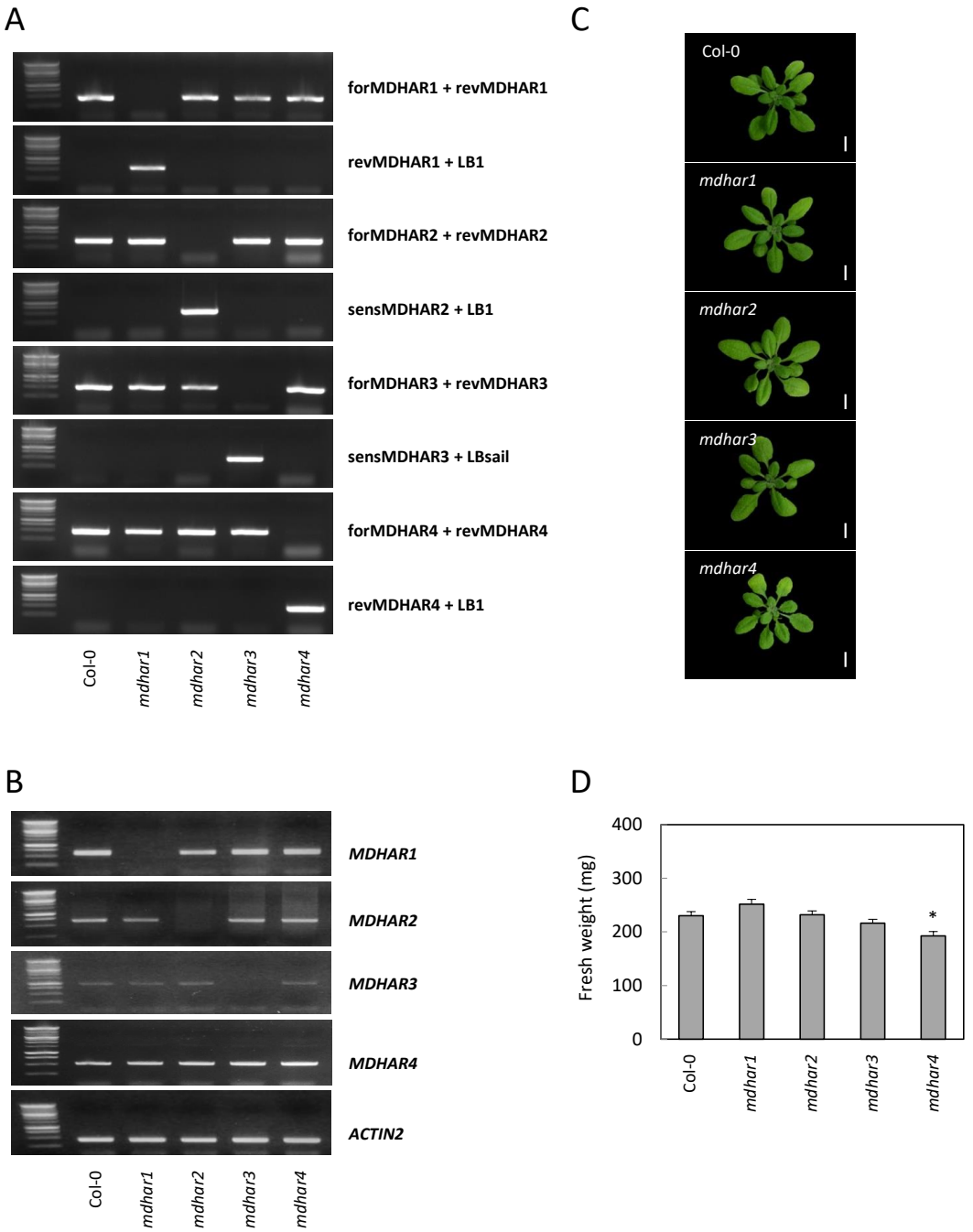

Figure 4.2 Genotyping and transcripts (RT-PCR) of all *mdhar* single mutants (*mdhar1*, *mdhar2*, *mdhar3*, *mdhar4*) and phenotype.

A. PCR analysis of homozygous single *mdhar* T-DNA insertion mutants.

B. RT-PCR analysis of different *mdhar* single mutants.

C. Photographs of plants grown in LD air for 3 weeks.

D. Fresh weight of rosettes after grown in LD air for 3 weeks. Data are means of at least 10 plants. * Indicates significant differences between *mdhar* mutants and Col-0 at $P < 0.05$.

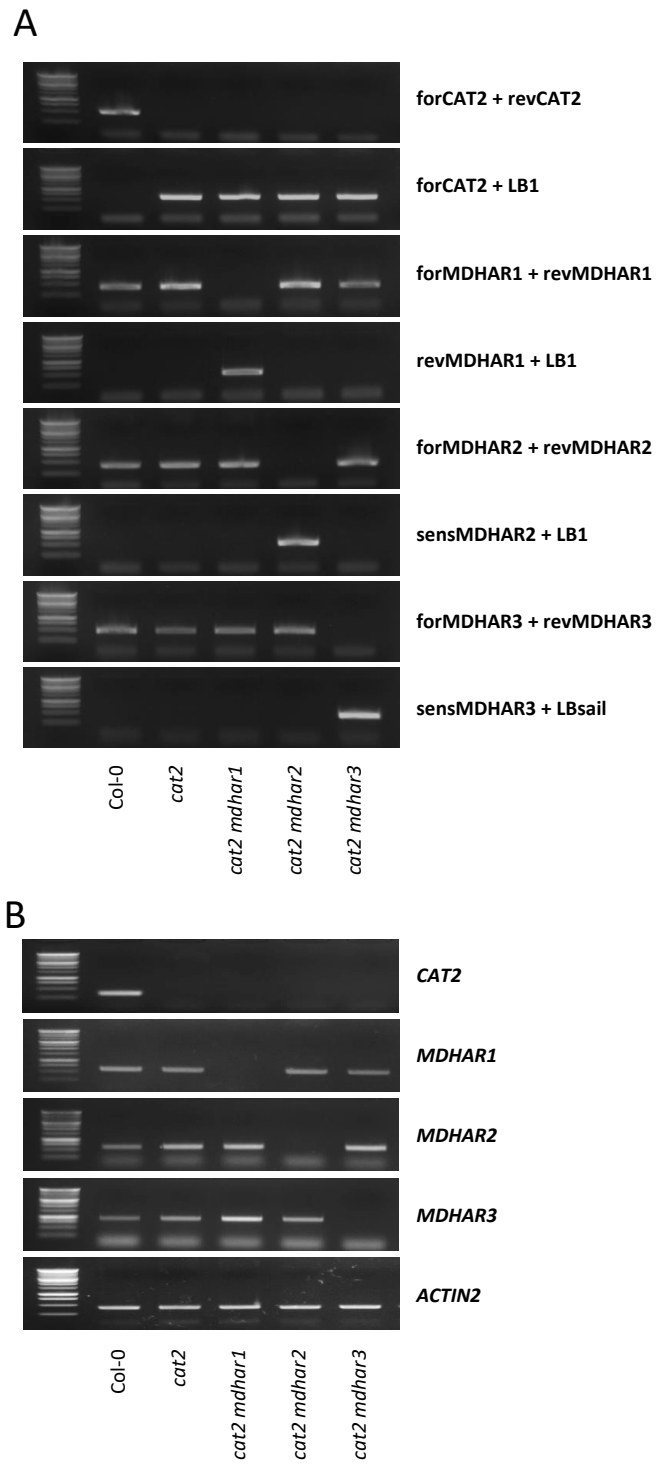

Figure 4.3. Genotyping and transcripts analysis of *cat2 mdhar1*, *cat2 mdhar2* and *cat2 mdhar3*.

A. PCR analysis of all double mutants.

B. Transcripts analysis by semi-quantitative RT-PCR.

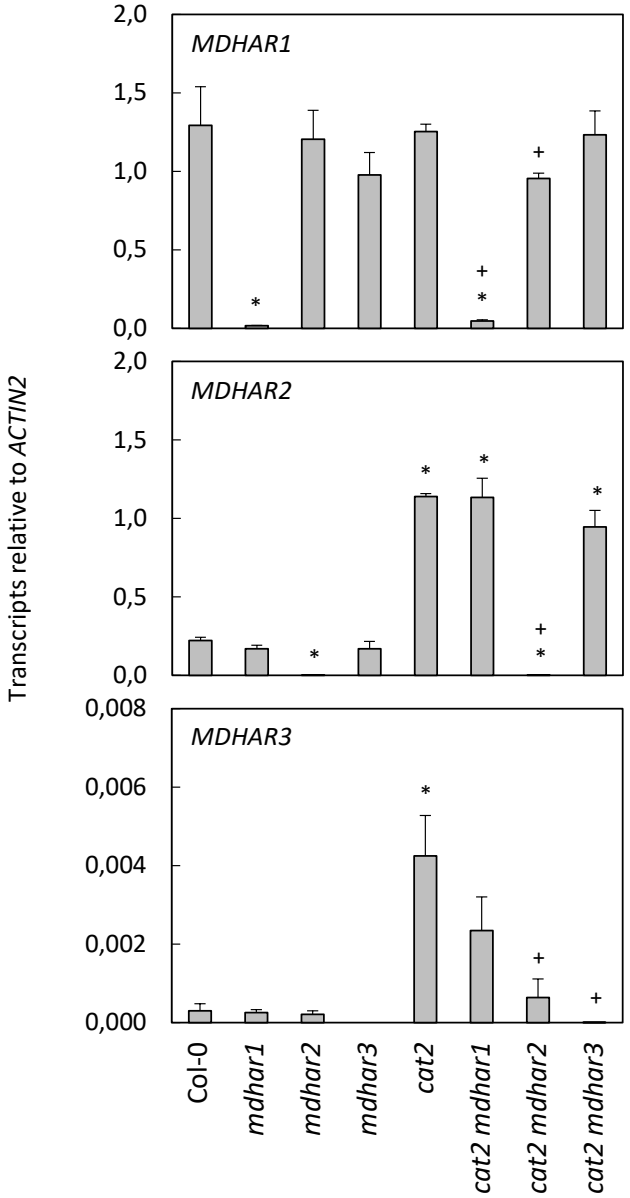

Figure 4.4. *MDHAR* genes expression in different *mdhar* mutants in Col-0 and *cat2* background. Data are means ± SE of four biological replicates. * Indicates significant differences of mutants to Col-0 at $P < 0.05$; $^{+}$ indicates significant differences of double mutants compared with *cat2* at $P < 0.05$.

weakened significantly in *cat2 mdhar2*. These results provide a first indication that *MDHAR2* and *MDHAR3* may be involved in the response to oxidative stress occurring in *cat2*.

4.2.3 Impact of *mdhar* mutations on *cat2*-triggered lesion formation and phytohormone signaling

To study the phenotypic impact of the *mdhar* mutations in an oxidative stress background, plants were grown in standard conditions in LD. Like *cat2*, all three double mutants were significantly smaller than the wild-type. While *cat2 mdhar1* was somewhat smaller than *cat2*, *cat2 mdhar2* and *cat2 mdhar3* showed a similar rosette mass to *cat2* (data not shown). The most striking phenotypic effect was on *cat2*-triggered lesion formation. While *cat2*-triggered HR-like lesions were clearly visible on *cat2 mdhar1* and *cat2 mdhar3* leaves, they were largely abolished by the loss of function of *MDHAR2* (Figure 4.5A and B). As described in Chapter 3, previous studies revealed that the lesion formation in *cat2* is associated with SA signaling (Queval et al., 2007; Chaouch et al., 2010). Hence, we analyzed the effects of each *mdhar* mutation on transcript levels for SA-associated genes. *PR1*, *PR2* and *PR5* are marker genes in SA-dependent PR responses, and *ICS1* is a gene involved in SA synthesis. None of the single *MDHAR* mutations affected these transcripts in the wild-type background in standard conditions, with all the markers maintained at the low basal level observed in the wild type (data not shown). In *cat2*, all four genes were markedly induced by the intracellular oxidative stress: while *mdhar1* did not affect this response, the *mdhar3* mutation tended to reinforce it, although this effect was only statistically significant for *PR1* (Figure 4.5C). The most dramatic effect was that of the *mdhar2* mutation, which strongly inhibited the induction of SA marker gene expression triggered by *cat2*. In *cat2 mdhar2*, transcripts for all four genes were similar to the basal levels observed in the wild-type, Col-0 (Figure 4.5C).

In view of the effects of the *mdhar2* mutation on lesions and SA marker transcripts, SA contents were measured by HPLC. Although some variability meant that differences were not always statistically significant, this analysis revealed that *cat2 mdhar2* showed similar SA levels to the wild-type while SA contents *in cat2 mdhar1* and *cat2 mdhar3* were similar to *cat2* (Figure 4.6). Therefore, loss of *MDHAR2* function appears to suppress SA contents, induction of SA-dependent genes and, to a large extent, lesion formation triggered by intracellular oxidative stress.

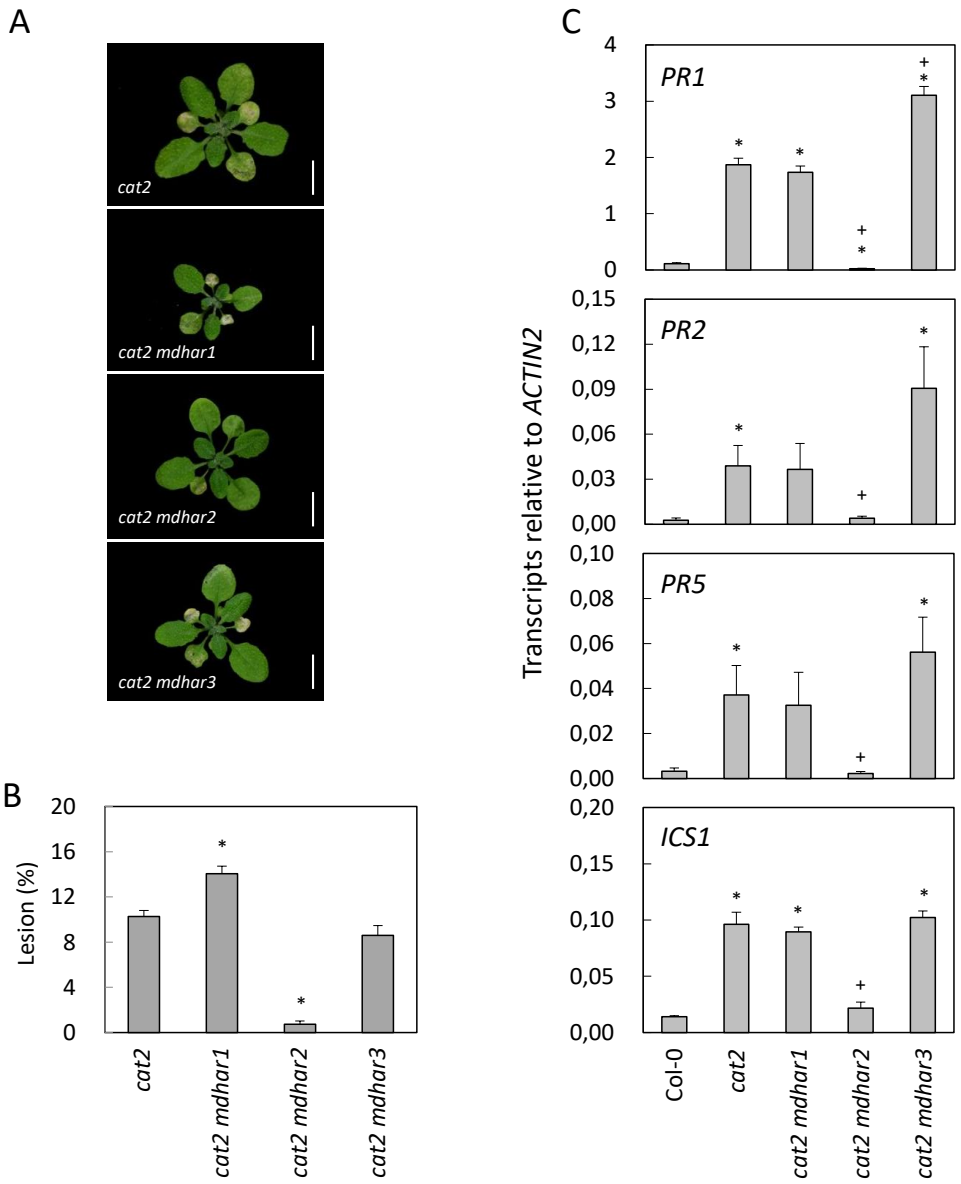

Figure 4.5. Effects of *mdhar* mutations on the *cat2* phenotype and SA marker transcripts.

A. Photographs of plants grown in LD air for 3 weeks.

B. Effects of different *mdhar* mutations on *cat2*-triggered lesions. Data are means ± SE of 12 plants. * Indicates significant differences in percentage of lesions on *cat2* background mutant leaves compared with *cat2*.

C. SA marker transcripts analysis in Col-0, *cat2*, and double mutants. Data are means ± SE of four biological replicates. * Indicates significant differences of mutants to Col-0 at $P < 0.05$; $^{+}$ indicates significant differences of double mutants compared with *cat2* at $P < 0.05$.

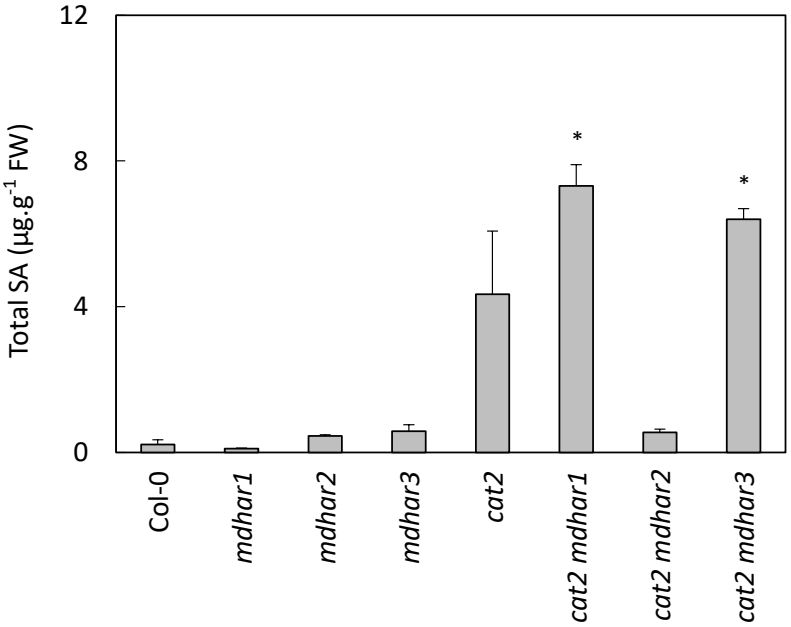

Figure 4.6. Total leaf salicylic acid (SA) contents in the different mutants. Data are means ± SE of three biological replicates. * Indicates significant differences of mutants to Col-0 at $P < 0.05$; $^{+}$ indicates significant differences of double mutants compared with *cat2* at $P < 0.05$.

At present, an allelic mutant for *MDHAR2* is not available (Table 4.1). A backcross strategy was therefore used to test the link between the *mdhar2* mutation and the phenotype by crossing the *cat2 mdhar2* line with *cat2*. Phenotype and genotype segregation were quantified and evaluated in F2 (Table 4.2). Data analysis showed that the lesion phenotype segregation ratio is close to 3:1, and most of the plants showing less or no lesions are *cat2 mdhar2* homozygotes. The semi-quantitative nature of the phenotype analysis meant that the genotype-phenotype link was not absolute. Nevertheless, the analysis revealed that about 90% of F2 segregants with one or two wild-type *MDHAR2* alleles showed phenotypes similar to *cat2*. In contrast, this figure was around 30% in *cat2 mdhar2* double homozygotes. These results suggest that *MDHAR2* is important in linking H_2O_2 to lesion formation and SA signaling induction.

As well as SA, JA is also a phytohormone that is closely linked to oxidative stress (Devoto and Turner, 2005; Maruta et al., 2011). A complex relationship between SA and JA signaling pathway has been reported (Dangl and Jones, 2001; Spoel et al., 2003; Takahashi et al., 2004; Koorneef et al., 2008).

Table 4.2. Backcross of *cat2 mdhar2* with *cat2.* At least four plants of *cat2 mdhar2* were crossed with *cat2*. Seeds were collected and pooled. F2 seeds were collected from two F1 plants, and lesion phenotypes were compared with genotypes for 90 (plant 1) and 86 (plant 2) F2 individuals.

	Total number of plants		Genotype at *MDHAR2* locus					
			MDHAR2 MDHAR2		*MDHAR2 mdhar2*		*mdhar2 mdhar2*	
	Plant 1	Plant 2	Plant 1	Plant 2	Plant 1	Plant 2	Plant 1	Plant 2
Number of plants	90	86	24	21	45	52	21	13
cat2 phenotype	69	71	22	20	41	47	6	4
Less or no lesions	21	15	2	1	4	5	15	9
cat2 phenotype/ less or no lesions	3.29	4.73	11	20	10.25	9.4	0.4	0.44
% *cat2* phenotype	76.7	82.6	91.7	95.2	91.1	90.4	28.6	30.8

Therefore, we analyzed levels of several marker transcripts involved in JA synthesis and signaling (Figure 4.7). *PDF1.2* and *JAZ10* are JA signaling marker genes, while *LOX3* encodes an enzyme involved in JA synthesis and *MYB95* is a transcription factor which responds to JA signaling. As observed for the SA markers, the single *mdhar* mutations did not affect the basal level of the JA markers in the wild-type background (data not shown). Also similar to the response of the SA marker genes, the *cat2* mutation induced all four genes, and this effect was not obviously impacted by loss of function of *MDHAR1* or *MDHAR3*. However, the *MDHAR2* mutation inhibited the transcript of *PDF1.2* in *cat2 mdhar2* to a basal level close to Col-0. It also slightly but significantly alleviated the induction of *LOX3* and *MYB95* (Figure 4.7). It is interesting that *PDF1.2* was the most strongly impacted, as this gene is also ethylene-responsive. These results suggest that *MDHAR2* may play roles in linking oxidative stress to signaling through several phytohormones, although its function seems to be particularly important for activation of the SA signaling pathway.

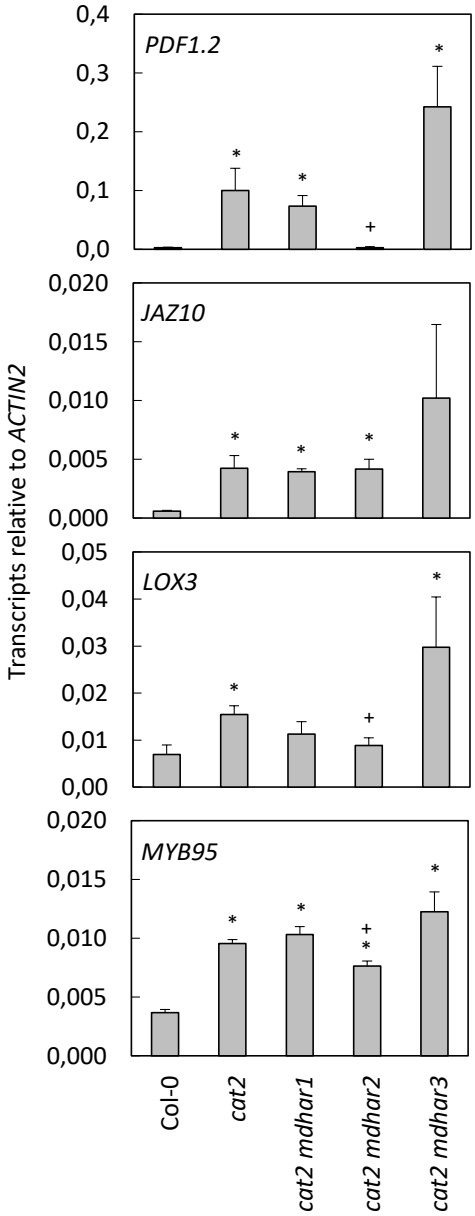

Figure 4.7. Effects of different *mdhar* mutations on *cat2*-induced JA-associated transcripts. Data are means ± SE of four biological replicates. * Indicates significant differences of mutants to Col-0 at $P < 0.05$; $^{+}$ indicates significant differences of double mutants compared with *cat2* at $P < 0.05$.

4.2.4 Impact of the loss of *MDHAR* functions on leaf redox status

To explore the functional impact of *mdhar* mutations in oxidative stress responses, several major antioxidative enzyme activities were analyzed in the different mutants. The single *mdhar* mutations did not affect any of the enzyme activities in the Col-0 background. As shown in Chapter 2, the *cat2*

mutation decreased leaf CAT activity to around 20% of that in the wild type. This effect was not substantially changed by the *mdhar* mutations although *cat2 mdhar2* showed slightly lower CAT activity than in *cat2*. To assess the effect of the mutations on the capacity of the ascorbate-glutathione system, the activities of APX, GR and DHAR were measured. All of them were increased by the *cat2* mutation, but none of the *mdhar* mutations had an obvious impact except *cat2 mdhar2*, which presented significantly lower APX activity than that in *cat2* (Figure 4.8).

As mentioned in Chapter 2, ROS signals are not easy to measure directly, especially in leaves, but transcripts known to be H_2O_2-responsive can serve as a useful proxy. Consequently, transcripts for the oxidative markers *GSTU24*, *UGT73b3* and *APX1* were quantified in both single and double mutants. The single *mdhar* mutations did not impact the expression of these marker genes in the Col-0 background, but the *cat2* mutation caused marked induction of all three (Figure 4.9). The up-regulation of *GSTU24* in response to the *cat2* mutation was not changed by blocking the function of *MDHAR1*, *MDHAR2* or *MDHAR3*. However, the induction of *UGT73b3* and *APX1* was partly reversed by the loss of function of *MDHAR2* (Figure 4.9).

Perturbation of redox homeostasis triggered by the *cat2* mutation notably involves increased oxidation of glutathione and total glutathione accumulation (Queval et al., 2007, 2009 ; Mhamdi et al., 2010b). As is shown in Figure 4.10, when grown in standard conditions, glutathione is kept in a highly reduced state in the wild type (>90% GSH). The *mdhar* single mutations did not in themselves affect glutathione status. In *cat2*, glutathione becomes much more oxidized and accumulates, almost entirely due to GSSG accumulation (Figure 4.10, upper panel). Loss of function of *MDHAR2* significantly exacerbated the oxidation of glutathione in *cat2*. While glutathione was almost 50% reduced in *cat2*, the pool fell to about 20% reduced in *cat2 mdhar2* (Figure 4.10). In contrast, the *mdhar3* mutation produced a slight but significant decrease in glutathione oxidation in the *cat2* background. In contrast to glutathione, ascorbate is less affected in *cat2* (Mhamdi et al., 2010b,c). No difference in the reduction state of ascorbate was found in any of the mutants compared with Col-0, but the total ascorbate pool was significantly decreased in *cat2 mdhar2* (Figure 4.10, lower panel). A slight effect of this type was also observed in the single *mdhar3* mutant. Taken together, these results suggest that

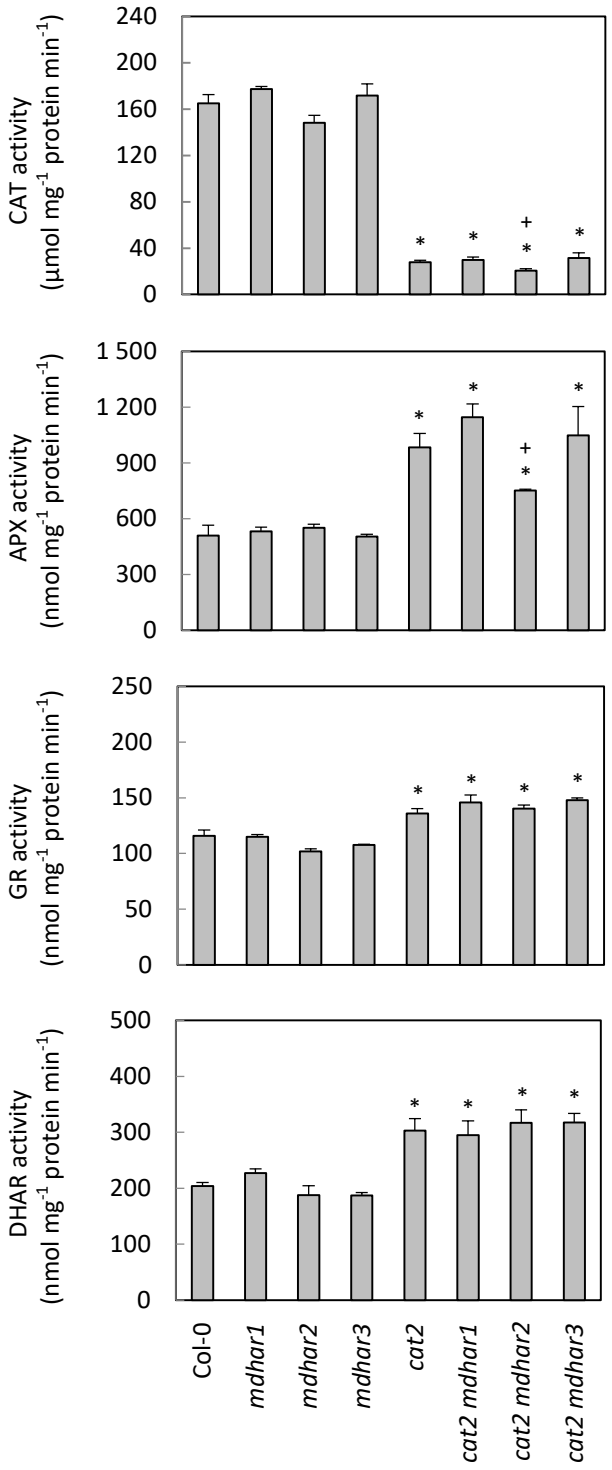

Figure 4.8. Major antioxidative enzyme activities in different *mdhar* mutants in Col-0 and *cat2* background. Data are means ± SE of three biological replicates. * Indicates significant differences of mutants to Col-0 at $P < 0.05$; $^{+}$ indicates significant differences of double mutants compared with *cat2* at $P < 0.05$.

MDHAR2 is involved in determining the cell redox state, and especially that of the glutathione pool, during oxidative stress.

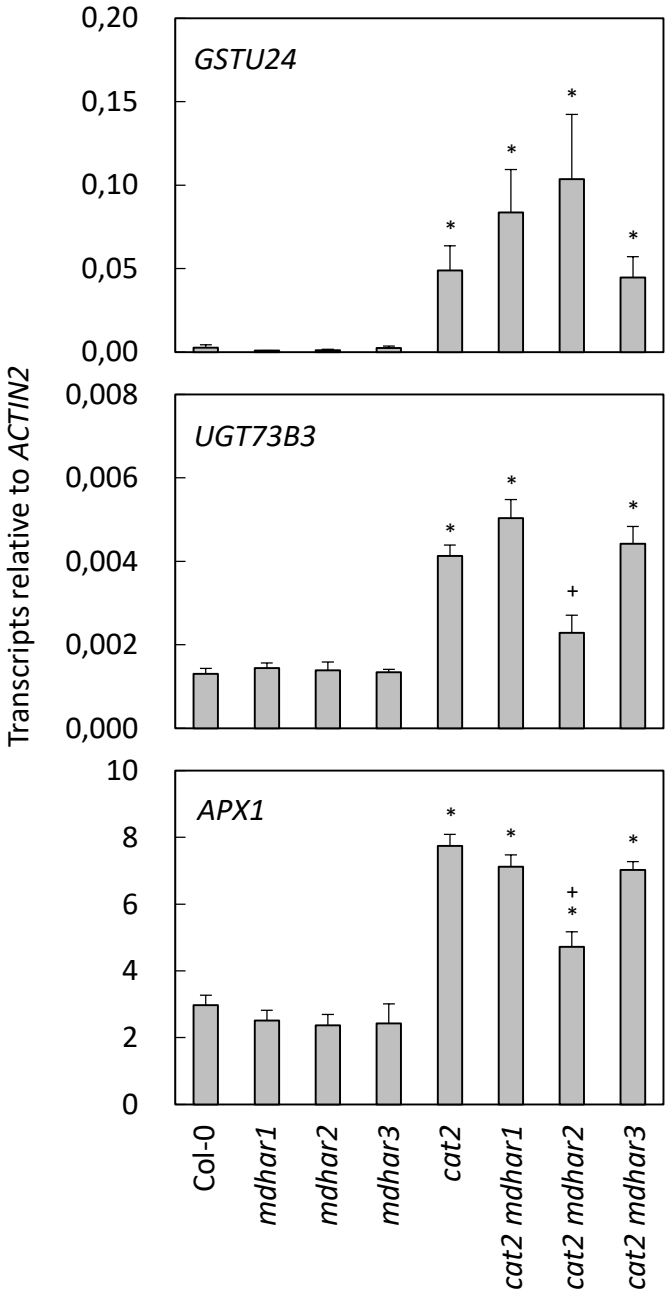

Figure 4.9. Oxidative marker transcripts in different *mdhar* mutants in Col-0 and *cat2* background. Data are means ± SE of four biological replicates. * Indicates significant differences of mutants to Col-0 at $P < 0.05$; $^{+}$ indicates significant differences of double mutants compared with *cat2* at $P < 0.05$.

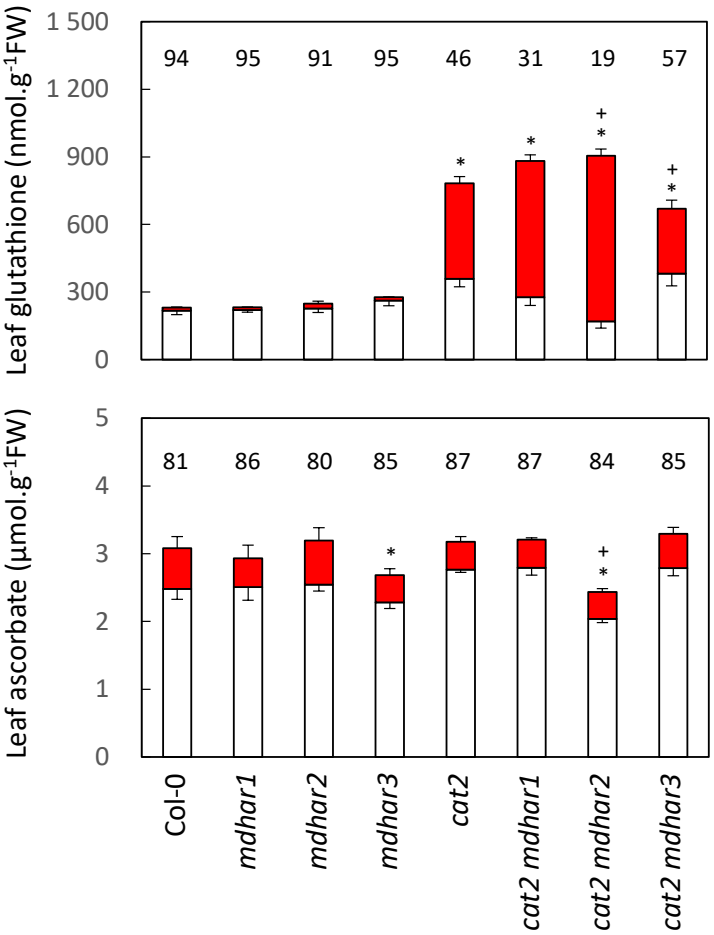

Figure 4.10. Effects of *mdhar* mutations on ascorbate and glutathione in both Col-0 and *cat2* background. White blocks, reduced forms. Red blocks, oxidized forms. Data are means ± SE of four biological replicates. * Indicates significant differences in total glutathione or ascorbate contents in mutants compared with Col-0 at $P < 0.05$; $^{+}$ indicates significant differences compared with *cat2* at $P < 0.05$. Numbers above the columns indicate percentage reduced (100 x reduced form/total content).

4.3 Discussion

The ascorbate-glutathione pathway has long been considered to be among the major components of plant antioxidative systems (Noctor and Foyer, 1998; Foyer and Noctor, 2013). While the enzymes and small molecules in this pathway have been well described, only limited information is available for the

role of specific enzyme isoforms in the response to oxidative stress. Previous studies from our and other laboratories have used *CAT*-deficient mutants to analyze this question, because decreased CAT capacity forces enhanced flux through the ascorbate-glutathione pathway, as has recently been quantitatively estimated using a modeling approach (Tuzet et al., 2018). Gene-specific studies have revealed an important role for cytosolic isoforms of APX, GR, and DHAR during oxidative stress conditions (Mhamdi et al., 2010b; Vanderauwera et al., 2011; Rahantaniaina et al., 2017). In addition to these enzymes, the cytosolic ascorbate-glutathione pathway is dependent on NAD(P)H that may be produced by several enzymes. As described in Chapter 3, a gene encoding a cytosolic G6PDH seems to be particularly important to link oxidative stress in *cat2* to downstream phytohormone signaling and lesion formation. The data in this chapter provide evidence that as specific cytosolic MDHAR isoform is also important in this respect.

MDHAR has been found to be induced by different external stresses at the levels of gene expression and/or enzyme activity (Kayıhan et al., 2016; Sudan et al., 2015). Genetic studies by Eastmond (2007) found that MDHAR4 is required for storage oil hydrolysis during Arabidopsis seed germination and that this effect is linked to removal of H_2O_2 derived from β-oxidation of fatty acids. During post-germination development of photosynthetic tissues, however, photorespiration becomes more important than fatty acid β-oxidation in generating large quantities of H_2O_2. Our phenotypic analyses of single *mdhar* mutants in standard conditions (LD, moderate light intensity) did not reveal a marked impact of loss of *MDHAR1*, *MDHAR2* or *MDHAR3* functions. The slightly decreased rosette size of *mdhar4* might be consistent with previous analyses on Arabidopsis seedlings (Eastmond, 2007) but since this mutant did not show decreased *MDHAR4* transcripts, the biological relevance of this observation is unclear. Nevertheless, some evidence that peroxisomal isoforms might be important in supporting H_2O_2 metabolism in leaves comes from the smaller size of *cat2 mdhar1* compared to *cat2* (Figure 4.5). Taken together, however, our data suggest that none of *MDHAR1, MDHAR2 or MDHAR3* is critical for plant growth and development in standard conditions, suggesting there may be functional redundancy among them or with other systems. Interestingly, none of the *mdhar* mutations affected leaf ascorbate pools to a great extent (Figure 4.10). Along with DHAR, MDHAR is considered one of the enzymes responsible for regenerating the reduced form of ascorbate after its

oxidation by reactions such as that catalyzed by APX. However, none of the mutant combinations for the three DHARs in Arabidopsis, including a triple *dhar1 dhar2 dhar3* mutant, affected the leaf ascorbate pool in either optimal or oxidative stress conditions (Rahantaniaina et al., 2017). This may reflect the existence of multiple routes for ascorbate recycling. As well as enzymatic reduction by MDHAR and DHAR, non-enzymatic reactions may also contribute. Nevertheless, it will be interesting to analyze ascorbate pools in double or triple *mdhar* mutants generated by crossing. This work is currently underway.

A key outstanding question is the effect of the specific *mdhar* mutations on extractable MDHAR activity. To what extent does each gene contribute to the total leaf MDHAR capacity? Unfortunately, this enzyme is not so easy to measure, notably because the substrate, MDHA, is an unstable free radical that must be generated in the assay. I have not been able to resolve this question within the timescale of the thesis, but it will be addressed soon by developing appropriate procedures to enable an accurate assay of MDHAR activities in the different lines.

Irrespective of their relative contributions to total leaf MDHAR activity, the data provide further evidence that cytosolic isoform of enzymes involved in the ascorbate-glutathione pathway play key roles in responses to oxidative stress. First, analysis of different *MDHAR* transcripts showed that *MDHAR2* expression is obviously induced in response to *cat2*-induced oxidative stress (Figure 4.4). The second gene encoding a cytosolic isoform, *MDHAR3*, was also significantly induced in the *cat2* background. In addition to database evidence that these genes are induced by oxidative stress in Arabidopsis, reports have described induction of certain *MDHAR* transcripts in other plants such as *Brassica campestris* (Yoon et al., 2004). Our analyses of double mutants suggest that cytosolic MDHAR isoforms play a role in responses to intracellular oxidative stress. Based on the analysis of *cat2 mdhar* mutants, MDHAR3 may be less important than MDHAR2 because the block of MDHAR3 expression had little effect on the *cat2* phenotype whereas the *mdhar2* mutation largely abolished lesions and the induction of the SA pathway (Figure 4.5A-C). While the backcross analysis suggests that this effect was not all-or-nothing, it is remarkable because it shows that knocking out an additional antioxidative enzyme can down-regulate rather than up-regulate *cat2*-triggered cell death. It should be

noted, however, that this observation is consistent with previous reports on *cat2 apx1* and *cat2 gr1* lines (Mhamdi et al., 2010b; Vanderauwera et al., 2011). It offers a further indication that oxidative stress-induced lesions are not simply the result of accumulated damage, but occur rather through a process of signaling linked to cell redox state.

As well as SA, JA is also an important defence hormone whose signaling is closely linked to ROS (Maruta et al., 2011; Han et al., 2013b). According to the marker transcripts analysis (Figure 4.7), JA signaling is activated by the *cat2* mutation, consistent with a previous report of our group (Han et al., 2013b). Among all the four genes analyzed, *PDF1.2* induction was abolished by loss of *MDHAR2* function (Figure 4.6), but this effect was slight for other genes, suggesting that MDHAR2 may influence *cat2*-induced JA signaling rather than JA synthesis. Further analyses will be required to establish whether the effect on JA signaling is a secondary effect of the marked impact of *mdhar2* on oxidative stress-induced SA signaling.

As a lesion-mimic mutant, *cat2*-induced lesion formation has been shown to share many features with the HR response, including induction of *PR* genes, accumulation of SA and phytoalexins, and enhanced resistance to pathogens (Chaouch et al., 2010). The present results on SA signaling in the *cat2* mutant are therefore consistent with previous reports. Strikingly, even though neither the *mdhar1* nor the *mdhar3* mutation markedly affected gene expression in *cat2*, the specific loss of *MDHAR2* function almost completely abolished the *cat2*-induced accumulation of SA and SA-associated transcripts. Since the *cat2* lesion phenotype has been shown to be dependent on SA synthesis through ICS1 (Chaouch et al., 2010; Chapter 3), the effect of *mdhar2* on this phenotype likely occurs by suppression of the SA pathway during oxidative stress.

What could be the link between MDHAR2 and uncoupling of the SA pathway from oxidative stress? Oxidative stress in *cat2* is accompanied by the induction of multiple oxidative marker transcripts and antioxidative enzyme activities (Noctor et al., 2016). Our analysis revealed that the up-regulation of APX, one of the major antioxidative enzymes, is partly antagonized by the *mdhar2* mutation when plants are exposed to intracellular oxidative stress caused by the *cat2* mutation. This effect is also

observed at the level of *APX* transcripts, with a decreased induction of the gene encoding cytosolic APX1 in *cat2 mdhar2* (Figures 4.8 and 4.9). These effects may be a compensatory response to perturbed regeneration of ascorbate in conditions that impose an accelerated oxidation of this molecule. This would be consistent with the decreased ascorbate pools in *cat2 mdhar2* (Figure 4.10), possibly caused by an imbalance between ascorbate and MDHA. The plant might be configured to respond by measures that decrease the efficiency of ascorbate oxidation to slow down the flux through the pathway. Further evidence that redox state is perturbed when *MDHAR2* function is lost in the *cat2* background comes from the decreased induction of *UGT73B3* transcripts and decreased CAT activity. All these observations reveal that *MDHAR2* plays some role in regulating plant redox state in response to intracellular oxidative stress caused by enhanced H_2O_2 availability.

Whether or not flux through the ascorbate-glutathione pathway is indeed decreased in response to loss of *MDHAR2* function, a striking effect is enhanced oxidation of glutathione in *cat2 mdhar2* (Figure 4.10). As previously described, the *cat2* mutation alone causes a marked oxidation of glutathione, and this effect is somehow required for activation of the SA pathway by oxidative stress (Mhamdi et al., 2010b; Han et al., 2013a). The enhanced oxidation in *cat2 mdhar2* suggests that MDHAR2 is required for maintaining glutathione redox state in oxidative stress conditions, even though glutathione is not a substrate or a product of the MDHAR reaction. The simplest explanation is that decreased capacity to regenerate ascorbate from MDHA leads to enhanced dismutation of MDHA to DHA, leading in turn to faster rates of DHA-dependent glutathione oxidation. Indeed, this explanation receives support from kinetic modelling analyses that suggest there is an inverse relationship between MDHAR capacity and glutathione oxidation in oxidative stress conditions (Tuzet et al., 2018).

As well as documenting an important role for MDHAR2 in oxidative stress responses, the data presented in this chapter offer an intriguing explanation of the effects of loss of *G6PD5* function discussed in Chapter 3. As outlined in Chapter 3, the *g6pd5* mutation abolishes the *cat2* lesion phenotype and modifies *cat2* transcriptomes in a similar manner to *sid2*. While work by our group and others has shown that various loss-of-function mutants for reductive pathways of H_2O_2 metabolism (ascorbate-glutathione-NADPH systems) can impact *cat2* responses, the *mdhar2* and *g6pd5* mutations

are those we have so far identified that produce the most striking effects on the SA pathway and lesion formation. Both genes encode cytosolic proteins, one that produces NADPH (G6PD5) and one that requires NADPH (MDHAR2). One possibility, therefore, is that at least part of the effect of the *g6pd5* mutation is due to compromised production of NADPH for MDHAR2 activity. Since glutathione status is a critical factor for induction of the SA pathway by oxidative stress (Han et al., 2013a; Rahantaniaina et al., 2017), the hyper-oxidation of glutathione linked to compromised MDHAR activity may be key in suppressing induction of the SA pathway in *cat2.* This could occur either by direct genetic loss of *MDHAR2* function or sub-optimal production of NADPH for MDHAR2 when *G6PD5* function is lost. Evidence that this is an interesting avenue to pursue comes from data showing that *g6pd5* produces a similar effect on *cat2* glutathione status to *mdhar2* (Amna Mhamdi, unpublished results).

In conclusion, the results in this chapter suggest that a specific isoform of MDHAR is replaceable in unchallenging conditions but is particularly important in response to oxidative stress. In oxidative stress conditions, the *mdhar2* mutation mimics the effects of the *sid2* and *g6pd5* mutations described in Chapter 3. This observation, and some of the perspectives it raises, will be discussed further in the next chapter.

CHAPTER 5

GENERAL CONCLUSIONS AND PERSPECTIVES

5.1 Conclusions

Numerous studies have revealed that H_2O_2 plays an important role in response to various environmental constraints and that this mainly occurs through its effect as a signaling molecule rather than as a toxic byproduct. Although a lot of attention has focused on H_2O_2 accumulation, metabolism and its role in signal transduction, many of the underlying mechanisms that convert redox changes to phenotypic and functional outputs still remain to be elucidated.

A primary factor in governing oxidative signaling is the rate of H_2O_2 processing systems by various systems existing in plants. Among these systems, CATs and the ascorbate-glutathione pathways are recognized as key players. In Arabidopsis, CAT2 has been demonstrated to be the major isoform of CAT in leaves and its function has been shown to be closely linked to photorespiration. In contrast, the contribution of CAT1 and CAT3 to physiological processes is less well established. NADPH is one of the components involved in both ROS metabolism and production. At the outset of my thesis, work in our group had found that loss of function of a specific enzyme catalyzing NADPH production, G6PD5, abolished H_2O_2-triggered lesion formation in *cat2*. However, the underlying mechanism was unknown. The role of the ascorbate-glutathione pathway in processing H_2O_2 largely depends on NADPH, as this co-factor is the source of reductant for MDHAR and GR. When I began this work, little information was available on the importance of specific isoforms of MDHAR in response to oxidative stress. The following sections outline how my work has provided new information on these different aspects of H_2O_2 metabolism and its consequences.

5.1.1 The function of specific CAT isoforms

Most studies on CAT have focused on roles of this enzyme in leaves. In the work reported in Chapter 2, the role of CAT in roots was also investigated. Functional analysis by using different CAT single and double mutants showed that CAT2 is the most important isoform in roots as well as in leaves. The decreased root length caused by the *cat2* mutation was partly rescued in the presence of sugar. Moreover, the hCO_2 growth condition rescued it almost completely. As is well established, the hCO_2

condition blocks photorespiration in photosynthetic cells, so the *cat2* root phenotype is probably a secondary nutritional effect of insufficient CAT activity in leaves. The data from CAT activities and plant growth suggest that, compared to CAT2, the other two CATs do not play a major role in plant development in non-stressful conditions.

Previous work in our laboratory showed a day length-dependent effect of the *cat2* mutation in that the transcripts of rapidly induced oxidative stress marker genes accumulated more strongly in SD than in LD (Queval et al., 2007, 2012). However, it was still unclear whether this effect of day length was simply caused by the duration of oxidative stress or some other factor related to photoperiod. In this work we avoided the differences in the duration of exposure to photorespiration by keeping plants grown in LD or SD hCO_2 to a similar development stage before inducing oxidative stress. Consequently, the analysis of H_2O_2 marker gene expression after an equal-time exposure to air revealed that the day length-dependent effect is not simply due to the differences in the duration of stress.

5.1.2 Effect of G6PD5 on the H_2O_2-induced SA signaling pathway

Based on the crucial role of CAT2 in consuming H_2O_2 produced in photorespiration, a T-DNA knockout *cat2* mutant has been extensively used as a tool to mimic oxidative stress. Unpublished work in our laboratory reveals that the loss of function of *G6PD5*, a gene involved in NADPH production, abolished the lesion phenotype as well as a large part of the *cat2* transcriptome. Interestingly, these effects are quite similar to those caused by the *sid2* mutation. With the aim of identifying the underlying mechanisms via an unbiased approach, we used a forward genetics strategy to try to find revertants of the *cat2 g6pd5* phenotype. As described in Chapter 3 of the thesis, two genes have so far been identified with some confidence. In addition, novel candidate genes were identified in two other revertants but further work is required to identify exactly which genes are regulating lesion formation in *cat2 g6pd5* in these lines.

The first two genes that we have identified are *MIPS1* and *CPR5*. Mutants for both of these genes have

previously been found to stimulate lesion formation in Arabidopsis (Bowling et al., 1997; Meng et al., 2009; Donahue et al., 2010). MIPS1 catalyzes the conversion of glucose-6-phospate to *myo*-Inositol phosphate, which shares the same substrate with G6PD5 in the cytosol. In addition, the lesion formation in *mips1* is linked to day length or light regime and is regulated by SA, features that are quite similar to those observed for *cat2*-triggered lesions. In contrast to *mips1*, *cpr5* displays a day length-independent lesion phenotype, even though it is linked with HR response (Bowling et al., 1997). Further work is required to establish the linkage between these genes and the *cat2* mutation in determining lesion formation. Possible approaches will be discussed in the following perspectives section.

5.1.3 Functions of specific MDHAR isoforms in response to oxidative stress

As one of the enzymes in the ascorbate-glutathione pathway, the function of MDHAR requires NADPH as an electron donor. These enzymes are considered to function in maintenance of the reduced state of ascorbate, together with DHAR. However the roles of specific MDHAR isoforms are still unclear. As noted in Chapter 4, recent work in our laboratory showed that the loss of DHAR function did not affect the leaf ascorbate pools in either optimal or oxidative stress conditions (Rahantaniaina et al., 2017). Thus, we explored the potential importance of MDHAR in the function of the NADPH-dependent ascorbate-glutathione pathway.

The functional analysis in Chapter 4 showed that single *mdhar1*, *mdhar2* and *mdhar3* mutations did not affect the phenotype markedly in standard conditions, suggesting functional redundancy among these genes or with other systems. This is further confirmed by similar redox states compared with the wild-type, as indicated by analysis of ascorbate, glutathione, and oxidative marker transcripts. The mutants also showed similar levels of *PR* gene expression and SA content to the wild type. Interestingly, transcripts analysis in the *cat2* background suggested that the cytosolic isoforms MDHAR2 and MDHAR3 are involved in responses to intracellular oxidative stress. Direct analysis of double mutants to test this hypothesis showed that MDHAR2 is important for lesion formation and induction of the SA pathway in *cat2*. Subsequently, SA content analysis confirmed the effect of

MDHAR2 on *cat2*-induced SA signaling in that the loss of *MDHAR2* function largely abolished the *cat2*-induced SA accumulation. Activation of JA signaling by the *cat2* mutation was also affected by the *mdhar2* mutation, albeit to a lesser extent than up-regulation of the SA pathway.

In addition to the effect on lesion formation and phytohormone pathways, MDHAR2 is involved in the up-regulation of antioxidative marker transcripts and enzyme activities in *cat2*. Our analysis showed that both accumulation of *APX1* transcripts and induction of extractable APX activity, which are observed in *cat2*, were partly antagonized by the loss of *MDHAR2* function. One explanation of this effect could be that the plant responds to decreased efficiency of ascorbate regeneration by decreasing the capacity for H_2O_2-dependent ascorbate oxidation by APX. Some evidence that ascorbate pools were affected by loss of *MDHAR2* function is apparent from decreased ascorbate in *cat2 mdhar2*. Intriguingly, however, redox analysis also revealed an effect of the *mdhar2* mutation on *cat2*-induced glutathione oxidation, an effect that is discussed further below. Together, these observations suggest that MDHAR2 is required for maintaining redox homeostasis in oxidative stress conditions.

5.2 Perspectives

5.2.1 Specificity of CAT functions and interactions between oxidative signaling and day length

The work reported in Chapter 2 underscored the crucial role of CAT2 in plant growth and development. In addition to the well described effect on leaf CAT activity, loss of *CAT2* function markedly decreased the root CAT activity and this was accompanied by a decrease in root length. By contrast, loss of either *CAT1* or *CAT3* function did not produce a substantial effect on plant growth. One possibility is that there is functional redundancy between these two genes. Because of the contiguous position of the two genes, it is very difficult to test this hypothesis by simple crossing. Although the *cat2* mutation strongly affects root and shoot growth, linked to an 80% decrease in extractable CAT activity, the mutation is not lethal under standard growth conditions. This raises the question of whether plants can survive without any CAT at all. Analysis of this question would require

production of triple loss-of-function lines, in which all three genes are inactivated. Recently, a preliminary analysis of such lines was reported, by using triple mutants by CRISPR/Cas9 technology to inactivate *CAT1* expression in the *cat2 cat3* double mutant (Su et al., 2018). While the authors reported that the plants showed a somewhat exacerbated phenotype compared to *cat2 cat3*, no lethality was observed (Su et al., 2018).

Data shown in Chapter 2 provide evidence that the effect of day length on oxidative signaling in *cat2* is not simply the result of differences in oxidative stress. One possibility is that the effect of day length is somehow linked to differences in photosynthesis. Alternatively, some light-dependent signaling pathway that is differentially active in SD and LD growth conditions might modulate the response to oxidative stress. Further analysis of photosynthetic characteristics in LD and SD could throw some light on the first possibility. One way to test a signaling role of day length would be to cross *cat2* with photoreceptor mutants and analyze whether the effect of day length on marker transcripts is altered. Photoreceptors include phytochromes and cryptochromes, both of which have been implicated in some stress responses as well as in light signaling (Kangasjärvi et al., 2012). Such genetic resources are currently being characterized in the laboratory.

5.2.2 Further analysis of revertant mutations that allow lesion formation in *cat2 g6pd5*

As noted in Chapter 3, two genes have been identified in the revertant screen. Genome sequencing results suggest that mutations in *MIPS1* and *CPR5* were responsible for the reversion of the lesion phenotype in four lines of the mutated *cat2 g6pd5* plants. Given that three *MIPS1* alleles have been identified, it seems highly likely that inactivation of this gene function is responsible for reversion of the *cat2 g6pd5* phenotype in these lines. Like *mips1*, *cpr5*, which was the top hit in another revertant line, is known to promote lesion formation and PR responses. As recognized lesion-mimic mutants, both *mips1* and *cpr5* show spontaneous lesion formation (Bowling et al., 1997; Meng et al., 2009; Donahue et al., 2010), albeit with some phenotypic differences and a different dependence on growth conditions. Further work is envisaged to establish the extent to which these genes are involved in mechanisms by which *g6pd5* mutation prevents *cat2*-triggered lesion formation and SA signaling.

Confirmation with T-DNA insertion mutants is one of the possible approaches. Such mutants can be crossed to *cat2*, *g6pd5* and *cat2 g6pd5*. Functional analysis of double and triple mutants will establish whether the mutations identified in the revertant screen are indeed causal in allowing lesion formation. If so, loss of function of the identified genes in the T-DNA lines should revert the phenotype in *cat2 g6pd5*, and allow lesions to appear. Furthermore, based on the fact that the *g6pd5* mutation mimics the *sid2* mutation in abolishing transcriptome responses triggered by *cat2*, it will be worthwhile to check if the SA signaling pathway is affected when introducing the identified mutation into *cat2 g6pd5*, e.g. at the levels of *PR* gene expression, SA contents, and pathogen resistance. Currently, a T-DNA mutant for *mips1* has been crossed into *cat2 g6pd5* by Amna Mhamdi (Ghent university). Crosses between other candidates and *cat2 g6pd5* are underway.

5.2.3 MDHAR isoforms in responses to H_2O_2

The work presented in Chapter 4 reported that the functional analysis of *mdhar1*, *mdhar2* and *mdhar3* mutants revealed an irreplaceable role of *MDHAR2* in regulating lesion formation and SA signaling pathway in response to oxidative stress. MDHAR1 may play some role in H_2O_2 metabolism because the loss of *MDHAR1* function slightly decreased the rosette size of *cat2*. *MDHAR3* may also be involved to some extent in the oxidative stress responses, since this gene was significantly induced in *cat2*. However, introduction of the *mdhar3* mutation into the *cat2* background did not cause substantial changes in the *cat2* phenotype or associated SA signaling. One interesting perspective would be to extend this analysis to include mutants for *MDHAR4* or *MDHAR5/6*. Previous reports suggest that MDHAR4 is involved in ascorbate recycling in the peroxisomes (Lisenbee et al., 2005), while loss of function of *MDHAR4* also affected seed oil hydrolysis and seedling development (Eastmond, 2007). New evidence revealed a pro-oxidant effect of *MDHAR6* in mediating TNT toxicity by promoting reactive oxygen production (Johnston et al., 2015; Noctor, 2015). It would be interesting to do the functional analysis of *mdhar4* and *mdhar6* in optimal growth condition and in oxidative stress, e.g. by introducing mutations for these two genes into the *cat2* background. Analyses of all *mdhar* mutants in other stress conditions (e.g. pathogens, salt, heavy metals) is also an interesting perspective. This work is currently underway in the laboratory.

Phenotype analysis of the *mdhar* single mutants showed no difference when compared with the wild type, suggesting functional redundancy among MDHAR isoforms or with other systems in standard conditions. Therefore it would be interesting to produce the mutants with loss of function of multiple *MDHAR* isoforms. Based on the location of subcellular MDHARs, crosses between *MDHAR1* and *MDHAR4*, as well as between *MDHAR2* and *MDHAR3* seem to be most interesting, because the first two genes are targeted to the peroxisome and the second two are targeted to the cytosol. Furthermore, according to the effects of different *MDHAR* genes, especially *MDHAR2*, in response to oxidative stress as reported in Chapter 4, the study of multiple *MDHAR* mutations in oxidative stress could help us to understand more about the function and relationship of different *MDHAR* isoforms. With this objective, it would be interesting to produce triple mutants of *cat2 mdhar1 mdhar4* and *cat2 mdhar2 mdhar3*. . The production of such double and triple mutants is in progress.

In Chapter 4 of the thesis, by a direct genetic approach, it was shown that *MDHAR2* is required for *cat2*-triggered lesion formation and SA signaling pathway. As the laboratory had previously established for the *g6pd5* mutation, the loss of *MDHAR2* function largely abolished *PR* gene expression and SA accumulation induced by *cat2*. As noted in the introduction, SA signaling is involved in resistance to certain types of pathogen, and is also involved in localized cell death that occurs to restrict pathogen spread within the plant (HR response; Mur et al., 2008). In *cat2*, SA accumulation occurs alongside HR-like lesion formation, and is accompanied by increased resistance to pathogens (Chaouch et al., 2012; Han et al., 2013a). Thus, it seems that the *mdhar2* mutation, like that for *G6PD5*, abolishes PR responses that are triggered by perturbation of intracellular redox state. Hence, it would be interesting to do pathogen tests on *cat2 mdhar2* mutants, to confirm that the effect on SA-dependent responses is accompanied by a loss of *cat2*-induced resistance.

At present, we do not have an allelic line of *mdhar2* to confirm the effect of *MDHAR2* in oxidative stress responses. Even though the backcross of *cat2 mdhar2* with *cat2* showed a phenotype segregation ratio close to 3:1, the semi-quantitative nature of the phenotype analysis does not provide an absolute confirmation of the link between *mdhar2* genotype and phenotype. Hence, we cannot discount a possible influence of other unknown T-DNA-related mutations in the single line of *mdhar2*

and *cat2 mdhar2*. In the absence of an allelic mutant line, it would therefore be very interesting to complement the *mdhar2* and *cat2 mdhar2* lines with the wild-type MDHAR2. One possibility would be to use a construct to express MDHAR2-GFP, as this would enable the subcellular compartmentation of MDHAR2 to be confirmed as well as functional analysis to evaluate if the complementation restores the phenotype and SA responses in *cat2 mdhar2*.

A key point is the contribution of the specific MDHAR isoforms to total activity in leaves. Thus far, I have not been able to do these measurements. One difficulty is that the unstable nature of the substrate, MDHA, which is a free radical, makes the assay somewhat more difficult than those of the other antioxidative enzymes I measured during this work. Nevertheless, such experiments are important, and likely to add useful information to clarify the contribution of specific MDHAR isoforms to overall activity. The technique will be developed soon, with the view of analyzing the impact of the different *mdhar* mutations on enzyme activity in Col-0 and *cat2* backgrounds.

5.2.4 A functional link between G6PD5 and MDHAR2 in H_2O_2 signaling?

One intriguing avenue of enquiry generated by this work is the possibility that specific isoforms of G6PDH and MDHAR are critical in determining signaling outcomes of intracellular oxidative stress. As noted in Chapter 4, the loss of function of *MDHAR2* largely abolished the lesion phenotype and activation of SA signaling induced by *cat2*. The analyses conducted so far suggest that these effects are quite similar to those produced by the mutation of *g6pd5* (Chapter 3). G6PDH is one of the sources of NADPH for the function of MDHAR in the ascorbate-glutathione pathway. Moreover, both *G6PD5* and *MDHAR2* are targeted to the cytosol. These characteristics suggest that the effect of the *g6pd5* mutation in the *cat2* background could be due to compromised production of NADPH for MDHAR2 activity. Another result that supports this interpretation is the hyper-oxidation of glutathione linked to the *mdhar2* mutation. As shown in Chapter 4, *cat2 mdhar2* shows a significantly more oxidized glutathione status compared to *cat2*. This effect is consistent with modelling analyses that suggest that MDHAR is a key fulcrum that determines the degree of glutathione oxidation in response to increased H_2O_2 availability (Tuzet et al., 2018). Intriguingly, a similar hyper-oxidation of glutathione has also

been found in *cat2 g6pd5* (Amna Mhamdi, unpublished results). Previous reports point to a crucial role for glutathione status in linking SA signaling pathway with intracellular oxidative stress (Han et al., 2013a; Rahantaniaina et al., 2017).

A scheme that summarizes the possible interactions is shown in Figure 5.1. Down-regulation of MDHAR may compromise MDHA reduction to ascorbate, allowing more MDHA to dismutate to DHA, which engages the glutathione pool and leads to increased glutathione oxidation (Figure 5.1). Exacerbated oxidation of glutathione caused by the *mdhar2* mutation may lead to the inhibition of SA pathway induction in *cat2*. All these effects could also occur by indirect perturbation of MDHAR function when NADPH availability is compromised in *cat2 g6pd5* (Figure 5.1). To provide a first confirmation of this hypothesis, it would be interesting to do a side-by-side analysis of glutathione and ascorbate in *cat2 mdhar2* and *cat2 g6pd5*.

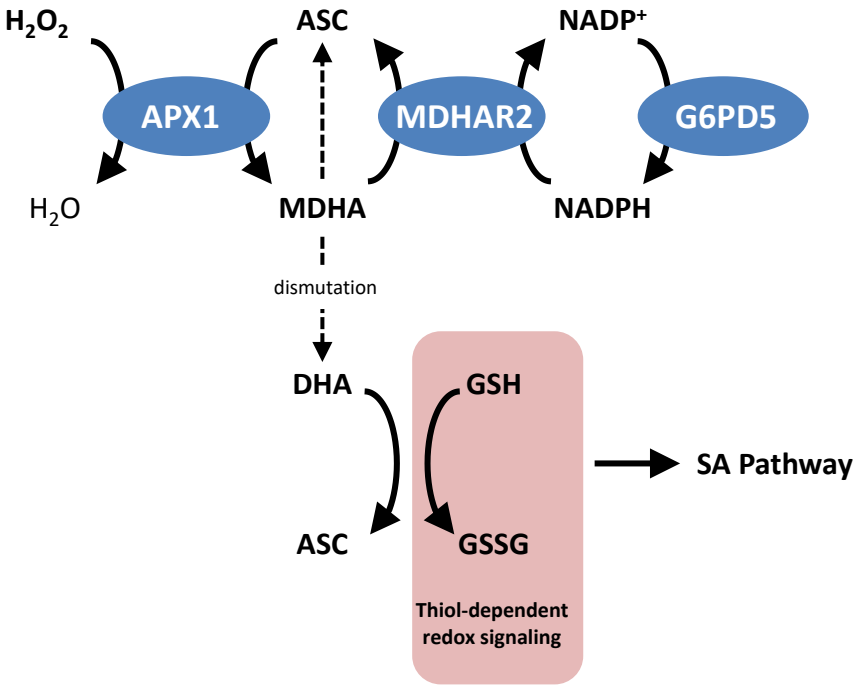

Figure 5.1. Scheme showing possible interplay between G6PD5 and MDHAR2 in activation of the SA pathway through their effects on cytosolic glutathione status. G6PD5-supported MDHAR2 activity is required to allow efficient regeneration of ascorbate from MDHA and to avoid excessive production of DHA that could over-oxidize the glutathione pool and inhibit the activation of signaling responses such as the SA pathway.

As noted in Chapter 3, the *g6pd5* mutation largely abolishes the transcriptomic response in *cat2*, thereby mimicking the *sid2* mutation. This result underscores the role of G6PD5 in linking SA signaling pathway to intracellular oxidative stress. Given the similar effect of *mdhar2* reported in this thesis, it would be interesting to analyze how loss of *MDHAR2* function affects the transcriptome response in *cat2*. A direct transcriptomic comparison of *cat2 mdhar2*, *cat2 g6pd5* and *cat2 sid2* can help us to understand if the *mdhar2* mutation indeed modifies the transcriptome response induced by *cat2* in a similar manner to that of the *g6pd5* and *sid2* mutations. This comparison could shed further light on the possible links between *G6PD5* and *MDHAR2* in regulating the SA signaling pathway in response to intracellular oxidative stress.

Alongside the direct transcriptomic comparison of *cat2 g6pd5* and *cat2 mdhar2*, it could also be interesting to identify whether there is overlap between MDHAR2 and G6PD5 interactants at the protein level. This can be achieved by analysis of protein interactions. For example, pulldown experiments can identify unknown proteins interacting with a protein of interest, using tags such as GFP fused to the protein of interest. Pulldown experiments using a G6PD5-GFP construct have already identified a number of possible *in planta* protein partners for G6PD5 (Amna Mhamdi, unpublished results). The MDHAR2-GFP constructs which will be produced for transformation of *cat2 mdhar2* (Section 5.2.3) could also be applied in pulldown experiments to find possible proteins interacting with MDHAR2. Thereafter, the protein partners of G6PD5 and MDHAR2 can be compared to see how much overlap there is between them. This will help us to further understand the relationship between G6PD5 and MDHAR2 in H_2O_2 signaling.

CHAPTER 6

MATERIALS AND METHODS

6.1 Plant materials and growth conditions

6.1.1 Plant materials

The T-DNA mutants were obtained from Nottingham Arabidopsis Stock Centre (NASC), Nottingham University, UK. While *cat2*, *cat3*, *mdhar1*, *mdhar2* and *mdhar4* are from the SALK collection and are in the Col-0 background, *cat1* and *mdhar3* are in the Col-3 background. The polymorphisms were SAIL_311_d07 for *cat1*, SALK_076998 for *cat2* (*cat2-1*, Queval et al., 2009), SALK_092911 for *cat3*, SALK_034893 for *mdhar1*, SALK_028874 for *mdhar2*, SAIL_31_A09 for *mdhar3*, SALK_015596 for *mdhar4*. Genotyping was performed by PCR using the primers listed in Table 6.1. Double mutants were generated by crossing *cat2* with the other single mutants. After heterozygote verification for both genes in the F1 generation by PCR, double homozygotes were identified in F2 in the same way. Thee F3 seeds produced were used for experiments. This work was accomplished with the collaboration of my colleagues in the group.

6.1.2 Growth and sampling

For plants grown in soil or on agar, seeds were first placed at 4 °C for 2 d in the dark and then transferred to a controlled-environment growth chamber in LD (16 h light/8 h dark) or SD (8 h light/16 h dark), an irradiance of 200 μmol m^{-2} s^{-1} at the leaf surface, 20°C/18°C, 65% humidity, and given nutrient solution twice per week. CO_2 concentration was maintained at 400 μL L^{-1} (air) or 3000 μL L^{-1} (hCO_2). For chemical treatment, the surface of the leaf was sprayed with 2 mM 3-AT and samples were collected 8 h later. Once collected at the stated developmental stage, samples were immediately frozen in liquid nitrogen and stored at -80 °C. Unless otherwise stated, data are means ± SE of three independent experiments with samples from different plants.

6.2 Methods

6.2.1 Phenotypic analysis and lesion quantification

Rosette diameter, leaf number and fresh weight from at least 18 plants of each genotype were quantified for phenotypic comparison. Photographs were also taken at the same time and then analyzed with IQ materials software to estimate the percentage of the rosette area that showed lesions.

6.2.2 DNA extraction and plant genotyping

Tissue samples were pre-cooled together with beads in 2 ml eppendorf tubes by liquid nitrogen. Then fine powder was obtained using a bead shaker. After adding 400 µl extraction buffer (200 mM Tris pH 7.5, 250 mM NaCl, 25 mM EDTA and 0.5% SDS), the solution was thoroughly vortexed and centrifuged at 11,000 rpm for 10 min at 4°C. 200 µl supernatant was mixed well with 200 µl isopropanol by vortex and centrifuged at 11,000 rpm for 10 min at room temperature. The pellet was washed with 1 ml 70% ethanol (v/v) and then dried in a fume hood. The pellet was redissolved in 100 µl sterile water. For T-DNA insertion lines, leaf DNA was amplified by PCR using primers specific for left T-DNA borders and the respective gene coding sequences (See Table 6.1).

6.2.3 RNA extraction and transcripts analysis

Total RNA was extracted with Trizol following the manufacturer's protocols. Around 100 mg leaf sample was thoroughly ground using a bead shaker following pre-cooling with beads in a 2 ml eppendorf tube in liquid nitrogen. For qPCR, the samples were shaken twice. Then 1 ml Trizol was added and the tube vortexed. For qPCR, the homogenate was incubated for 5 min at room temperature. 200 µl chloroform was added and mixed well by gentle shaking for 15 s. After incubation for 2-3 min at room temperature, the solution was centrifuged at 11,000 rpm for 15 min at 4°C. The upper aqueous phase was transferred into 200 µl isopropanol and vortexed. The solution was incubated at room temperature for 10 min and then centrifuged at 11,000 rpm for 10 min at 4 °C. The precipitate was

washed with 1 ml 70% ethanol (v/v) and centrifuged for another 5 min. The remaining liquid was removed and the pellet was dried at room temperature for 10 min. Then 40 µl RNase-free water was added, and the pellet resuspended by 10 min incubation at 65°C. The RNA solution was stored at -80°C.

The RNA concentration was estimated using a NanoDrop spectrophotometer. Then 4 µg RNA was reverse-transcribed using imPromll reverse transcriptase (Promega). For semi-quantitative RT-PCR, *ACTIN2* transcripts were used as a constitutive control. Quantitative real-time RT-PCR was performed with the LightCycler® 480 SYBR Green I Master (Roche) according to Queval et al. (2009). For qPCR, both *ACTIN2* and *RCE1* transcripts were used as controls. Gene-specific primer sequences used in this study are listed in Table 6.1.

Table 6.1. Oligonucleotide sequences used in this study

°	**Oligonucleotide**	**Sequence**	**Technique**
1	ForCAT1	TCCAGGTCAATTACTTCCCTTCA	Genotyping
2	RevCAT1	AGGCTCCGAAAGCGCTTCAA	Genotyping
3	ForCAT2	CCCAGAGGTACCTCTTCTTCTCCCATG	Genotyping
4	RevCAT2	TCAGGGAACTTCATCCCATCGC	Genotyping
5	ForCAT3	TCGATTGTTTAGACGTCCGAC	Genotyping
6	RevCAT3	AGGTTTGAAATGTCATGGGTG	Genotyping
7	ForG6PD5	CTTGTCGCCATGGAGAAACC	Genotyping
8	RevG6PD5	ATTTGGGAAGGTTTGATTTGG	Genotyping
9	ForMDHAR1	TGTTGGCGGAGGTTACATTG	Genotyping
10	RevMDHAR1	TCGTCAAACGAAACCAAACC	Genotyping
11	ForMDHAR2	TGGTTTATCCAGAACCTTGG	Genotyping
12	RevMDHAR2	GTCTACCACCGACACCCACT	Genotyping
13	ForMDHAR3	TTGCAACCGGTTCTACTGTG	Genotyping
14	RevMDHAR3	TTGATTCCCTTGTTGGCATAG	Genotyping
15	ForMDHAR4	CAAGTCGTGCAAGCAAAGAG	Genotyping
16	RevMDHAR4	TTACGGGTTCTTCGGAAATG	Genotyping

17	Lb1	TGGACCGCTTGCTGCAACTCT	Genotyping
18	LBSail	GAAATGGATAAATAGCCTTGCTTCC	Genotyping
19	ForACTIN2	TTCCCTCAGCACATTCCAGCAG	RT-PCR
20	RevACTIN2	TTAACATTGCAAAGAGTTTCAAGG	RT-PCR
21	ForCAT1	TACTCCAGACCCGGATCTTC	RT-PCR
22	RevCAT1	AAACCAAACCGTAAGAGGAGC	RT-PCR
23	ForCAT2	GTGCTGACTTTCTCCGAGCT	RT-PCR
24	RevCAT2	CCTGAACCATCCATGTGCCT	RT-PCR
25	ForCAT3	AGAAAGTTCCCACCCCTACAAACTCC	RT-PCR
26	RevCAT3	TGAATTAATAATATGTATAACGACCACCATA AATCT	RT-PCR
27	ForMDHAR1	GACTTCCAGGTTTCCATTGC	RT-PCR
28	RevMDHAR1	TATCACAATGTCGGCTTCCA	RT-PCR
29	ForMDHAR2	TGGTTTATCCAGAACCTTGG	RT-PCR
30	RevMDHAR2	TCCAACCACTTTCCGTTCTT	RT-PCR
31	ForMDHAR3	TGGCGGAAGAGAAAAGCTAC	RT-PCR
32	RevMDHAR3	CCCGCCATACATTTTCATTG	RT-PCR
33	ForMDHAR4	CATGGGAAGAGCTTTCGTG	RT-PCR
34	RevMDHAR4	ATATAGCCACCGCCGATAAC	RT-PCR
35	ForACTIN2	CTGTACGGTAACATTGTGCTCAG	qRT-PCR
36	RevACTIN2	CCGATCCAGACACTGTACTTCC	qRT-PCR
37	ForRCE1	CTGTTCACGGAACCCAATTC	qRT-PCR
38	RevRCE1	GGAAAAAGGTCTGACCGACA	qRT-PCR
39	ForCAT1	AAGTGCTTCATCGGGAAGG	qRT-PCR
40	RevCAT1	CTCCGAAAGCGCTTCAAC	qRT-PCR
41	ForCAT2	TGCTGGAAACTACCCTGAATGG	qRT-PCR
42	RevCAT2	TCAACACCATACGTCCAACAGG	qRT-PCR
43	ForCAT3	CCACTTGATGTGACCAAGATCTG	qRT-PCR
44	RevCAT3	GTAGATTCCAGGAACCACAAGACC	qRT-PCR
45	ForMDHAR1	ATCTGAGTGAAACACAACCACC	qRT-PCR
46	RevMDHAR1	GGGTTTCCTCTGCCGTAGAC	qRT-PCR
47	ForMDHAR2	CGAGCACAACCTTCTGTTGAG	qRT-PCR
48	RevMDHAR2	GCCACTCTGAACTCAAAGCTC	qRT-PCR
49	ForMDHAR3	TAAAGTGGCACGAGCACAAC	qRT-PCR

50	RevMDHAR3	CTATAGAACTTGGTGGCGAAAG	qRT-PCR
51	ForGSTU24	TCCATAGCTGGTTTGCAGTG	qRT-PCR
52	RevGSTU24	TAGCGACGCTCTCTCTCTCC	qRT-PCR
53	ForUGT73B3	CCTCACCACACCTCTCAACTC	qRT-PCR
54	RevUGT73B3	TCTGGTAACCCGAGATCCAC	qRT-PCR
55	ForAPX1	GCACTATTGGACGACCCTGT	qRT-PCR
56	RevAPX1	GCAAACCCAAGCTCAGAAAG	qRT-PCR
57	ForPR1	AGGCTAACTACAACTACGCTGCG	qRT-PCR
58	RevPR1	GCTTCTCGTTCACATAATTCCCAC	qRT-PCR
59	ForPR2	TCAAGGAGCTTAGCCTCACC	qRT-PCR
60	RevPR2	CGCCTAGCATCCCGTAGC	qRT-PCR
61	ForPR5	GCCCTACCACCGTCTGG	qRT-PCR
62	RevPR5	CGGGAAGCACCTGGAGTC	qRT-PCR
63	ForICS1	TTGGTGGCGAGGAGAGTG	qRT-PCR
64	RevICS1	CTTCCAGCTACTATCCCTGTCC	qRT-PCR
65	ForPDF1.2	CCAAACATGGATCATGCAAC	qRT-PCR
66	RevPDF1.2	CACACGATTTAGCACCAAAGA	qRT-PCR
67	ForJAZ10	CATCGGCTAAATCTCGTTCG	qRT-PCR
68	RevJAZ10	CGGTACTAGACCTGGCGAGA	qRT-PCR
69	ForLOX3	GTGGCCGGAGTTATCAACC	qRT-PCR
70	RevLOX3	GGGACGTAGCCACCGTAAG	qRT-PCR
71	ForMYB95	TCGATGTCACCTCCTCATCA	qRT-PCR
72	RevMYB95	GCGAGCTTGTTAAGGAAACG	qRT-PCR

6.2.4 Antioxidative enzyme activity measurements

6.2.4.1 Extraction

For CAT, GR and DHAR activity analysis, around 150 mg leaves or 100 mg roots from different plants was ground in liquid nitrogen with 50-100 mg PVP. Following grinding, 1.5 ml 0.1 M NaH_2PO_4 (pH 7.5) containing 1 mM EDTA was added immediately. If APX activity was involved in the analysis, 1 mM L-ascorbic acid was included in the buffer. Once thawed, the homogenate was transferred into a 2 ml Eppendorf tube, and centrifuged at 14,000 rpm for 10 min at 4°C. 1.1 ml

supernatant was transferred into a fresh tube, then 0.5 ml was desalted on a NAP-5 column that had been previously washed with 10 ml sterile water and pre-equilibrated with 10 ml 0.1 M NaH_2PO_4 containing 1 mM EDTA (pH 7.5). After desalting, the elution was performed with 1 ml of the same buffer. To prepare proteins for analysis of APX activity, pre-equilibration and elution were carried out separately with 0.1 M NaH_2PO_4 containing 1 mM EDTA and 1 mM L-ascorbic acid (pH 7.5).

6.2.4.2 Activity assay

Extractable enzyme activities were measured as described by Noctor et al. (2016). CAT activity was measured by H_2O_2 consumption at 240 nm. 20 µl H_2O_2 was added to 880-930 µl 0.1 M NaH_2PO_4, 1 mM EDTA (pH 7.5). The reaction was started by the addition of 50-100 µl desalted extract. The absorbance decrease at 240 nm was monitored for 1-2 min, and the linear part of the curve (first 30-60 s) was used for calculation. APX activity was measured as ascorbate oxidation at 290 nm. 50 µl 10 mM L-ascorbic acid was added to 890 µl 0.1 M NaH_2PO_4, 1 mM EDTA (pH 7.5), followed by the addition of 50 µl desalted extract. Then, the absorbance decrease at 290 nm was monitored for 2 min after adding 10 µl 20 mM H_2O_2. GR activity was measured as the absorbance decrease at 340 nm caused by NADPH oxidation. 10 µl 10 mM NADPH was added to 880 µl 0.1 M NaH_2PO_4, 1 mM EDTA (pH 7.5), followed by 100 µl desalted extract. Then the reaction was started by adding 10 µl 50 mM GSSG and the decrease in 340 nm was monitored for 2 min. DHAR activity was monitored as the increase in 265 nm due to DHA reduction to ascorbate. 50 µl 4 mM DHA and 25 µl 100 mM GSH were added to 905 µl 0.1 M NaH_2PO_4, 1 mM EDTA (pH 7.0). Then the absorbance increase at 265 nm was monitored for 2 min after the addition of 20 µl desalted extract.

6.2.5 Metabolite analysis

6.2.5.1 Glutathione and ascorbate assay by plate reader

6.2.5.1.1 Extraction

Oxidized and reduced forms of ascorbate and glutathione analysis were performed following a plate-reader method which was described in Queval and Noctor (2007). Around 100 mg leaves was ground to a fine powder in liquid nitrogen with a pestle and mortar. 1 ml 0.2 mM HCl was added immediately and the homogenate was ground again. After centrifuging at 14000 rpm for 10 min at 4 ℃, 500 µl supernatant was transferred to a fresh tube and mixed with 50 µl of 0.2 M NaH_2PO_4 (pH 5.6). Then the solution was neutralized to pH 4.5-5 with 0.2 M NaOH for the following assay.

6.2.5.1.2 Glutathione analysis

Glutathione measurements were performed by monitoring GR-dependent reduction of 5,5'-dithiobis (2-nitro-benzoic acid) (DTNB, Ellman's reagent) by GSH at 412 nm (Tietze, 1969). For total glutathione, the reaction system contained 0.1 ml of 0.2 M NaH_2PO_4, 10 mM EDTA (pH 7.5), 60 µl H_2O, 10 µl of 12 mM DTNB, 10 µl of 10 mM NADPH and 10 µl neutralized extract. The components were mixed three times by programmed shaking, and then 10 µl GR (20 U/ml) was added to start the reaction. The absorbance increase at 412 nm was monitored for 5 min and rates were calculated over the first 90 s. For GSSG, the measurement was based on the same principle except that an additional incubation step was performed to complex GSH in extract aliquots before reaction. For this, 200 µl neutralized extract was incubated with 2 µl 2-vinylpyridine (VPD) for 30 min at room temperature (Griffith, 1980). Excess VPD in the extract was then removed by centrifugation twice at 14000 rpm for 15 min at 4 ˚C. Finally 20 µl supernatant was added to the reaction system. Rates were converted to quantities of glutathione. Triplicate assays were performed for each extract as well as standards in the same plate.

6.2.5.1.3 Ascorbate analysis

Ascorbate measurements were done by monitoring the A_{265} which is specifically removable by ascorbate oxidase (AO). For ASC, the reaction system contained 100 µl 0.2 M NaH_2PO_4 (pH 5.6), 55 µl H_2O and 40 µl neutralized extract. Following programmed shaking (three times), the A_{265} was read. Then, 5µl AO (40 U/ml) was added and A_{265} was recorded again after 5 min. For total ascorbate, 100 µl neutralized extract was incubated with 140 µl 0.12 M NaH_2PO_4 (pH 7.5) and 10 µl 25 mM DTT for 30 min at room temperature. This treatment converts DHA to ASC. Then, the assay was performed as described for ASC. Triplicate assays were done for each extract in the same plate (Queval and Noctor, 2007).

6.2.5.2 Total SA assay by High Performance Liquid Chromatography (HPLC)

Total SA was measured following a protocol described in Langlois-Meurinne et al. (2005). Approximately 200 mg leaf sample was ground in liquid nitrogen and homogenized with 1.5 ml 90% methanol. Extracts were vortexed and centrifuged at 16000 g for 15 min at 4 ˚C. The supernatant was transferred to a new tube and set aside, and the precipitate was re-suspended with 0.5 ml 100% methanol by vortex. The supernatant obtained by centrifuging for 15 min at 16000 g was then mixed with the first supernatant. Subsequently, the combined supernatant was recentrifuged to produce the final supernatant, which was dried in a speed-vac for at least two hours. The dried extracts were subjected to acid hydrolysis by adding 600 µl 3 N HCl and incubating for 45 mins at 80 ˚C. 1 ml diethylether was added to the extracts. After vortexing for 20 mins, the preparation was centrifuged for 1 min at 16000 g, and the organic phase was transferred to a new tube. The remaining liquid was re-extracted by adding another 1 ml diethylether and the organic phase was mixed with the first one. The combined organic phase was evaporated to dryness in the fume hood. Finally, the dried extracts were dissolved in 200 µl resuspension buffer for HPLC analysis. Identification and quantification were performed by comparison of peaks with SA standards.

6.2.6 ROS visualization in roots

ROS visualization was performed using $DCFH_2$-DA staining, following a method adapted from Mhamdi et al. (2010b). 10 d-old seedlings were incubated in 50 µM staining solution at room temperature for 20 min in dark. Excess staining solution was removed by washing seedlings three times in phosphate buffer for 5 min in the dark. The fluorescence was observed with a Zeiss Axio Imager 2 fluorescence microscope.

6.2.7 EMS screen

6.2.7.1 EMS mutagenesis

Two 50 ml plastic tubes were prepared, each containing approximately 1000 seeds of *cat2 g6pd5,* and 25 ml 0.3% EMS (300 µl EMS stock solution/100 ml distilled water) was added. The tubes were incubated for 15 h at room temperature with gentle rotating. Because of the hazardous nature of EMS, a face-mask and gloves were worn, and all procedures were carried out in a fume hood. After the incubation with EMS, the M1 seeds were rinsed eight to nine times with 50 ml sterilized water. The waste washing solution was poured into a special container and deactivated with 0.1 N NaOH solution for 12 h in a fume hood. For the final rinse, seeds were kept in water and rotated for at least 1 h. Waste water was then poured off and the seeds were suspended with 0.1% agarose (0.1 g agarose powder/100 ml TBE).

The seeds were pipetted one by one into soil (9 seeds per square pot) immediately after mutagenesis. In total, approximately 1700 seeds were sown in the experiment. After vernalization for 2 d in the cold room, plants were transferred into a controlled-environment growth chamber in LD (16 h light/8 h dark), an irradiance of 200 µmol m^{-2} s^{-1} at leaf level, 20°C/18°C. To assess the EMS effect and the efficiency of the mutagenesis treatment, we quantified embryo lethality in M1 plants. Five plants were randomly chosen and 10 mature siliques from each plant were dissected under a stereomicroscope. Fruits were categorized into three classes based on the visual determination of the number of normal

and aborted seeds in each silique. Class A has a proportion of 3:1 or smaller (aborted seeds > 20 %), class B has a proportion between 4:1 and 13:1 (20 % ≥ aborted seeds > 6.7 %), and class C has a proportion of 14:1 or larger (aborted seeds < 6.7%). A frequency of fertile fruits (B+C) between 2% and 35% is regarded as an acceptable range to continue the work (Martín et al., 2009).

6.2.7.2 Phenotype screen

M2 seeds were harvested from all plants in bulk. The screen was carried out in a photoperiod of 16 h light/8 h dark with irradiance of 200 µmol m^{-2} s^{-1} at leaf level. Nine seeds were sown in each square pot and approximately 1600 plants were screened in each batch. Plants showing clear lesion phenotypes on the leaf surface were selected and genotyped by PCR to confirm that they were *cat2 g6pd5* homozygotes.

6.2.7.3 Backcross with *cat2 g6pd5*

For identified *cat2 g6pd5* M2 mutants that showed lesions, seeds of the next generation were grown to confirm the phenotype and genotype. At least twelve M3 plants of each potential mutant line were grown to confirm the stability of the previously recorded phenotype. For those lines in which all M3 plants showed clear lesions and which were reconfirmed as *cat2 g6pd5* homozygotes, plants were backcrossed with the non-mutagenized parental line *cat2 g6pd5*. Theoretically, the first filial generation (F1) plants obtained by backcross should be heterozygotes for the causal mutation. The F1 phenotype gives an important indication of whether the mutation is dominant or recessive. A lesion phenotype in all F1 plants indicates that the mutation is dominant; if none show lesions, the causal mutation is likely to be recessive.

F2 progeny were obtained by self-pollination of F1 plants. Seeds were collected from single plants and more than 60 seeds from four F1 plants were sown for phenotype segregation analysis. Those showing obvious lesions were identified, the genotype was confirmed again by PCR, and the segregation ratio was calculated. This ratio provides an indicator of the number of potential causal mutations in a given

line. In theory, if the segregation ratio of plants without lesions to those showing lesions is 3:1, it indicates that a single recessive mutation is probably responsible for the phenotype. Two mutations could be causal if the ratio is 15:1. The screened F2 plants with lesions were backcrossed to *cat2 g6pd5* for a second time, and genotypes and phenotypes analyzed in the resulting F2 generation. For a given line, F2 segregation ratios should be similar for the first and second backcrosses.

6.2.7.4 Sample collection for sequencing

Leaves from at least 50 F2 individuals that showed lesions following the first or second backcross were pooled and the bulked genomic DNA was sequenced. In parallel, the parental line *cat2 g6pd5* was also sequenced as the reference genome.

6.2.8 Nuclear DNA isolation for sequencing

Rosette material from approximately fifty plants was ground in liquid nitrogen then reground in 15 ml HBM buffer (25 mM Tris-HCl, pH 7.5, 440 mM sucrose, 10 mM $MgCl_2$, 0.1% Triton X-100, 10 mM β-mercaptoethanol) with continued grinding during thawing. The suspension was vortexed, kept on ice for 20 min, then filtered through Miracloth into 50 ml Falcon tubes. The filtrate was centrifuged at 3000 *g* for 10 min at 4°C, then the supernatant was discarded and the pellet resuspended in 0.5 ml NIB buffer (20 mM Tris-HCl, pH 7.5, 250 mM sucrose, 5 mM $MgCl_2$, 5 mM KCl, 0.1% Triton X-100, 10 mM β-mercaptoethanol). The resuspended pellet was carefully layered onto a 15-50% Percoll gradient in NIB buffer and centrifuged at 3000 rpm for 10 min at 4°C. Pelleted nuclei were washed and recentrifuged at 3000 rpm for 10 min at 4°C. The pellet was then resuspended in 0.5 mL pre-heated CTAB solution and incubated at 60°C for 30 min with frequent agitation. The suspension was clarified by centrifugation at 12000 *g* for 5 min and then combined with 0.5 ml chloroform:isoamyl alcohol (24:1) and gently mixed for about 1 min. After centrifugation for 5 min at 7000 *g* (4°C), the upper phase was transferred to a fresh Eppendorf tube and treated with RNAse for 30 min at 37°C. Then, 350 µl isopropanol was added with gentle mixing. Following overnight incubation at -20°C, the suspension was centrifuged at 13000 *g* for 6 min at 4°C. The supernatant was removed, washed twice

with 0.5 ml 70% ethanol, then dried in air for at least 15 min before being resuspended in 55 µl DNAse-free water. The DNA concentration was determined with a NanoDrop spectrophotometer.

6.2.9 Statistical analysis

Unless stated otherwise, the statistical analysis of data was based on Student's t-tests. Calculations were performed on a minimum of three independent data sets, assuming two sample equal variance and a two-tailed distribution. Unless otherwise indicated, significant difference is expressed using t-test at $P < 0.05$.

REFERENCES

Abe A, Kosugi S, Yoshida K, Natsume S, Takagi H, Kanzaki H, Matsumura H, Yoshida K, Mitsuoka C, Tamiru M, et al (2012) Genome sequencing reveals agronomically important loci in rice using MutMap. Nat Biotechnol **30**: 174-178

Abou-Attia MA, Wang X, Nashaat Al-Attala M, Xu Q, Zhan G, Kang Z (2016) *TaMDAR6* acts as a negative regulator of plant cell death and participates indirectly in stomatal regulation during the wheat stripe rust-fungus interaction. Physiol Plant **156**: 262-267

Abuharbeid S, Apel J, Sander M, Fiedler B, Langer M, Zuzarte ML, Czubayko F, Aigner A (2004) Cytotoxicity of the novel anti-cancer drug rViscumin depends on HER-2 levels in SKOV-3 cells. Biochem Biophys Res Commun **321**: 403-412

Achard P, Renou JP, Berthomé R, Harberd NP, Genschik P (2008) Plant DELLAs restrain growth and promote survival of adversity by reducing the levels of reactive oxygen species. Curr Biol **18**: 656-660

Agrawal V, Zhang C, Shapiro AD, Dhurjati PS (2004) A dynamic mathematical model to clarify signaling circuitry underlying programmed cell death control in *Arabidopsis* disease resistance. Biotechnol Prog **20**: 426-442

Alessandra Devoto, John G. Turner (2004) Jasmonate-regulated *Arabidopsis* stress signalling network. Physiologia Plantarum **123**: 161 - 172

Alfonso-Prieto M, Biarnés X, Vidossich P, Rovira C (2009) The molecular mechanism of the catalase reaction. J Am Chem Soc **131**: 11751-11761

Anjum NA, Gill SS, Gill R, Hasanuzzaman M, Duarte AC, Pereira E, Ahmad I, Tuteja R, Tuteja N (2014) Metal/metalloid stress tolerance in plants: role of ascorbate, its redox couple, and associated enzymes. Protoplasma **251**: 1265-1283

Arakaki AK, Ceccarelli EA, Carrillo N (1997) Plant-type ferredoxin-$NADP^+$ reductases: a basal structural framework and a multiplicity of functions. FASEB J **11**: 133-140

Arnon DI, Rosenberg LL, Whatley FR (1954) A new glyceraldehyde phosphate dehydrogenase from photosynthetic tissues. Nature **173**: 1132-1134

Arondel V, Lemieux B, Hwang I, Gibson S, Goodman HM, Somerville CR (1992) Map-based cloning of a gene controlling omega-3 fatty acid desaturation in *Arabidopsis*. Science **258**: 1353-1355

Asada K (2006) Production and scavenging of reactive oxygen species in chloroplasts and their functions. Plant Physiol **141**: 391-396

Asada K (2000) The water-water cycle as alternative photon and electron sinks. Philos Trans R Soc Lond B Biol Sci **355**: 1419-1431

Asada K (1999) THE WATER-WATER CYCLE IN CHLOROPLASTS: scavenging of active oxygens and dissipation of excess photons. Annu Rev Plant Physiol Plant Mol Biol **50**: 601-639

Asada K, Kiso K, Yoshikawa K (1974) Univalent reduction of molecular-oxygen by spinach-chloroplasts on illumination. J Biol Chem **249**: 2175-2181

Assmann SM (2005) G protein regulation of disease resistance during infection of rice with rice blast fungus. Sci STKE **310**: cm13

Austin RS, Vidaurre D, Stamatiou G, Breit R, Provart NJ, Bonetta D, Zhang J, Fung P, Gong Y, Wang PW, McCourt P, Guttman DS (2011) Next-generation mapping of *Arabidopsis* genes. Plant J **67**: 715-725

Awad J, Stotz HU, Fekete A, Krischke M, Engert C, Havaux M, Berger S, Mueller MJ (2015) 2-cysteine peroxiredoxins and thylakoid ascorbate peroxidase create a water-water cycle that is essential to protect the photosynthetic apparatus under high light stress conditions. Plant Physiol **167**: 1592-1603

Belhaj K, Lin B, Mauch F (2009) The chloroplast protein RPH1 plays a role in the immune response of *Arabidopsis* to Phytophthora brassicae. Plant J **58**: 287-298

Borraccino G, Dipierro S, Arrigoni O (1986) Purification and properties of ascorbate free-radical reductase from potato tubers. Planta **167**: 521-526

Bowler C, Fluhr R (2000) The role of calcium and activated oxygens as signals for controlling cross-tolerance. Trends Plant Sci **5**: 241-246

Bowling SA, Clarke JD, Liu Y, Klessig DF, Dong X (1997) The *cpr5* mutant of *Arabidopsis* expresses both NPR1-dependent and NPR1-independent resistance. Plant Cell **9**: 1573-1584

Brown NJ, Palmer BG, Stanley S, Hajaji H, Janacek SH, Astley HM, Parsley K, Kajala K, Quick WP, Trenkamp S, et al (2010) C_4 acid decarboxylases required for C_4 photosynthesis are active in the mid-vein of the C_3 species *Arabidopsis thaliana*, and are important in sugar and amino acid metabolism. Plant J **61**: 122-133

Bruggeman Q, Raynaud C, Benhamed M, Delarue M (2015) To die or not to die? Lessons from lesion mimic mutants. Front Plant Sci **6**: 24

Brunner NA, Hensel R (2001) Nonphosphorylating glyceraldehyde-3-phosphate dehydrogenase from Thermoproteus tenax. Methods Enzymol **331**: 117-131

Bueso E, Alejandro S, Carbonell P, Perez-Amador MA, Fayos J, Bellés JM, Rodriguez PL, Serrano R (2007) The lithium tolerance of the *Arabidopsis cat2* mutant reveals a cross-talk between oxidative stress and ethylene. Plant J **52**: 1052-1065

Bulley S, Laing W (2016) The regulation of ascorbate biosynthesis. Curr Opin Plant Biol **33**: 15-22

Bunkelmann JR, Trelease RN (1996) Ascorbate peroxidase. A prominent membrane protein in oilseed glyoxysomes. Plant Physiol **110**: 589-598.

Bustos DM, Iglesias AA (2002) Non-phosphorylating glyceraldehyde-3-phosphate dehydrogenase is post-translationally phosphorylated in heterotrophic cells of wheat (*Triticum aestivum*). FEBS Lett **530**: 169-173

Bustos DM, Iglesias AA (2003) Phosphorylated non-phosphorylating glyceraldehyde-3- phosphate dehydrogenase from heterotrophic cells of wheat interacts with 14-3-3 proteins. Plant Physiol **133**: 2081-2088

Cairns NG, Pasternak M, Wachter A, Cobbett CS, Meyer AJ (2006) Maturation of *Arabidopsis* seeds is dependent on glutathione biosynthesis within the embryo. Plant Physiol **141**: 446-455

Chamnongpol S, Willekens H, Moeder W, Langebartels C, Sandermann H, Van Montagu M, Inzé D, Van Camp W (1998) Defense activation and enhanced pathogen tolerance induced by H_2O_2 in transgenic tobacco. Proc Natl Acad Sci USA **95**: 5818-5823

Chang GG, Tong L (2003) Structure and function of malic enzymes, a new class of oxidative decarboxylases. Biochemistry **42**: 12721-12733

Chaouch S, Queval G, Noctor G (2012) AtRbohF is a crucial modulator of defence-associated metabolism and a key actor in the interplay between intracellular oxidative stress and pathogenesis responses in *Arabidopsis*. Plant J **69**: 613-627

Chaouch S, Queval G, Vanderauwera S, Mhamdi A, Vandorpe M, Langlois-Meurinne M, Van Breusegem F, Saindrenan P, Noctor G (2010) Peroxisomal hydrogen peroxide is coupled to biotic defense responses by ISOCHORISMATE SYNTHASE1 in a daylength-related manner. Plant Physiol **153**: 1692-1705

Cheng Y, Long M (2007) A cytosolic NADP-malic enzyme gene from rice (*Oryza sativa* L.) confers salt tolerance in transgenic *Arabidopsis*. Biotechnol Lett **29**: 1129-1134

Cobbett CS, May MJ, Howden R, Rolls B (1998) The glutathione-deficient, cadmium-sensitive mutant, *cad2-1*, of *Arabidopsis thaliana* is deficient in γ-glutamylcysteine synthetase. Plant J **16**: 73-78

Coego A, Ramirez V, Gil MJ, Flors V, Mauch-Mani B, Vera P (2005) An *Arabidopsis* homeodomain transcription factor, OVEREXPRESSOR OF CATIONIC PEROXIDASE 3, mediates resistance to infection by necrotrophic pathogens. Plant Cell **17**: 2123-2137

Cornic G, Briantais JM (1991) Partitioning of photosynthetic electron flow between CO_2 and O_2

reduction in a C_3 leaf (*Phaseolus vulgaris* L.) at different CO_2 concentrations and during drought stress. Planta **183**: 178-184

Corpas FJ, Barroso JB (2014) NADPH-generating dehydrogenases: their role in the mechanism of protection against nitro-oxidative stress induced by adverse environmental conditions. Front Environ Sci **2**: 1-5

Corpas FJ, Barroso JB, Del Río LA (2001) Peroxisomes as a source of reactive oxygen species and nitric oxide signal molecules in plant cells. Trends Plant Sci **6**: 145-150

Corpas FJ, Fernández-Ocaña A, Carreras A, Valderrama R, Luque F, Esteban FJ, Rodríguez-Serrano M, Chaki M, Pedrajas JR, Sandalio LM, et al (2006) The expression of different superoxide dismutase forms is cell-type dependent in olive (*Olea europaea* L.) leaves. Plant Cell Physiol **47**: 984-994

Corpas FJ, Palma JM, del Río LA, Barroso JB (2009) Evidence supporting the existence of L-arginine-dependent nitric oxide synthase activity in plants. New Phytol **184**: 9-14

Creissen G, Firmin J, Fryer M, Kular B, Leyland N, Reynolds H, Pastori G, Wellburn F, Baker N, Wellburn A, et al (1999) Elevated glutathione biosynthetic capacity in the chloroplasts of transgenic tobacco plants paradoxically causes increased oxidative stress. Plant Cell **11**: 1277-1292

Cuperus JT, Montgomery TA, Fahlgren N, Burke RT, Townsend T, Sullivan CM, Carrington JC (2010) Identification of MIR390a precursor processing-defective mutants in *Arabidopsis* by direct genome sequencing. Proc Natl Acad Sci USA **107**: 466-471

Dal Santo S, Stampfl H, Krasensky J, Kempa S, Gibon Y, Petutschnig E, Rozhon W, Heuck A, Clausen T, Jonak C (2012) Stress-induced GSK3 regulates the redox stress response by phosphorylating glucose-6-phosphate dehydrogenase in *Arabidopsis*. Plant Cell **24**: 3380-3392

Dalton DA, Baird LM, Langeberg L, Taugher CY, Anyan WR, Vance CP, Sarath G (1993) Subcellular localization of oxygen defense enzymes in soybean (*Glycine max* [L.] Merr.) root nodules. Plant Physiol **102**: 481-489

Dalton DA, Langeberg L, Robbins M (1992) Purification and characterization of monodehydroascorbate reductase from soybean root nodules. Arch Biochem Biophys **292**: 281-286

Dangl JL, Jones JD (2001) Plant pathogens and integrated defence responses to infection. Nature **411**: 826-833

Dat JF, Inzé D, Van Breusegem F (2001) Catalase-deficient tobacco plants: tools for in planta studies on the role of hydrogen peroxide. Redox Rep **6**: 37-42

Daudi A, Cheng Z, O'Brien JA, Mammarella N, Khan S, Ausubel FM, Bolwell GP (2012) The

apoplastic oxidative burst peroxidase in *Arabidopsis* is a major component of pattern-triggered immunity. Plant Cell **24**: 275-287

De Leonardis S, De Lorenzo G, Borraccino G, Dipierro S (1995) A specific ascorbate free radical reductase isozyme participates in the regeneration of ascorbate for scavenging toxic oxygen species in potato tuber mitochondria. Plant Physiol **109**: 847-851

Desikan R, A-H-Mackerness S, Hancock JT, Neill SJ (2001) Regulation of the *Arabidopsis* transcriptome by oxidative stress. Plant Physiol **127**: 159-172

Dghim AA, Mhamdi A, Vaultier MN, Hasenfratz-Sauder MP, Le Thiec D, Dizengremel P, Noctor G, Jolivet Y (2013) Analysis of cytosolic isocitrate dehydrogenase and glutathione reductase 1 in photoperiod-influenced responses to ozone using *Arabidopsis* knockout mutants. Plant Cell Environ **36**: 1981-1991

Dietrich RA, Delaney TP, Uknes SJ, Ward ER, Ryals JA, Dangl JL (1994) *Arabidopsis* mutants simulating disease resistance response. Cell **77**: 565-577

Dietrich RA, Richberg MH, Schmidt R, Dean C, Dangl JL (1997) A novel zinc finger protein is encoded by the *Arabidopsis LSD1* gene and functions as a negative regulator of plant cell death. Cell **88**: 685-694

Dietz KJ (2003) Plant peroxiredoxins. Annu Rev Plant Biol **54**: 93-107

Dietz KJ (2008) Redox signal integration: From stimulus to networks and genes. Physiol Plant **133**: 459-468

Dietz KJ, Mittler R, Noctor G (2016) Recent progress in understanding the role of reactive oxygen species in plant cell signaling. Plant Physiol **171**: 1535-1539

Dixon DP, Hawkins T, Hussey PJ, Edwards R (2009) Enzyme activities and subcellular localization of members of the *Arabidopsis* glutathione transferase superfamily. J Exp Bot **60**: 1207-1218

Dizengremel P, Le Thiec D, Hasenfratz-Sauder MP, Vaultier MN, Bagard M, Jolivet Y (2009) Metabolic-dependent changes in plant cell redox power after ozone exposure. Plant Biology **11**: 35-42

Dodd AN, Kudla J, Sanders D (2010) The language of calcium signaling. Annu Rev Plant Biol **61**: 593-620

Doke N (1983) Generation of superoxide anion by potato tuber protoplasts during the hypersensitive response to hyphal wall components of *Phytophthora infestans* and specific inhibition of the reaction by suppressors of hypersensitivity. Physiol Plant Pathol **23**: 359-367

Donahue JL, Alford SR, Torabinejad J, Kerwin RE, Nourbakhsh A, Ray WK, Hernick M,

Huang X, Lyons BM, Hein PP, et al (2010) The *Arabidopsis thaliana* Myo-Inositol 1-phosphate synthase1 gene is required for Myo-inositol synthesis and suppression of cell death. Plant Cell **22**: 888-903

Dowdle J, Ishikawa T, Gatzek S, Rolinski S, Smirnoff N (2007) Two genes in *Arabidopsis thaliana* encoding GDP-L-galactose phosphorylase are required for ascorbate biosynthesis and seedling viability. Plant J **52**: 673-689

Drincovich MF, Casati P, Andreo CS (2001) NADP-malic enzyme from plants: a ubiquitous enzyme involved in different metabolic pathways. FEBS Lett **490**: 1-6

Drouaud J, Camilleri C, Bourguignon PY, Canaguier A, Bérard A, Vezon D, Giancola S, Brunel D, Colot V, Prum B, Quesneville H, Mézard C (2006) Variation in crossing-over rates across chromosome 4 of *Arabidopsis thaliana* reveals the presence of meiotic recombination "hot spots". Genome Res **16**: 106-114

Eastmond PJ (2007) *MONODEHYROASCORBATE REDUCTASE4* is required for seed storage oil hydrolysis and postgerminative growth in *Arabidopsis*. Plant Cell **19**: 1376-1387

Eltayeb AE, Kawano N, Badawi GH, Kaminaka H, Sanekata T, Shibahara T, Inanaga S, Tanaka K (2007) Overexpression of monodehydroascorbate reductase in transgenic tobacco confers enhanced tolerance to ozone, salt and polyethylene glycol stresses. Planta **225**: 1255-1264

Eltelib HA, Badejo AA, Fujikawa Y, Esaka M (2011) Gene expression of monodehydroascorbate reductase and dehydroascorbate reductase during fruit ripening and in response to environmental stresses in acerola (*Malpighia glabra*). J Plant Physiol **168**: 619-627

Emes MJ, Neuhaus HE (1997) Metabolism and transport in non-photosynthetic plastids. J Exp Bot **48**: 1995-2005

Esaka M, Yamada N, Kitabayashi M, Setoguchi Y, Tsugeki R, Kondo M, Nishimura M (1997) cDNA cloning and differential gene expression of three catalases in pumpkin. Plant Mol Biol **33**: 141-155

Feng H, Liu W, Zhang Q, Wang X, Wang X, Duan X, Li F, Huang L, Kang Z (2014a) *TaMDHAR4*, a monodehydroascorbate reductase gene participates in the interactions between wheat and *Puccinia striiformis* f. sp. *tritici*. Plant Physiol Biochem **76**: 7-16

Feng H, Wang X, Zhang Q, Fu Y, Feng C, Wang B, Huang L, Kang Z (2014b) Monodehydroascorbate reductase gene, regulated by the wheat PN-2013 miRNA, contributes to adult wheat plant resistance to stripe rust through ROS metabolism. Biochim Biophys Acta **1839**: 1-12.

Ferguson IB and Dunning SJ (1986) Effect of 3-amino-1,2,4-triazole, a catalase inhibitor, on peroxide content of suspension-cultured pear fruit cells. Plant Sci **43**: 7-11

Ferretti M, Destro T, Tosatto SC, La Rocca N, Rascio N, Masi A (2009) Gamma-glutamyl transferase in the cell wall participates in extracellular glutathione salvage from the root apoplast. New Phytol **181**: 115-126

Finkel T, Holbrook NJ (2000) Oxidants, oxidative stress and the biology of ageing. Nature **408**: 239-247

Finkemeier I, König AC, Heard W, Nunes-Nesi A, Pham PA, Leister D, Fernie AR, Sweetlove LJ (2013) Transcriptomic analysis of the role of carboxylic acids in metabolite signaling in Arabidopsis leaves. Plant Physiol **162**: 239-253

Fischer BB, Hideg É, Krieger-Liszkay A (2013) Production, detection, and signaling of singlet oxygen in photosynthetic organisms. Antioxid Redox Signal **18**: 2145-2162

Foreman J, Demidchik V, Bothwell JH, Mylona P, Miedema H, Torres MA, Linstead P, Costa S, Brownlee C, Jones JD, et al (2003) Reactive oxygen species produced by NADPH oxidase regulate plant cell growth. Nature **422**: 442-446

Foyer CH, Bloom AJ, Queval G, Noctor G (2009) Photorespiratory metabolism: genes, mutants, energetics, and redox signaling. Annu Rev Plant Biol **60**: 455-484

Foyer CH, Halliwell B (1977) Purification and properties of dehydroascorbate reductase from spinach leaves. Phytochemistry **9**: 1347-1350

Foyer CH, Halliwell B (1976) The presence of glutathione and glutathione reductase in chloroplasts: a proposed role in ascorbic acid metabolism. Planta **133**: 21-25

Foyer CH, Neukermans J, Queval G, Noctor G, Harbinson J (2012) Photosynthetic control of electron transport and the regulation of gene expression. J Exp Bot **63**: 1637-1661

Foyer CH, Noctor G (2011) Ascorbate and glutathione: the heart of the redox hub. Plant Physiol **155**: 2-18

Foyer CH, Noctor G (2012) Managing the cellular redox hub in photosynthetic organisms. Plant Cell Environ **35**: 199-201

Foyer CH, Noctor G (2005a) Oxidant and antioxidant signalling in plants: a re-evaluation of the concept of oxidative stress in a physiological context. Plant Cell Environ **28**: 1056-1071

Foyer CH, Noctor G (2000) Oxygen processing in photosynthesis: regulation and signalling. New Phytol **146**: 359-388

Foyer CH, Noctor G (2005b) Redox homeostasis and antioxidant signaling: a metabolic interface between stress perception and physiological responses. Plant Cell **17**: 1866-1875

Foyer CH, Noctor G (2009) Redox regulation in photosynthetic organisms: signaling, acclimation, and practical implications. Antioxid Redox Signal **11**: 861-905

Foyer CH, Noctor G (2003) Redox sensing and signalling associated with reactive oxygen in chloroplasts, peroxisomes and mitochondria. Physiol Plant **119**: 355-364

Foyer CH, Noctor G (2016) Stress-triggered redox signalling: what's in pROSpect? Plant Cell Environ **39**: 951-964

Foyer CH, Ruban AV, Noctor G (2017) Viewing oxidative stress through the lens of oxidative signalling rather than damage. Biochem J **474**: 877-883

Frugoli JA, Zhong HH, Nuccio ML, McCourt P, McPeek MA, Thomas TL, McClung CR (1996) Catalase is encoded by a multigene family in Arabidopsis thaliana (L.) Heynh. Plant Physiol **112**: 327-336

Fryer MJ, Ball L, Oxborough K, Karpinski S, Mullineaux PM, Baker NR (2003) Control of *Ascorbate Peroxidase 2* expression by hydrogen peroxide and leaf water status during excess light stress reveals a functional organisation of Arabidopsis leaves. Plant J **33**: 691-705

Fryer MJ, Oxborough K, Mullineaux PM, Baker NR (2002) Imaging of photooxidative stress responses in leaves. J Exp Bot **53**: 1249-1254

Gao X, Yuan HM, Hu YQ, Li J, Lu YT (2014) Mutation of *Arabidopsis* CATALASE2 results in hyponastic leaves by changes of auxin levels. Plant Cell Environ **37**: 175-188

Gao Z, Loescher WH (2000) NADPH supply and mannitol biosynthesis. Characterization, cloning, and regulation of the non-reversible glyceraldehyde-3-phosphate dehydrogenase in celery leaves. Plant Physiol **124**: 321-330

Gatzek S, Wheeler GL, Smirnoff N (2002) Antisense suppression of l-galactose dehydrogenase in *Arabidopsis thaliana* provides evidence for its role in ascorbate synthesis and reveals light modulated l-galactose synthesis. Plant J **30**: 541-553

Genaro-Mattos TC, Maurício ÂQ, Rettori D, Alonso A, Hermes-Lima M (2015) Antioxidant activity of caffeic acid against iron-induced free radical generation-a chemical approach. PLoS One **10**: 1-12

Gerrard Wheeler MC, Arias CL, Tronconi MA, Maurino VG, Andreo CS, Drincovich MF (2008) *Arabidopsis thaliana* NADP-malic enzyme isoforms: high degree of identity but clearly distinct properties. Plant Mol Biol **67**: 231-242

Gerrard Wheeler MC, Tronconi MA, Drincovich MF, Andreo CS, Flügge UI, Maurino VG (2005) A comprehensive analysis of the NADP-malic enzyme gene family of Arabidopsis. Plant

Physiol **139**: 39-51

Gest N, Garchery C, Gautier H, Jiménez A, Stevens R (2013) Light-dependent regulation of ascorbate in tomato by a monodehydroascorbate reductase localized in peroxisomes and the cytosol. Plant Biotechnol J **11**: 344-354

Godoy Herz MA, Kornblihtt AR, Barta A, Kalyna M, Petrillo E (2014) Shedding light on the chloroplast as a remote control of nuclear gene expression. Plant Signal Behav **9**: e976150

Gorman AA, Rodgers MA (1992) Current perspectives of singlet oxygen detection in biological environments. J Photochem Photobiol B **14**: 159-176

Graham IA, Eastmond PJ (2002) Pathways of straight and branched chain fatty acid catabolism in higher plants. Prog Lipid Res **41**: 156-181

Greene EA, Codomo CA, Taylor NE, Henikoff JG, Till BJ, Reynolds SH, Enns LC, Burtner C, Johnson JE, Odden AR, et al (2003) Spectrum of chemically induced mutations from a large-scale reverse-genetic screen in *Arabidopsis*. Genetics **164**: 731-740.

Griffith OW (1980) Determination of glutathione and glutathione disulfide using glutathione reductase and 2-vinylpyridine. Anal Biochem **106**: 207-212

Guan L, Scandalios JG (1996) Molecular evolution of maize catalases and their relationship to other eukaryotic and prokaryotic catalases. J Mol Evol **42**: 570-579

Gustin MC, Albertyn J, Alexander M, Davenport K (1998) MAP Kinase pathways in the yeast *Saccharomyces cerevisiae*. Microbiol Mol Biol Rev **62**: 1264-1300

Gutiérrez J, González-Pérez S, García-García F, Daly CT, Lorenzo Ó, Revuelta JL, McCabe PF, Arellano JB (2014) Programmed cell death activated by Rose Bengal in *Arabidopsis thaliana* cell suspension cultures requires functional chloroplasts. J Exp Bot **65**: 3081-3095

Halliwell B (2006) Oxidative stress and neurodegeneration: where are we now? J Neurochem **97**: 1634-1658

Halliwell B, Gutteridge JMC (2015) Free Radicals in Biology and Medicine (5th Ed, Oxford University Press, Oxford)

Han Y, Chaouch S, Mhamdi A, Queval G, Zechmann B, Noctor G (2013a) Functional analysis of Arabidopsis mutants points to novel roles for glutathione in coupling H_2O_2 to activation of salicylic acid accumulation and signaling. Antioxid Redox Signal **18**: 2106-2121

Han Y, Mhamdi A, Chaouch S, Noctor G (2013b) Regulation of basal and oxidative stress-triggered jasmonic acid-related gene expression by glutathione. Plant Cell Environ **36**: 1135-1146

Harms K, Von Ballmoos P, Brunold C, Höfgen R, Hesse H (2000) Expression of a bacterial serine acetyltransferase in transgenic potato plants leads to increased levels of cysteine and glutathione. Plant J **22**: 335-343

Hartwig B, James GV, Konrad K, Schneeberger K, Turck F (2012) Fast isogenic mapping-by-sequencing of ethyl methanesulfonate-induced mutant bulks. Plant Physiol **160**: 591-600

Havir EA, McHale NA (1989) Enhanced-peroxidatic activity in specific catalase isozymes of tobacco, barley, and maize. Plant Physiol **91**: 812-815

Henikoff S, Comai L (2003) Single-nucleotide mutations for plant functional genomics. Annu Rev Plant Biol **54**: 375-401

Herbette S, Lenne C, Leblanc N, Julien JL, Drevet JR, Roeckel-Drevet P (2002) Two GPX-like proteins from *Lycopersicon esculentum* and *Helianthus annuus* are antioxidant enzymes with phospholipid hydroperoxide glutathione peroxidase and thioredoxin peroxidase activities. Eur J Biochem **269**: 2414-2420

Hideg E, Kálai T, Hideg K, Vass I (1998) Photoinhibition of photosynthesis in vivo results in singlet oxygen production detection via nitroxide-induced fluorescence quenching in broad bean leaves. Biochemistry **37**: 11405-11411

Hodges M (2002) Enzyme redundancy and the importance of 2-oxoglutarate in plant ammonium assimilation. J Exp Bot **53**: 905-916

Hodges M, Flesch V, Gálvez S, Bismuth E (2003) Higher plant $NADP^+$-dependent isocitrate dehydrogenases, ammonium assimilation and NADPH production. Plant Physiol Biochem **41**: 577-585

Hossain MA, Asada K (1985) Monodehydroascorbate reductase from cucumber is a flavin adenine dinucleotide enzyme. J Biol Chem **260**: 12920-12926

Hossain MA, Nakano Y, Asada K (1984) Monodehydroascorbate reductase in spinach chloroplasts and its participation in regeneration of ascorbate for scavenging hydrogen peroxide. Plant Cell Physiol **25**: 385-395

Huner NP, Maxwell DP, Gray GR, Savitch LV, Krol M, Ivanov AG, Falk S (1996) Sensing environmental temperature change through imbalances between energy supply and energy consumption: Redox state of photosystem II. Physiol Plant **98**: 358-364

Hu X, Zhang A, Zhang J, Jiang M (2006) Abscisic acid is a key inducer of hydrogen peroxide production in leaves of maize plants exposed to water stress. Plant Cell Physiol **47**: 1484-1495

Hu YQ, Liu S, Yuan HM, Li J, Yan DW, Zhang JF, Lu YT (2010) Functional comparison of

catalase genes in the elimination of photorespiratory H_2O_2 using promoter- and 3'-untranslated region exchange experiments in the *Arabidopsis cat2* photorespiratory mutant. Plant Cell Environ 33: 1656-1670

Ichimura K, Shinozaki K, Tena G, Sheen J, Henry Y, Champion A, Kreis M, Zhang S, Hirt H, Wilson C, et al (2002) Mitogen-activated protein kinase cascades in plants: a new nomenclature. Trends Plant Sci **7**: 301-308

Iddar A, Valverde F, Assobhei O, Serrano A, Soukri A (2005) Widespread occurrence of non-phosphorylating glyceraldehyde-3-phosphate dehydrogenase among gram-positive bacteria. Int Microbiol **8**: 251-258

Iglesias AA (1990) On the metabolism of triose-phosphates in photosynthetic cells. Their involvement on the traffic of ATP and NADPH. Biochem Educ **18**: 2-5

Iqbal A, Yabuta Y, Takeda T, Nakano Y, Shigeoka S (2006) Hydroperoxide reduction by thioredoxin-specific glutathione peroxidase isoenzymes of Arabidopsis thaliana. FEBS J **273**: 5589-5597

Iwamoto M, Higo H, Higo K (2000) Differential diurnal expression of rice catalase genes: the 5'-flanking region of *CatA* is not sufficient for circadian control. Plant Sci **151**: 39-46

Jannat R, Uraji M, Morofuji M, Hossain MA, Islam MM, Nakamura Y, Mori IC, Murata Y (2011) The roles of *CATALASE2* in abscisic acid signaling in *Arabidopsis* guard cells. Biosci Biotechnol Biochem **75**: 2034-2036

Jezek P, Hlavatá L (2005) Mitochondria in homeostasis of reactive oxygen species in cell, tissues, and organism. Int J Biochem Cell Biol **37**: 2478-2503

Jiménez A, Hernandez JA, Del Rio LA, Sevilla F (1997) Evidence for the presence of the ascorbate-glutathione cycle in mitochondria and peroxisomes of pea leaves. Plant Physiol **114**: 275-284

Jiménez A, Hernández JA, Pastori G, del Río LA, Sevilla F (1998) Role of the ascorbate-glutathione cycle of mitochondria and peroxisomes in the senescence of pea leaves. Plant Physiol **118**: 1327-1335

Jing HC, Anderson L, Sturre MJ, Hille J, Dijkwel PP (2007) *Arabidopsis CPR5* is a senescence-regulatory gene with pleiotropic functions as predicted by the evolutionary theory of senescence. J Exp Bot **58**: 3885-3894

Jing HC, Hebeler R, Oeljeklaus S, Sitek B, Stühler K, Meyer HE, Sturre MJ, Hille J, Warscheid B, Dijkwel PP (2008) Early leaf senescence is associated with an altered cellular redox balance in *Arabidopsis cpr5*/*old1* mutants. Plant Biol **1**: 85-98

Jing HC, Sturre MJ, Hille J, Dijkwel PP (2002) *Arabidopsis* onset of leaf death mutants identify a regulatory pathway controlling leaf senescence. Plant J **32**:51-63

Johnston EJ, Rylott EL, Beynon E, Lorenz A, Chechik V, Bruce NC (2015) Monodehydroascorbate reductase mediates TNT toxicity in plants. Science **349**: 1072-1075

Joo JH, Wang S, Chen JG, Jones AM, Fedoroff NV (2005) Different signaling and cell death roles of heterotrimeric **G** protein α and β subunits in the *Arabidopsis* oxidative stress response to ozone. Plant Cell **17**: 957-970

Kadota Y, Shirasu K, Zipfel C (2015) Regulation of the NADPH oxidase RBOHD during plant immunity. Plant Cell Physiol **56**: 1472-1480

Kaminaka H, Näke C, Epple P, Dittgen J, Schütze K, Chaban C, Holt BF, Merkle T, Schäfer E, Harter K, et al (2006) bZIP10-LSD1 antagonism modulates basal defense and cell death in Arabidopsis following infection. EMBO J **25**: 4400-4411

Kangasjärvi S, Neukermans J, Li S, Aro EM, Noctor G (2012) Photosynthesis, photorespiration, and light signalling in defence responses. J Exp Bot **63**: 1619-1636

Karpinski S, Escobar C, Karpinska B, Creissen G, Mullineaux PM (1997) Photosynthetic electron transport regulates the expression of cytosolic ascorbate peroxidase genes in *Arabidopsis* during excess light stress. Plant Cell **9**: 627-640

Kayıhan DS, Kayıhan C, Çiftçi YÖ (2016) Excess boron responsive regulations of antioxidative mechanism at physio-biochemical and molecular levels in *Arabidopsis thaliana*. Plant Physiol Biochem **109**: 337-345

Kelly GJ, Gibbs M (1973) A mechanism for the indirect transfer of photosynthetically reduced nicotinamide adenine dinucleotide phosphate from chloroplasts to the cytoplasm. Plant Physiol **52**: 674-676

Kendall AC, Keys AJ, Turner JC, Lea PJ, Miflin BJ (1983) The isolation and characterisation of a catalase-deficient mutant of barley (*Hordeum vulgare* L.). Planta 159: 505-511.

Khokon AR, Okuma E, Hossain MA, Munemasa S, Uraji M, Nakamura Y, Mori IC, Murata Y (2011) Involvement of extracellular oxidative burst in salicylic acid-induced stomatal closure in *Arabidopsis*. Plant Cell Environ **34**: 434-443

Kim C, Apel K (2013) $^{1}O2$-mediated and EXECUTER-dependent retrograde plastid-to-nucleus signaling in norflurazon-treated seedlings of *Arabidopsis thaliana*. Mol Plant **6**: 1580-1591

Kimura S, Kaya H, Kawarazaki T, Hiraoka G, Senzaki E, Michikawa M, Kuchitsu K (2012) Protein phosphorylation is a prerequisite for the Ca^{2+}-dependent activation of *Arabidopsis* NADPH

oxidases and may function as a trigger for the positive feedback regulation of Ca^{2+} and reactive oxygen species. Biochim Biophys Acta **1823**: 398-405

Kirkman HN, Gaetani GF (2007) Mammalian catalase: a venerable enzyme with new mysteries. Trends Biochem Sci **32**: 44-50

Koornneef A, Leon-Reyes A, Ritsema T, Verhage A, Den Otter FC, Van Loon LC, Pieterse CM (2008) Kinetics of salicylate-mediated suppression of jasmonate signaling reveal a role for redox modulation. Plant Physiol **147**: 1358-1368

Koornneef M, Dellaert LW, van der Veen JH (1982) EMS- and radiation-induced mutation frequencies at individual loci in *Arabidopsis thaliana* (L.) Heynh. Mutat Res **93**: 109-123

Koussevitzky S, Nott A, Mockler TC, Hong F, Sachetto-martins G, Surpin M, Lim J, Mittler R, Chory J (2007) Signals from chloroplasts converge to regulate nuclear gene expression. Science **316**: 715-719.

Kovtun Y, Chiu WL, Tena G, Sheen J (2000) Functional analysis of oxidative stress-activated mitogen-activated protein kinase cascade in plants. Proc Natl Acad Sci USA **97**: 2940-2945

Krieger-Liszkay A (2005) Singlet oxygen production in photosynthesis. J Exp Bot **56**: 337-346

Kruse A, Fieuw S, Heineke D, Müller-Röber B (1998) Antisense inhibition of cytosolic NADP-dependent isocitrate dehydrogenase in transgenic potato plants. Planta **205**: 82-91

Kwak JM, Mori IC, Pei ZM, Leonhardt N, Torres MA, Dangl JL, Bloom RE, Bodde S, Jones JD, Schroeder JI (2003) NADPH oxidase *AtrbohD* and *AtrbohF* genes function in ROS-dependent ABA signaling in *Arabidopsis*. EMBO J **22**: 2623-2633

Kyriakis JM, Avruch J (1996) Sounding the alarm: protein kinase cascades activated by stress and inflammation. J Biol Chem **271**: 24313-24316

Laloi C, Stachowiak M, Pers-Kamczyc E, Warzych E, Murgia I, Apel K (2007) Cross-talk between singlet oxygen- and hydrogen peroxide-dependent signaling of stress responses in *Arabidopsis thaliana*. Proc Natl Acad Sci U S A **104**: 672-677

Langlois-Meurinne M, Gachon CM, Saindrenan P (2005) Pathogen-responsive expression of glycosyltransferase genes *UGT73B3* and *UGT73B5* is necessary for resistance to *Pseudomonas syringae pv tomato* in *Arabidopsis*. Plant Physiol **139**: 1890-1901

Lee KP, Kim C, Landgraf F, Apel K (2007) EXECUTER1- and EXECUTER2-dependent transfer of stress-related signals from the plastid to the nucleus of *Arabidopsis thaliana*. Proc Natl Acad Sci USA **104**: 10270-10275

Lee M, Choi Y, Burla B, Kim YY, Jeon B, Maeshima M, Yoo JY, Martinoia E, Lee Y (2008) The ABC transporter AtABCB14 is a malate importer and modulates stomatal response to CO_2. Nat Cell Biol **10**: 1217-1223

Leister D (2012) Retrograde signaling in plants: from simple to complex scenarios. Front Plant Sci **3**: 1-9

Liebthal M, Maynard D, Dietz K-J (2018) Peroxiredoxins and redox signaling in plants. Antioxid Redox Signal **28**: 609-624

Li F, Wu QY, Sun YL, Wang LY, Yang XH, Meng QW (2010) Overexpression of chloroplastic monodehydroascorbate reductase enhanced tolerance to temperature and methyl viologen-mediated oxidative stresses. Physiol Plant **139**: 421-34

Li H, Shang J, Yang Z, Shen W, Ai Z, Zhang L (2017) Oxygen vacancy associated surface fenton chemistry: surface structure dependent hydroxyl radicals generation and substrate dependent reactivity. Environ Sci Technol **51**: 5685-5694

Li J, Chen G, Wang X, Zhang Y, Jia H, Bi Y (2011) Glucose-6-phosphate dehydrogenase-dependent hydrogen peroxide production is involved in the regulation of plasma membrane H^+-ATPase and Na^+/H^+ antiporter protein in salt-stressed callus from *Carex moorcroftii*. Physiol Plant **141**: 239-250

Li M, Ma F, Liang D, Li J, Wang Y (2010) Ascorbate biosynthesis during early fruit development is the main reason for its accumulation in kiwi. PLoS One **5**: 1-14

Linster CL, Clarke SG (2008) L-Ascorbate biosynthesis in higher plants : the role of VTC2. Trends Plant Sci **13**: 567-573

Lisenbee CS, Lingard MJ, Trelease RN (2005) *Arabidopsis* peroxisomes possess functionally redundant membrane and matrix isoforms of monodehydroascorbate reductase. Plant J **43**: 900-914

Li S, Mhamdi A, Clement C, Jolivet Y, Noctor G (2013) Analysis of knockout mutants suggests that *Arabidopsis NADP-MALIC ENZYME2* does not play an essential role in responses to oxidative stress of intracellular or extracellular origin. J Exp Bot **64**: 3605-3614

Li S, Mhamdi A, Trotta A, Kangasjärvi S, Noctor G (2014) The protein phosphatase subunit PP2A-B'γ is required to suppress day length-dependent pathogenesis responses triggered by intracellular oxidative stress. New Phytol **202**: 145-160

Liu J, Wang X, Hu Y, Hu W, Bi Y (2013) Glucose-6-phosphate dehydrogenase plays a pivotal role in tolerance to drought stress in soybean roots. Plant Cell Rep **32**: 415-429

Liu S, Cheng Y, Zhang X, Guan Q, Nishiuchi S, Hase K, Takano T (2007) Expression of an

NADP-malic enzyme gene in rice (*Oryza sativa* L) is induced by environmental stresses; over-expression of the gene in *Arabidopsis* confers salt and osmotic stress tolerance. Plant Mol Biol **64**: 49-58

Liu WC, Han TT, Yuan HM, Yu ZD, Zhang LY, Zhang BL, Zhai S, Zheng SQ, Lu YT (2017) CATALASE2 functions for seedling post-germinative growth by scavenging H_2O_2 and stimulating ACX2/3 activity in *Arabidopsis*. Plant Cell Environ **40**: 2720-2728

Liu Y, Fiskum G, Schubert D (2002) Generation of reactive oxygen species by the mitochondrial electron transport chain. J Neurochem **80**: 780-787

Li Y, Trush MA (1993) DNA damage resulting from the oxidation of hydroquinone by copper: role for a Cu(II)/Cu(I) redox cycle and reactive oxygen generation. Carcinogenesis **14**: 1303-1311.

Loewus FA, Loewus MW (1983) Myo-inositol: its biosynthesis and metabolism. Annu Rev Plant Physiol **34**: 137-161

Loewus FA, Murthy PP (2000) Myo-Inositol metabolism in plants. Plant Sci **150**: 1-19

Lorrain S, Vailleau F, Balagué C, Roby D (2003) Lesion mimic mutants: keys for deciphering cell death and defense pathways in plants? Trends Plant Sci **8**: 263-271

Lund ST, Stall RE, Klee HJ (1998) Ethylene regulates the susceptible response to pathogen infection in tomato. Plant Cell **10**: 371-382

Lynn A, Koehler KE, Judis L, Chan ER, Cherry JP, Schwartz S, Seftel A, Hunt PA, Hassold TJ (2002) Covariation of synaptonemal complex length and mammalian meiotic exchange rates. Science **296**: 2222-2225

Margoliash E, Novogrodsky A, Schejter A (1960) Irreversible reaction of 3-amino-1:2:4-triazole and related inhibitors with the protein of catalase. Biochem J **74**: 339-348

Martín B, Ramiro M, Martínez-Zapater JM, Alonso-Blanco C (2009) A high-density collection of EMS-induced mutations for TILLING in Landsberg erecta genetic background of *Arabidopsis*. BMC Plant Biol **9**: 147

Maruta N, Trusov Y, Brenya E, Parekh U, Botella JR (2015) Membrane-localized extra-large G proteins and Gbg of the heterotrimeric G proteins form functional complexes engaged in plant immunity in *Arabidopsis*. Plant Physiol **167**: 1004-1016

Maruta T, Inoue T, Tamoi M, Yabuta Y, Yoshimura K, Ishikawa T, Shigeoka S (2011) Arabidopsis NADPH oxidases, AtrbohD and AtrbohF, are essential for jasmonic acid-induced expression of genes regulated by MYC2 transcription factor. Plant Sci **180**: 655-660

Masi A, Destro T, Turetta L, Varotto S, Caporale G, Ferretti M (2007) Localization of gamma-glutamyl transferase activity and protein in *Zea mays* organs and tissues. J Plant Physiol **164**: 1527-1535

Mateos MI, Serrano A (1992) Occurrence of phosphorylating and non-phosphorylating $NADP^+$-dependent glyceraldehyde-3-phosphate dehydrogenases in photosynthetic organisms. Plant Sci **84**: 163-170

Maurino VG, Gerrard Wheeler MC, Andreo CS, Drincovich MF (2009) Redundancy is sometimes seen only by the uncritical: does *Arabidopsis* need six malic enzyme isoforms? Plant Sci **176**: 715-721

Maxwell DP, Wang Y, McIntosh L (1999) The alternative oxidase lowers mitochondrial reactive oxygen production in plant cells. Proc Natl Acad Sci USA **96**: 8271-8276

May MJ, Leaver CJ (1994) *Arabidopsis thaliana* gamma-glutamylcysteine synthetase is structurally unrelated to mammalian, yeast, and Escherichia coli homologs. Proc Natl Acad Sci USA **91**: 10059-10063

May MJ, Leaver CJ (1993) Oxidative stimulation of glutathione synthesis in *Arabidopsis thaliana* suspension cultures. Plant Physiol **103**: 621-627

McAinsh MR, Pittman JK (2009) Shaping the calcium signature. New Phytol **181**: 275-294

McCallum CM, Comai L, Greene EA, Henikoff S (2000) Targeted screening for induced mutations. Nat Biotechnol **18**: 455-457

McClung CR (1997) Regulation of catalases in *Arabidopsis*. Free Radic Biol Med **23**: 489-496

Mehler AH (1951) Studies on reactions of illuminated chloroplasts. I. Mechanism of the reduction of oxygen and other Hill reagents. Arch Biochem Biophys **33**: 65-77

Meister A (1988) Glutathione metabolism and its selective modification. J Biol Chem **263**: 17205-17208

Melotto M, Underwood W, Koczan J, Nomura K, He SY (2006) Plant stomata function in innate immunity against bacterial invasion. Cell **126**: 969-980

Meng PH, Raynaud C, Tcherkez G, Blanchet S, Massoud K, Domenichini S, Henry Y, Soubigou-Taconnat L, Lelarge-Trouverie C, Saindrenan P, et al (2009) Crosstalks between myo-inositol metabolism, programmed cell death and basal immunity in *Arabidopsis*. PLoS One **4**: e7364

Meyer AJ (2008) The integration of glutathione homeostasis and redox signaling. J Plant Physiol **165**: 1390-1403

Meyer AJ, Brach T, Marty L, Kreye S, Rouhier N, Jacquot JP, Hell R (2007) Redox-sensitive GFP in *Arabidopsis thaliana* is a quantitative biosensor for the redox potential of the cellular glutathione redox buffer. Plant J **52**: 973-986

Meyer K, Leube MP, Grill E (1994) A protein phosphatase 2C involved in ABA signal transduction in *Arabidopsis thaliana*. Science **264**: 1452-1455

Mhamdi A, Hager J, Chaouch S, Queval G, Han Y, Taconnat L, Saindrenan P, Gouia H, Issakidis-Bourguet E, Renou J-P, et al (2010b) *Arabidopsis* GLUTATHIONE REDUCTASE1 plays a crucial role in leaf responses to intracellular hydrogen peroxide and in ensuring appropriate gene expression through both salicylic acid and jasmonic acid signaling pathways. Plant Physiol **153**: 1144-1160

Mhamdi A, Mauve C, Gouia H, Saindrenan P, Hodges M, Noctor G (2010c) Cytosolic NADP-dependent isocitrate dehydrogenase contributes to redox homeostasis and the regulation of pathogen responses in *Arabidopsis* leaves. Plant, Cell Environ **33**: 1112-1123

Mhamdi A, Noctor G (2016) High CO_2 primes plant biotic stress defences through redox-linked pathways. Plant Physiol **172**: 929-942

Mhamdi A, Noctor G, Baker A (2012) Plant catalases: peroxisomal redox guardians. Arch Biochem Biophys **525**: 181-194

Mhamdi A, Queval G, Chaouch S, Vanderauwera S, Van Breusegem F, Noctor G (2010a) Catalase function in plants: a focus on *Arabidopsis* mutants as stress-mimic models. J Exp Bot **61**: 4197-4220

Mittler R (2002) Oxidative stress, antioxidants and stress tolerance. Trends Plant Sci **7**: 405-410

Mittler R (2017) ROS are good. Trends Plant Sci 22: 11-19

Mittler R, Herr EH, Orvar BL, van Camp W, Willekens H, Inzé D, Ellis BE (1999) Transgenic tobacco plants with reduced capability to detoxify reactive oxygen intermediates are hyperresponsive to pathogen infection. Proc Natl Acad Sci USA **96**: 14165-14170

Mittler R, Vanderauwera S, Gollery M, Van Breusegem F (2004) Reactive oxygen gene network of plants. Trends Plant Sci **9**: 490-498

Mittler R, Vanderauwera S, Suzuki N, Miller G, Tognetti VB, Vandepoele K, Gollery M, Shulaev V, Van Breusegem F (2011) ROS signaling: the new wave? Trends Plant Sci **16**: 300-309

Miura K, Okamoto H, Okuma E, Shiba H, Kamada H, Hasegawa PM, Murata Y (2013) *SIZ1* deficiency causes reduced stomatal aperture and enhanced drought tolerance via controlling salicylic acid-induced accumulation of reactive oxygen species in *Arabidopsis*. Plant J **73**: 91-104

Møller IM (2001) PLANT MITOCHONDRIA AND OXIDATIVE STRESS : electron transport, NADPH turnover, and metabolism of reactive oxygen species. Annu Rev Plant Physiol Plant Mol Biol **52**: 561-591

Møller IM, Rasmusson AG (1998) The role of NADP in the mitochondrial matrix. Trends Plant Sci **3**: 21-27

Monshausen GB, Bibikova TN, Weisenseel MH, Gilroy S (2009) Ca^{2+} regulates reactive oxygen species production and pH during mechanosensing in *Arabidopsis* roots. Plant Cell **21**: 2341-2356

Mullen RT, Lee MS, Trelease RN (1997) Identification of the peroxisomal targeting signal for cottonseed catalase. Plant J **12**: 313-322

Mullen RT, Trelease RN (1996) Biogenesis and membrane properties of peroxisomes: does the boundary membrane serve and protect? Trends Plant Sci **1**: 389-394

Mullineaux PM, Rausch T (2005) Glutathione, photosynthesis and the redox regulation of stress-responsive gene expression. Photosynth Res **86**: 459-474

Mur LA, Kenton P, Lloyd AJ, Ougham H, Prats E (2008) The hypersensitive response; the centenary is upon us but how much do we know? J Exp Bot **59**: 501-520

Mutsuda M, Ishikawa T, Takeda T, Shigeoka S (1996) The catalase-peroxidase of *Synechococcus* PCC 7942: purification, nucleotide sequence analysis and expression in *Escherichia coli*. Biochem J **316**: 251-257

Nakano Y, Asada K (1981) Hydrogen peroxide is scavenged by ascorbate-specific peroxidase in spinach chloroplasts. Plant Cell Phyisol **22**: 867-880

Nathan C (2003) Specificity of a third kind: reactive oxygen and nitrogen intermediates in cell signaling. J Clin Invest **111**: 769-778

Nitschke S, Cortleven A, Iven T, Feussner I, Havaux M, Riefler M, Schmülling T (2016) Circadian stress regimes affect the circadian clock and cause jasmonic acid-dependent cell death in cytokinin-deficient *Arabidopsis* plants. Plant Cell **28**: 1616-1639

Noctor G (2015) Lighting the fuse on toxic TNT. Science **349**: 1052-1053.

Noctor G (2006) Metabolic signalling in defence and stress: the central roles of soluble redox couples. Plant Cell Environ **29**: 409-425

Noctor G, Arisi AC, Jouanin L, Foyer CH (1998) Manipulation of glutathione and amino acid biosynthesis in the chloroplast. Plant Physiol **118**: 471-482

Noctor G, Foyer CH (1998) ASCORBATE AND GLUTATHIONE: keeping active oxygen under control. Annu Rev Plant Physiol Plant Mol Biol **49**: 249-279

Noctor G, Gomez L, Vanacker H, Foyer CH (2002) Interactions between biosynthesis, compartmentation and transport in the control of glutathione homeostasis and signalling. J Exp Bot **53**: 1283-1304

Noctor G, Lelarge-Trouverie C, Mhamdi A (2015) The metabolomics of oxidative stress. Phytochemistry **112**: 33-53

Noctor G, Mhamdi A, Chaouch S, Han Y, Neukermans J, Marquez-Garcia B, Queval G, Foyer CH (2012) Glutathione in plants: an integrated overview. Plant Cell Environ **35**: 454-484

Noctor G, Mhamdi A, Foyer CH (2016) Oxidative stress and antioxidative systems: Recipes for successful data collection and interpretation. Plant Cell Environ **39**: 1140-1160

Noctor G, Mhamdi A, Foyer CH (2014) The roles of reactive oxygen metabolism in drought: not so cut and dried. Plant Physiol **164**: 1636-1648

Noctor G, Reichheld JP, Foyer CH (2017) ROS-related redox regulation and signaling in plants. Semin Cell Dev Biol. **80**: 3-12

Noji M, Saito K (2002) Molecular and biochemical analysis of serine acetyltransferase and cysteine synthase towards sulfur metabolic engineering in plants. Amino Acids **22**: 231-243

Nordman T, Xia L, Björkhem-Bergman L, Damdimopoulos A, Nalvarte I, Arnér ESJ, Spyrou G, Eriksson LC, Björnstedt M, Olsson JM (2003) Regeneration of the antioxidant ubiquinol by lipoamide dehydrogenase, thioredoxin reductase and glutathione reductase. Biofactors **18**: 45-50

Nühse TS, Bottrill AR, Jones AME, Peck SC (2007) Quantitative phosphoproteomic analysis of plasma membrane proteins reveals regulatory mechanisms of plant innate immune responses. Plant J **51**: 931-940

Nyathi Y, Baker A (2006) Plant peroxisomes as a source of signalling molecules. Biochim Biophys Acta **1763**: 1478-1495

Obara K, Sumi K, Fukuda H (2002) The use of multiple transcription starts causes the dual targeting of *Arabidopsis* putative monodehydroascorbate reductase to both mitochondria and chloroplasts. Plant Cell Physiol **43**: 697-705.

Ohkama-Ohtsu N, Sasaki-Sekimoto Y, Oikawa A, Jikumaru Y, Shinoda S, Inoue E, Kamide Y, Yokoyama T, Hirai MY, Shirasu K, et al (2011) 12-Oxo-phytodienoic acid-glutathione conjugate is transported into the vacuole in *Arabidopsis*. Plant Cell Physiol **52**: 205-209

Orzáez D, Granell A (1997) DNA fragmentation is regulated by ethylene during carpel senescene in *Pisum sativum*. Plant J **11**: 137-144

Ossowski S, Schneeberger K, Clark RM, Lanz C, Warthmann N, Weigel D (2008) Sequencing of natural strains of *Arabidopsis thaliana* with short reads. Genome Res **18**: 2024-2033

Overmyer K, Tuominen H, Kettunen R, Betz C, Langebartels C, Sandermann H Jr, Kangasjärvi J (2000) Ozone-sensitive arabidopsis *rcd1* mutant reveals opposite roles for ethylene and jasmonate signaling pathways in regulating superoxide-dependent cell death. Plant Cell **12**: 1849-1862

Page DR, Grossniklaus U (2002) The art and design of genetic screens: *Arabidopsis thaliana*. Nat Rev Genet **3**: 124-136

Parisy V, Poinssot B, Owsianowski L, Buchala A, Glazebrook J, Mauch F (2006) Identification of *PAD2* as a γ-glutamylcysteine synthetase highlights the importance of glutathione in disease resistance of *Arabidopsis*. Plant J **49**: 159-172

Parker D, Beckmann M, Zubair H, Enot DP, Caracuel-Rios Z, Overy DP, Snowdon S, Talbot NJ, Draper J (2009) Metabolomic analysis reveals a common pattern of metabolic re-programming during invasion of three host plant species by *Magnaporthe grisea*. Plant J **59**: 723-737

Pasternak M, Lim B, Wirtz M, Hell R, Cobbett CS, Meyer AJ (2008) Restricting glutathione biosynthesis to the cytosol is sufficient for normal plant development. Plant J **53**: 999-1012

Pastori GM, Foyer CH (2002) Common components, networks, and pathways of cross-tolerance to stress. The central role of "Redox" and abscisic acid-mediated controls. Plant Physiol **129**: 460-468

Pastori GM, Kiddle G, Antoniw J, Bernard S, Veljovic-Jovanovic S, Verrier PJ, Noctor G, Foyer CH (2003) Leaf vitamin C contents modulate plant defense transcripts and regulate genes that control development through hormone signaling. Plant Cell **15**: 939-951

Pérez-Ruiz JM, Cejudo FJ (2009) A proposed reaction mechanism for rice NADPH thioredoxin reductase C, an enzyme with protein disulfide reductase activity. FEBS Lett **583**: 1399-1402

Peters JL, Cnudde F, Gerats T (2003) Forward genetics and map-based cloning approaches. Trends Plant Sci **8**: 484-491

Petrov VD, Van Breusegem F (2012) Hydrogen peroxide-a central hub for information flow in plant cells. AoB Plants **2012**: pls014

Pfannschmidt T, Nilsson A, Allen JF (1999) Photosynthetic control of chloroplast gene expression. Nature **397**: 625-628

Piattoni CV, Bustos DM, Guerrero SA, Iglesias AÁ (2011) Nonphosphorylating glyceraldehyde-3-

phosphate dehydrogenase is phosphorylated in wheat endosperm at serine-404 by an SNF1-related protein kinase allosterically inhibited by ribose-5-phosphate. Plant Physiol **156**: 1337-1350

Pitzschke A, Hirt H (2006) Mitogen-activated protein kinases and reactive oxygen species signaling in plants. Plant Physiol **141**: 351-356

Plaxton WC (1996) The organization and regulation of plant glycolysis. Annu Rev Plant Physiol Plant Mol Biol **47**: 185-214

Pogson BJ, Woo NS, Förster B, Small ID (2008) Plastid signalling to the nucleus and beyond. Trends Plant Sci **13**: 602-609

Polle A (2001) Dissecting the superoxide dismutase-ascorbate-glutathione-pathway in chloroplasts by metabolic modeling. Computer simulations as a step towards flux analysis. Plant Physiol **126**: 445-462

Qi J, Wang J, Gong Z, Zhou JM (2017) Apoplastic ROS signaling in plant immunity. Curr Opin Plant Biol **38**: 92-100

Queval G, Issakidis-Bourguet E, Hoeberichts FA, Vandorpe M, Gakière B, Vanacker H, Miginiac-Maslow M, Van Breusegem F, Noctor G (2007) Conditional oxidative stress responses in the *Arabidopsis* photorespiratory mutant *cat2* demonstrate that redox state is a key modulator of daylength-dependent gene expression, and define photoperiod as a crucial factor in the regulation of H_2O_2-induced cell death. Plant J **52**: 640-657

Queval G, Jaillard D, Zechmann B, Noctor G (2011) Increased intracellular H_2O_2 availability preferentially drives glutathione accumulation in vacuoles and chloroplasts. Plant Cell Environ **34**: 21-32

Queval G, Neukermans J, Vanderauwera S, Van Breusegem F, Noctor G (2012) Daylength is a key regulator of transcriptomic responses to both CO_2 and H_2O_2 in *Arabidopsis*. Plant Cell Environ **35**: 374-387

Queval G, Noctor G (2007) A plate reader method for the measurement of NAD, NADP, glutathione, and ascorbate in tissue extracts: application to redox profiling during *Arabidopsis* rosette development. Anal Biochem **363**: 58-69

Queval G, Thominet D, Vanacker H, Miginiac-Maslow M, Gakière B, Noctor G (2009) H_2O_2-activated up-regulation of glutathione in *Arabidopsis* involves induction of genes encoding enzymes involved in cysteine synthesis in the chloroplast. Mol Plant **2**: 344-356

Qu LJ, Qin G (2014) Generation and identification of *Arabidopsis* EMS mutants. Methods Mol Biol. **1062**: 225-239

Rahantaniaina MS, Li S, Chatel-Innocenti G, Tuzet A, Issakidis-Bourguet E, Mhamdi A, Noctor

G (2017) Cytosolic and chloroplastic DHARs cooperate in oxidative stress-driven activation of the salicylic acid pathway. Plant Physiol **174**: 956-971

Regelsberger G, Jakopitsch C, Furtmüller PG, Rueker F, Switala J, Loewen PC, Obinger C (2001) The role of distal tryptophan in the bifunctional activity of catalase-peroxidases. Biochem Soc Trans **29**: 99-105

Regelsberger G, Jakopitsch C, Plasser L, Schwaiger H, Furtmüller PG, Peschek GA, Zámocký M, Obinger C (2002) Occurrence and biochemistry of hydroperoxidases in oxygenic phototrophic prokaryotes (cyanobacteria). Plant Physiol Biochem **40**: 479-490

Rennenberg H (1980) Glutathione metabolism and possible biological roles in higher plants. **21**: 2771-2781

Rentel MC, Lecourieux D, Ouaked F, Usher SL, Petersen L, Okamoto H, Knight H, Peck SC, Grierson CS, Hirt H, et al (2004) OXI1 kinase is necessary for oxidative burst-mediated signalling in *Arabidopsis*. Nature **427**: 858-861

Rius SP, Casati P, Iglesias AA, Gomez-Casati DF (2006) Characterization of an *Arabidopsis thaliana* mutant lacking a cytosolic non-phosphorylating glyceraldehyde-3-phosphate dehydrogenase. Plant Mol Biol **61**: 945-957

Rumpho ME, Edwards GE, Loescher WH (1983) A pathway for photosynthetic carbon flow to mannitol in celery leaves : activity and localization of key enzymes. Plant Physiol **73**: 869-873

Rouhier N, Jacquot JP (2005) The plant multigenic family of thiol peroxidases. Free Radical Bio Med **38**: 1413-1421

Sano S, Tao S, Endo Y, Inaba T, Hossain MA, Miyake C, Matsuo M, Aoki H, Asada K, Saito K (2005) Purification and cDNA cloning of chloroplastic monodehydroascorbate reductase from spinach. Biosci Biotechnol Biochem **69**: 762-772

Sattler SE, Mène-Saffrané L, Farmer EE, Krischke M, Mueller MJ, DellaPenna D (2006) Nonenzymatic lipid peroxidation reprograms gene expression and activates defense markers in *Arabidopsis* tocopherol-deficient mutants. Plant Cell **18**: 3706-3720

Scharte J, Schön H, Tjaden Z, Weis E, von Schaewen A. (2009) Isoenzyme replacement of glucose-6-phosphate dehydrogenase in the cytosol improves stress tolerance in plants. Proc Natl Acad Sci USA **106**: 8061-8066

Scheibe R, Dietz KJ (2012) Reduction-oxidation network for flexible adjustment of cellular metabolism in photoautotrophic cells. Plant Cell Environ **35**: 202-216

Schneeberger K, Ossowski S, Lanz C, Juul T, Petersen AH, Nielsen KL, Jørgensen JE, Weigel D,

Andersen SU (2009) SHOREmap: simultaneous mapping and mutation identification by deep sequencing. Nat Methods **6**: 550-551

Schützendübel A, Polle A (2002) Plant responses to abiotic stresses: heavy metal-induced oxidative stress and protection by mycorrhization. J Exp Bot **53**: 1351-1365

Schwarzländer M, Fricker MD, Müller C, Marty L, Brach T, Novak J, Sweetlove LJ, Hell R, Meyer AJ (2008) Confocal imaging of glutathione redox potential in living plant cells. J Microsc **231**: 299-316

Serrato AJ, Fernández-Trijueque J, Barajas-López JD, Chueca A, Sahrawy M (2013) Plastid thioredoxins: a "one-for-all" redox-signaling system in plants. Front Plant Sci **4**: 1-10

Sewelam N, Jaspert N, Van Der Kelen K, Tognetti VB, Schmitz J, Frerigmann H, Stahl E, Zeier J, Van Breusegem F, Maurino VG (2014) Spatial H_2O_2 signaling specificity: H_2O_2 from chloroplasts and peroxisomes modulates the plant transcriptome differentially. Mol Plant **7**: 1191-1210

Sewelam N, Kazan K, Schenk PM (2016) Global plant stress signaling: reactive oxygen species at the cross-road. Front Plant Sci **7**: 1-21

Sewelam N, Kazan K, Thomas-Hall SR, Kidd BN, Manners JM, Schenk PM (2013) Ethylene response factor 6 is a regulator of reactive oxygen species signaling in *Arabidopsis*. PLoS One **8**: e70289

Sierla M, Rahikainen M, Salojärvi J, Kangasjärvi J, Kangasjärvi S (2013) Apoplastic and chloroplastic redox signaling networks in plant stress responses. Antioxid Redox Signal **18**: 2220-2239

Smirnoff N (2000) Ascorbate biosynthesis and function in photoprotection. Philos Trans R Soc Lond B Biol Sci **355**: 1455-1464

Smirnoff N (2011) Vitamin C: The metabolism and functions of ascorbic acid in plants. Adv Bot Res **59**: 107-177

Smith IK, Kendall AC, Keys AJ, Turner JC, Lea PJ (1985) The regulation of the biosynthesis of glutathione in leaves of barley (*Hordeum vulgare* L.). Plant Sci **41**: 11-17

Spoel SH, Koornneef A, Claessens SM, Korzelius JP, Van Pelt JA, Mueller MJ, Buchala AJ, Métraux JP, Brown R, Kazan K, et al (2003) NPR1 modulates cross-talk between salicylate- and jasmonate-dependent defense pathways through a novel function in the cytosol. Plant Cell **15**: 760-770

Strohm M, Jouanin L, Kunert KJ, Pruvost C, Polle A, Foyer CH, Rennenberg H (1995) Regulation of glutathione synthesis in leaves of transgenic poplar (*Populus tremula X P. alba*) overexpressing glutathione synthetase. Plant J **7**: 141-145

Sudan J, Negi B, Arora S (2015) Oxidative stress induced expression of monodehydroascorbate reductase gene in *Eleusine coracana*. Physiol Mol Biol Plants **21**: 551-558

Suharsono U, Fujisawa Y, Kawasaki T, Iwasaki Y, Satoh H, Shimamoto K (2002) The heterotrimeric G protein α subunit acts upstream of the small GTPase Rac in disease resistance of rice. Proc Natl Acad Sci USA **99**: 13307-13312

Sung DY, Kim TH, Komives EA, Mendoza-Cózatl DG, Schroeder JI (2009) ARS5 is a component of the 26S proteasome complex, and negatively regulates thiol biosynthesis and arsenic tolerance in *Arabidopsis*. Plant J **59**: 802-813

Su T, Wang P, Li H, Zhao Y, Lu Y, Dai P, Ren T, Wang X, Li X, Shao Q, et al (2018) The *Arabidopsis* catalase triple mutant reveals important roles of catalases and peroxisome derived signaling in plant development. J Integr Plant Biol **60**: 591-607

Su T, Xu J, Li Y, Lei L, Zhao L, Yang H, Feng J, Liu G, Ren D (2011) Glutathione-Indole-3-Acetonitrile is required for camalexin biosynthesis in *Arabidopsis thaliana*. Plant Cell **23**: 364-380

Tada Y, Spoel SH, Pajerowska-Mukhtar K, Mou Z, Song J, Wang C, Zuo J, Dong X (2008) Plant immunity requires conformational changes of NPR1 via S-nitrosylation and thioredoxins. Science **321**: 952-956

Takahama U (2004) Oxidation of vacuolar and apoplastic phenolic substrates by peroxidase: physiological significance of the oxidation reactions. Phytochem Rev **3**: 207-219

Takahashi H, Chen Z, Du H, Liu Y, Klessig DF (1997) Development of necrosis and activation of disease resistance in transgenic tobacco plants with severely reduced catalase levels. Plant J **11**: 993-1005

Takahashi H, Kanayama Y, Zheng MS, Kusano T, Hase S, Ikegami M, Shah J (2004) Antagonistic interactions between the SA and JA signaling pathways in *Arabidopsis* modulate expression of defense genes and gene-for-gene resistance to cucumber mosaic virus. Plant Cell Physiol **45**: 803-809

Tena G, Asai T, Chiu WL, Sheen J (2001) Plant mitogen-activated protein kinase signaling cascades. Curr Opin Plant Biol **4**: 392-400

Thole JM, Strader LC (2015) Next-generation sequencing as a tool to quickly identify causative EMS-generated mutations. Plant Signal Behav **10**: e1000167

Thom E, Möhlmann T, Quick WP, Camara B, Neuhaus HE (1998) Sweet pepper plastids: enzymic equipment, characterisation of the plastidic oxidative pentose-phosphate pathway, and transport of phosphorylated intermediates across the envelope membrane. Planta **204**: 226-233

Tietze F (1969) Enzymic method for quantitative determination of nanogram amounts of total and oxidized glutathione: applications to mammalian blood and other tissues. Anal Biochem **27**: 502-522

Till BJ, Reynolds SH, Greene EA, Codomo CA, Enns LC, Johnson JE, Burtner C, Odden AR, Young K, Taylor NE, et al (2003) Large-scale discovery of induced point mutations with high-throughput TILLING. Genome Res **13**: 524-530

Tognetti VB, Van Aken O, Morreel K, Vandenbroucke K, van de Cotte B, De Clercq I, Chiwocha S, Fenske R, Prinsen E, Boerjan W, et al (2010) Perturbation of indole-3-butyric acid homeostasis by the UDP-glucosyltransferase UGT74E2 modulates *Arabidopsis* architecture and water stress tolerance. Plant Cell **22**: 2660-2679

Torres MA, Dangl JL (2005) Functions of the respiratory burst oxidase in biotic interactions, abiotic stress and development. Curr Opin Plant Biol **8**: 397-403

Torres MA, Dangl JL, Jones JDG (2002) *Arabidopsis* gp91phox homologues AtrbohD and AtrbohF are required for accumulation of reactive oxygen intermediates in the plant defense response. Proc Natl Acad Sci USA **99**: 517-522

Torres MA, Jones JD, Dangl JL (2005) Pathogen-induced, NADPH oxidase-derived reactive oxygen intermediates suppress spread of cell death in *Arabidopsis thaliana*. Nat Genet **37**: 1130-1134

Torres MA, Jones JD, Dangl JL (2006) Reactive oxygen species signaling in response to pathogens. Plant Physiol **141**: 373-378

Trotta A, Wrzaczek M, Scharte J, Tikkanen M, Konert G, Rahikainen M, Holmström M, Hiltunen HM, Rips S, Sipari N, et al (2011) Regulatory subunit B'gamma of protein phosphatase 2A prevents unnecessary defense reactions under low light in *Arabidopsis*. Plant Physiol **156**: 1464-1480

Trusov Y, Sewelam N, Rookes JE, Kunkel M, Nowak E, Schenk PM, Botella JR (2009) Heterotrimeric G proteins-mediated resistance to necrotrophic pathogens includes mechanisms independent of salicylic acid-, jasmonic acid/ethylene- and abscisic acid-mediated defense signaling. Plant J **58**: 69-81

Tuzet A, Rahantaniana MS, Noctor G (2018) Analyzing the function of catalase and the ascorbate-glutathione pathway in H_2O_2 processing: Insights from an experimentally constrained kinetic model. AntioxidRedox Signal (accepted)

Ullmann P, Gondet L, Potier S, Bach TJ (1996) Cloning of *Arabidopsis thaliana* glutathione synthetase (GSH2) by functional complementation of a yeast *gsh2* mutant. Eur J Biochem **669**: 662-669

Umezawa T, Nakashima K, Miyakawa T, Kuromori T, Tanokura M, Shinozaki K, Yamaguchi-Shinozaki K (2010) Molecular basis of the core regulatory network in ABA responses: sensing,

signaling and transport. Plant Cell Physiol **51**: 1821-1839

Vadassery J, Tripathi S, Prasad R, Varma A, Oelmüller R (2009) Monodehydroascorbate reductase 2 and dehydroascorbate reductase 5 are crucial for a mutualistic interaction between *Piriformospora indica* and *Arabidopsis*. J Plant Physiol **166**: 1263-1274

Valderrama R, Corpas FJ, Carreras A, Gómez-Rodríguez MV, Chaki M, Pedrajas JR, Fernández-Ocaña A, Del Río LA, Barroso JB (2006) The dehydrogenase-mediated recycling of NADPH is a key antioxidant system against salt-induced oxidative stress in olive plants. Plant Cell Environ **29**: 1449-1459

Van Breusegem F, Dat JF (2006) Reactive oxygen species in plant cell death. Plant Physiol **141**: 384-390

Vandenabeele S, Vanderauwera S, Vuylstecke M, Rombauts S, Langebartels C, Seidlitz HK, Zabeau M, Van Montagu M, Inzé D, Van Breusegem F (2004) Catalase deficiency drastically affects gene expression induced by high light in *Arabidopsis thaliana*. Plant J **39**: 45-58

Vandenabeele S, Van Der Kelen K, Dat J, Gadjev I, Boonefaes T, Morsa S, Rottiers P, Slooten L, Van Montagu M, Zabeau M, et al (2003) A comprehensive analysis of hydrogen peroxide-induced gene expression in tobacco. Proc Natl Acad Sci USA **100**: 16113-16118

Vandenbroucke K, Robbens S, Vandepoele K, Inzé D, Van de Peer Y, Van Breusegem F (2008) Hydrogen peroxide-induced gene expression across kingdoms: A comparative analysis. Mol Biol Evol **25**: 507-516

Vanderauwera S, Suzuki N, Miller G, van de Cotte B, Morsa S, Ravanat JL, Hegie A, Triantaphylidès C, Shulaev V, Van Montagu MC, et al (2011) Extranuclear protection of chromosomal DNA from oxidative stress. Proc Natl Acad Sci USA **108**: 1711-1716

Vanderauwera S, Zimmermann P, Rombauts S, Vandenabeele S, Langebartels C, Gruissem W, Inzé D, Van Breusegem F (2005) Genome-wide analysis of hydrogen peroxide-regulated gene expression in *Arabidopsis* reveals a high light-induced transcriptional cluster involved in anthocyanin biosynthesis. Plant Physiol **139**: 806-821

Vernoux T, Wilson RC, Seeley KA, Reichheld JP, Muroy S, Brown S, Maughan SC, Cobbett CS, Van Montagu M, Inzé D, et al (2000) The ROOT MERISTEMLESS1/CADMIUM SENSITIVE2 gene defines a glutathione-dependent pathway involved in initiation and maintenance of cell division during postembryonic root development. Plant Cell **12**: 97-110

Vlot AC, Dempsey DA, Klessig DF (2009) Salicylic Acid, a multifaceted hormone to combat disease. Annu Rev Phytopathol **47**: 177-206

Voll LM, Zell MB, Engelsdorf T, Saur A, Wheeler MG, Drincovich MF, Weber APM, Maurino

VG (2012) Loss of cytosolic NADP-malic enzyme 2 in *Arabidopsis thaliana* is associated with enhanced susceptibility to *Colletotrichum higginsianum*. New Phytol **195**: 189-202

Vollsnes AV, Erikson AB, Otterholt E, Kvaal K, Oxaal U, Futsaether C (2009) Visible foliar injury and infrared imaging show that daylength affects short-term recovery after ozone stress in *Trifolium subterraneum*. J Exp Bot **60**: 3677-3686

Wachter A, Wolf S, Steininger H, Bogs J, Rausch T (2005) Differential targeting of GSH1 and GSH2 is achieved by multiple transcription initiation: implications for the compartmentation of glutathione biosynthesis in the *Brassicaceae*. Plant J **41**: 15-30

Wagner D, Przybyla D, Op den Camp R, Kim C, Landgraf F, Lee KP, Würsch M, Laloi C, Nater M, Hideg E, et al (2004) The genetic basis of singlet oxygen-induced stress responses of *Arabidopsis thaliana*. **306**: 1183-1185

Wakao S, Andre C, Benning C (2008) Functional analyses of cytosolic glucose-6-phosphate dehydrogenases and their contribution to seed oil accumulation in *Arabidopsis*. Plant Physiol **146**: 277-288

Wakao S, Benning C (2005) Genome-wide analysis of glucose-6-phosphate dehydrogenases in *Arabidopsis*. Plant J **41**: 243-256

Wang X, Ma Y, Huang C, Wan Q, Li N, Bi Y (2008) Glucose-6-phosphate dehydrogenase plays a central role in modulating reduced glutathione levels in reed callus under salt stress. Planta **227**: 611-623

Weigel D, Glazebrook J (2002) *Arabidopsis*: A Laboratory Manual. CSHL Press **2**: 20-30

Wendt UK, Hauschild R, Lange C, Pietersma M, Wenderoth I, von Schaewen A (1999) Evidence for functional convergence of redox regulation in G6PDH isoforms of cyanobacteria and higher plants. Plant Mol Biol **40**: 487-494

Wheeler G, Ishikawa T, Pornsaksit V, Smirnoff N (2015) Evolution of alternative biosynthetic pathways for vitamin C following plastid acquisition in photosynthetic eukaryotes. Elife **4**: e06369

Wheeler GL, Jones MA, Smirnoff N (1998) The biosynthetic pathway of vitamin C in higher plants. Nature **393**: 365-369

Willekens H, Chamnongpol S, Davey M, Schraudner M, Langebartels C, Van Montagu M, Inzé D, Van Camp W (1997) Catalase is a sink for H_2O_2 and is indispensable for stress defence in C3 plants. EMBO J **16**: 4806-4816.

Willekens H, Inzé D, Van Montagu M, van Camp W (1995) Catalases in plants. Mol Breed **1**: 207-228

Winterbourn CC (2013) The biological chemistry of hydrogen peroxide. Methods Enzymol **528**: 3-25

Wirtz M, Hell R (2007) Dominant-negative modification reveals the regulatory function of the multimeric cysteine synthase protein complex in transgenic tobacco. Plant Cell **19**: 625-639

Wrzaczek M, Hirt H (2001) Plant MAP kinase pathways : how many and what for? Biol Cell **93**: 81-87

Xiang C, Oliver DJ (1998) Glutathione metabolic genes coordinately respond to heavy metals and jasmonic acid in *Arabidopsis*. Plant Cell **10**: 1539-1550

Xing Y, Jia W, Zhang J (2008) AtMKK1 mediates ABA-induced *CAT1* expression and H_2O_2 production via AtMPK6-coupled signaling in *Arabidopsis*. Plant J **54**: 440-451

Yoon HS, Lee H, Lee IA, Kim KY, Jo J (2004) Molecular cloning of the monodehydroascorbate reductase gene from *Brassica campestris* and analysis of its mRNA level in response to oxidative stress. Biochim Biophys Acta **1658**: 181-186

Yoshida S, Ito M, Nishida I, Watanabe A (2002) Identification of a novel gene *HYS1/CPR5* that has a repressive role in the induction of leaf senescence and pathogen-defence responses in *Arabidopsis thaliana*. Plant J **29**: 427-437

Yuan HM, Liu WC, Lu YT (2017) CATALASE2 coordinates SA-mediated repression of both Auxin accumulation and JA biosynthesis in plant defenses. Cell Host Microbe **21**: 143-155

Zamocky M, Furtmüller PG, Obinger C (2008) Evolution of catalases from bacteria to humans. Antioxid Redox Signal **10**: 1527-1548

Zechmann B (2011) Subcellular distribution of ascorbate in plants. Plant Signal Behav **6**: 360-363

Zhang J, Shao F, Li Y, Cui H, Chen L, Li H, Zou Y, Long C, Lan L, Chai J, et al (2007) A Pseudomonas syringae effector inactivates MAPKs to suppress PAMP-induced immunity in plants. Cell Host Microbe **1**: 175-185

Zhong HH, Young JC, Pease EA, Hangarter RP, McClung CR (1994) Interactions between light and the circadian clock in the regulation of *CAT2* expression in *Arabidopsis*. Plant Physiol **104**: 889-898

Zimmermann P, Heinlein C, Orendi G, Zentgraf U (2006) Senescence-specific regulation of catalases in *Arabidopsis thaliana* (L.) Heynh. Plant Cell Environ **29**: 1049-1060

Zurbriggen MD, Carrillo N, Tognetti VB, Melzer M, Peisker M, Hause B, Hajirezaei MR (2009) Chloroplast-generated reactive oxygen species play a major role in localized cell death during the non-

host interaction between tobacco and *Xanthomonas campestris* pv. *vesicatoria*. Plant J **60**: 962-973

Résumé

Les plantes sont des organismes sessiles et ne peuvent donc pas s'éloigner de conditions défavorables. Parce qu'elles sont constamment mises au défi par les changements environnementaux tels que l'infection par des agents pathogènes, les fluctuations de température et d'intensité lumineuse, la disponibilité de l'eau et la pollution chimique, les plantes ont mis au point de vastes systèmes physiologiques pour faire face à divers stimuli et maintenir une croissance et un développement normaux. Il existe un vif intérêt pour comprendre les réactions des plantes au stress, car elles peuvent souvent déterminer les rendements agricoles. Le rôle central des ROS dans les réponses au stress explique l'explosion de l'intérêt porté à la recherche sur ces molécules au cours des dernières décennies. Alors que les concepts antérieurs considéraient les ROS comme des sous-produits toxiques, ils sont désormais considérés comme des molécules de signalisation clés impliquées dans de nombreux processus physiologiques (Foreman et al., 2003; Wagner et al., 2004; Han et al., 2013a, b; Foyer et al. ., 2017). Il est important de noter que, dans les environnements naturels et sur le terrain, les plantes sont souvent exposées simultanément à plusieurs types de conditions de stress. Par exemple, une plante peut être confrontée à la fois à des polluants du sol, à un excès de sel et à une attaque d'agents pathogènes. Bien qu'il soit accepté que les ROS soient des régulateurs clés du résultat de telles conditions, le réseau qui contrôle les ROS et les réponses des usines à ces ROS reste à élucider. L'une des principales lacunes de nos connaissances concerne le rôle spécifique de différentes enzymes impliquées dans le contrôle de l'accumulation de ROS et de l'état d'oxydo-réduction cellulaire. C'est dans ce contexte que les travaux présentés dans cette thèse ont été conduits.

Trois gènes encodent CAT chez Arabidopsis. Bien que le rôle de *CAT2* dans la photorespiration soit bien établi, l'importance des différents CAT dans d'autres processus est moins claire. Dans ce travail, nous avons examiné les fonctions de la CAT en utilisant des mutants d'ADN-T pour *cat1*, *cat2*, *cat3* ainsi que les doubles mutants *cat1 cat2* et *cat2 cat3*. Dans les racines et les feuilles, les mutants *cat2* ont montré le plus grand effet sur l'activité. Comme la croissance de la rosette, la croissance des racines était inhibée dans toutes les lignées contenant *cat2*. L'inhibition de la croissance des racines a été empêchée par la croissance à hCO_2, ce qui suggère qu'il s'agit d'un effet indirect du stress oxydatif sur les feuilles. Les phénotypes marqués n'ont pas été identifiés chez les mutants simples *cat1* ou *cat3*, mais l'analyse des mutants doubles a suggéré un certain chevauchement entre *CAT2* et *CAT3* dans les feuilles et *CAT1* et *CAT2* dans les semences. La réponse des gènes marqueurs H_2O_2 à une exposition égale de la cat2 au stress oxydatif était fortement influencée par le contexte de la longueur de la journée de croissance. Des réponses similaires dans *cat2* et *cat2 cat3* suggèrent que cela n'est pas lié aux effets de la durée du jour sur l'expression de *CAT3*. Le 3-aminotriazole (3-AT), un inhibiteur non spécifique de la CAT, a produit des effets dépendants de la longueur du jour qualitativement similaires à ceux observés chez *cat2*. Ensemble, nos données (1) soulignent l'importance de CAT2 chez Arabidopsis; (2) suggèrent que CAT1 et CAT3 sont principalement des enzymes de «sauvegarde»; et (3) établir que les réponses au déficit en CAT dépendant de la longueur du jour sont indépendantes de la durée du stress oxydatif.

La formation de lésions et la signalisation associée à l'acide salicylique (SA) déclenchée par la mutation *cat2* peuvent être supprimées en inactivant la voie de synthèse de la SA par la mutation *sid2*. Il est intéressant de noter que la neutralisation d'une isoforme spécifique de la glucose-6-phosphate déshydrogénase (G6PD5) dans l'arrière-plan *cat2* produit un effet très similaire, mais les raisons restent à élucider. Pour identifier les gènes impliqués dans

la liaison de H_2O_2 intracellulaire et de G6PD5 dans la signalisation SA, un criblage génétique classique (en avant) a été utilisé. Des graines de *cat2 g6pd5* ont été mutagénisées avec du méthanesulfonate d'éthyle et la population M2 a été examinée visuellement pour rechercher des individus présentant un phénotype similaire à *cat2* (lésions sur les feuilles). Six révertants candidats présentant ce phénotype ont été obtenus. Après au moins un rétrocroisement avec *cat2 g6pd5*, l'ADN a été isolé d'individus F2 regroupés qui présentaient des lésions et les gènes candidats ont été identifiés par séquençage du génome. Les données montrent que quatre de ces six lignées sont mutées dans des gènes connus pour être impliqués dans la régulation de la mort cellulaire liée à la voie SA. Sur ces quatre, trois portent des mutations dans le gène codant pour la *myo*-INOSITOL PHOSPHATE SYNTHASE 1 (MIPS1), tandis que l'un est muté dans *CONSTITUTIVE EXPRESSOR OF PR GENES 5* (CPR5). Dans les deux autres lignées, les mutations identifiées ne concernaient pas des acteurs reconnus impliqués dans la formation de lésions, offrant des perspectives intéressantes pour des travaux ultérieurs visant à caractériser les rôles des gènes impliqués.

Avec la catalase, la voie de l'ascorbate-glutathion est considérée comme un acteur clé dans le métabolisme de H_2O_2 produit à l'intérieur de la cellule. Les données de la littérature suggèrent que le flux par la voie ascorbate-glutathion est accéléré pendant le stress et dans les systèmes génétiques mimant le stress, tels que le mutant *cat2*. Quatre types d'enzymes différents fonctionnent dans la voie ascorbate-glutathion et sont codés par plus d'un gène. Une de ces enzymes est la monodéhydroascorbate réductase (MDHAR) dépendante de NAD (P) H, pour laquelle cinq gènes sont annotés dans Arabidopsis. Pour analyser l'importance des isoformes spécifiques du MDHAR, des mutants spécifiques du gène ont été obtenus pour un isoforme peroxisomal (MDHAR1) et deux isoformes cytosoliques (MDHAR2, MDHAR3). Les conséquences de la perte de ces fonctions MDHAR ont été analysées dans un contexte de type sauvage et déficient en catalase. Bien qu'aucune des mutations de *mdhar* n'ait eu d'effet marqué sur la croissance ou le phénotype de rosette dans le contexte de type sauvage, *mdhar2* a eu plusieurs effets saisissants sur les modifications de l'état redox déclenchées par *cat2* et l'activation de la voie SA. Comparé à *cat2*, un double mutant *cat2 mdhar2* a montré une formation de lésion beaucoup plus réduite accompagnée d'une activation plus faible de la voie SA. Ces effets étaient liés à une perturbation de la voie ascorbate-glutathion et, plus particulièrement, à une oxydation accrue du glutathion par rapport à *cat2*. Ensemble, les résultats suggèrent qu'un MDHAR cytosolique spécifique joue un rôle important dans la signalisation des réponses au H_2O_2 intracellulaire.

université PARIS-SACLAY | ÉCOLE DOCTORALE Sciences du végétal : du gène à l'écosystème

Titre : Analyse fonctionnelle des mutants de la catalase et de leur application à l'analyse des voies liées au NADPH dans signalisation oxydative chez *Arabidopsis thaliana*

Mots clés : catalase, NADPH, stress oxydant, H_2O_2, signalisation

Résumé : Les conditions contraignantes provoquent la modification de l'état redox et la signalisation liée aux formes actives de l'oxygène (ROS), dont les concentrations sont régulées par des systèmes antioxydant complexes. Mais nous avons toujours des connaissances fragmentaires quant à l'importance des ROS pour la signalisation cellulaire chez les plantes. Cette étude a utilisé des approches de génétique classique et inverse chez *Arabidopsis thaliana* dans le but d'élucider les rôles des catalases et des systèmes NADPH-glutathion-ascorbate dans le métabolisme du H_2O_2 et la signalisation qui en dépend. Une analyse de mutants ADN-T a révélé que la mutation *cat2*, à la différence de *cat1* et de *cat3*, a fortement affecté la croissance et le développement de la plante. Mais ces effets étaient absents lors de la culture des plantes sous un taux de CO_2 élevé, suggérant que la taille diminuée est causée, directement ou indirectement, par une capacité compromise de métaboliser le H_2O_2 produit par la photorespiration. Une étude de *cat2* cultivé dans des photopériodes différentes a mis en évidence une forte influence de la période d'illumination sur la signalisation oxydative et ceci d'une manière qui est indépendante de l'intensité du stress. Lorsque *cat2* est cultivé en jours longs, le stress oxydant induit la voie de l'acide salicylique (SA), provoquant des lésions visibles sur les feuilles. Cette réponse au stress oxydant est annulée dans un double mutant *cat2 g6pd5*, chez lequel l'expression d'une forme spécifique de la glucose-6-phosphate déshydrogénase (G6PDH) a également été inactivée. Une approche de génétique classique a permis d'identifier plusieurs gènes susceptibles d'être impliqués dans la régulation de la formation de lésions SA-dépendante dans ce double mutant. Afin d'explorer les rôles des monodéshydroascorbate réductases (MDHAR) spécifiques dans des conditions optimales et de stress, des mutants d'insertion pour plusieurs gènes codant la MDHAR ont été obtenus. A la suite de son introduction dans le fond *cat2*, l'un d'entre eux a fortement modifié l'induction de la voie SA par le stress oxydant. Pris dans leur ensemble, les résultats soulignent l'importance de CAT2 et permettent de dessiner un lien fonctionnel entre des G6PDH et MDHAR spécifiques dans les voies de signalisation oxydative chez Arabidopsis, lien qui pourrait s'expliquer par la production de NADPH par la G6PDH et son utilisation par la MDHAR.

Title : Functional analysis of catalase mutants and their application to the analysis of NADPH-linked pathways in oxidative signaling in *Arabidopsis thaliana*

Keywords : catalase, NADPH, oxidative stress, H_2O_2, signaling

Abstract: Stress conditions lead to modified redox states and signaling linked to reactive oxygen species (ROS), whose cellular concentrations are regulated by complex antioxidative systems. While the importance of ROS in cell signaling remains very fragmentary. This work used forward and reverse genetics to analyze the roles of catalases and the NADPH-glutathione-ascorbate systems in H_2O_2 metabolism and related signaling in *Arabidopsis thaliana*. An analysis of T-DNA mutants revealed that *cat2*, but not *cat1* or *cat3*, substantially impacted plant growth and development. These effects were annulled by growth at high CO_2, suggesting that they were caused, directly or indirectly, by compromised capacity to metabolize photorespiratory H_2O_2. An analysis conducted in *cat2* rosettes following growth in different photoperiods revealed that oxidative signaling is strongly influenced by day length in a manner that is independent of stress intensity. When *cat2* is grown in long days, oxidative stress induces the salicylic acid (SA) pathway, leading to visible lesions on the leaves. This response to oxidative stress is annulled in *cat2 g6pd5*, which has additionally lost the function of a specific glucose-6-phosphate dehydrogenase (G6PDH). A forward genetics approach identified several genes that may be involved in regulating SA-dependent lesion formation in this double mutant. To explore the roles of specific monodehydroascorbate reductases (MDHAR) in optimal and stress conditions, insertion mutants for several MDHAR-encoding genes were obtained. One of them markedly altered induction of the SA pathway by oxidative stress when introduced into the *cat2* background. Together, the results underline the importance of CAT2 and point to functional coupling between specific NADPH-producing G6PDH and NADPH-requiring MDHAR in oxidative stress signaling pathways in Arabidopsis.

Université Paris-Saclay
Espace Technologique / Immeuble Discovery
Route de l'Orme aux Merisiers RD 128 / 91190 Saint-Aubin, France